



universität
wien

DISSERTATION / DOCTORAL THESIS

Titel der Dissertation / Title of the Doctoral Thesis

New Dehydrogenative Coupling Reactions and Borrowing Hydrogen Processes Using Iron and Manganese Catalysts

verfasst von / submitted by

Natalie Christine Hofmann, BSc. MSc.

angestrebter akademischer Grad / in partial fulfilment of the requirements for the degree of
Doktorin der Naturwissenschaften (Dr. rer. nat.)

Wien, 2021 / Vienna 2021

Studienkennzahl lt. Studienblatt /
degree programme code as it appears on the student
record sheet:

A 796 605 419

Dissertationsgebiet lt. Studienblatt /
field of study as it appears on the student record sheet:

Chemie / Chemistry

Betreut von / Supervisor:

Univ.- Prof. Dr. Kai Carsten Hultsch

*„Man merkt nie, was schon getan wurde,
man sieht immer nur, was noch zu tun bleibt.“*

Marie Skłodowska Curie

Danksagung

Meine Dissertation wäre in dieser Form ohne die Unterstützung vieler Personen nicht zustande gekommen. Deshalb möchte ich jetzt die Gelegenheit nutzen, all jenen zu danken, die diese Arbeit möglich gemacht haben.

Mein besonderer Dank gilt zunächst *Univ. Prof. Dr. Kai Carsten Hultsch* für die Betreuung und die Möglichkeit meine Dissertation in seiner Forschungsgruppe durchzuführen. Ebenfalls möchte ich mich bei *Univ. Prof. Dr. Mario Waser* und *Privatdoz. Dr. Roman Lichtenacker* bedanken, die sich bereit erklärt haben diese Arbeit als Gutachter zu bewerten.

Großer Dank gilt auch allen MitarbeiterInnen der analytischen Teams, die mich bei diversen Analysen unterstützt haben. Speziell erwähnen möchte ich hier das NMR-Team rund um *Ass.-Prof. Dr. Hanspeter Kählig*, das MS-Team von *Dr. Martin Zehl*, das Elementaranalyse-Team von *Mag. Johannes Theiner* und natürlich auch *Peter Frühauf*, der mich bei jeglichen Fragen und Problemen bezüglich unserer GC-Geräte unterstützt hat.

Danken möchte ich außerdem meinen Kollegen in der Arbeitsgruppe der chemischen Katalyse, die mich in den letzten Jahren begleitet haben und fachlich, sowie moralisch unterstützt haben. Zunächst möchte ich mich bei der 1. Generation an Gruppenmitgliedern *Agnieszka*, *Felicity*, *John*, *Leo*, *Lisa* und *Rudi* bedanken, die mich sehr herzlich aufgenommen haben und mich vor allem am Beginn meiner praktischen Arbeit mit sehr vielen Tipps und neuen Ideen unterstützt haben. Im Laufe meiner Arbeitszeit hat sich die Gruppe wesentlich verändert und somit möchte ich auch der 2. Generation *Christoph*, *Fereshteh*, *Lara*, *Mariusz* und *Olivera* meinen Dank aussprechen. Durch die vielen lustigen und spannenden Gespräche wurde der Arbeitsalltag deutlich aufgelockert und es sind immer wieder neue Ideen für Experimente entstanden. Bei *Lara* und *Rudi* möchte ich mich auch zusätzlich für das Korrekturlesen meiner Arbeit bedanken. Speziell erwähnen möchte ich auch *Mirjana*, die uns immer auf jegliche Art und Weise unterstützt. Ein Dankeschön hier auch an meine Studenten *Josefine*, *Adam*, *Eszter*, *Isabella*, *Marc-Andé* und *Anna*, die mit ihren Arbeiten auch einen wesentlichen Beitrag zu meinen Ergebnissen beigetragen haben.

Darüber hinaus gilt mein größter Dank vor allem meiner *Familie* und meinen *Freunden*, die mich auf meinem Weg durch das Studium begleitet haben. Danke, dass ihr mich immer für mich da wart und mich wieder aufgebaut und motiviert habt. Ihr könnt euch nicht vorstellen, wie wichtig dieser Rückhalt für mich war.

Abstract

Heterocycles and heteroatom containing molecules in general are essential substructures of synthetically valuable compounds, such as pharmaceuticals and industrially relevant bulk and fine chemicals. Hence, their easy and atom-efficient synthesis starting from simple, commercially available precursors plays a pivotal role in modern synthetic chemistry. The borrowing hydrogen strategy (BH) and related approaches, including acceptorless dehydrogenative couplings (ADH) and oxidative dehydrogenative coupling reactions (ODC), provide outstanding opportunities for a variety of transformations of alcohols and amines, in particular the formation of new carbon-carbon or carbon-nitrogen bonds. The overall goal of this thesis was the extension of the applicability of these methods. Thus, one strategy was to identify and optimize suitable cascade reactions promoted by abundant metal catalysts in combination with organocatalysis. The first part of this research was focused on the switchable *N*-alkylation of anilines with benzylic alcohols, catalyzed by the nitrile-ligated variant of the Knölker complex. Hence, an enantioselective one-pot, three-component condensation to form α -alkylamino phosphonates (yields up to 83 %, 50 % *ee*) was developed. For that purpose, a sequential iron-catalyzed dehydrogenative condensation was combined with a hydrophosphonylation step, promoted by a chiral BINOL-based phosphoric acid. Secondly, the reaction scope of the highly active PN^3 manganese pincer complex, prepared *in situ* starting from the bipyridine-derived ligand $\text{bpy-}^6\text{NH}^i\text{PrP}$ and $\text{Mn}(\text{CO})_5\text{Br}$, was extended. Thereby, on the one hand the coupling of 2-aminobenzyl alcohols with nitriles to form 2-aminoquinolines could be performed using noticeable low catalyst (1 mol%) and base loadings (10 mol%). On the other hand, the first selective synthesis of 1,2,3,4-tetrahydroquinolines (yields up to 91 %) starting from 2-aminobenzyl alcohols and secondary alcohols *via* homogeneous catalysis was established. The third approach comprised the synthesis, characterization and investigation of new manganese PN^3 -pincer complexes. Thus, a novel acyl manganese catalyst was formed upon complexation of $\text{phen-}^2\text{NH}^i\text{PrP}$ with the $\text{MeMn}(\text{CO})_5$ metal precursor. The complex showed remarkable stability and catalytic activity under atmospheric conditions. Particularly noteworthy is the *N*-alkylation of aniline with benzyl alcohol under air, in which a conversion of 61 % was achieved.

Zusammenfassung

Stickstoff- und phosphorhaltige organische Verbindungen dienen als Grundkörper für Arzneimittel, Basis- und Feinchemikalien. Es ist daher von besonderem Interesse diese Substanzen möglichst kostengünstig und einfach zu synthetisieren. Aus Alkoholen und Aminen lassen sich mittels Wasserstoff-Transfer-Reaktionen oder dehydrierenden Kupplungsreaktionen Verbindungen mit neuen Kohlenstoff-Kohlenstoff- oder Kohlenstoff-Stickstoff-Bindungen herstellen. Die Anwendungsmöglichkeiten dieser Verfahren sollten im Rahmen der vorliegenden Arbeit erweitert werden. Dazu wurden neue Synthesewege unter Verwendung bekannter Katalysatoren untersucht und optimiert. Als erster Schwerpunkt wurde eine modifizierbare *N*-Alkylierung von Anilinen mit benzyllischen Alkoholen, katalysiert mit einer Variante des Knölker Komplexes, untersucht. Im Zuge dessen konnte eine enantioselektive Mehrkomponentenreaktion zur Synthese von α -Alkylaminophosphonaten (bis zu 83 % Ausbeute, bis zu 50 % *ee*) entwickelt werden. In diesem „Eintopfverfahren“ wurde eine eisenkatalysierte Kondensation mit einer Hydrophosphonylierungsreaktion, katalysiert mit einer chiralen BINOL-basierten Phosphorsäure, kombiniert. Darüber hinaus ließ sich das Anwendungsgebiet eines reaktiven PN^3 Mangan-Pincer-Katalysators, der *in situ* ausgehend von dem Bipyridin-basierten Liganden $\text{bpy-}^6\text{NH}^{\text{Pr}}\text{P}$ und $\text{Mn}(\text{CO})_5\text{Br}$ hergestellt wurde, erweitern. Somit konnten einerseits 2-Aminochinoline aus 2-Aminobenzylalkoholen und Nitrilen mit sehr geringer Katalysator- (1 mol%) und Basen-Beladung (10 mol%) hergestellt werden. Andererseits konnten 1,2,3,4-Tetrahydrochinoline erstmals selektiv ausgehend von 2-Aminobenzylalkoholen und sekundären Alkoholen mittels homogener Katalyse synthetisiert werden. Ein dritter Ansatz beinhaltet die Synthese, Charakterisierung und Anwendung neuer Mangan- PN^3 -Pincer Komplexe. Hierbei zeigte vor allem ein neuer Acyl-Mangan Komplex, hergestellt durch Komplexierung von $\text{phen-}^2\text{NH}^{\text{Pr}}\text{P}$ mit $\text{MeMn}(\text{CO})_5$, großes Potential. Der Katalysator weist hohe Stabilität und katalytische Aktivität an Luft auf. Besonders bemerkenswert ist hierbei die *N*-Alkylierung von Anilin mit Benzylalkohol an Luft, die einen Umsatz von 61% erzielte.

Table of Contents

Danksagung	iii
Abstract	v
Zusammenfassung	vii
Table of Contents	ix
1. Introduction	1
1.1. Homogeneous base metal catalysis	1
1.2. Redox non-innocent ligands	2
1.3. Borrowing hydrogen methodology	7
1.4. Hydrophosphonylation Reactions	12
2. Scope of Work	16
3. Results and Discussion.....	17
3.1. Publication 1	18
3.1. Publication 2.....	33
3.2. Publication 3.....	56
3.4. Unpublished Results.....	98
4. Conclusion and Outlook.....	127
5. References	129
6. Appendix.....	134
6.1. Abbreviations	134
6.2. Figures	135
6.3. Schemes	136
6.4. Tables	137

1. Introduction

1.1. Homogeneous base metal catalysis

The development of atom-efficient, sustainable and highly selective synthetic strategies plays a fundamental role in modern chemistry.^[1] For this purpose, catalysis provides a promising tool, which is already widely used in industrial applications.^[2] However, until now, the vast majority of industrially applied catalytic systems have relied on noble metals. In recent years, based on the global emphasis on sustainable chemistry, the replacement of precious metals by base metals became a topic of great interest.^[3] Due to their abundance in the earth crust (Figure 1)^[4] and the resulting lower costs, base metals are particularly attractive.^[5]

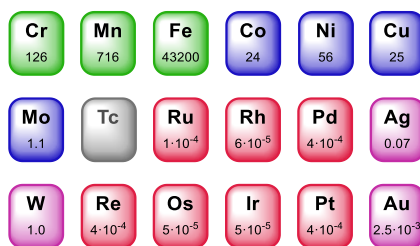


Figure 1: Concentration [ppm] of middle to late transition metals in the continental earth crust.^[4-6]

However, for overall cost-considerations it should be taken into account that the robustness and the activity of base metal catalysts are often significantly lower compared to noble metal catalytic systems. Therefore, the relative costs for developing suitable ligand systems need to be considered as well.^[6] Moreover, a generally lower toxicity for non-precious metals is often listed as an outstanding advantage, though the toxicity levels have to be viewed critically.^[7]

Comparison of the significantly more abundant 3d-metals with the more precious 4d- and 5d- metals reveals crucial differences in the electronic structure and in the bonding. For instance, the redox potentials or the free reaction energies for homo- and heterolytic bond dissociations, as well as the stability of ground states or the preference for higher spin-states show large discrepancies, which influence homogeneous catalytic reactions drastically.^[5] Generally, 4d- and 5d- metal complexes are prone to undergo 2-electron pathways, such as oxidative addition and reductive elimination, whereas 3d-metals prefer to undergo 1-electron steps.^[8] However, recent research proved that so-called 'redox non-

innocent' ligands can act as 'electron reservoirs' expanding the scope of metalorganic reactions of 3d- metals significantly (see Section 1.2.).^[9]

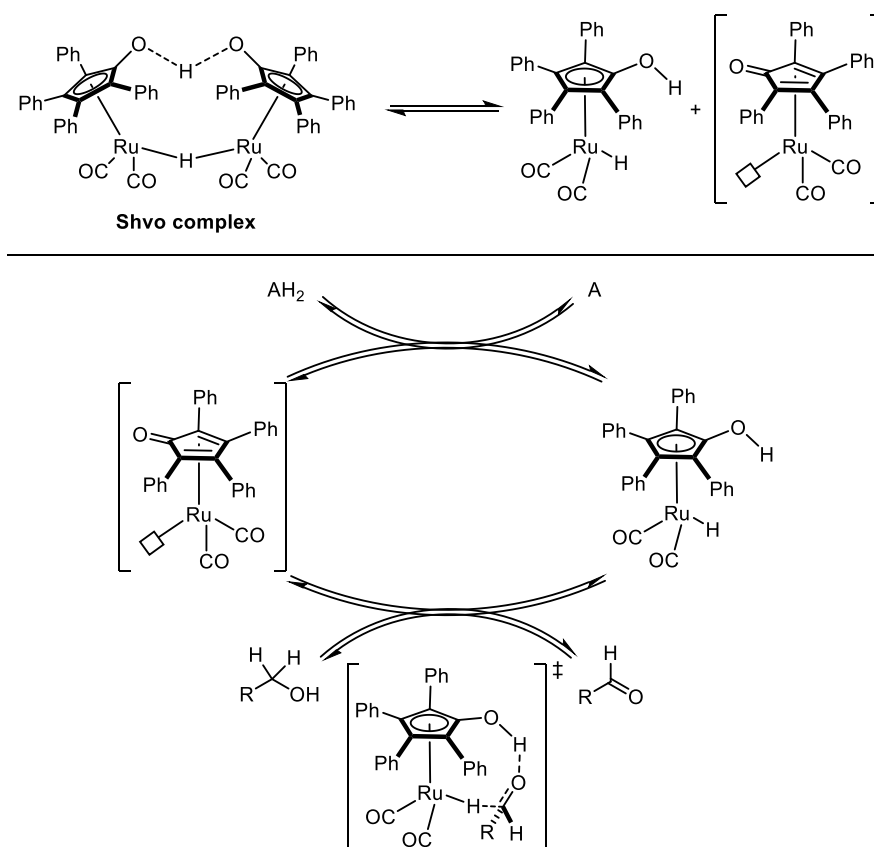
1.2. Redox non-innocent ligands

In 'classical' catalytic reactions, ligands activate the metal center by affecting its electronic properties. Moreover, they provide steric hindrance and thus direct the substrates to free coordination sites, affecting the selectivity of the reaction. However, commonly the ligands remain unchanged and do not actively participate in the catalytic cycle such as undergoing bond breaking or bond forming reaction steps. In contrast, functional (non-innocent) ligands directly participate in substrate activation and product forming processes by undergoing reversible structural changes. In general, one can distinguish between two different types of redox non-innocent ligands. The first group acts by accepting and donating electrons, whereas the second takes part in bond forming or breaking reactions of the substrate.^[9] Thus, the utilization of metal-ligand cooperation expands the reaction scope compared to 'classical' transition metal catalysis.^[10]

Among the wide range of redox non-innocent ligand systems,^[9c] the focus of this PhD thesis lies on the application of cyclopentadienone and pincer ligated complexes, which interact with the metal through aromatization and dearomatization processes.^[10b]

1.2.2. Cyclopentadienone complexes

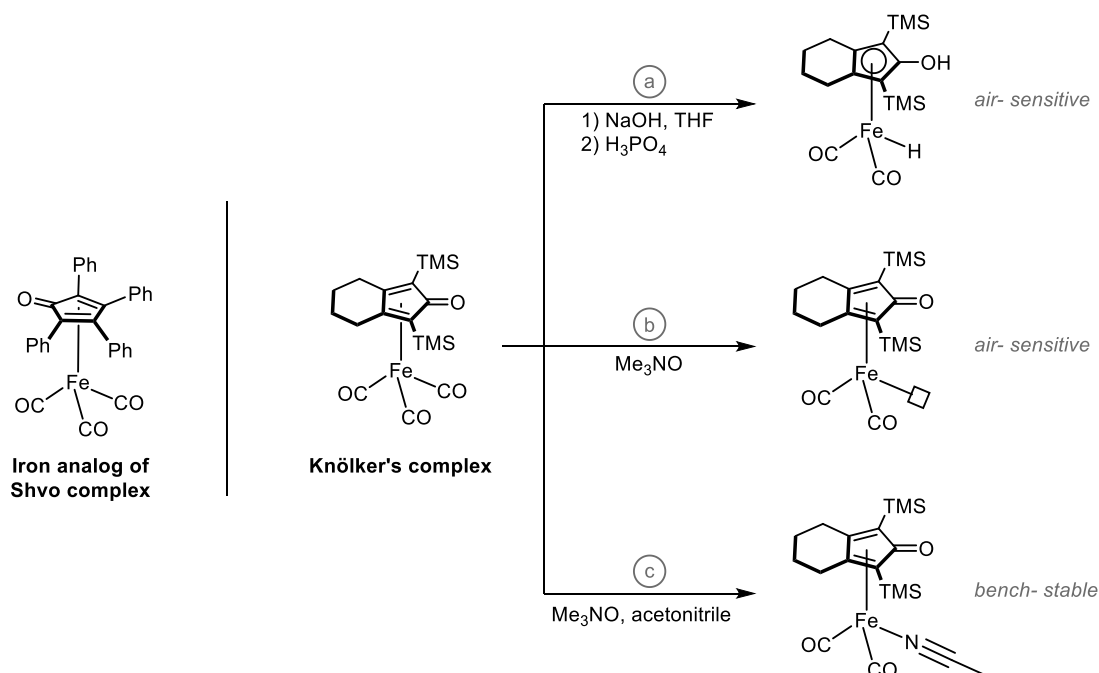
Cyclopentadienone catalysts make an important class of complexes. Generally, they can be easily synthesized and the coordinated non-innocent ligand induces powerful redox properties.^[11] The Shvo catalyst, discovered in 1984 by Shvo *et al.*,^[12] represents one of the first examples of a hydrogen transfer catalyst that promotes the reaction based on metal-ligand cooperation (Scheme 1). The complex itself is formed *via* ruthenium-promoted [2+2+1]- cycloaddition. As solid, it forms a dimeric structure, though its catalytic activity originates from dissociation into two monomeric complexes.^[10b] The reaction proceeds through interconversion of η^5 -ligated hydroxycyclopentadienyl and η^4 -ligated cyclopentadienone.^[10b, 12b] In the suggested outer-sphere mechanism the hydrogenation of the carbonyl moiety proceeds *via* simultaneous hydride-transfer from the metal center and proton transfer from the hydroxy group of the cyclopentadienyl ligand.^[13]



Scheme 1: Proposed mechanism for the dehydrogenation of alcohols promoted by ruthenium-based Shvo catalyst.^[10b, 12b]

The iron analog of the Shvo complex (Scheme 2) was already reported in the late 1960s by Schrauzer,^[14] though this complex showed poor activity in the hydrogenation of ketones.^[12b] In 1992 Knölker *et al.* developed a bicyclic tricarbonyl iron complex – the so called Knölker complex. The bench-stable η^4 -ligated cyclopentadienone variant can get activated by treatment with NaOH followed by H_3PO_4 , generating the air-sensitive and highly reactive η^5 -ligated hydroxycyclopentadienyl complex (Scheme 2a). The addition of trimethylamine-*N*-oxide activates the complex by creating a free coordination site (Scheme 2b). Both highly active complexes are air-sensitive.^[15] Another possibility is the exchange of a CO-ligand against acetonitrile (Scheme 2c), leading to a bench-stable, active complex which achieves higher turnover numbers compared to the tricarbonyl complex.^[15c, 16] Casey and coworkers found this complex to be highly active in the hydrogenation of ketones and aldehydes using H_2 or *i*PrOH as hydrogen donor, which is suggested to proceed *via* a similar outer-sphere mechanism compared to the ruthenium analogon.^[11, 17] In the last decade, the reaction scope of the Knölker complex and its derivatives has been thoroughly investigated and a vast number of reactions based on the borrowing hydrogen and the acceptorless dehydrogenation strategy (see Section 1.3) has been developed.^[11, 18] In doing so, the alkylation of amines^[19] and alcohols^[20] was promoted successfully and various heterocyclic

compounds such as quinolines,^[20] 1,2,3,4-tetrahydroquinoxalines,^[19a] pyrroles,^[21] pyrrolidines and piperidines^[19a] were synthesized in an atom-efficient manner.



Scheme 2: Cyclopentadienyl-ligated iron complexes.

1.2.3. Pincer complexes

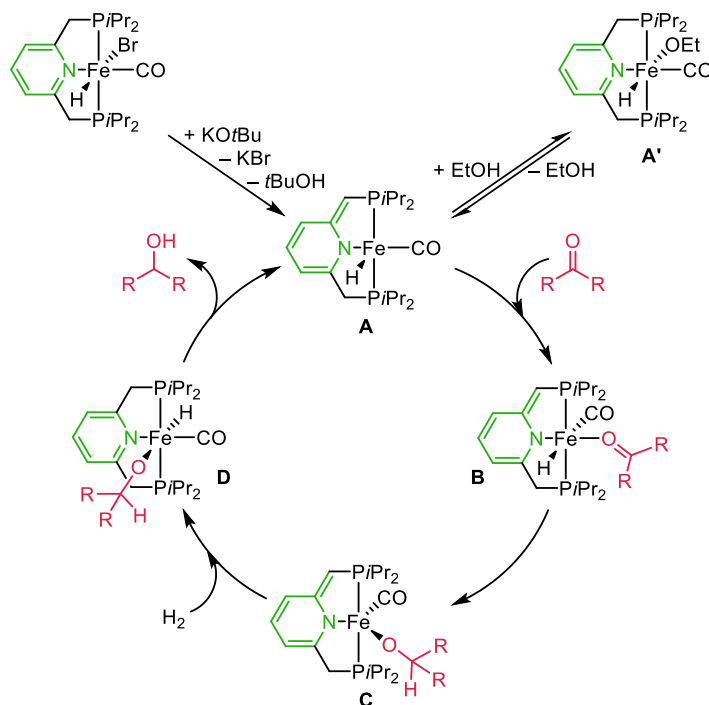
The term 'pincer ligand' generally refers to a tridentate ligand that occupies three adjacent binding sites in meridional geometry in a metal complex. Two fused metallacycles are formed between the pincer ligand and the metal center, providing a well-defined geometry of the metal environment and stabilizing the formed complex.^[22] Initial reports on these type of ligands date back to the 1970s.^[23] Figure 2 displays a common example of a pincer ligand with a 2,6-disubstituted aromatic ring as backbone coordinated to a metal center. This example shows that the steric and electronic properties of these complexes can be modified easily without changing the coordination geometry significantly.

	Function	Typical groups
R...	- steric control - introduction of chirality	
L...	- electronic control	P, N, O
Y...	- ring- size determination - bite angle effect - introduction of chirality - metal-ligand cooperation	(CH ₂) _n , O, NH
X...	- electronic control	C, N
Z...	- electronic control (fine-tuning)	Hal, RO, R

Figure 2: Tuning possibilities of pincer ligands.^[22d, 22e]

First of all, the central ligand atom (X) provides electronic control, in particular caused by the *trans* influence. The other coordinating atoms (L) show a significant impact on the electronic properties as well. Besides, modification of substituent Z can be used for electronic fine-tuning. Substituents R directly influence the steric hindrance and can be used to introduce chirality, whereas the linker arms (Y) define the ring size and thus affect the bite angle and the metal-ligand cooperation (MLC).^[10, 22]

The exact classification is based on the coordinating donor atoms (LXL), such as common ligands designs PCP, NCN, PNP and NNP. The three-dentate chelation ensures a strong bonding to the metal leading to a high stability of the formed complexes. This renders them suitable for promoting the activation of inert bonds, which generally requires harsh reaction conditions.^[22e] Aromatic pincer ligands are a prime example of non-innocent ligands, as they are capable to undergo electron delocalization over their backbones. Deprotonation by strong bases dearomatizes the heteroaromatic core and forms an exocyclic double bond creating a reactive center for metal-ligand cooperation.^[10b, 24] Milstein and coworkers discovered this mode of metal-ligand cooperation and developed a variety of catalytic systems.^[10a, 25] A textbook example of an aromatization-dearomatization mechanism is depicted in Scheme 3 using a non-innocent PNP pincer ligand in combination with an iron-metal center to promote the hydrogenation of ketones.



Scheme 3: Proposed aromatization-dearomatization mechanism by using a non-innocent PNP pincer ligand for the hydrogenation of ketones.^[25d]

The addition of KO^tBu leads to deprotonation at the pyridinylmethylenic carbon and thus to the formation of the reactive dearomatized hydride species (**A**). This intermediate is stabilized by rearomatization through a reversible addition of ethanol forming **A'**. Coordination of the ketone gives intermediate **B**. Then the ketone undergoes migratory insertion into the Fe-H bond, forming a pentacoordinate alkoxy complex (**C**). Reaction with external hydrogen leads to the rearomatized hydrido alkoxy complex (**D**). In the final step elimination of the reduced product regenerates active species **A**.^[25d]

Manganese Pincer Complexes

In modern catalytic research, the development of abundant metal pincer complexes has become of increasing interest.^[22c, 26] Based on the ability of manganese to form complexes with coordination numbers up to 7 and its high redox potential, manganese compounds used to be applied for oxidation and coupling reactions.^[27] Though in more recent years, manganese pincer-complexes have shown high potential in catalytic (de)hydrogenation and transfer hydrogenation reactions.^[28] Figure 3 displays some examples of manganese pincer complexes with different scaffolds.

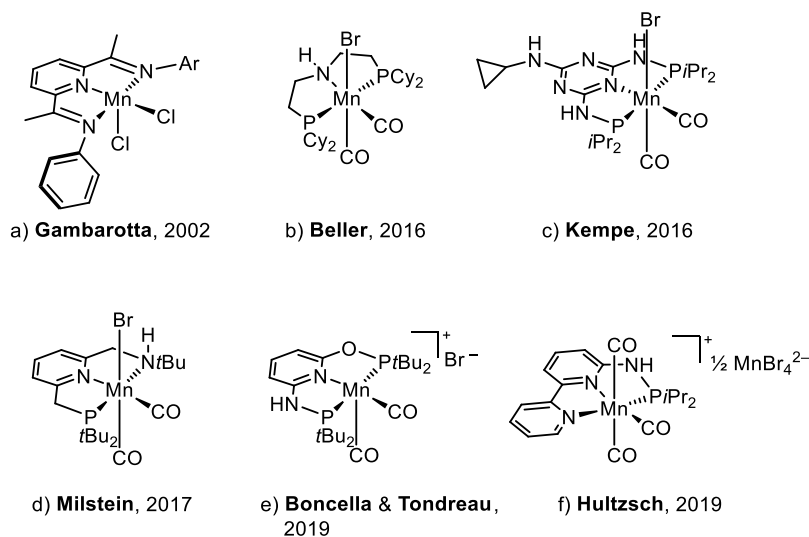


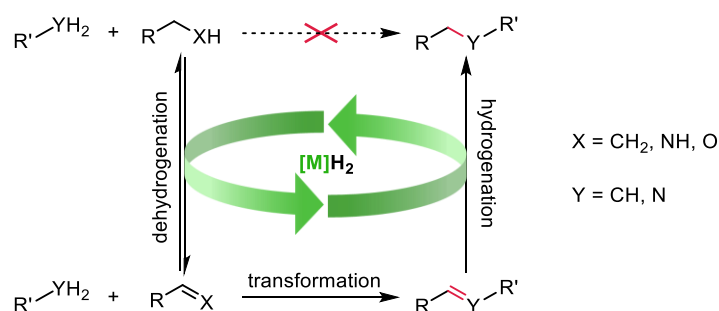
Figure 3: Different scaffolds of manganese-based pincer complexes.

Gambarotta and coworkers for example studied the alkylation of diiminepyridine ligated manganese complexes (Figure 3a).^[29] The groups of Beller, Kempe, and Milstein investigated different ligands for various hydrogenation reactions. Aliphatic PNP manganese complex (Figure 3b) hydrogenates nitriles, ketones and aldehydes,^[30] whereas the PN₅P-ligated complex (Figure 3c) was exclusively applied to hydrogenate aldehydes and ketones.^[31] The pincer complex with the pyridine backbone (Figure 3d) was reported to reduce esters.^[25i] PNNOP manganese-based pincer complex (Figure 3e) reported by

Boncella and Tondreau showed high catalytic activity in the dehydrogenation of formic acid.^[32] Our group reported an NNP-system with a bipyridine backbone (Figure 3f) which showed high activities for the *N*-alkylation of amines under mild reaction conditions.^[33]

1.3. Borrowing hydrogen methodology

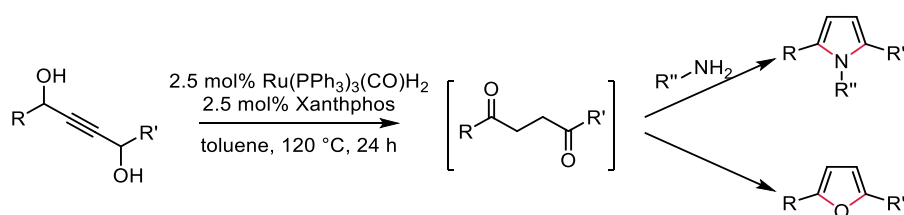
Heterocycles and carbon-heteroatom containing molecules in general are indispensable substructures of synthetically valuable compounds. Hence, their easy and atom-efficient synthesis starting from simple, commercially available precursors plays a pivotal role in modern synthetic chemistry.^[1] The borrowing hydrogen strategy provides outstanding opportunities as a green method for a variety of transformations utilizing cheap and harmless starting materials. Most commonly alcohols and amines are used as substrates for the formation of new carbon-carbon or carbon-nitrogen bonds. The general pathway is depicted in Scheme 4. The first step involves a temporary activation by dehydrogenation (oxidation). The activated substrate can undergo various functionalization reactions, for example different types of condensation reactions, forming unsaturated intermediates. In the end, the hydrogen which was generated in the first step will facilitate the catalyzed reduction to the saturated product. Consequently, there is no net oxidation (hydrogen loss) or reduction (hydrogen gain) after the completed reaction sequence. The most important benefit of combining catalytic dehydrogenation and hydrogenation is the minimization of the application of stoichiometric activation agents such as oxygen, quinones or TEMPO. Instead H_2 (= the smallest possible molecule) is used as activation agent. Moreover, tedious workup and purification steps of the intermediates can be avoided as this cascade strategy proceeds as a one-pot reaction.^[34]



Scheme 4: General principle of the borrowing hydrogen methodology.^[34a]

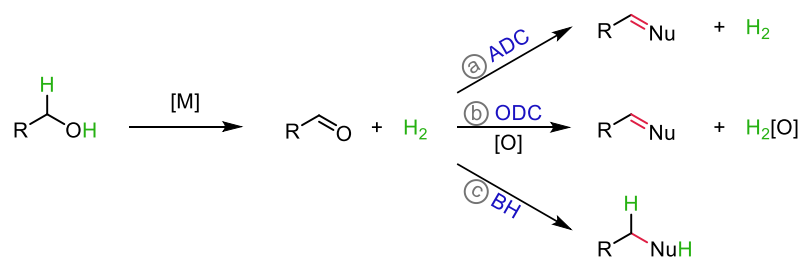
1.3.1. Borrowing hydrogen strategies and dehydrogenative coupling reactions

It should be noted that there are various examples which are not strictly following this dehydrogenation/hydrogenation-sequence, such as the ruthenium-promoted synthesis of pyrroles obtained through cyclization of 1,4-alkynediols with amines (Scheme 5).^[35]



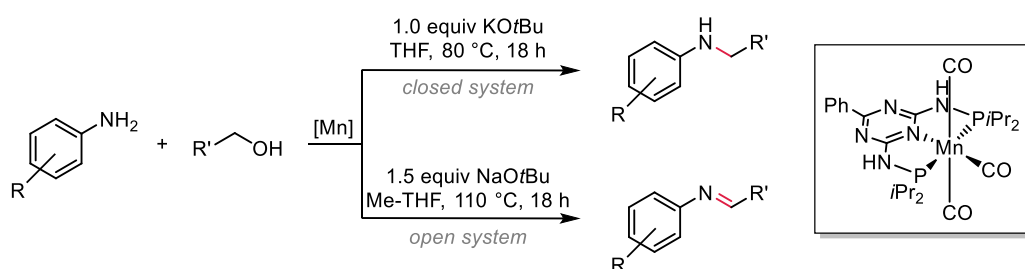
Scheme 5: Ruthenium-promoted pyrrole synthesis from 1,4-alkynediols and amines.^[35]

Moreover, it is important to distinguish between different mechanisms based on the role of the hydrogen (Scheme 6). In the course of acceptorless dehydrogenative coupling reactions (ADC) the generated hydrogen is released (Scheme 6a), whereas for the oxidative-dehydrogenative coupling (ODC) an additional oxidant or hydrogen acceptor is applied (Scheme 6b). Strictly speaking, in a borrowing hydrogen (BH) reaction the overall reaction sequence is redox neutral. The hydrogen which is generated during substrate activation is used in the end as reducing agent (Scheme 6c and Scheme 4).^[36]



Scheme 6: Mechanistic differences based on the role of hydrogen.^[36]

However, all these strategies are closely related and often discussed together. Several metal complexes are highly active for more than one pathway simply by changing the reaction conditions. For instance, Kempe and coworkers reported a base switchable synthesis of *N*-alkylated amines (*via* BH) or imines (*via* ADC) (Scheme 7)^[37]



Scheme 7: Switchable selective synthesis of *N*-alkylated amines and imines.^[37]

These methods provide access to various different products – such as imines, amines, amides, alcohols and esters, as well as a broad range of different heterocycles – utilizing simple and cheap starting materials.^[34] The most important obtained structural motifs are depicted in Figure 4.

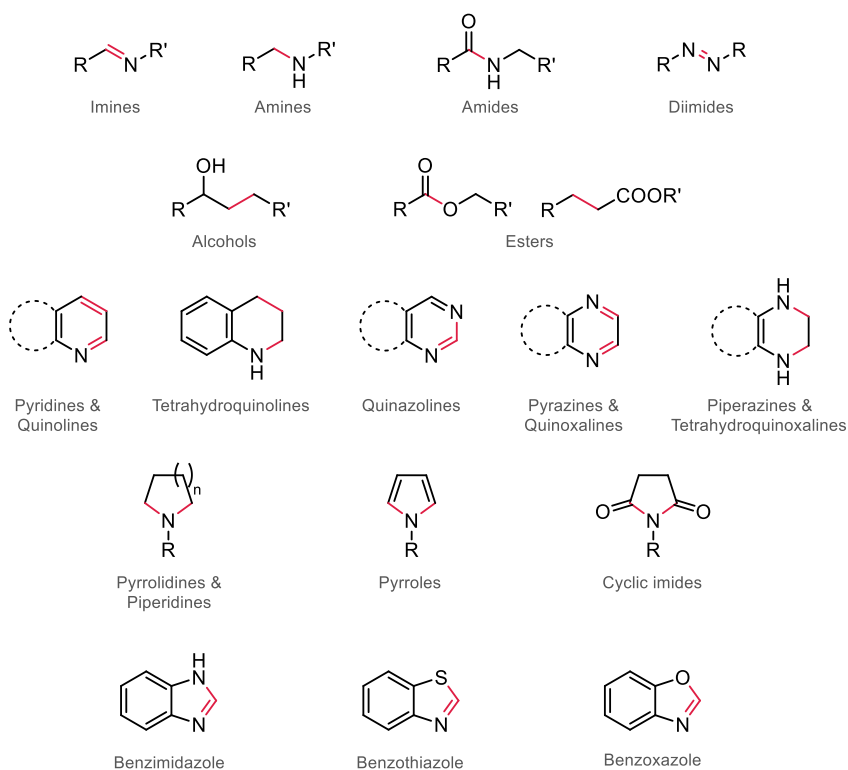
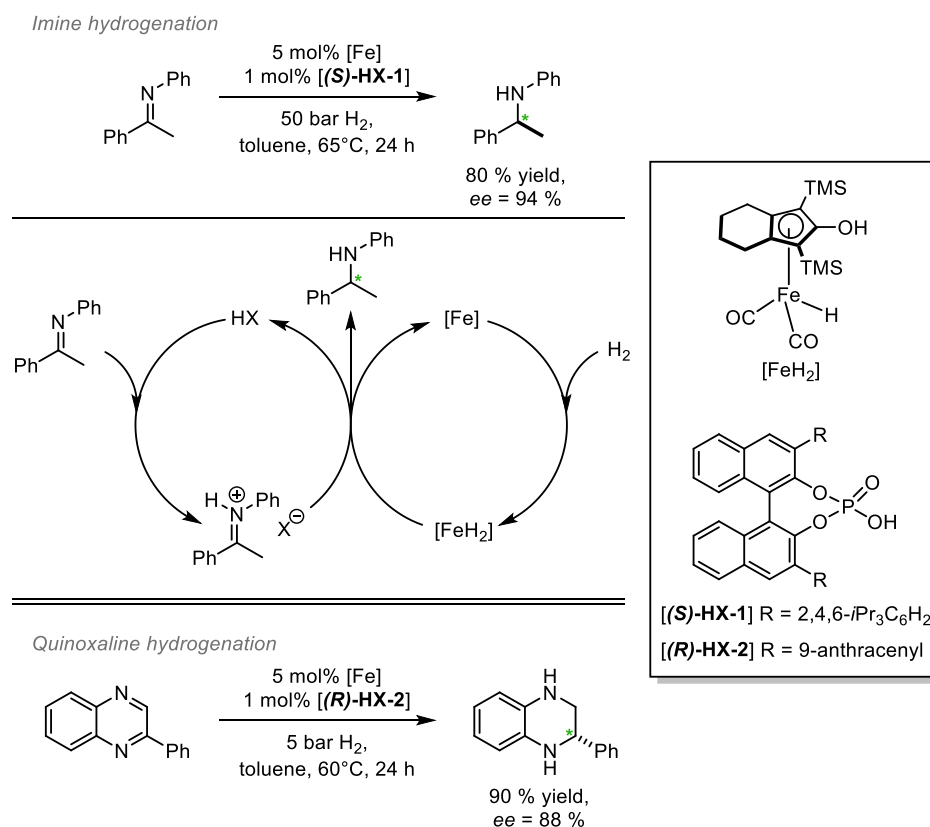


Figure 4: Important structural motifs obtained through ACD, ODC or BH strategies (the newly formed chemical bonds are highlighted in red).

For detailed information on this topic, we summarized the work on multicomponent reactions based on dehydrogenative coupling strategies and the borrowing hydrogen methodology for the formation of *N*-containing heterocycles in a review (see chapter 3.1).

1.3.2. Multicatalytic approaches

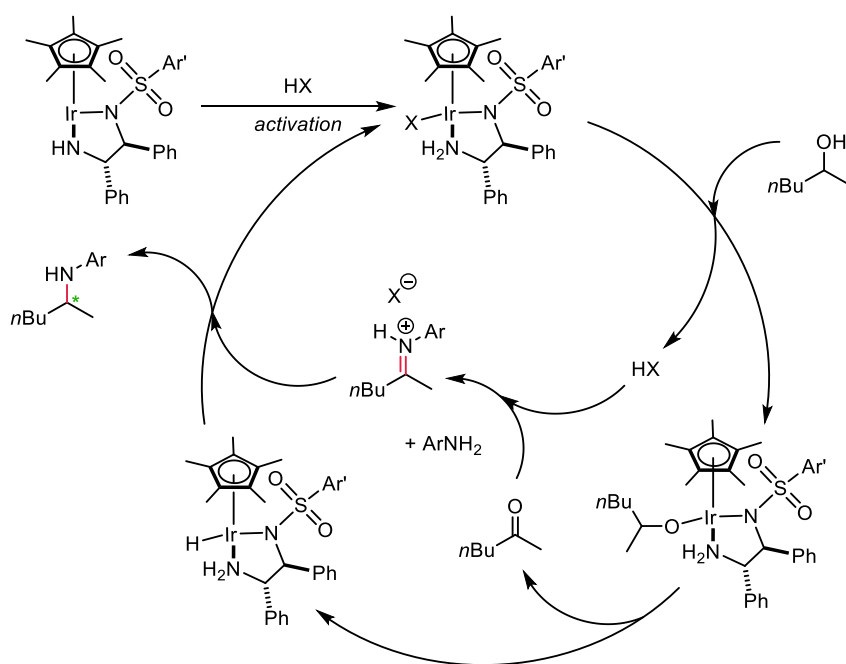
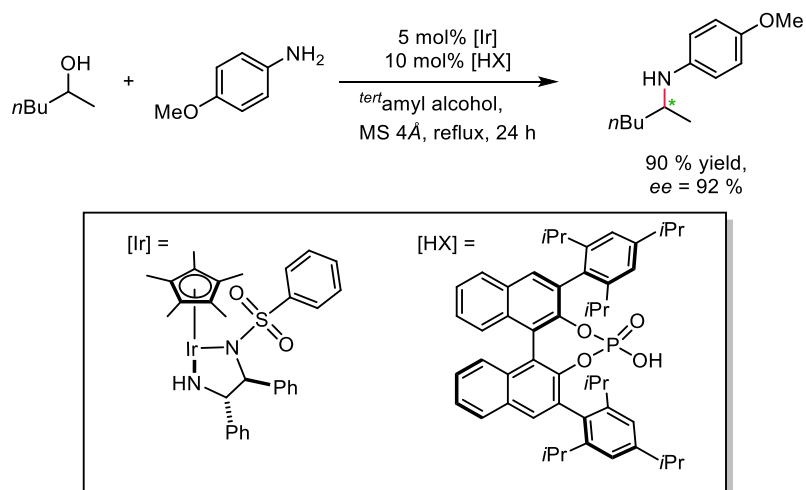
The application of multicatalytic approaches – in this case the combination of metal-catalyzed borrowing hydrogen processes with organocatalytic reactions – allows to gain access to even higher functionalized products. Moreover, the application of chiral organocatalysts opens the way towards stereoselective reactions *via* one-pot procedures. In the following three outstanding examples which served as basis for the first part of this doctoral thesis (see Section 3.2.) will be explained briefly. Beller and coworkers developed a cooperative catalytic system combining the highly active hydride derivative of the Knölker complex with chiral BINOL-based phosphoric acids for the enantioselective hydrogenation of imines and quinoxalines. Scheme 8 depicts the cooperation of the catalytic systems for the reduction of imines.^[38] The reaction starting from quinoxalines proceeds in a similar fashion only with slightly modified reaction conditions and a different phosphoric acid.^[39]



Scheme 8: Enantioselective hydrogenation of imines and quinoxalines promoted by a cooperative catalytic system. ^[38-39]

Zhao and coworkers reported a synthesis of chiral amines *via* catalysis by a mono-Cp diamine iridium and a chiral BINOL based phosphoric acid. Both catalysts are assumed to function cooperatively. The iridium complex is involved in the dehydrogenation of the alcohol and the final reduction of the formed product. The acid cocatalyst (HX) is believed

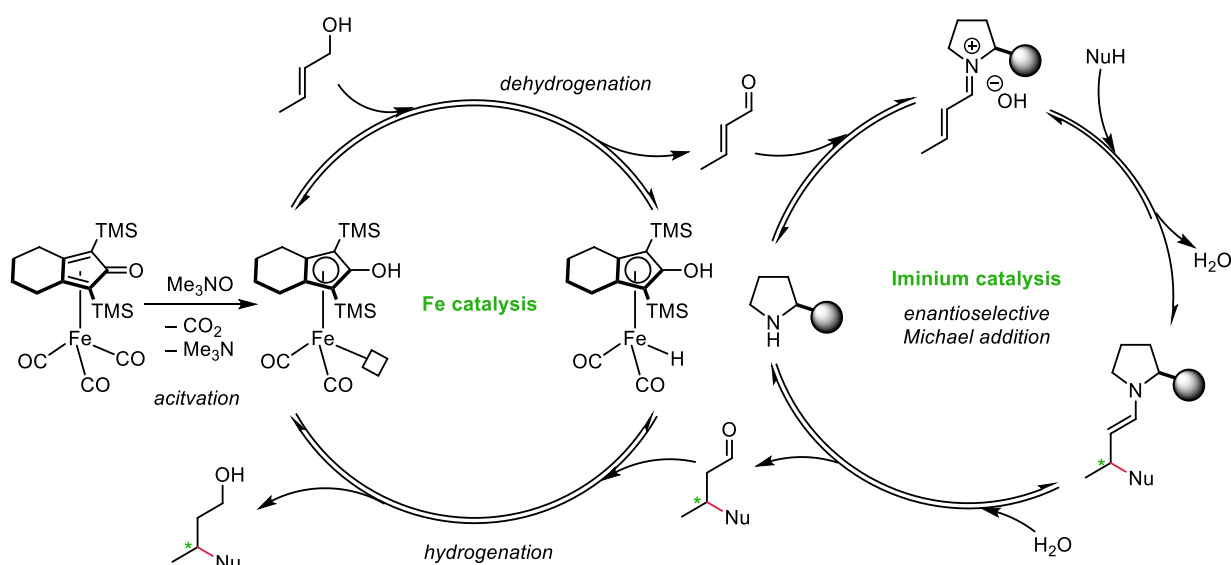
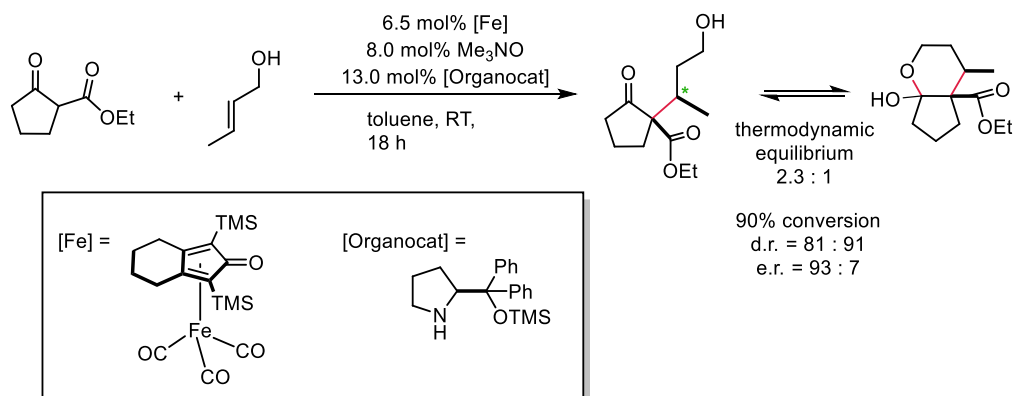
to promote the imine condensation as well as activating the imine intermediate as iminium species (Scheme 9).^[40]



Scheme 9: Synthesis of chiral amines via cooperative catalysis by iridium and a chiral phosphoric acid.^[40]

Quintard and Rodriguez combined an iron promoted borrowing hydrogen process with iminium catalysis in a dual manner in order to transform simple allylic alcohols into β -chiral saturated alcohols (Scheme 10). The iron-based Knölker complex oxidizes the alcohol and thereby activates it for the enantioselective Michael addition promoted by a derivative of *L*-proline. In the end, the metal complex reduces the formed Michael product, which tends to undergo a lactone formation.^[41] In contrast to the other two examples the chirality is

introduced during the organocatalyzed Michael addition and is retained throughout the reduction step.

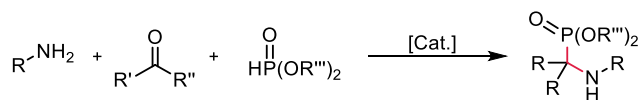


Scheme 10: Enantioselective functionalization of allylic alcohols through dual catalysis by iron and an amino acid derivative.^[41]

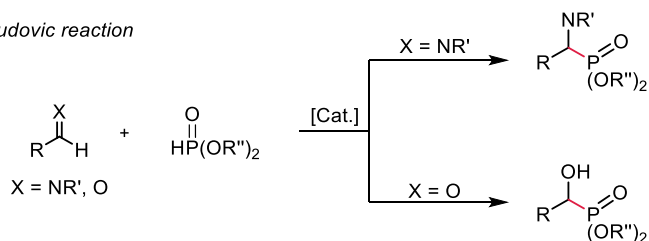
1.4. Hydrophosphonylation Reactions

As hydrophosphonylation reactions play an important role in the first part of this doctoral thesis (see Section 3.2.), the theoretical background will be briefly discussed herein. A hydrophosphonylation reaction allows the formation of a new C-P bond by adding alkyl- or aryl- phosphites to aldehydes or imines generating phosphonates. The most straightforward and widely used synthetic strategies are the Kabachnik-Fields and the Pudovic reaction (Scheme 11).^[42] The Kabachnik-Fields reaction is a three-component condensation of a carbonyl, an amine and a phosphite *via* hydrophosphonylation of an *in situ* formed imine.^[43] The direct addition of phosphites to carbonyls or imines leading to α -hydroxy or α -amino phosphonates is called Pudovic reaction^[42a, 44]

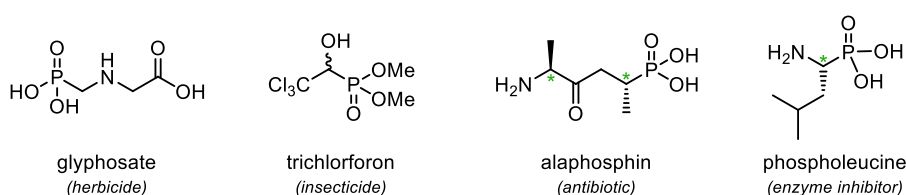
Kabachnik- Fields reaction



Pudovic reaction

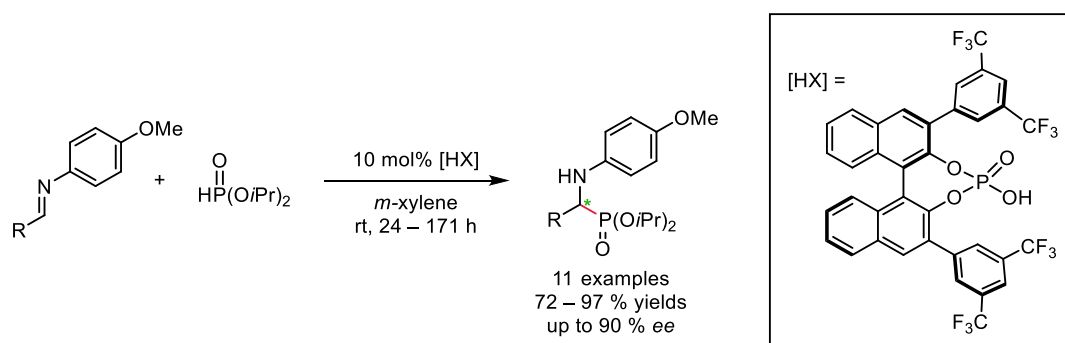
Scheme 11: Synthesis of α -amino and α -hydroxy phosphonates.

The obtained phosphonate diesters are valuable precursors of α -amino and α -hydroxy phosphonic acids. The diesters show a high solubility in organic and neutral aqueous media, which allows easy functionalization, followed by conversion into the corresponding phosphonic acids under acidic reaction conditions. Both structural motifs serve as building blocks for herbicides, fungicides, insecticides as well as antibiotics and anti-viral agents (Figure 5).^[42, 45] In many cases the biological activity of these compounds is highly dependent on the absolute configuration at the stereogenic α -carbon to the phosphorous. For example only the displayed (*S,R*)-diastereomer (alaphosphin, Figure 5) shows inhibitory activity in the peptidoglycan biosynthesis in gram-positive and gram-negative bacteria, whereas the other stereoisomers of alanyl-1-aminoethylphosphonic acid are inactive.^[45a, 46] In the case of phospholeucine the (*R*)-enantiomer is a significantly more potent inhibitor of leucine aminopeptidase compared to the (*S*)- enantiomer.^[47]

Figure 5: Selected examples of biologically important α -amino phosphonates and phosphonic acids

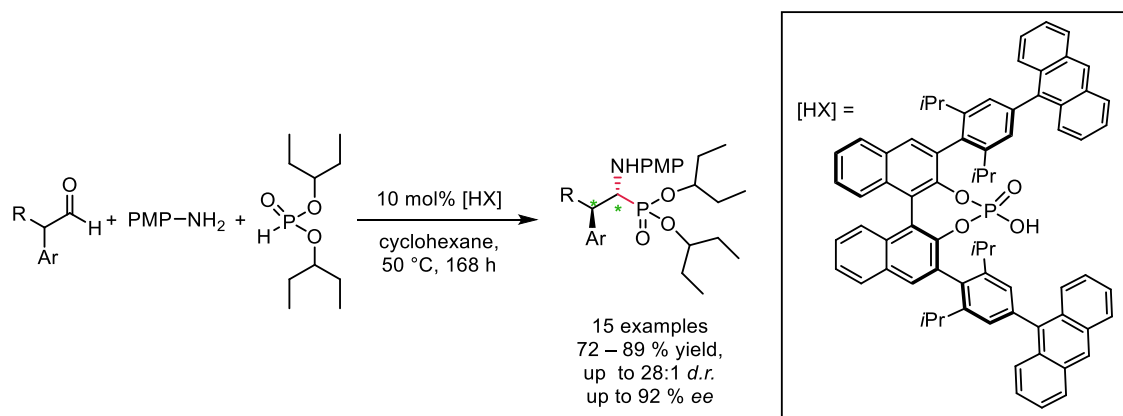
Due to the importance of chiral phosphonate diesters, a vast number of stereoselective synthetic procedures was developed. Initial approaches generally applied enantiopure amines or imines as starting materials in order to generate the desired enantiomer or diastereomer of corresponding phosphonate diester.^[45a, 48] Within the last 25 years a great variety of organocatalytic enantioselective hydrophosphonylation strategies were developed.^[42, 49] Among the wide range of highly active organocatalysts, chiral BINOL-based phosphoric acids were chosen to promote the one-pot synthesis of enantioenriched

α -*N*-alkylaminophosphonates, which was developed in the course of the first project of this doctoral thesis (see Section 3.2.). At this point two landmark publications using chiral BINOL-based phosphoric acids as organocatalysts shall be highlighted. The application of these phosphoric acids was pioneered by Fuchibe and coworkers to produce α -amino phosphonates with moderate to good enantioselectivities starting from aldimines and diisopropylphosphine (Scheme 12).^[49g]



Scheme 12: Asymmetric hydrophosphonylation of aldimines promoted by a chiral BINOL-based phosphoric acid.

List *et al.* extended the applicability by conducting a direct asymmetric three-component Kabachnik-Fields reaction of an aldehyde, *p*-anisidine and di(3-pentyl)phosphite (Scheme 13).^[43c]



Scheme 13: Direct asymmetric three-component Kabachnik-Fields reaction promoted by a chiral BINOL-based phosphoric acid.^[43c]

It is assumed that the addition of phosphites to imines is based on a bifunctional activation mechanism. On the one hand the phosphoric acid acts as a Brønsted acid protonating the imine. On the other hand it coordinates the hydrogen of the phosphite by acting as Brønsted base (Figure 6a).^[49g] The phosphite is considered as the nucleophilic and reactive tautomer, whereas the non-nucleophilic phosphonate form is generally favoured (Figure 6b).^[49d, 50]

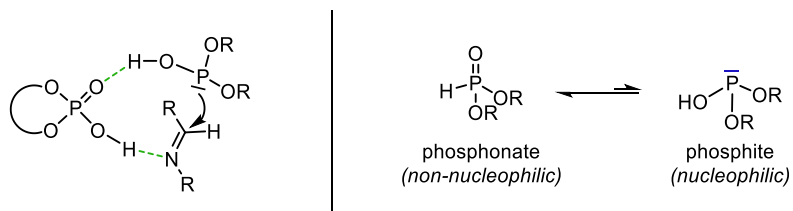


Figure 6: a) Bifunctional activation mechanism of BINOL-based chiral phosphoric acids.^[49g] b) Phosphonate-phosphite tautomerism.^[49d, 50a]

2. Scope of Work

The borrowing hydrogen methodology and related acceptorless dehydrogenative coupling strategies have become ever more important in current organic synthesis, providing attractive atom-efficient synthetic pathways. Within the last decade the reaction scope increased significantly.^[34] However, there is still a high potential for further developments, in particular in the field of base metal catalysis. The aim of this work was to further broaden the scope of application. Thus, one approach was the combination of known metal complexes with chiral organocatalysts. In doing so the metal species should catalyze the (de)hydrogenation steps, whereas the organocatalyst should promote the functionalization reaction, hence generating enantioenriched products. The second strategy involved modification of reaction conditions of known reactions, which should lead to a new, previously unobserved product. In order to reach these goals, the first step was the identification of suitable reactions, followed by optimization of the reaction conditions. With the optimized synthetic strategies in hand, the applicability and selectivity were examined by substrate screenings. In the course of this study, investigations to get insights into the mechanistic pathways were conducted as well. Lastly new pincer complexes were synthesized, characterized and tested with respect to their catalytic activity.

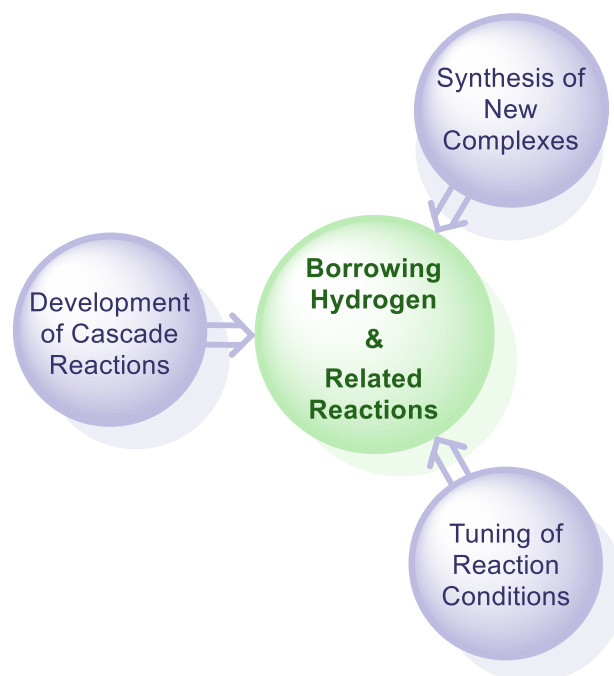


Figure 7: Strategies to broaden the applicability of borrowing hydrogen reactions and related methods.

3. Results and Discussion

This PhD thesis is based on the following scientific publications.

3.1. Publication 1

Borrowing Hydrogen and Acceptorless Dehydrogenative Coupling in the Multicomponent Synthesis of Heterocycles: A Comparison between Base and Noble Metals (*Review*)

N. Hofmann, K. C. Hultsch,

manuscript submitted to *Eur. J. Org. Chem.* (submission date: 10.06.2021)

3.2. Publication 2

Switching the *N*-Alkylation of Arylamines with Benzyl Alcohols to Imine Formation Enables the One-Pot Synthesis of Enantioenriched α -*N*-Alkylaminophosphonates

N. Hofmann, K. C. Hultsch, *Eur. J. Org. Chem.* **2019**, 3105–3111.

3.3. Publication 3

Synthesis of Tetrahydroquinolines via Borrowing Hydrogen Methodology Using a Manganese PN³ Pincer Catalyst

N. Hofmann, L. Homberg, K. C. Hultsch, *Org. Lett.* **2020**, 22, 7964–7970.

3.4. Unpublished results

Some additional experiments which were not reported in a publication are summarized in Section 3.4.

3.1. Publication 1

Borrowing Hydrogen and Acceptorless Dehydrogenative Coupling in the Multicomponent Synthesis of Heterocycles: A Comparison between Base and Noble Metals (Review)

Natalie Hofmann^[a] and Kai C. Hultzsch^{*[a]}

^[a] Universität Wien, Fakultät für Chemie, Institut für Chemische Katalyse
Währinger Straße 38, 1090 Wien
<https://chemcat@univie.ac.at/>

* Corresponding author; email: kai.hultzsch@univie.ac.at

Manuscript submitted to *Eur. J. Org. Chem.* (submission date: 10.06.2021)

In this review various strategies for the multicomponent synthesis of *N*-containing heterocycles based on the borrowing hydrogen principle and on acceptorless dehydrogenative coupling reactions are described. The focus of this review lies on homogeneous abundant metal catalytic systems. Besides, selected examples of state-of-the-art noble metal catalysts are listed to allow a comparison between base and noble metal complexes.

As first author I conducted a strategic literature research and extracted the most important scientific facts. Moreover, the draft of the manuscript was prepared.

Borrowing Hydrogen and Acceptorless Dehydrogenative Coupling in the Multicomponent Synthesis of Heterocycles: A Comparison Between Base and Noble Metal Catalysis

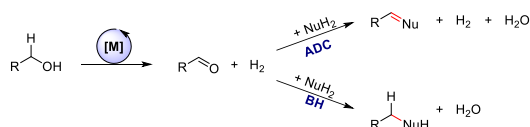
Natalie Hofmann,^[a] and Kai C. Hultsch^{*[a]}

[a] N. Hofmann, MSc., Univ.-Prof. Dr. K. C. Hultsch
University of Vienna, Faculty of Chemistry,
Institute of Chemical Catalysis
Währinger Straße 38, 1090 Wien (Austria)
E-mail: kai.hultsch@univie.ac.at

Abstract: Acceptorless dehydrogenative coupling reactions (ADC) and hydrogen transfer strategies (HT) provide a powerful tool in the multicomponent formation of *N*-heterocycles. A broad variety of complex products can be obtained starting from simple, cheap and commercially available reagents. The protocols are highly atom-efficient, as water, dihydrogen, or in some cases hydrogen peroxide, are the only by-products. Besides, in general neither further reducing or oxidizing agents, nor external hydrogen are required. Especially base metal-catalyzed strategies become ever more important. Therefore, in recent years, various different iron, cobalt, nickel and manganese catalysts have been developed. In this mini-review we want to highlight the progress that has been made using abundant metal complexes to promote multicomponent cyclizations for the formation of *N*-heterocycles and compare their capabilities with available noble metal catalyst systems.

1. Introduction

Nitrogen-containing heterocycles are indispensable substructures of a variety of important compounds which play an essential role in biological systems and processes. Therefore, they are used as fundamental building blocks for pharmaceuticals and industrially relevant basic and fine chemicals.^[1] Based on the strong demand for *N*-heterocycles and as part of increased efforts to implement processes following green chemistry guidelines, the development of sustainable, atom-efficient and waste-minimizing synthetic strategies plays an important role.^[2] A variety of acceptorless dehydrogenative coupling reactions and hydrogen transfer strategies for the formation of new carbon-carbon and carbon-heteroatom bonds within a cascade reaction leading to heteroatom containing products have been established in recent years (Scheme 1). These approaches are interesting in particular, since water, hydrogen, and in very few cases hydrogen peroxide, are generated as the only by-products.^[3]



Scheme 1. Differences between acceptorless dehydrogenative couplings (ADC) and the borrowing hydrogen strategy (BH).

Until recently the majority of studies focused on noble metal-based catalyst systems. However, catalyst systems based on abundant metals have received increasing attention in recent

years, in an effort to conserve scarce precious metal resources and in order to develop greener, more sustainable and more cost-effective processes (Figure 1).^[4]

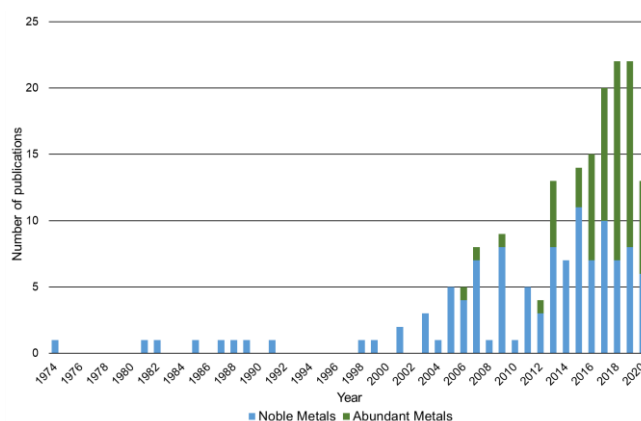


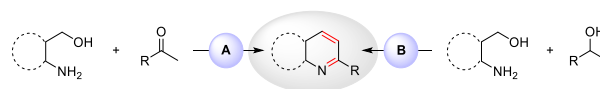
Figure 1. Number of publications on the formation of nitrogen-containing heterocycles through hydrogen transfer reactions and dehydrogenative couplings promoted by noble metal catalysts vs. abundant metal catalysts.

In this mini-review we want to give an overview on the reported homogeneous base metal catalyst systems which have been used for the synthesis of nitrogen-containing heterocycles in multicomponent acceptorless dehydrogenative coupling reactions and hydrogen transfer reactions. Some related dehydrogenative coupling reactions that make use of an external hydrogen acceptor are included as well. In addition, we will compare these strategies and results with state-of-the-art noble metal catalyst systems.

2. Synthesis of diverse heterocycles

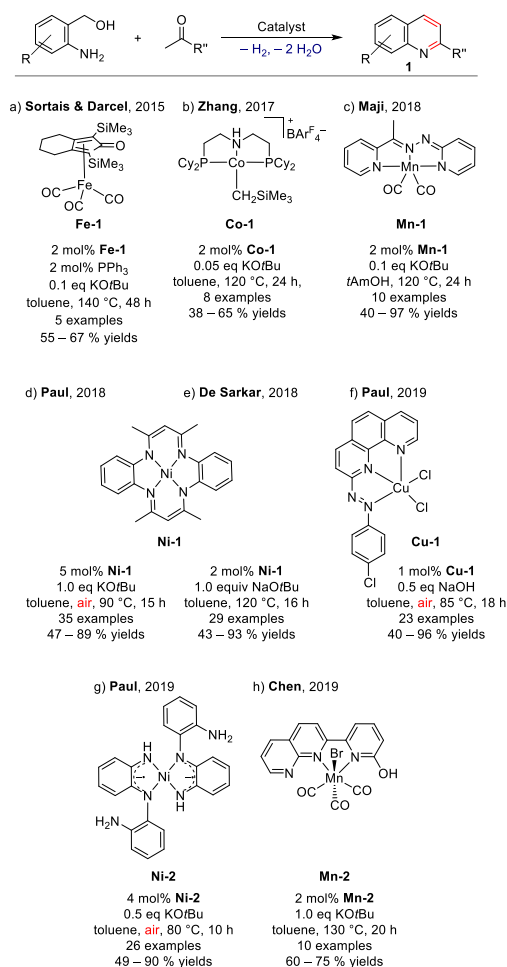
2.1. Quinolines

In general, quinolines can be synthesized through a mono dehydrogenative coupling of 2-aminobenzyl alcohols and ketones or via double dehydrogenative coupling using secondary alcohols and 2-aminobenzyl alcohols (Scheme 2).



Scheme 2. Mono and double dehydrogenative Friedlander-type annulation of ketones (A) or secondary alcohols (B) with 2-aminobenzyl alcohols.

The first base metal-catalyzed Friedländer annulation through coupling of ketones and 2-aminobenzyl alcohols was reported in 2015 utilizing the Knölker-type iron complex **Fe-1** in combination with catalytic amounts of KO^tBu (Scheme 3a).^[5] Applying the ionic cobalt-PNP complex **Co-1** in this reaction allowed to lower the reaction temperature and base loading (Scheme 3b).^[6] **Co-1** exhibited a broader substrate scope, successfully converting aliphatic and heterocyclic ketones. Non-methyl ketones (propiophenone and α -tetralone) were converted as well, although the conversion was significantly lower. Two catalysts based on manganese showed catalytic activity in this coupling reaction as well. The application of NNN-pincer ligated complex **Mn-1** led to higher yields compared to **Fe-1** and **Co-1** (Scheme 3c).^[7] The bidentate bipy-based manganese(I)-complex **Mn-2** (Scheme 3h) required a stoichiometric amount of base.^[8]

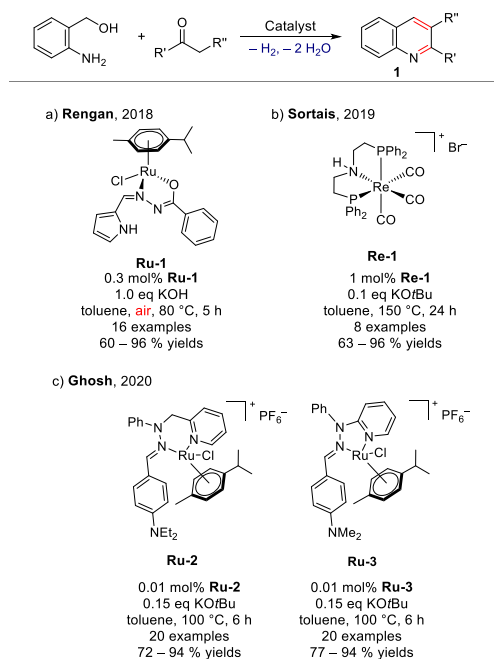


Scheme 3. Base metal-catalyzed mono dehydrogenative formation of quinolines.

The 2-hydroxy group and the uncoordinated *N*-heterocycle were crucial for the efficiency of this catalytic system. The nickel-based catalyst system **Ni-1**,^[9] featuring a tetraaza-macrocyclic ligand, was utilized in mono and double dehydrogenative coupling processes to form quinolines (Scheme 3d). The double dehydrogenative coupling strategy required higher catalyst and base loadings, as well as longer reaction times, to obtain the corresponding quinolines in satisfying yields. While the catalyst and base loading is on the higher end of the spectrum, the required reaction temperatures are significantly lower. Removal of H₂ from the reaction mixture is crucial for these type of coupling reactions whereas the presence of air is less detrimental to the reaction outcome. Therefore, reactions with **Ni-1** could be

conducted under atmospheric conditions in an open system. Shortly after, another report emerged studying both coupling reactions utilizing the same catalyst **Ni-1** in combination with NaO^tBu using a lower catalyst loading, but higher reaction temperatures (Scheme 3e).^[10] In contrast to the first report,^[9] the mono and the double dehydrogenative coupling were both performed using the same reaction conditions and the reactions were conducted under an argon atmosphere in a closed system.^[10] The diradical nickel(II)-catalyst **Ni-2**, featuring two antiferromagnetically coupled singlet diradical diamine-type ligands, were applied in the synthesis of quinolines (Scheme 3g), 2-aminoquinolines and quinazolines (see Section 2.3) *via* dehydrogenative coupling.^[11] Finally, the air-stable copper(II) complex **Cu-1**, containing a redox-active azo-aromatic scaffold, operates under relatively mild, aerobic conditions (Scheme 3f).^[12]

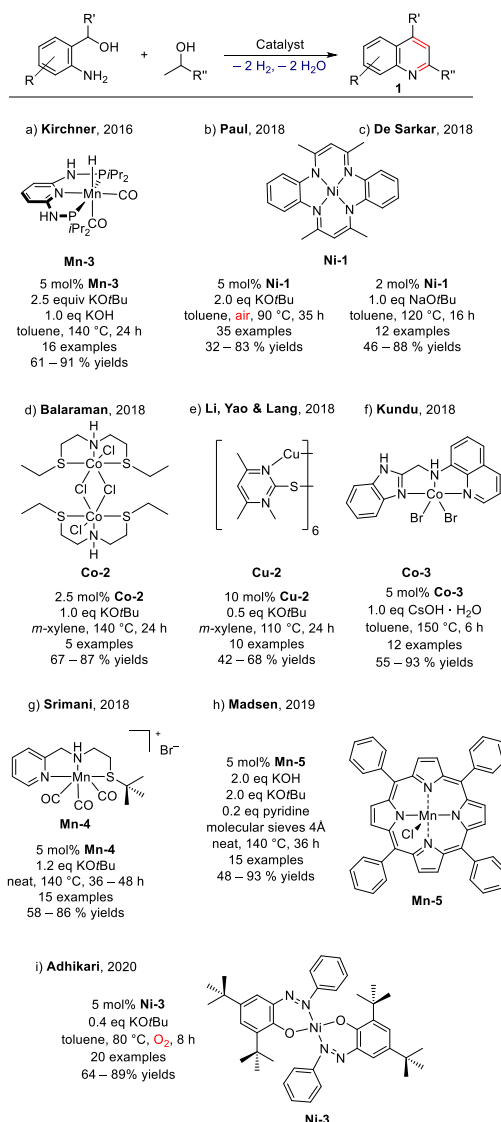
Compared to the noble metal catalysts which are used for the mono dehydrogenative cyclization of 2-aminobenzyl alcohols and ketones,^[13] base metal catalyst systems tend to require higher catalyst and base loadings, as well as higher reaction temperatures, in order to show similar efficiencies. The most active systems based on noble metals require low catalyst or base loadings and they are based on the arene ruthenium(II) benzhydrazone complex **Ru-1**,^[13j] the PN(H)P-rhenium complex **Re-1**^[13m] and two recently reported piano-stool ruthenium complexes (**Ru-2**, **Ru-3**)^[13n] (Scheme 4). Interestingly, most of the noble metal-based catalyst systems require a H₂-acceptor, such as benzophenone, for the mono dehydrogenative coupling or utilize the ketone in large excess^[13a, 13b, 13e-g, 13i, 13j], whereas the abundant metal-based systems generally only require a slight excess of the ketone.



Scheme 4. State-of-the-art noble metal catalyst systems for the mono dehydrogenative formation of quinolines.

The first report on the abundant metal-promoted double dehydrogenative coupling of 2-aminobenzyl alcohols and secondary alcohols was reported by Kirchner and co-workers (Scheme 5a).^[14] The application of the PNP-manganese(I) hydride complex **Mn-3** allowed the synthesis of various quinolines starting from substituted benzylic, cyclic aliphatic and heterocyclic alcohols. However, a major drawback of this system was the large

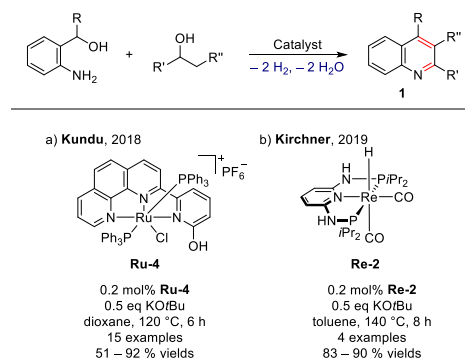
amount of base which was required in order to obtain decent conversions and its limitation to 2-aminobenzhydrols as substrates. Subsequently, the dimeric, sulfur-based and phosphine-free SNS-cobalt(II) pincer catalyst **Co-2** (Scheme 5d) was reported to exhibit high activity in the reaction with linear aliphatic secondary alcohols.^[15] Besides, this catalyst was further employed in the cyclization of unprotected aminoalcohols and secondary alcohols to obtain pyridine (see Section 2.5) and pyrrole derivatives (see Section 2.12). The reaction was also facilitated with the copper(I) *N*-heterocycle thiolate cluster **Cu-2** (Scheme 5e).^[16] The base loading was low in comparison to the other reported systems; however, the catalyst loading was relatively high (10 mol% based on Cu atoms) in comparison to all other systems and the yields were generally moderate. The NNN-cobalt(II) pincer complex **Co-3** was applied as catalyst in combination with CsOH · H₂O in the synthesis of quinolines (Scheme 5f), 2-alkylaminoquinolines (see Section 2.3) and quinoxalines (see Section 2.6), but the system required rather harsh reaction temperatures (150 °C).^[17] The catalyst system tolerated benzylic secondary alcohols containing various electron-donating or electron-withdrawing groups and heterocycles. However, the sole example using an aliphatic secondary alcohol led to a lower conversion.



Scheme 5. Base metal-catalyzed double dehydrogenative coupling in the formation of quinolines.

The less air and moisture sensitive phosphine-free NNS-manganese(I) complex **Mn-4** (Scheme 5g)^[18] was reported to require significantly lower base loading compared to the two other manganese-based systems.^[14, 19] **Mn-4** was able to convert the more challenging aliphatic alcohols, although longer reaction times (48 h) were required to obtain decent yields. While most manganese-based catalyst systems utilize Mn(I), the porphyrin Mn(III) chloride complex **Mn-5** was recently reported to promote the dehydrogenative synthesis of quinolines (Scheme 5h).^[19] The air-stable, phosphine-free nickel complex **Ni-3** allowed this formation using milder reaction conditions, though an oxygen atmosphere was required (Scheme 5i). Mechanistic studies revealed that the oxygen is required for regeneration of the catalyst *via* aerobic oxidation, producing hydrogen peroxide as by-product.^[20]

Precious metal catalyst systems generally require lower catalyst loadings (0.2 mol% – 2.0 mol%) and base loadings (0.1 equiv – 2.0 equiv)^[13f, 13l, 13m, 21] for this particular reaction in comparison to abundant metal systems. The systems requiring the lowest catalyst loading (0.2 mol%) in combination with a low base loading (50 mol%) are on the one hand NNN-ruthenium(II) pincer-complex **Ru-4** (Scheme 6a)^[21e] and on the other hand the PNP-rhenium(I) hydride complex **Re-2**.^[21g] However, **Re-2** was only applied in the dehydrogenative coupling of 2-aminobenzhydrol instead of 2-aminobenzyl alcohol (Scheme 6b).



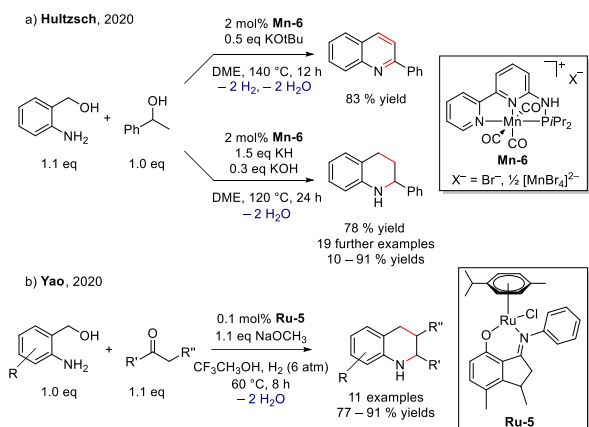
Scheme 6. State-of-the-art precious metal catalyst systems for the double dehydrogenative formation of quinolines.

2.2. 1,2,3,4-Tetrahydroquinolines and 1,2,3,4-Tetrahydronaphthyrindines

Compared to the synthesis of quinolines, the reports on the formation of 1,2,3,4-tetrahydroquinolines are scarce. Recently, the first method for the synthesis of the latter, based on the borrowing hydrogen methodology, was published. An earth-abundant PN³-manganese(I) pincer complex (**Mn-6**) was used to promote the reaction sequence.^[22] Both, quinolines and 1,2,3,4-tetrahydroquinolines could be selectively synthesized thanks to a targeted choice of base (Scheme 7a). The combination of two distinct bases (KH and KOH) was crucial for the completion of the borrowing hydrogen cycle and, thus, the synthesis of the reduced tetrahydroquinolines in good yields. Moreover, this catalytic system allowed the synthesis of 1,2,3,4-tetrahydronaphthyrindines through cyclization of 2-aminopyridyl methanols and secondary alcohols. In accordance to a previously reported ruthenium system,^[23] the transfer hydrogenation mainly occurs at the pre-existing pyridyl ring. While outside the scope of this review, it should be mentioned that the synthesis of tetrahydroquinolines starting from 2-aminobenzyl alcohols and a primary alcohol has

been achieved using a heterogeneous nickel-catalyst, but the system was limited to primary alcohols.^[24]

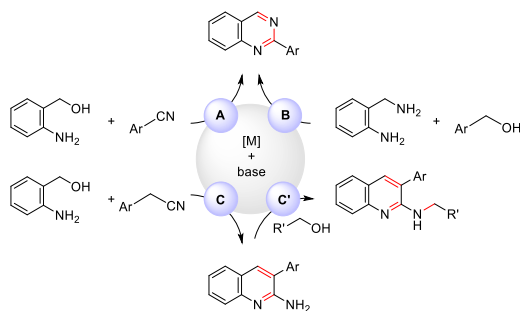
Another approach to synthesize 1,2,3,4-tetrahydroquinolines was pursued with the N,O-chelate half-sandwich ruthenium complex **Ru-5** starting from 2-aminobenzyl alcohols and ketones.^[25] The cyclization to form the corresponding quinoline and its hydrogenation were combined to a one-pot synthesis. Thus, usage of hydrogen pressure, low catalyst loading (0.1 mol%) and a stoichiometric amount of base produced the desired 1,2,3,4-tetrahydroquinolines in good yields. (Scheme 7b).



Scheme 7. Catalytic approaches to 1,2,3,4-tetrahydroquinolines.

2.3. 2-Aminoquinolines and Quinazolines

Different strategies have been developed over the last decade for the biomimetic syntheses of 2-aminoquinolines and quinazolines promoted by base^[11, 17, 26] and noble^[13m, 21e, 27] metal catalysts utilizing hydrogen transfer methodologies (Scheme 8).

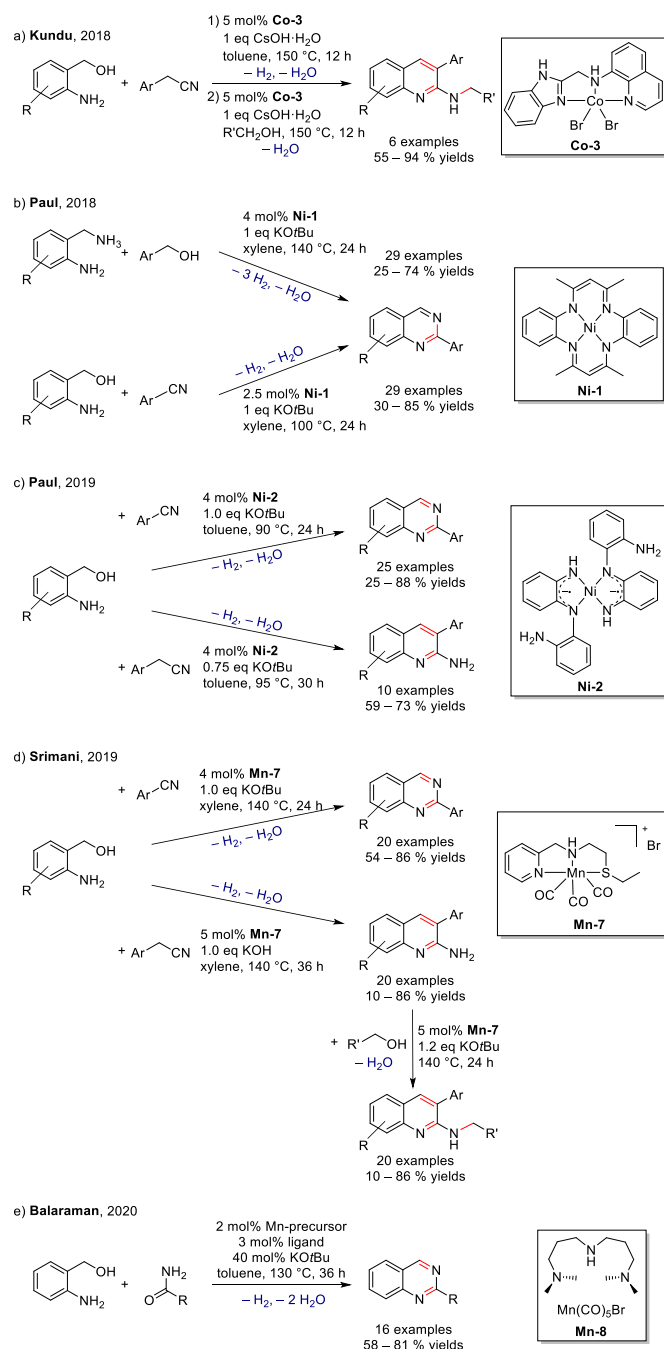


Scheme 8. Selected synthetic strategies for the formation of 2-aminoquinolines and quinazolines based on transfer hydrogenation processes.

The synthesis of quinazolines has been reported for nickel- and manganese-based catalyst systems (Scheme 9). The tetraaza-macrocyclic complex **Ni-1** catalyzed two pathways. On the one hand, the coupling of 2-aminobenzylamine with benzyl alcohol and on the other hand the coupling of 2-aminobenzyl alcohol with benzonitrile (Scheme 9b).^[26a] The singlet diradical nickel(II) catalyst **Ni-2** was not only able to promote the synthesis of quinolines (see Section 2.1) and quinazolines, but also the formation of 2-aminoquinolines (Scheme 9c).^[11] The NNS-ligated manganese(I) complex **Mn-7** catalyzed the synthesis of benzimidazoles, benzothiazoles (see Section 2.13), quinazolines and 2-(alkylamino)quinolines (Scheme 9d).^[26b] The latter are obtained *via* a one-pot, two-step procedure; however, the *N*-alkylation step required additional catalyst and base. A similar

approach was reported utilizing the NNN-cobalt(II) pincer complex **Co-3** (Scheme 9a).^[17] A different strategy to form quinazolines was pursued with manganese catalyst system **Mn-8**, which was prepared *in situ* from commercially available $\text{Mn}(\text{CO})_5\text{Br}$ and an aliphatic NNN ligand. It promoted the dehydrogenative annulation of 2-aminobenzyl alcohol and primary amides (Scheme 9e). A broad functional group tolerance was observed, though, benzamides with strong electron-withdrawing groups were unreactive.^[28]

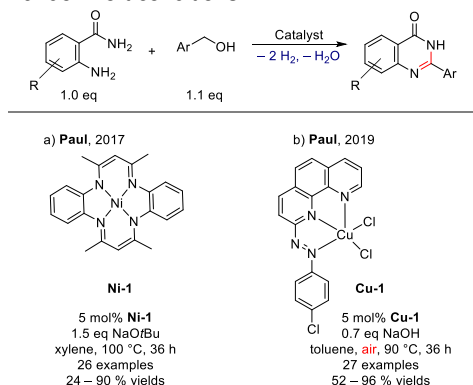
Ruthenium-based catalyst systems are superior for this cascade reaction,^[21e, 27c] as significant lower catalyst loadings (1 – 3 mol%) suffice and the second reaction step (*N*-alkylation) does not require supplementary catalyst or base.



Scheme 9. Overview and comparison of abundant metal-based processes for the synthesis of 2-aminoquinolines and quinazolines.

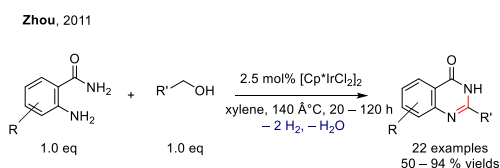
2.4. Quinazolinone

Dehydrogenative condensation reactions for the formation of quinazolinones have made significant progress in the past ten years using both, precious^[29] and base^[12, 30] metal catalyst systems. The coupling of 2-aminobenzamides with alcohols was reported with two earth-abundant metal complexes. The tetraaza-macrocyclic nickel(II) complex **Ni-1** generally promoted the reaction under inert conditions (Scheme 10a)^[30b] without addition of a hydrogen acceptor, but the application of styrene increased the yield by 12 – 23 %. The air-stable copper(II) complex **Cu-1** catalyzed the reaction under atmospheric conditions, whereby H₂O₂ is generated as by-product instead of H₂ (Scheme 10b).^[12] It should be noted that no reaction was observed in the absence of oxygen under inert conditions.



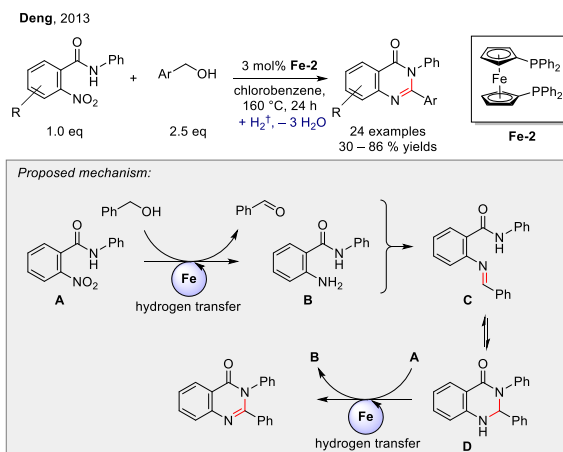
Scheme 10. Abundant metal-catalyzed strategies for the dehydrogenative quinazolinone formation.

Among the precious metal catalysts, only the iridium-based catalyst system [Cp*IrCl₂]₂^[29a] provided significant advantages compared to the discussed base metal catalyst systems. A moderate low catalyst loading of 2.5 mol% of [Cp*IrCl₂]₂ led to good yields of the corresponding quinazolinones and no additional base was required (Scheme 11). Moreover, the more challenging alcohols with extended carbon chains were converted successfully using prolonged reaction times. However, a higher reaction temperature (140 °C) was required and styrene was added as H₂-acceptor to convert electron-rich alcohols.



Scheme 11. Iridium-catalyzed dehydrogenative quinazolinone formation.

Another approach is the redox neutral synthesis of 2,3-diarylquinazolines starting from 2-nitro-*N*-arylbenzamides and benzylic alcohols. The commercially available iron complex 1,1'-bis(diphenylphosphino)ferrocene (**Fe-2**) showed high reactivity to promote this reaction without any external oxidant or reductant (Scheme 12).^[30a]



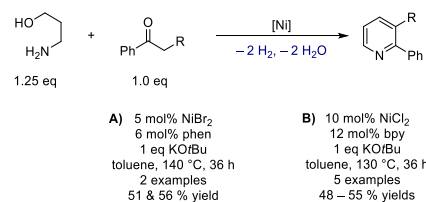
Scheme 12. Iron-catalyzed 2,3-diarylquinazolinone formation. [†] The added hydrogen equivalent stems from the excess of benzylic alcohol added to the reaction mixture.

The hydrogen generated through oxidation of the primary alcohol and intermediate D acted as reducing agent for the nitro group. However, the precise role of the 18 valence electron ferrocene derivative **Fe-2** in the hydrogen transfer process is unclear.

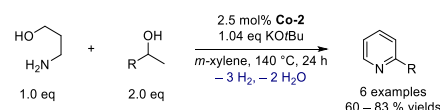
2.5. Pyridines

Pyridines can be synthesized in a similar manner compared to quinolines. However, the cyclization of secondary alcohols with γ -aminoalcohols without aromatic backbone is rarely reported for base metal catalyst systems.

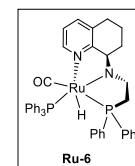
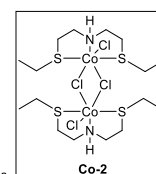
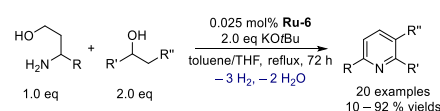
a) Banerjee, 2018



b) Balaraman, 2018



c) Liu & Sun, 2016



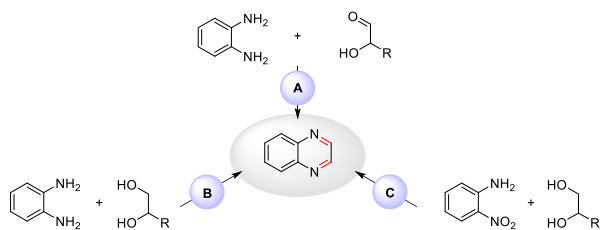
Scheme 13. State-of-the-art noble metal catalyzed pyridine synthesis compared with published base metal catalyst systems.

A bipyridine-^[31] and a phenanthroline-based^[32] nickel catalyst system were applied in the double dehydrogenative cyclization of 3-amino-1-propanol with ketones, providing the corresponding pyridines in moderate yields, whereby the bipyridine-based system required the double amount of catalyst (Scheme 13a). The application of these catalyst systems and reaction conditions using 2-amino-1-propanol instead of 3-amino-1-propanol led to the formation of quinolines as well. The dimeric sulfur-based and phosphine-free SNS-cobalt(II) pincer complex **Co-2** promoted the double dehydrogenative coupling to form the corresponding

pyridines in good yields (Scheme 13b).^[15] As noted for the quinoline syntheses, catalyst loadings are significantly lower (0.2 – 1.0 mol%) when using noble metal catalysts.^[21b, 21h, 33] The PNN-tridentate ruthenium complex **Ru-6** stands out with a low catalyst loading of only 0.025 mol% (Scheme 13c).^[33b] However, the necessity to use 2 equivalents of base represents a significant drawback compared to other noble metal-based catalyst systems.

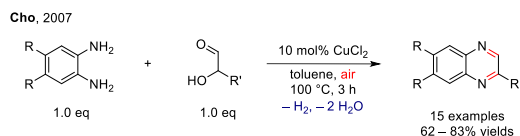
2.6. Quinoxalines

Three strategies for the formation of quinoxalines have been reported. The mono dehydrogenative coupling of 2-phenylenediamines with α -hydroxyketones (Scheme 14, **A**), the double dehydrogenative coupling of 2-phenylenediamines with 1,2-diols (**B**) and the redox neutral reaction of 2-nitroanilines with 1,2-diols (**C**).



Scheme 14. Three different pathways for the synthesis of quinoxalines.

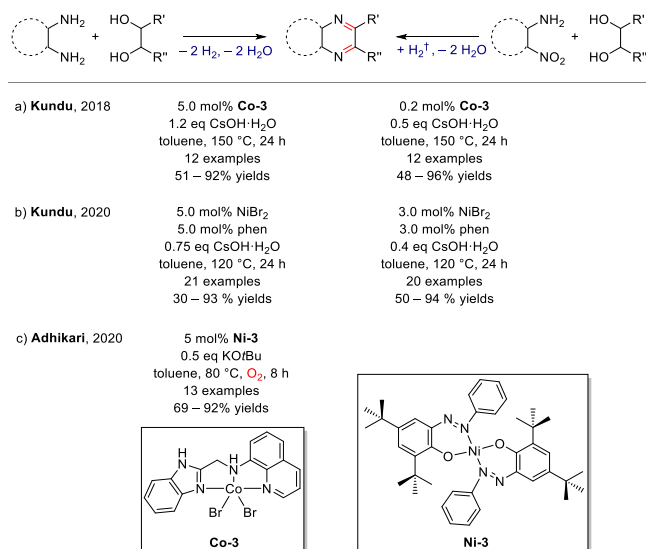
In 2007 Cho reported an oxidative cyclization in the presence of a copper catalyst to synthesize quinoxalines from 2-phenylenediamines and α -hydroxyketones (Scheme 15).^[34] The reaction could be performed either in air or under argon, although the latter conditions led to a significant drop in yield from 94 % to 55 %. Interestingly, no base was applied for catalyst activation; on the contrary, the application of KOH decreased the yield significantly. This observation stands in contrast to results obtained with the ruthenium-based system $\text{RuCl}_2(\text{PPh}_3)_3$, which was applied to promote the formation of quinoxalines starting from 2-phenylenediamines and vicinal diols.^[35]



Scheme 15. Oxidative cyclization of 2-phenylenediamines and α -hydroxyketones to form quinoxalines.

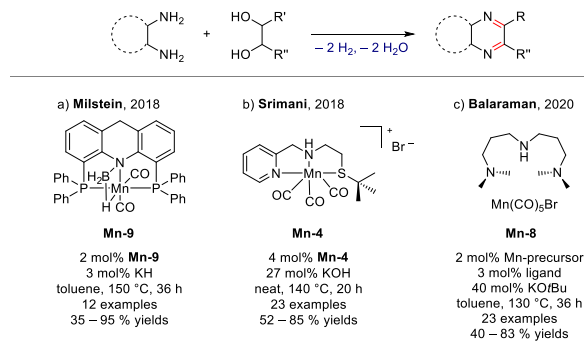
Some examples for the acceptorless dehydrogenative coupling of 2-phenylenediamines and vicinal diols were reported with abundant metals as well.^[17, 18, 36] The NNN-cobalt(II) pincer complex **Co-3** was found to be active in the formation of quinoxalines starting from vicinal diols and 2-phenylenediamines (Scheme 16a).^[17] A large excess of diol (5 equivalents) was required in order to obtain the quinoxaline in satisfying yield. For the redox neutral synthesis of quinoxalines from vicinal diols and 2-nitroanilines the required catalyst and base loadings were significantly lower and the excess of diol was lowered to 3 equivalents. The nitro group served as hydrogen acceptor, while the alcohols acted as hydrogen donor. The catalyst loading was even lower compared to a dppp-ruthenium(II) catalyst system (1 mol%).^[37] A phenanthroline nickel catalyst system that was recently reported for its high reactivity in the synthesis of pyridines (see Section 2.5) and pyrrolidines (see Section 2.12) was applied

to these two reactions as well (Scheme 16b).^[38] Particular noteworthy is that heterogeneous Ni-particles were detected during the catalytic reaction and were characterized by PXRD, XPS, and TEM techniques. The air-stable, phosphine-free nickel complex **Ni-3**, which was reported for the formation of quinolines under aerobic conditions (see Section 2.1), was shown to be active to promote the reaction of diols and diamines to quinoxalines as well (Scheme 16c).^[20] A slightly higher amount of base was required compared to the synthesis of quinolines in order to obtain decent yields.



Scheme 16. Quinoxaline synthesis starting from vicinal diols and 2-phenylenediamines or nitroanilines. † The added hydrogen equivalent stems from the excess of diol added to the reaction mixture.

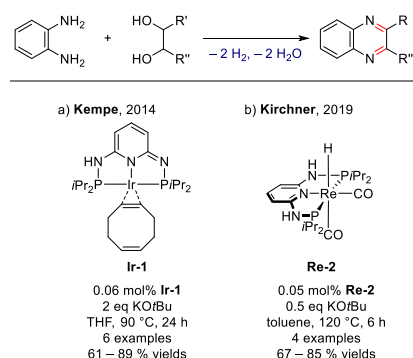
Three manganese-based catalyst systems have been reported for the double dehydrogenative synthesis of quinoxalines. The acridine-based pincer system **Mn-9** only required a catalytic amount of base (Scheme 17a).^[36] However, it should be noted that only long-chain vicinal diols can be converted under these conditions, whereas short-chain diols require a stoichiometric amount of base. The phosphine-free NNS-manganese(II) complex **Mn-4** is less air and moisture sensitive, but required higher catalyst and base loading (Scheme 17b).^[18] Manganese catalyst system **Mn-8** could not only be used for the synthesis of quinazolines (Section 2.3), but it also promoted the synthesis of quinoxalines, showing a broad functional group tolerance (Scheme 17c).^[28]



Scheme 17. Manganese-catalyzed formation of quinoxalines.

Various noble metal catalyst systems are known for the formation of quinoxalines.^[21b, 35, 37, 39] Thereof, two catalyst systems with low catalyst loading stand out. The PNP-iridium complex **Ir-1** required a stoichiometric amount of base (Scheme 18a),^[39a] whereas the

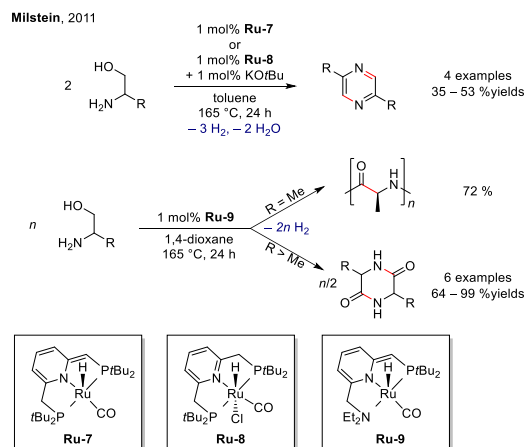
PNP-rhenium(I) hydride complex **Re-2** combined low catalyst loading and a substoichiometric amount of base (Scheme 18b).^[219]



Scheme 18. Iridium- and rhenium-promoted formation of quinoxalines.

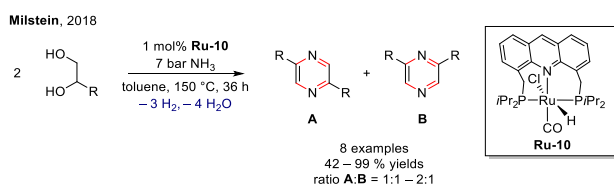
2.7. Pyrazines

Reports on the synthesis of pyrazines based on the borrowing hydrogen principle are limited in general. In 2011, Milstein reported the first self-coupling of 2-aminoalcohols to form 2,5-disubstituted symmetrical pyrazines catalyzed by the PNP-ruthenium pincer complex **Ru-7** without the addition of base or **Ru-8** in combination with a catalytic amount of base.^[40] Cyclic dipeptides were formed by using the NNP-ruthenium pincer complex **Ru-9** (Scheme 19). Interestingly, a methyl-group in α -position to the amine group (alaninol) did not lead to the formation of the corresponding cyclic dipeptide, but to poly(alanine), whereas all larger substituents led selectively to the cyclic dipeptide.



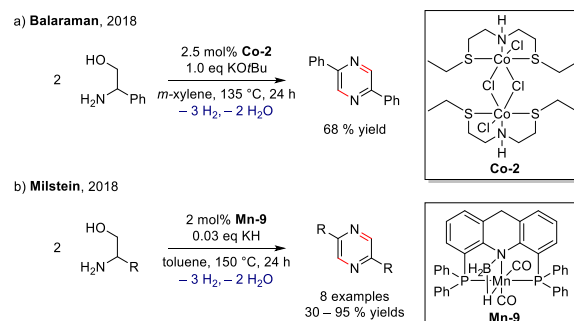
Scheme 19. Self-coupling of 2-aminoalcohols promoted by ruthenium pincer complexes.

In 2018 mixtures of 2,5- and 2,6-substituted pyrazines were synthesized from 1,2-diols using ammonia as nitrogen source promoted by the acridine-based ruthenium pincer complex **Ru-10** (Scheme 20).^[41] In a similar manner pyrroles were formed as well.



Scheme 20. Synthesis of pyrazines starting from 1,2-diols and ammonia.

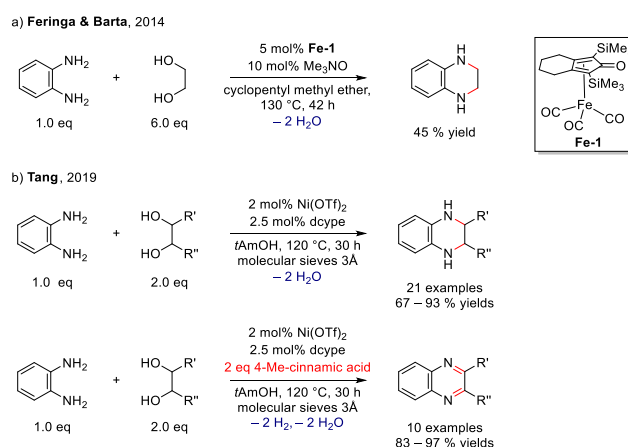
The SNS-cobalt(II) pincer complex **Co-2** was found to be active for the acceptorless self-condensation of 2-amino-2-phenylethan-1-ol using equimolar amounts of base. (Scheme 21a).^[15] The first earth-abundant metal-promoted self-coupling of 2-aminoalcohols with a catalytic amount of base (KH) was reported using the acridine-based manganese pincer complex **Mn-9** (Scheme 21b).^[36]



Scheme 21. Base metal-promoted synthesis of pyrazines.

2.8. 1,2,3,4-Tetrahydroquinoxalines

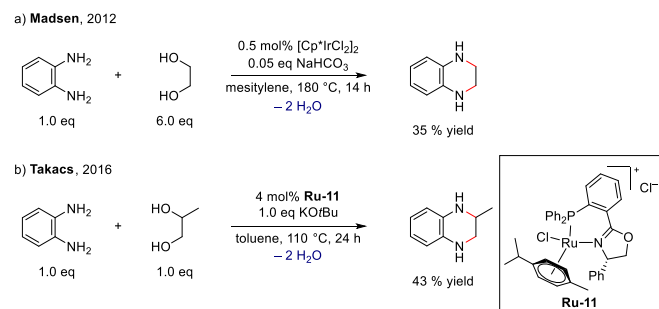
Compared to quinoxalines, there are only few examples for the synthesis of their hydrogenated derivatives based on the borrowing hydrogen strategy. In 2014 Feringa and Barta published the first example for the synthesis of 1,2,3,4-tetrahydroquinoxalines.^[42] They applied the iron-based Knölker complex **Fe-1**, which was activated with trimethylamine *N*-oxide, to promote the double alkylation of 1,2-benzenediamine with ethylene glycol and obtained 45 % of the corresponding cyclization product. No base was required, though a large excess of the vicinal diol was used (Scheme 22a). The application of nickel triflate/1,2-bis(dicyclohexylphosphino)ethane (dcype) allowed a base-free cyclocondensation (Scheme 22b).^[43] A broader substrate screening proved the applicability of the catalyst system. The aromatic quinoxaline could be obtained selectively by introducing 4-methylcinnamic acid to capture the Ni-H species.



Scheme 22. Base metal-catalyzed formation of 1,2,3,4-tetrahydroquinoxalines and quinoxalines based on the borrowing hydrogen strategy.

The number of reports with noble metal catalysts for this type of reaction is small as well, mainly the synthesis of the corresponding piperazines (see Section 2.9.) and decahydroquinolines was reported.^[44] Only the dimeric iridium complex [Cp*IrCl₂]₂^[44c] and the air-stable **Ru-11**^[44d] were reported

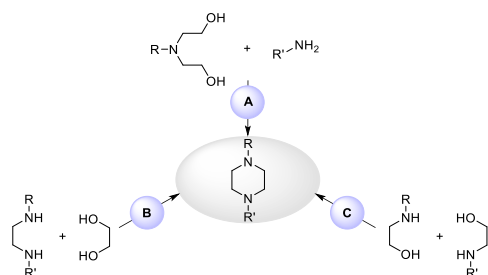
to promote the synthesis of 1,2,3,4-tetrahydroquinoxalines in moderate yields. Both systems required additional base, the ruthenium-based system even stoichiometric amounts (Scheme 23).



Scheme 23. Noble metal-catalyzed formation of 1,2,3,4-tetrahydroquinoxalines via borrowing hydrogen methodology.

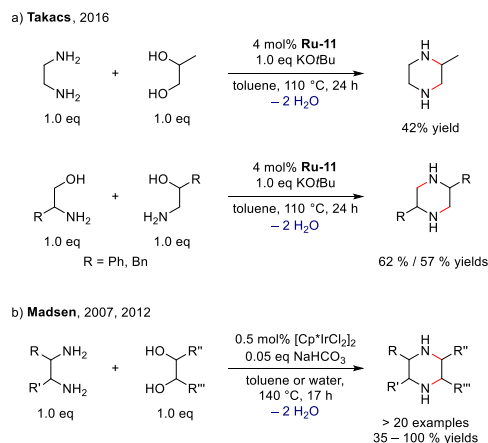
2.9. Piperazines

The borrowing hydrogen strategy provides three pathways for the synthesis of piperazines (Scheme 24). So far solely noble metal catalyst systems have been reported to promote these reactions,^[44, 45] some of them will be mentioned briefly.



Scheme 24. Three pathways for the synthesis of piperidines and its derivatives.

The pioneering work was published by Watanabe in 1985, in which 1,5-diols and primary amines were converted into *N*-arylated or *N*-alkylated piperazines using catalytic amounts of ruthenium catalysts ($\text{RuCl}_2(\text{PPh}_3)_3$ or $\text{RuCl}_3 \cdot \text{H}_2\text{O}$).^[45a] The first synthesis of piperazines by cyclocondensation of 1,2-diamines and 1,2-diols was achieved by applying the ruthenium-based catalyst $\text{Ru}_3(\text{CO})_{12}/\text{PBU}_3$.^[44a]

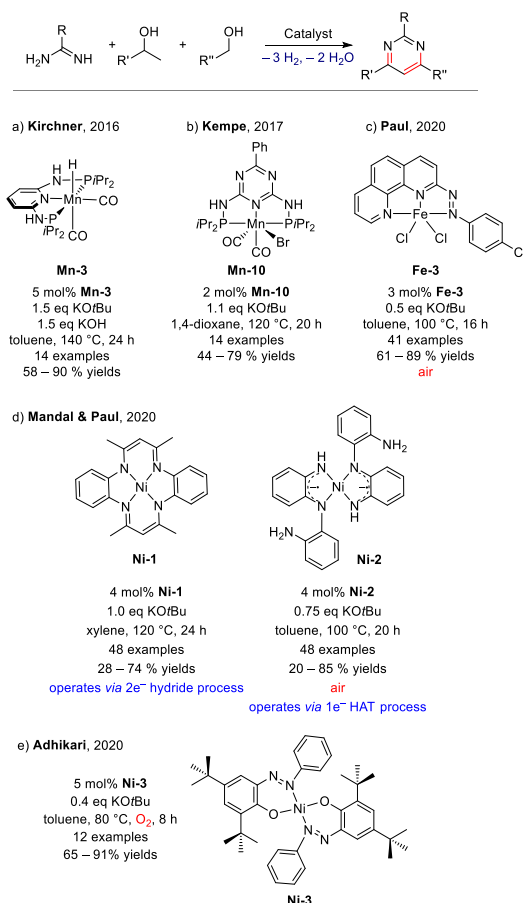


Scheme 25. Noble metal-promoted synthesis of piperazines.

The ruthenium phosphinooxazoline complex **Ru-11** was not only used for the cross-coupling of diols and diamines, but also for the cyclodimerization of ethanolamine derivatives (Scheme 25a).^[44d] Significantly higher yields in the cyclisation of 1,2-diamines and 1,2-diols were obtained using $[\text{Cp}^*\text{IrCl}_2]_2$ as catalyst in combination with a catalytic amount of base (Scheme 25b).^[44b, 44c]

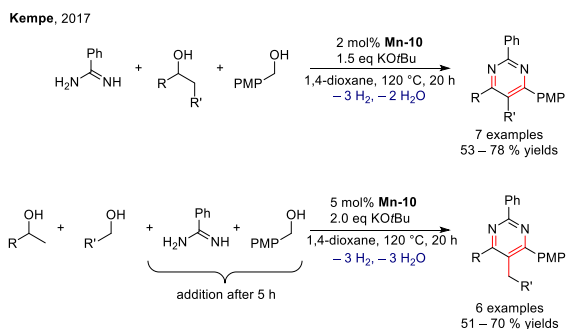
2.10. Pyrimidines

In 2016 Kirchner and coworkers established the first base metal-promoted synthesis of trisubstituted pyrimidines via three component condensation of benzamidine with two alcohols using PNP-manganese(I) hydride complex **Mn-3** (Scheme 26a).^[14]



Scheme 26. Base metal-catalyzed three component condensation for the synthesis of pyrimidines.

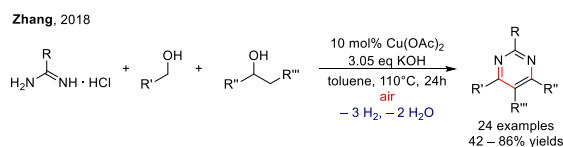
The PNP -manganese(I) pincer complex **Mn-10** promoted this reaction with lower catalyst and base loading and at a lower reaction temperature (Scheme 26b).^[46] Besides, tetra-substituted pyrimidines were synthesized through either a one-pot one-step three component reaction or a consecutive one-pot four component cyclization (Scheme 27). The air-stable iron complex **Fe-3** promoted the multicomponent dehydrogenative functionalization of alcohols to form 2,4,6-trisubstituted pyrimidines (Scheme 26c).^[47] The $\text{Fe}(\text{II})$ -complex, featuring a redox non-innocent 2-phenylazo-(1,10-phenanthroline) ligand enabled the synthesis at moderate reaction temperatures with a substoichiometric amount of base in air.



Scheme 27. Synthesis of tetra-substituted pyrimidines *via* three or four component reaction.

Recently a comparative study of nickel-catalyzed dehydrogenative formation of pyrimidines was reported (Scheme 26d).^[48] The two catalyst systems are operating in two different pathways. **Ni-1** catalyzes the reaction *via* a two-electron hydride transfer process under inert conditions requiring harsher reaction conditions, whereas the generally more active **Ni-2** operates *via* a one-electron hydrogen atom transfer (HAT) pathway in air. The air-stable **Ni-3**, with an azo motif in the ligand backbone, promoted the dehydrogenative annulation under oxygen atmosphere as well through a HAT-based oxidation mechanism (Scheme 26e).^[49] Moreover, triazines could be synthesized by coupling primary alcohols and 4-methylbenzimidazole using the same reaction conditions.

Various copper salts, such as CuBr₂, CuCl₂, CuI, CuO and Cu(OAc)₂, were screened on their catalytic activity for the pyrimidine formation based on the borrowing hydrogen principle.^[50] Cu(OAc)₂ was found to be a simple and air-stable catalyst which was capable to perform the reaction in air (Scheme 28). However, catalyst and base loadings were significantly higher compared to other published systems.



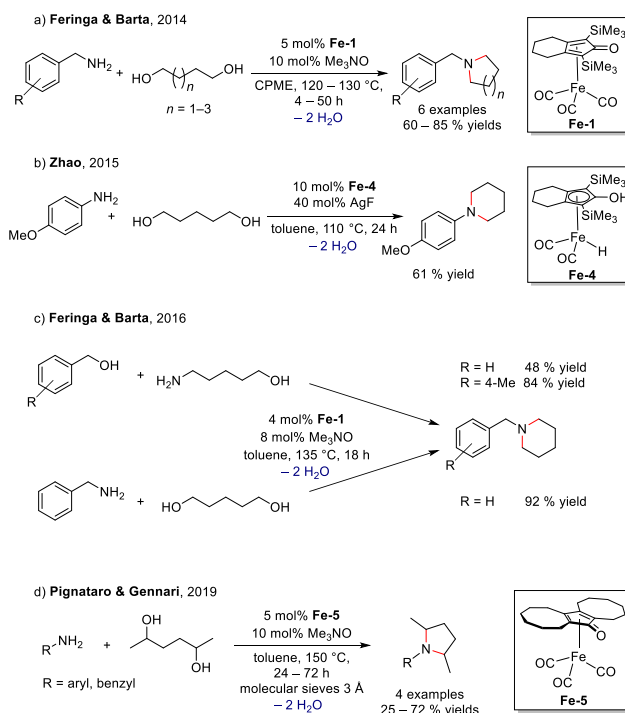
Scheme 28. Synthesis of pyrimidines *via* condensation of amidine hydrochloride and alcohols promoted by a copper salt.

Precious metal based catalysts should also be taken into account. For example the application of a PN₅P-iridium complex,^[51] rhenium-pincer complex **Re-2**,^[21g] or a 2-(2-benzimidazolyl)-pyridine ligated ruthenium complex^[52] allowed the synthesis of pyrimidines. They did not only require a significantly lower catalyst loading of 1 mol%, but also smaller amounts of base (0.5 – 0.75 equiv). However, the nonprecious metal catalysts are less expensive and three examples also provide the huge advantage of being stable in air, thus avoiding the necessity to operate under inert conditions.

2.11. Pyrrolidines, Piperidines and derivatives

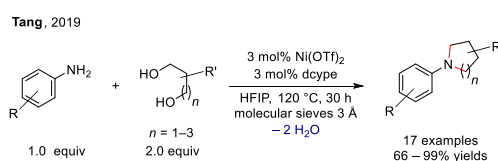
The first reports on the synthesis of pyrrolidines and piperidines *via* cyclization of diols with amines date back to the 1980's, when noble metal catalysts were used under forcing reaction conditions.^[45a, 53] Over the years more and more catalyst systems based on precious metals were published^[44d, 45b, 54] and within the last decade abundant metal complexes became more and more

present. Various publications state the ability of iron cyclopentadienone catalysts to promote the cyclization of diols with amines, leading to pyrrolidines, piperazines and derivatives of larger ring size. Six different piperidines were synthesized with the well-known Knölker complex **Fe-1** after activation with trimethylamine *N*-oxide, (Scheme 29a).^[42] The double alkylation was only observed for benzylamines featuring electron withdrawing groups, whereas benzylamine itself only led to a conversion of 50%, yielding a mixture of mono- and double alkylation product. Subsequently two synthetic routes for the intermolecular formation of *N*-benzylpiperidines promoted by **Fe-1** were established (Scheme 29c).^[55] A single example for the synthesis of 1-(4-methoxyphenyl)piperidine was reported by activating a derivative of the Knölker complex **Fe-4** with AgF (Scheme 29b).^[56] Application of the further modified **Fe-5** allowed the first reaction of anilines or benzylamines with secondary 1,4-diols to form substituted pyrrolidines (Scheme 29d).^[57]



Scheme 29. Application of (cyclopentadienone)iron complexes for the formation of pyrrolidines, piperidines and derivatives.

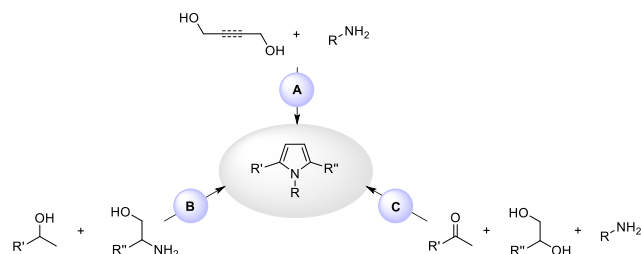
A detailed investigation of the cyclization of diols with arylamines was conducted using a catalyst system derived from nickel triflate and 1,2-bis(dicyclohexylphosphine)ethane (dcype) (Scheme 30).^[43] The reaction required the more acidic 1,1,1,3,3,3-hexafluoroisopropanol (HFIP) as solvent. The optimized reaction conditions can be applied for the synthesis of several piperidines, pyridines and some larger heterocycles. This system was highly active for the synthesis of 1,2,3,4-tetrahydroquinoxalines as well (see Section 2.8).



Scheme 30. Nickel-promoted cyclization of diols with arylamines to form pyrrolidines, piperidines and derivatives.

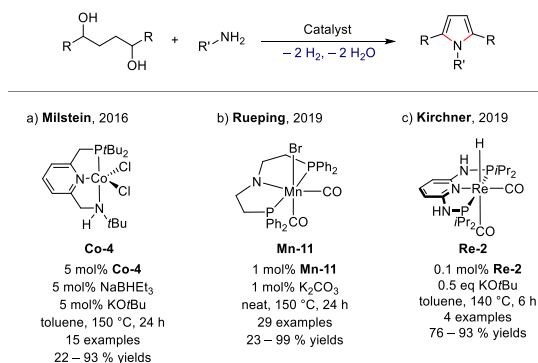
2.12. Pyrroles

There are different pathways to synthesize pyrroles based on the borrowing hydrogen concept (Scheme 31). The cyclization of primary amines and unsaturated or saturated diols, the reaction of secondary alcohols and 2-aminoalcohols or a three-component condensation of ketones with primary amines and 1,2-diols can lead to pyrroles.



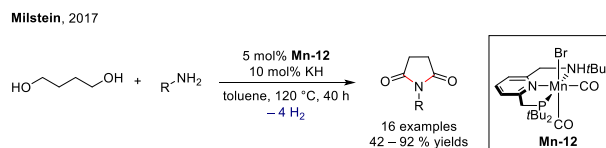
Scheme 31. Strategies for the synthesis of pyrroles following the borrowing hydrogen concept.

The number of examples for the selective synthesis of *N*-substituted pyrroles starting from readily available diols and simple anilines is scarce. In 2011 the research group around Crabtree reported the first dehydrogenative Paal-Knorr synthesis to form pyrroles by a ruthenium diphosphine diamine complex.^[58] The reaction was performed under a constant flow of nitrogen to facilitate the dehydrogenative process. The first base metal-promoted dehydrogenative coupling of diols and amines to form *N*-substituted pyrroles was achieved by using the cobalt(II) pincer complex **Co-4** (Scheme 32a).^[59] The combination of NaBHET₃ as activator and a catalytic amount of base (KO^tBu) allowed the synthesis of various pyrroles in moderate to good yields. Lower catalyst and base loadings were achieved and the substrate scope was broadened when the PNP-manganese(I) pincer complex **Mn-11** was employed (Scheme 32b).^[60] Particularly noteworthy is the successful conversion of the primary diol 1,4-butanediol to the corresponding pyrroles in good yields, for which the cobalt-system **Co-4** only obtained moderate yields and unidentified by-products. The precious metal PNP-rhenium(I) complex **Re-2** promoted the dehydrogenation reaction to form pyrroles as well (Scheme 32c).^[219] The catalyst loading (0.1 mol%) is significantly lower compared to the two base metal systems; however, the base loading (0.5 equiv) is higher and only the secondary diol 2,4-hexanol was applied as substrate.



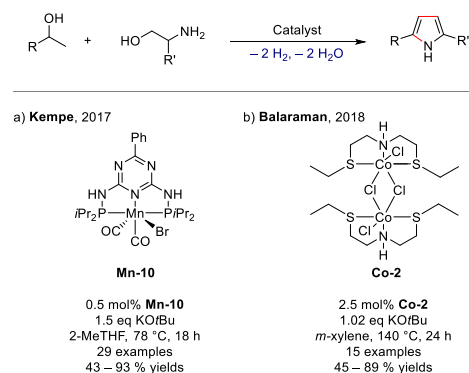
Scheme 32. Comparison of the state-of-the-art abundant and precious metal-promoted dehydrogenative coupling of diols and amines to form *N*-substituted pyrroles.

It should be taken into account that the same starting materials can undergo a dehydrogenative coupling leading to the corresponding cyclic imides.^[61] For instance, the PNN-manganese(I) pincer complex **Mn-12** exhibited high activity in this reaction with catalytic amounts of KH as base (Scheme 33).^[61b]



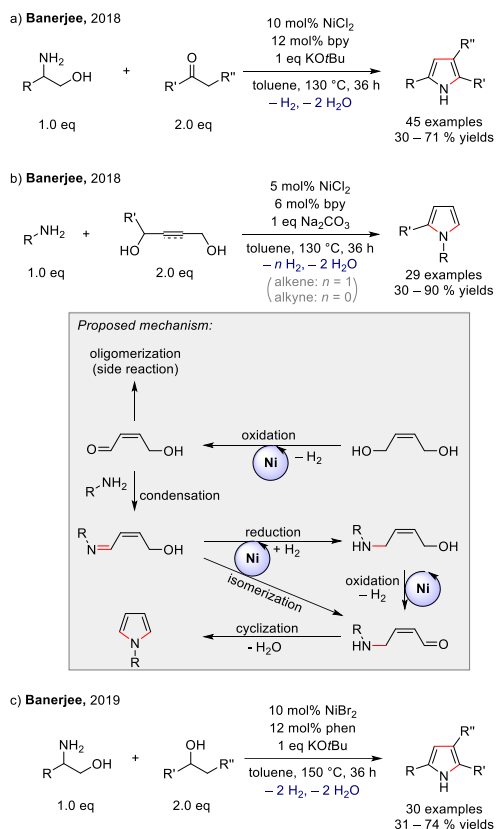
Scheme 33. Manganese-promoted dehydrogenative coupling of alcohols and amines to form cyclic imides.

Significantly more catalyst systems based on precious metals have been reported for the formation of pyrroles *via* dehydrogenative coupling of secondary alcohols with 2-aminoalcohols.^[219, 33c, 62] In 2013 Kempe *et al.* reported the first example promoted by an iridium-based catalyst system.^[62a] In this case it was proposed that the alcohols are dehydrogenated to form the corresponding carbonyl compounds which condense with the amine compound to form the pyrrole. In 2017, the first catalyst system based on an abundant metal was reported (Scheme 34a).^[63] The PN⁵P-manganese(I) pincer complex **Mn-10**, which is a highly active catalyst for the synthesis of pyrimidines as well (see Section 2.10), was shown to promote the formation of pyrroles under relatively mild conditions (78 °C). The phosphine-free SNS-cobalt(II) catalyst **Co-2** was not only active for the dehydrogenative formation of quinolines (see Section 2.1), pyridines (see Section 2.5) and pyrazines (see Section 2.7), but also for pyrroles (Scheme 34b).^[15] Interestingly, the reaction of 1-(4-nitrophenyl)ethan-1-ol with 2-amino-3-methylbutan-1-ol led to the corresponding pyrrole with a reduced nitro-group from the hydrogen generated in the reaction. A relatively high catalyst loading and harsh reaction conditions were required in comparison to the manganese-based system.



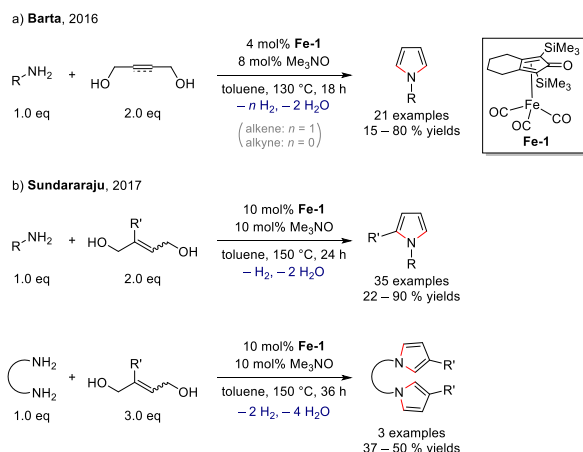
Scheme 34. Base metal-promoted dehydrogenative coupling of diols and amines to form *N*-substituted pyrroles.

The application of bipyridine- and phenanthroline-ligated nickel catalysts gave access to different synthetic routes for the synthesis of pyrroles based on the borrowing hydrogen methodology (Scheme 35). Bipyridine-ligated nickel chloride promoted the cyclization of 2-amino alcohols with ketones (Scheme 35a)^[31] and the cyclization of butene-1,4-diols and butyne-1,4-diols with different aryl- and alkylamines (Scheme 35b).^[64] The latter reaction is supposed to proceed through a sequence of internal hydrogen-transfer isomerization and condensation reactions.



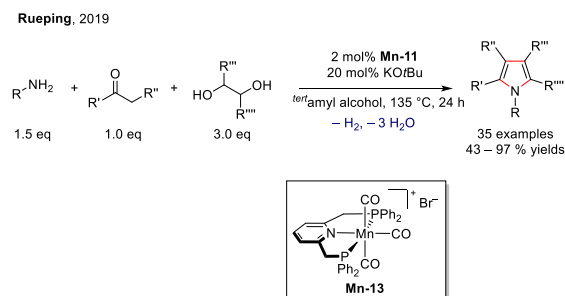
Scheme 35. Nickel-promoted dehydrogenative coupling strategies for the synthesis of pyrroles.

A later study described the double dehydrogenative condensation of β -amino alcohols with secondary alcohols. For this reaction the phenanthroline-ligated nickel bromide showed higher catalytic activity (Scheme 35c).^[65] Early pioneering work for this particular reaction was reported by Moritani in 1974 using Pd black.^[66] More recently ruthenium-based catalysts have been developed.^[67,68] The iron complex **Fe-1** promoted the cyclization of butene-1,4-diols and butyne-1,4-diols with alkyl- and aryl-amines using only catalytic amounts of trimethylamine *N*-oxide as activator without the need for an external base (Scheme 36a).^[69] With higher catalyst loadings the methodology was extended, allowing the synthesis of symmetrical bis-pyrroles *via* a one-pot procedure starting from diamines and (*E*)/(*Z*)-butene-1,4-diols (Scheme 36b).^[70]



Scheme 36. Iron-promoted strategies for the synthesis of pyrroles.

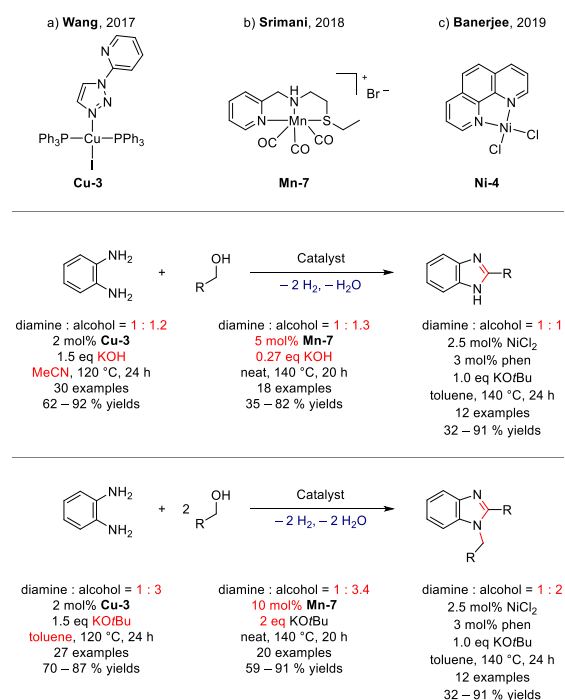
Again, the aforementioned rhenium-based complex **Re-2** represents the state-of-the-art catalyst system for the acceptorless dehydrogenative formation of pyrroles with respect to the catalyst (0.1 mol%) and KOtBu (0.5 equiv) base-loading.^[21g] A $[\text{Ru}_3(\text{CO})_{12}]$ /Xantphos system promoted a three-component pyrrole synthesis in which ketones with different types of amines and vicinal diols were coupled in analogy to the Hantzsch pyrrole synthesis.^[62d, 62e] The PNP^{Ph}-ligated manganese(I)-complex **Mn-13** was the first base metal catalyst system which promoted this heterocyclization (Scheme 37).^[71]



Scheme 37. Manganese-promoted three component reaction for the formation of pyrroles.

2.13. Benzimidazoles, Benzothiazoles and Benzoxazoles

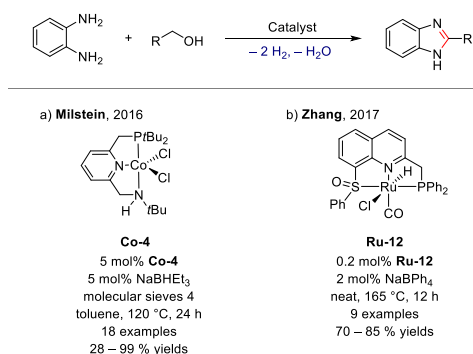
Watanabe and coworkers applied ruthenium phosphine complexes at high reaction temperatures for the synthesis of benzimidazoles and benzoxazoles through acceptorless dehydrogenation.^[72] Since then several precious metal-based catalyst systems^[39b, 73] and a few abundant metal catalyst systems^[8, 74] have been reported to promote the formation of benzimidazoles, benzothiazoles and benzoxazoles. Base metal complexes based on copper,^[74b] manganese,^[74d] and nickel^[74e] promoted the synthesis of 2-monosubstituted and 1,2-disubstituted benzimidazoles (Scheme 38).



Scheme 38. Base metal-promoted synthesis of mono- and disubstituted benzimidazoles.

Particularly for **Ni-4**, the product selectivity was solely controlled by the diamine to alcohol ratio (Scheme 38c), whereas the applied solvent and/or base needed to be adapted in case of **Cu-3** and **Mn-7**. Further studies showed the versatility of the established NNS-manganese(I) catalyst system **Mn-7** in the synthesis of 2,3-dihydro-1H-perimidine derivatives through coupling of 1,8-diaminonaphthalene with benzylic alcohols.^[75]

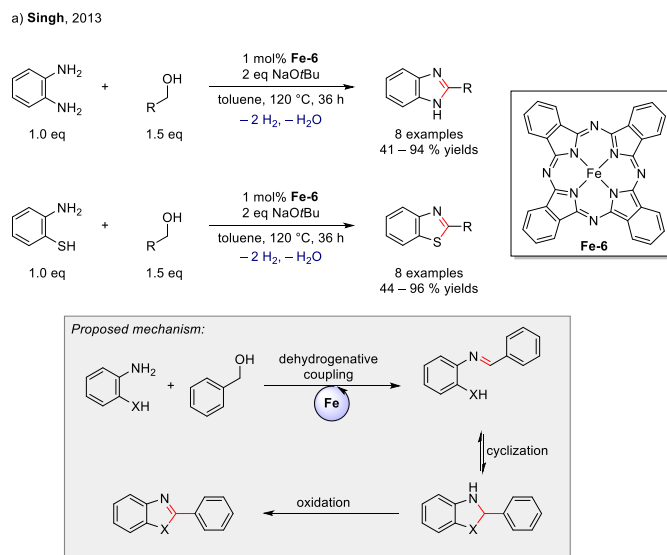
The PNNH-cobalt(II) pincer complex **Co-4** represents the first homogeneous earth-abundant metal-promoted catalyst system that operated after activation with NaBHET₃ under otherwise base-free conditions (Scheme 39a).^[74a] The same catalyst system was applied for the synthesis of pyrroles as well, though a catalytic amount of base was required (see Section 2.12). Among the noble metals, the ruthenium(II) hydride complex **Ru-12** bearing a quinoline-based pincer ligand showed high activity after activation with a catalytic amount of NaBPh₄, avoiding stoichiometric amounts of base (Scheme 39b).^[73d]



Scheme 39. Comparison of the state-of-the-art abundant and noble metal-promoted synthesis of benzimidazoles.

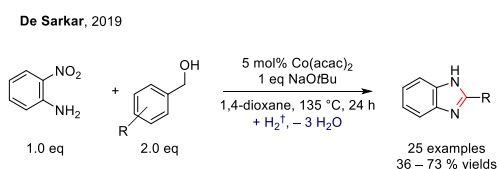
Iron phthalocyanine (**Fe-6**) was utilized in dehydrogenative reactions of various alcohols with 2-phenyldiamines to yield benzimidazoles, while 2-aminothiophenol produced the corresponding 2-substituted benzothiazoles (Scheme 40a).^[76] Initial studies concerning the mechanism suggest that the catalyst is only required for the oxidation step of the alcohol in the first place, but not in the final dehydrogenation step of 2,3-dihydrobenzothiazole, as this reaction proceeds without catalyst under the reaction conditions as well.

The NNS-manganese(I) complex **Mn-4** was found to be not only active for the formation of quinolines (see Section 2.1) and quinoxalines (see Section 2.6), but also for the synthesis of benzothiazoles (Scheme 40b).^[18] Compared to the iron-based system **Fe-6**, a significantly higher catalyst loading was required, though the amount of base was reduced significantly. Coupling of the more stable 2-nitroanilines and benzylic alcohols has been investigated and reported as well.



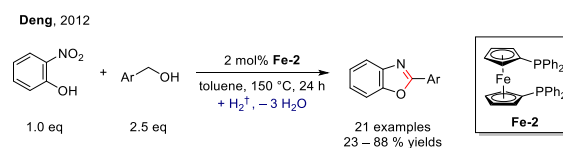
Scheme 40. Iron- and manganese-catalyzed synthesis of benzimidazoles and benzothiazoles.

Various benzimidazoles were synthesized using the commercially available Co(acac)₃ in combination with a stoichiometric amount of base (Scheme 41).^[77] Two equivalents of alcohol were applied in order to ensure the complete reduction of the nitro group; thus, the alcohol is not only acting as substrate but as hydrogen donor as well.



Scheme 41. Redox economical synthesis of benzimidazoles promoted by Cu(OAc)₂. [†] The added hydrogen equivalent stems from the excess of alcohol added to the reaction mixture.

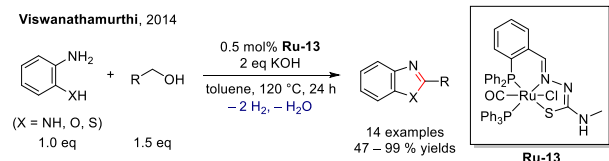
In 2012 an iron-catalyzed procedure for the oxygen containing derivatives benzoxazoles was established. 1,1-bis(diphenylphosphino)ferrocene (**Fe-2**) promoted the reaction of 2-nitrophenols with benzylic alcohols affording a range of 2-arylbenzoxazoles (Scheme 42).^[78] A 2.5-fold excess of benzylic alcohol was necessary, as the alcohol acts as coupling reagent and reductant. The precise mechanism how **Fe-2** facilitates the hydrogen transfer in this reaction is not known.



Scheme 42. Iron-catalyzed formation of 2-arylbenzoxazoles. [†] The added hydrogen equivalent stems from the excess of alcohol added to the reaction mixture.

Benzoxazoles, benzimidazoles and benzothiazoles were synthesized starting from 2-heterosubstituted anilines and

primary alcohols by using the noble metal ruthenium(II) carbonyl complex **Ru-13** containing a thiosemicarbazone ligand. (Scheme 43).^[73c] Low catalyst loadings allowed good conversions; however, two equivalents of base were required.



Scheme 43. Ruthenium-catalyzed formation of benzoxazoles, benzimidazoles and benzothiazoles.

3. Conclusion and Perspective

Homogeneous abundant metal catalysts seem to have a high potential in multicomponent dehydrogenative condensation reactions and transfer hydrogenations to form *N*-containing heterocycles. Still, the majority of base metal promoted reactions requires higher catalyst or base loading compared to noble metal catalysts. However, the number and variety of base metal catalyst systems is increasing and the systems steadily improve further. Besides, for selected examples, such as the formation of 1,2,3,4-tetrahydroquinoxalines or for certain types of pyrrole syntheses, base metal complexes are superior.

Keywords: multicomponent reactions • *N*-heterocycles • acceptorless dehydrogenation • transfer hydrogenation • abundant metal catalysts

- [1] A. Ricci, Amino Group Chemistry: From Synthesis to the Life Sciences, Wiley–VCH, Weinheim, 2008.
- [2] a) R. A. Sheldon, I. Arends, U. Hanefeld, *Green chemistry and catalysis*, Vol. 21, Wiley–VCH, Weinheim, 2007; b) R. A. Sheldon, *Chem. Commun.* 2008, 3352–3365; c) M. North, *Sustainable Catalysis: With Non-endangered Metals*, Royal Society of Chemistry, Cambridge, 2015.
- [3] a) A. Corma, J. Navas, M. J. Sabater, *Chem. Rev.* 2018, 118, 1410–1459; b) T. Irrgang, R. Kempe, *Chem. Rev.* 2019, 119, 2524–2549; c) B. G. Reed-Berendt, K. Polidano, L. C. Morrill, *Org. Biomol. Chem.* 2019, 17, 1595–1607; d) B. Paul, M. Maji, K. Chakrabarti, S. Kundu, *Org. Biomol. Chem.* 2020, 18, 2193–2214; e) M. Maji, D. Panja, I. Borthakur, S. Kundu, *Org. Chem. Fron.* 2021, 8, 2673–2709; f) B. G. Reed-Berendt, D. E. Latham, M. B. Dambatta, L. C. Morrill, *ACS Cent. Sci.* 2021, 7, 570–585.
- [4] Robertus J. M. Klein Gebbink, M. E. Moret, *Non-Noble Metal Catalysis: Molecular Approaches and Reactions*, Wiley–VCH, Weinheim, 2019.
- [5] S. Elangovan, J.-B. Sortais, M. Beller, C. Darcel, *Angew. Chem. Int. Ed.* 2015, 54, 14483–14486; *Angew. Chem.* 2015, 127, 14691–14694.
- [6] G. Zhang, J. Wu, H. Zeng, S. Zhang, Z. Yin, S. Zheng, *Org. Lett.* 2017, 19, 1080–1083.
- [7] M. K. Barman, A. Jana, B. Maji, *Adv. Synth. Catal.* 2018, 360, 3233–3238.
- [8] C. Zhang, B. Hu, D. Chen, H. Xia, *Organometallics* 2019, 38, 3218–3226.
- [9] S. Parua, R. Sikari, S. Sinha, S. Das, G. Chakraborty, N. D. Paul, *Org. Biomol. Chem.* 2018, 16, 274–284.
- [10] S. Das, D. Maiti, S. De Sarkar, *J. Org. Chem.* 2018, 83, 2309–2316.
- [11] G. Chakraborty, R. Sikari, S. Das, R. Mondal, S. Sinha, S. Banerjee, N. D. Paul, *J. Org. Chem.* 2019, 84, 2626–2641.
- [12] S. Das, S. Sinha, D. Samanta, R. Mondal, G. Chakraborty, P. Brandaõ, N. D. Paul, *J. Org. Chem.* 2019, 84, 10160–10171.
- [13] a) C. S. Cho, B. T. Kim, T.-J. Kim, S. C. Shim, *Chem. Commun.* 2001, 2576–2577; b) C. S. Cho, H. J. Seok, S. O. Shim, *J. Heterocyclic Chem.* 2005, 42, 1219–1222; c) C. S. Cho, S.-C. Shim, *Bull. Korean Chem. Soc.* 2005, 26, 2038–2040; d) K. Taguchi, S. Sakaguchi, Y. Ishii, *Tetrahedron Lett.* 2005, 46, 4539–4542; e) R. Martínez, G. J. Brand, D. J. Ramón, M. Yus, *Tetrahedron Lett.* 2005, 46, 3683–3686; f) R. Martínez, D. J. Ramón, M. Yus, *Tetrahedron* 2006, 62, 8982–8987; g) R. Martínez, D. J. Ramón, M. Yus, *Tetrahedron* 2006, 62, 8988–9001; h) R. Martínez, D. J. Ramón, M. Yus, *Eur. J. Org. Chem.* 2007, 1599–1605; i) H. Vander Mierde, N. Ledoux, B. Allaert, P. Van Der Voort, R. Drozdak, D. De Vos, F. Verpoort, *New. J. Chem.* 2007, 31, 1572–1574; j) H. Vander Mierde, P. Van Der Voort, D. De Vos, F. Verpoort, *Eur. J. Org. Chem.* 2008, 2008, 1625–1631; k) R. Wang, H. Fan, W. Zhao, F. Li, *Org. Lett.* 2016, 18, 3558–3561; l) M. Subramanian, S. Sundar, R. Rengan, *Appl. Organometal. Chem.* 2018, 32, e4582; m) D. Wei, V. Dorcet, C. Darcel, J.-B. Sortais, *ChemSusChem* 2019, 12, 3078–3082; n) A. Maji, A. Singh, N. Singh, K. Ghosh, *ChemCatChem* 2020, 12, 3108–3125.
- [14] M. Mastalir, M. Glatz, E. Pittenauer, G. Allmaier, K. Kirchner, *J. Am. Chem. Soc.* 2016, 138, 15543–15546.
- [15] S. P. Midya, V. G. Landge, M. K. Sahoo, J. Rana, E. Balaraman, *Chem. Commun.* 2018, 54, 90–93.
- [16] D.-W. Tan, H.-X. Li, D.-L. Zhu, H.-Y. Li, D.-J. Young, J.-L. Yao, J.-P. Lang, *Org. Lett.* 2018, 20, 608–611.
- [17] S. Shee, K. Ganguli, K. Jana, S. Kundu, *Chem. Commun.* 2018, 54, 6883–6886.
- [18] K. Das, A. Mondal, D. Srimani, *Chem. Commun.* 2018, 54, 10582–10585.
- [19] K. Azizi, S. Akrami, R. Madsen, *Chem. Eur. J.* 2019, 25, 6439–6446.
- [20] A. K. Bains, V. Singh, D. Adhikari, *J. Org. Chem.* 2020, 85, 14971–14979.
- [21] a) C. S. Cho, B. T. Kim, H.-J. Choi, T.-J. Kim, S. C. Shim, *Tetrahedron* 2003, 59, 7997–8002; b) D. Srimani, Y. Ben-David, D. Milstein, *Chem. Commun.* 2013, 49, 6632–6634; c) S. Ruch, T. Irrgang, R. Kempe, *Chem. Eur. J.* 2014, 20, 13279–13285; d) P. Premkumar, R. Manikandan, M. Nirmala, P. Viswanathamurthi, J. G. Malecki, *J. Coord. Chem.* 2017, 70, 3065–3079; e) M. Maji, K. Chakrabarti, B. Paul, B. C. Roy, S. Kundu, *Adv. Synth. Catal.* 2018, 360, 722–729; f) M. Maji, K. Chakrabarti, D. Panja, S. Kundu, *J. Catal.* 2019, 373, 93–102; g) M. Mastalir, M. Glatz, E. Pittenauer, G. Allmaier, K. Kirchner, *Org. Lett.* 2019, 21, 1116–1120; h) B. Guo, T.-Q. Yu, H.-X. Li, S.-Q. Zhang, P. Braunstein, D. J. Young, H.-Y. Li, J.-P. Lang, *ChemCatChem* 2019, 11, 2500–2510; i) S. N. R. Donthireddy, P. M. Illam, A. Rit, *Inorg. Chem.* 2020, 59, 1835–1847.
- [22] N. Hofmann, L. Homberg, K. C. Hultsch, *Org. Lett.* 2020, 22, 7964–7970.
- [23] B. Xiong, Y. Li, W. Lv, Z. Tan, H. Jiang, M. Zhang, *Org. Lett.* 2015, 17, 4054–4057.
- [24] J. Zhang, Z. An, Y. Zhu, X. Shu, H. Song, Y. Jiang, W. Wang, X. Xiang, L. Xu, J. He, *ACS Catal.* 2019, 9, 11438–11446.
- [25] X.-J. Yun, J.-W. Zhu, Y. Jin, W. Deng, Z.-J. Yao, *Inorg. Chem.* 2020, 59, 7841–7851.
- [26] a) S. Parua, R. Sikari, S. Sinha, G. Chakraborty, R. Mondal, N. D. Paul, *J. Org. Chem.* 2018, 83, 11154–11166; b) K. Das, A. Mondal, D. Pal, D. Srimani, *Org. Lett.* 2019, 21, 3223–3227.
- [27] a) J. Fang, J. Zhou, Z. Fang, *RSC Adv.* 2013, 3, 334–336; b) M. Chen, M. Zhang, B. Xiong, Z. Tan, W. Lv, H. Jiang, *Org. Lett.* 2014, 16, 6028–6031; c) W. Lv, B. Xiong, H. Jiang, M. Zhang, *Adv. Synth. Catal.* 2017, 359, 1202–1207; d) X.-M. Wan, Z.-L. Liu, W.-Q. Liu, X.-N. Cao, X. Zhu, X.-M. Zhao, B. Song, X.-Q. Hao, G. Liu, *Tetrahedron* 2019, 75, 2697–2705.
- [28] A. Mondal, M. K. Sahoo, M. Subramanian, E. Balaraman, *J. Org. Chem.* 2020, 85, 7181–7191.
- [29] a) J. Zhou, J. Fang, *J. Org. Chem.* 2011, 76, 7730–7736; b) H. Hikawa, Y. Ino, H. Suzuki, Y. Yokoyama, *J. Org. Chem.* 2012, 77, 7046–7051; c) A. J. A. Watson, A. C. Maxwell, J. M. J. Williams, *Org. Biomol. Chem.* 2012, 10, 240–243; d) F. Li, L. Lu, J. Ma, *Org. Chem. Fron.* 2015, 2, 1589–1597; e) F. Li, L. Lu, P. Liu, *Org. Lett.* 2016, 18, 2580–2583; f) J. Qiao, H. Jiang, X. Liu, C. Xu, Z. Sun, W. Chu, *Eur. J. Org. Chem.* 2019, 2428–2434.
- [30] a) H. Wang, X. Cao, F. Xiao, S. Liu, G.-J. Deng, *Org. Lett.* 2013, 15, 4900–4903; b) S. Parua, S. Das, R. Sikari, S. Sinha, N. D. Paul, *J. Org. Chem.* 2017, 82, 7165–7175.
- [31] K. Singh, M. Vellakkaran, D. Banerjee, *Green Chem.* 2018, 20, 2250–2256.
- [32] J. Das, K. Singh, M. Vellakkaran, D. Banerjee, *Org. Lett.* 2018, 20, 5587–5591.
- [33] a) S. Michlik, R. Kempe, *Angew. Chem. Int. Ed.* 2013, 52, 6326–6329; *Angew. Chem.* 2013, 125, 6450–6454; b) B. Pan, B. Liu, E. Yue, Q. Liu, X. Yang, Z. Wang, W.-H. Sun, *ACS Catal.* 2016, 6, 1247–1253; c) H. Chai, L. Wang, T. Liu, Z. Yu, *Organometallics* 2017, 36, 4936–4942; d)

- T. Hille, T. Irrgang, R. Kempe, *Angew. Chem. Int. Ed.* **2017**, *56*, 371–374; *Angew. Chem.* **2017**, *56*, 7261–7265.
- [34] C. S. Cho, S. G. Oh, *J. Mol. Catal. Chem.* **2007**, *276*, 205–210.
- [35] C. S. Cho, S. G. Oh, *Tetrahedron Lett.* **2006**, *47*, 5633–5636.
- [36] P. Daw, A. Kumar, N. A. Espinosa-Jalapa, Y. Diskin-Posner, Y. Ben-David, D. Milstein, *ACS Catal.* **2018**, *8*, 7734–7741.
- [37] F. Xie, M. Zhang, H. Jiang, M. Chen, W. Lv, A. Zheng, X. Jian, *Green Chem.* **2015**, *17*, 279–284.
- [38] S. Shee, D. Panja, S. Kundu, *J. Org. Chem.* **2020**, *85*, 2775–2784.
- [39] a) T. Hille, T. Irrgang, R. Kempe, *Chem. Eur. J.* **2014**, *20*, 5569–5572. b) K. Chakrabarti, M. Maji, S. Kundu, *Green Chem.* **2019**, *21*, 1999–2004.
- [40] B. Gnanaprakasam, E. Balaraman, Y. Ben-David, D. Milstein, *Angew. Chem. Int. Ed.* **2011**, *50*, 12240–12244; *Angew. Chem.* **2011**, *123*, 12448–12452.
- [41] P. Daw, Y. Ben-David, D. Milstein, *J. Am. Chem. Soc.* **2018**, *140*, 11931–11934.
- [42] T. Yan, B. L. Feringa, K. Barta, *Nat. Commun.* **2014**, *5*, 5602.
- [43] P. Yang, C. Zhang, W.-C. Gao, Y. Ma, X. Wang, L. Zhang, J. Yue, B. Tang, *Chem. Commun.* **2019**, *55*, 7844–7847.
- [44] a) G. Jenner, G. Bitsi, *J. Mol. Catal.* **1988**, *45*, 165–168; b) L. U. Nordström, R. Madsen, *Chem. Commun.* **2007**, 5034–5036; c) L. L. R. Lorentz-Petersen, L. U. Nordström, R. Madsen, *Eur. J. Org. Chem.* **2012**, 6752–6759; d) K. O. Marichev, J. M. Takacs, *ACS Catal.* **2016**, *6*, 2205–2210.
- [45] a) Y. Tsuji, K. T. Huh, Y. Ohsugi, Y. Watanabe, *J. Org. Chem.* **1985**, *50*, 1365–1370; b) R. A. T. M. Abbenhuis, J. Boersma, G. van Koten, *J. Org. Chem.* **1998**, *63*, 4282–4290; c) K. Fujita, Y. Kida, R. Yamaguchi, *Heterocycles* **2009**, *77*, 1371–1377.
- [46] N. Deibl, R. Kempe, *Angew. Chem. Int. Ed.* **2017**, *56*, 1663–1666; *Angew. Chem.* **2017**, *129*, 1685–1688.
- [47] R. Mondal, S. Sinha, S. Das, G. Chakraborty, N. D. Paul, *Adv. Synth. Catal.* **2020**, *362*, 594–600.
- [48] G. Chakraborty, R. Sikari, R. Mondal, S. Mandal, N. D. Paul, *Asian J. Org. Chem.* **2020**, *9*, 431–436.
- [49] A. K. Bains, D. Adhikari, *Catal. Sci. Technol.* **2020**, *10*, 6309–6318.
- [50] T. Shi, F. Qin, Q. Li, W. Zhang, *Org. Biomol. Chem.* **2018**, *16*, 9487–9491.
- [51] N. Deibl, K. Ament, R. Kempe, *J. Am. Chem. Soc.* **2015**, *137*, 12804–12807.
- [52] M. Maji, S. Kundu, *Dalton Trans.* **2019**, *48*, 17479–17487.
- [53] a) R. Grigg, T. R. B. Mitchell, S. Sutthivaiyakit, N. Tongpenyai, *Chem. Commun.* **1981**, 611–612; b) S.-I. Murahashi, K. Kondo, T. Hakata, *Tetrahedron Lett.* **1982**, *23*, 229–232; c) K. Felföldi, M. S. Klyavlin, M. Bartók, *J. Organomet. Chem.* **1989**, *362*, 193–195.
- [54] a) I. Yamaguchi, T. Sakano, H. Ishii, K. Osakada, T. Yamamoto, *J. Organomet. Chem.* **1999**, *584*, 213–216; b) K. Fujita, T. Fujii, R. Yamaguchi, *Org. Lett.* **2004**, *6*, 3525–3528; c) G. Cami-Kobeci, P. A. Slatford, M. K. Whittlesey, J. M. J. Williams, *Bioorg. Med. Chem. Lett.* **2005**, *15*, 535–537; d) K. Fujita, Y. Enoki, R. Yamaguchi, *Org. Synth.* **2006**, *83*, 217–221; e) M. H. S. A. Hamid, C. L. Allen, G. W. Lamb, A. C. Maxwell, H. C. Maytum, A. J. A. Watson, J. M. J. Williams, *J. Am. Chem. Soc.* **2009**, *131*, 1766–1774; f) L. Miao, S. C. DiMaggio, H. Shu, M. L. Trudell, *Org. Lett.* **2009**, *11*, 1579–1582; g) A. B. Enyong, B. Moasser, *J. Org. Chem.* **2014**, *79*, 7553–7563; h) A. Nandakumar, S. P. Midya, V. G. Landge, E. Balaraman, *Angew. Chem. Int. Ed.* **2015**, *54*, 11022–11034; *Angew. Chem.* **2015**, *127*, 11174–11186; i) A. E. R. Chamberlain, K. J. Paterson, R. J. Armstrong, H. C. Twin, T. J. Donohoe, *Chem. Commun.* **2020**, *56*, 3563–3566.
- [55] T. Yan, B. L. Feringa, K. Barta, *ACS Catal.* **2016**, *6*, 381–388.
- [56] H.-J. Pan, T. W. Ng, Y. Zhao, *Chem. Commun.* **2015**, *51*, 11907–11910.
- [57] X. Bai, F. Aiolfi, M. Cettolin, U. Piarulli, A. Dal Corso, L. Pignataro, C. Gennari, *Synthesis* **2019**, *51*, 3545–3555.
- [58] N. D. Schley, G. E. Dobereiner, R. H. Crabtree, *Organometallics* **2011**, *30*, 4174–4179.
- [59] P. Daw, S. Chakraborty, J. A. Garg, Y. Ben-David, D. Milstein, *Angew. Chem. Int. Ed.* **2016**, *55*, 14373–14377; *Angew. Chem.* **2016**, *128*, 14585–14589.
- [60] J. C. Borghs, Y. Lebedev, M. Rueping, O. El-Sepelgy, *Org. Lett.* **2019**, *21*, 70–74.
- [61] a) J. Zhang, M. Senthilkumar, S. C. Ghosh, S. H. Hong, *Angew. Chem. Int. Ed.* **2010**, *49*, 6391–6395; *Angew. Chem.* **2010**, *122*, 6535–6539. b) N. A. Espinosa-Jalapa, A. Kumar, G. Leitus, Y. Diskin-Posner, D. Milstein, *J. Am. Chem. Soc.* **2017**, *139*, 11722–11725.
- [62] a) S. Michlik, R. Kempe, *Nat. Chem.* **2013**, *5*, 140–144; b) D. Srimani, Y. Ben-David, D. Milstein, *Angew. Chem. Int. Ed.* **2013**, *52*, 4012–4015; *Angew. Chem.* **2013**, *125*, 4104–4107; c) K. Iida, T. Miura, J. Ando, S. Saito, *Org. Lett.* **2013**, *15*, 1436–1439; d) M. Zhang, X. Fang, H. Neumann, M. Beller, *J. Am. Chem. Soc.* **2013**, *135*, 11384–11388; e) M. Zhang, H. Neumann, M. Beller, *Angew. Chem. Int. Ed.* **2013**, *52*, 597–601; *Angew. Chem.* **2013**, *125*, 625–629; f) D. Deng, B. Hu, M. Yang, D. Chen, *Organometallics* **2018**, *37*, 2386–2394.
- [63] F. Kallmeier, B. Dudziec, T. Irrgang, R. Kempe, *Angew. Chem. Int. Ed.* **2017**, *56*, 7261–7265; *Angew. Chem.* **2017**, *129*, 7367–7371.
- [64] K. Singh, L. M. Kabadwal, S. Bera, A. Alanthadka, D. Banerjee, *J. Org. Chem.* **2018**, *83*, 15406–15414.
- [65] A. Alanthadka, S. Bera, M. Vellakkaran, D. Banerjee, *J. Org. Chem.* **2019**, *84*, 13557–13564.
- [66] S.-I. Murahashi, T. Shimamura, I. Moritani, *Chem. Commun.* **1974**, 931–932.
- [67] T. Yasushi, Y. Yasuharu, H. Keun-Tae, W. Yoshihisa, *Bull. Chem. Soc. Jpn.* **1987**, *60*, 3456–3458.
- [68] a) S. J. Pridmore, P. A. Slatford, A. Daniel, M. K. Whittlesey, J. M. J. Williams, *Tetrahedron Lett.* **2007**, *48*, 5115–5120; b) S. J. Pridmore, P. A. Slatford, J. E. Taylor, M. K. Whittlesey, J. M. J. Williams, *Tetrahedron* **2009**, *65*, 8981–8986.
- [69] T. Yan, K. Barta, *ChemSusChem* **2016**, *9*, 2321–2325.
- [70] B. Emayavaramban, M. Sen, B. Sundararaju, *Org. Lett.* **2017**, *19*, 6–9.
- [71] J. C. Borghs, L. M. Azofra, T. Biberger, O. Linnenberg, L. Cavallo, M. Rueping, O. El-Sepelgy, *ChemSusChem* **2019**, *12*, 3083–3088.
- [72] T. Kondo, S. Yang, K.-T. Huh, M. Kobayashi, S. Kotachi, Y. Watanabe, *Chem. Lett.* **1991**, *20*, 1275–1278.
- [73] a) A. J. Blacker, M. M. Farah, M. I. Hall, S. P. Marsden, O. Saidi, J. M. J. Williams, *Org. Lett.* **2009**, *11*, 2039–2042; b) A. J. Blacker, M. M. Farah, S. P. Marsden, O. Saidi, J. M. J. Williams, *Tetrahedron Lett.* **2009**, *50*, 6106–6109; c) R. Ramachandran, G. Prakash, S. Selvamurugan, P. Viswanathamurthi, J. G. Malecki, V. Ramkumar, *Dalton Trans.* **2014**, *43*, 7889–7902; d) Q. Luo, Z. Dai, H. Cong, R. Li, T. Peng, J. Zhang, *Dalton Trans.* **2017**, *46*, 15012–15022; e) L. Li, Q. Luo, H. Cui, R. Li, J. Zhang, T. Peng, *ChemCatChem* **2018**, *10*, 1607–1613.
- [74] a) P. Daw, Y. Ben-David, D. Milstein, *ACS Catal.* **2017**, *7*, 7456–7460; b) Z. Xu, D.-S. Wang, X. Yu, Y. Yang, D. Wang, *Adv. Synth. Catal.* **2017**, *359*, 3332–3340; c) U. Narang, K. K. Yadav, S. Bhattacharya, S. M. S. Chauhan, *ChemistrySelect* **2017**, *2*, 7135–7140; d) K. Das, A. Mondal, D. Srimani, *J. Org. Chem.* **2018**, *83*, 9553–9560; e) A. Bera, M. Sk, K. Singh, D. Banerjee, *Chem. Commun.* **2019**, *55*, 5958–5961.
- [75] K. Das, A. Mondal, D. Pal, H. K. Srivastava, D. Srimani, *Organometallics* **2019**, *38*, 1815–1825.
- [76] M. Bala, P. K. Verma, U. Sharma, N. Kumar, B. Singh, *Green Chem.* **2013**, *15*, 1687–1693.
- [77] S. Das, S. Mallick, S. De Sarkar, *J. Org. Chem.* **2019**, *84*, 12111–12119.
- [78] M. Wu, X. Hu, J. Liu, Y. Liao, G.-J. Deng, *Org. Lett.* **2012**, *14*, 2722–2725.

3.1. Publication 2

Switching the *N*-Alkylation of Arylamines with Benzyl Alcohols to Imine Formation Enables the One-Pot Synthesis of Enantioenriched α -*N*-Alkylaminophosphonates

Natalie Hofmann^[a] and Kai C. Hultzsch^{*[a]}

^[a] Universität Wien, Fakultät für Chemie, Institut für Chemische Katalyse
Währinger Straße 38, 1090 Wien
<https://chemcat@univie.ac.at/>

* Corresponding author; email: kai.hultzsch@univie.ac.at

Eur. J. Org. Chem. **2019**, 3105–3111; doi: 10.1002/ejoc.201900209.

Different variants of the Knölker complex and a broad range of chiral BINOL-based phosphoric acids were synthesized. Then their capability to promote the selective *N*-alkylation of arylamines, respectively the subsequent enantioselective hydrophosphonylation to form enantioenriched α -*N*-alkylaminophosphonates was investigated.

As first author I developed the idea of the described cascade reaction. Besides, I designed and conducted the experiments, evaluated the obtained results and prepared the draft of the manuscript.

Hydrogen Borrowing Catalysis

Switching the *N*-Alkylation of Arylamines with Benzyl Alcohols to Imine Formation Enables the One-Pot Synthesis of Enantioenriched α -*N*-Alkylaminophosphonates

Natalie Hofmann^[a] and Kai C. Hultzscht^{*[a]}

Abstract: The selective *N*-alkylation of anilines with benzylic alcohols can be switched in favor of the dehydrogenative condensation process using the nitrile-ligated Knölker's complex by conducting the reaction either in a closed system under inert conditions, or in an open system in air. The selective formation of imines, containing reactive C=N bonds, provides an opportu-

nity towards further functionalization. Indeed, a one-pot three-component condensation of alcohols, amines and phosphites, promoted by an iron-based Knölker-type complex in combination with a chiral BINOL-based phosphoric acid, provides access to enantioenriched α -*N*-alkylaminophosphonates.

Introduction

The development of atom-efficient transformations that lead to valuable compounds bearing carbon–heteroatom bonds starting from innocuous and cheap starting materials is in the focus of modern synthetic chemistry.^[1] Therefore, hydrogen borrowing catalysis is an important contemporary research topic as it provides a green method for a variety of transformations of alcohols, in particular the formation of new carbon–carbon or carbon–nitrogen bonds.^[2] In order to gain access to higher functionalized products the combination of metal-based hydrogen borrowing catalysis with organocatalysis provides promising possibilities.^[3–5] Our interest is primarily focused on different derivatives of the well-known iron-based Knölker's complex **1a–1c** (Figure 1).^[6]

Iron is particularly attractive as it is one of the most abundant metals in the earth crust. Besides, iron species are ubiquitous in biological systems and metabolic processes making them interesting for applications in the food and pharmaceutical industry.^[7] The low toxicity of iron is often used in the discussion on iron-based catalysts as well; however, the toxicity level of iron has to be viewed critically.^[8] Knölker's complex itself has been applied in combination with different organocatalysts. Rodriguez et al. established the enantioselective functionalization of allylic alcohols by applying, among others, a triple iron/copper/iminium activation,^[3] whereas Beller et al. re-

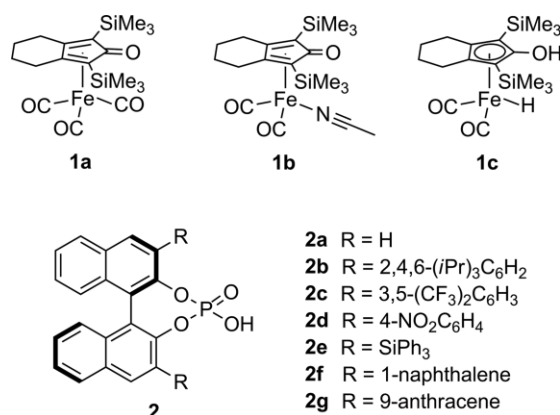


Figure 1. Applied metal and organocatalysts.

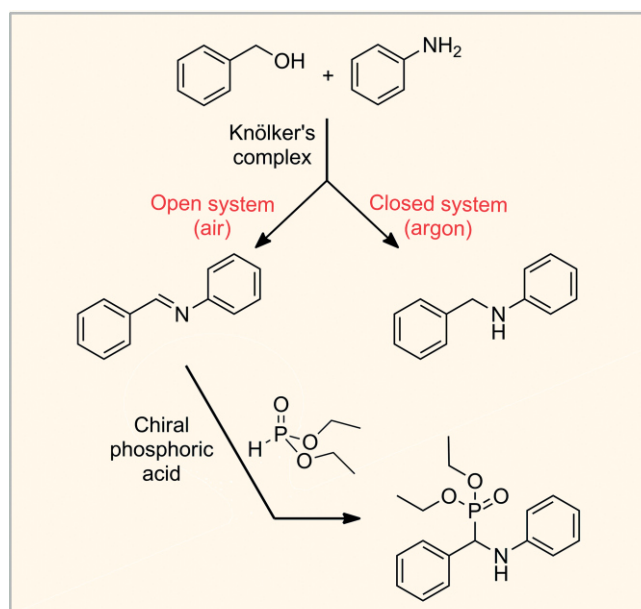
ported enantioselective hydrogenations of imines and quinoxalines by combining iron catalysis with chiral phosphoric acids **2**.^[4] In this work we focus on the synthesis of enantioenriched α -*N*-alkylaminophosphonates by combining a hydrogen-borrowing based *N*-alkylation with the Kabachnik–Fields reaction.^[9] As α -aminophosphonates are valuable replacements of α -amino carboxylic acids, which are building blocks of proteins and peptides and therefore play an important role in many physiological processes, their easy and waste-free synthesis is of particular interest.^[10] To the best of our knowledge there are only two heterogeneous systems for the one-pot condensation of anilines, alcohols and phosphites, but no homogeneous system at all. On one hand Hosseini et al. reported CuO@Fe₃O₄ nanoparticles to be suitable catalysts,^[11] on the other hand Fan and co-workers conducted the reaction with gold supported on hydroxyapatite.^[12] With this in mind we decided to develop a homogeneous system to synthesize enantioenriched α -aminophosphonates. As Beller and co-workers could combine the iron-based Knölker's complex **1c** with chiral phosphoric ac-

[a] Universität Wien, Fakultät für Chemie, Institut für Chemische Katalyse, Währinger Straße 38, 1090 Wien, Austria
E-mail: kai.hultzscht@univie.ac.at
<https://chemcat.univie.ac.at/>

Supporting information and ORCID(s) from the author(s) for this article are available on the WWW under <https://doi.org/10.1002/ejoc.201900209>.

© 2019 The Authors. Published by Wiley-VCH Verlag GmbH & Co. KGaA. This is an open access article under the terms of the Creative Commons Attribution-NonCommercial-NoDerivs License, which permits use and distribution in any medium, provided the original work is properly cited, the use is non-commercial and no modifications or adaptations are made.

ids **2** for hydrogenations^[4] and phosphoric acids are common organocatalysts for hydrophosphonylations,^[9b,13] we chose to combine similar systems for the exploration of the enantioselective one-pot condensation of anilines, alcohols and phosphites. In the course of our investigations we found that it is possible to control the selectivity of the *N*-alkylation of aniline promoted by Knölker's complex **1b** and **1c** by varying the reaction conditions (Scheme 1).^[14] So far, under base-free conditions iron is known to favor the formation of the respective amine, whereas manganese is prone to stop at the imine-intermediate.^[15] In this study we will show that a selective formation of the *N*-alkylated amine can be achieved by conducting the reaction under argon, whereas a selective imine formation is observed when the reaction is performed under atmospheric conditions. The reactive imine can subsequently undergo a hydrophos-



Scheme 1. Selective synthesis of *N*-alkylated amines, imines and α -*N*-alkylaminophosphonates.

phonylation reaction leading to α -*N*-alkylaminophosphonates. Therefore, three different products are accessible starting from anilines and benzylic alcohols simply by varying the reaction conditions and by combining metal catalysis with organocatalysis.

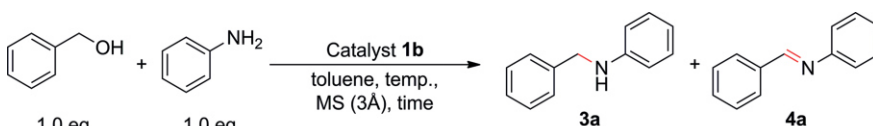
Results and Discussion

Selective *N*-Alkylation

Initially, we started our investigations on this topic using Knölker's complex **1a** (Figure 1),^[6] which was already successfully applied for the direct alkylation of amines with alcohols.^[14] However, applying this type of catalyst required additional base or activation reagents to achieve any reactivity in the *N*-alkylation of aniline. As our goal was to combine the *N*-alkylation with a subsequent hydrophosphonylation step promoted by chiral phosphoric acids **2**, we were searching for a way to avoid the application of base. Thus, we decided to utilize Knölker's complex **1b**,^[6b] in which one CO ligand is replaced by acetonitrile. This variant of Knölker's complex is a known catalyst for transfer hydrogenations of aldehydes, ketones and alkynes using 2-propanol as hydrogen source.^[16] Feringa and co-workers used this air-stable nitrile-ligated complex for the *N*-alkylation of amino acids.^[14f] Darcel et al. observed moderate activity in the α -alkylation of ketones with alcohols.^[17] Fortunately, this catalyst turned out to be highly active in our base-free benchmark reaction with aniline and benzyl alcohol as well. Besides, we synthesized the hydride derivative **1c** of the Knölker's complex,^[6c,18] which proved to be active as well.

To our delight we could control the selectivity of this reaction simply by switching between a closed system under argon atmosphere and an open system under atmospheric conditions with both catalysts (**1b** and **1c**, see Table S1 in supporting information). Realization under inert conditions resulted in the quantitative formation of *N*-benzylaniline (**3a**), whereas execution in an open system in air led to the selective formation of *N*-benzylideneaniline (**4a**). In general, the nitrile-ligated com-

Table 1. Selectivity studies for the *N*-alkylation of aniline with benzyl alcohol.^[a]

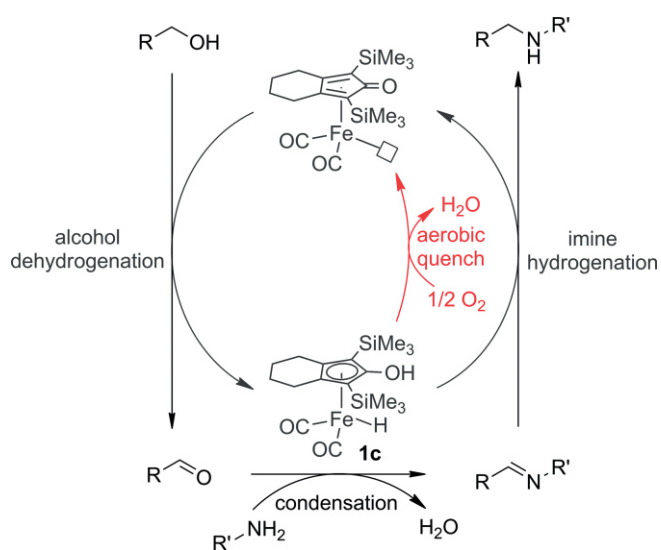
							
#	Cat. 1b [mol-%]	Open/ closed	Temp. [°C]	Time [h]	Conversion [%] ^[b] Overall	Amine 3a	Imine 4a
1	5.0	closed	100	24	93	92	< 1
2	5.0	closed	110	24	quant.	> 99	< 1
3	5.0	open	110	48	47	7	40
4	7.5	open	110	48	63	9	54
5	7.5	open	140	48	87	14	73
6	7.5	open	140	55	94	16	78
7	7.5	open^[c]	140	55	quant.	17	83

[a] Reaction conditions: 150 mg of molecular sieves (3 Å), 0.250 mmol benzyl alcohol, 0.250 mmol aniline, 0.3 mL of toluene. Closed = reaction in closed vial under an argon atmosphere. Open = reaction in opened vial in air at 60 °C for 15 min, then the vial was loosely capped in order for hydrogen to be able to escape and heated to 140 °C for 55 h. [b] Conversion was determined via GC/FID and GC/MS using mesitylene as internal standard. [c] *p*-Xylene was applied as solvent.

plex **1b** exhibits a higher reactivity and is easier to handle than **1c** thanks to its bench stability.^[6b] Therefore, this catalyst was used for the following screening and optimization reactions (Table 1).

We found that the application of 5 mol-% of **1b** at 110 °C in a closed system under argon leads to a quantitative formation of **3a**. Higher catalyst loadings (7.5 mol-%) and temperatures (140 °C) as well as longer reaction times (55 h) are required in an open system in order to achieve good conversions to **4a**. By changing the solvent from toluene to the higher boiling *p*-xylene the outcome was improved further. Despite these harsh conditions, a practical feature is that the selective formation of the imine can be conducted under atmospheric conditions, significantly simplifying the reaction's feasibility. Further investigations showed that the application of molecular sieves (3 Å) is crucial for the success of both reactions.

The change in product selectivity upon switching from a closed system under argon to an open system in air can be attributed to an oxidative quenching of the reduced Knölker's complex by oxygen, which bypasses the imine hydrogenation pathway (Scheme 2).^[19,20]



Scheme 2. Proposed mechanism for the aerobic quench of **1c** short-circuiting the hydrogen borrowing *N*-alkylation.

After optimization of the reaction conditions we explored the functional group tolerance and the selectivity of the catalyst. We applied benzylic alcohols and anilines with several electron-donating and electron-withdrawing groups. (Table 2). Methyl and methoxy substituents proved to be well tolerated leading to the corresponding secondary amines (**3b**, **3c**, **3f**, **3g**, **3i**, **3j**), respectively imines (**4b**, **4c**, **4f**, **4g**, **4i**, **4j**) in good to excellent yields. The reaction of *ortho*-hydroxybenzyl alcohol with aniline, preferentially led to the amine **3e** under both reaction conditions, while the respective imine **4e** was only formed in small amounts. Similar observations were made in the reaction of 2- and 3-aminopyridine with benzyl alcohol to preferentially form amines **3k** and **3l**, but here the overall conversion was also diminished. The converse was noticed in the reaction of *ortho*-chlorobenzyl alcohol with aniline (**3d**, **4d**). The reaction

of aniline with linear aliphatic alcohols *n*-butanol, *n*-pentanol, and *n*-hexanol led to the corresponding amines **3m–o** in good yields, similar to observations made by Kirchner et al. using an iron PNP pincer catalyst,^[15a] however, even under atmospheric conditions the amines **3m–o** remained the prevailing products and only trace amounts of imines **4m–o** were formed. Piper-

Table 2. Synthesis of amines and imines through coupling of various alcohols with amines.^[a]

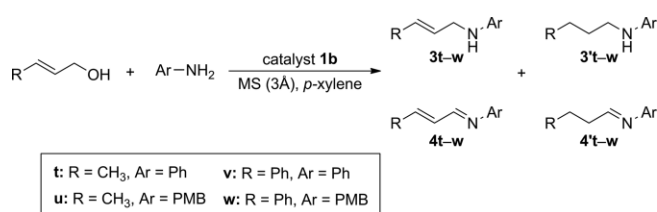
$R-OH + R'-NH_2 \xrightarrow[\text{MS (3Å), } p\text{-xylene}]{\text{catalyst 1b}}$		$R-NH-R'$	$R-N=R'$
		3a–3s	4a–4s
(A) select. formation of amines 3		(B) select. formation of imines 4	
	R = H 3a >99%		R = H 4a 83%
	R = CH ₃ 3b 75%		R = CH ₃ 4b 90%
	R = OCH ₃ 3c >99%		R = OCH ₃ 4c 69%
	R = Cl 3d 24%		R = Cl 4d 70% ^[e]
	R = OH 3e 94% ^[b]		R = OH 4e 11% ^[b]
	3f 96%		4f 86%
	R' = CH ₃ 3g 91%		R' = CH ₃ 4g 72%
	R' = F 3h 71%		R' = F 4h 67% ^[e]
	3i >99		4i 75%
	3j 97%		4j 77%
	3k 67%		4k 6%
	3l 47%		4l 13%
	n=1 3m 91% ^[c]		n=1 4m 9% ^[c]
	n=2 3n >99%		n=2 4n 5%
	n=3 3o 95%		n=3 4o <1%
	3p 99% ^[c]		4p none
	3q 36% ^[d]		4q 75% ^[d,e]
	3r 85%		4r 49%
	3s 86%		4s 23%

[a] Reaction conditions: A) selective formation of amine: 5 mol-% **1b**, 150 mg of molecular sieves (3Å), 0.250 mmol alcohol, 0.250 mmol aniline, 0.3 mL of *p*-xylene, 110 °C, 24 h, closed system, argon. B) selective formation of imine: 7.5 mol-% **1b**, 150 mg of molecular sieves (3Å), 0.300 mmol alcohol, 0.250 mmol aniline, 0.3 mL of *p*-xylene, 140 °C, 55 h, open system, air. Conversions and product ratios were determined via GC/FID and GC/MS using mesitylene as internal standard. Amine/imine-ratios for all reactions are listed in the supporting information in Tables S3A and S3B. [b] NMR-yield. [c] Reaction temperature: 130 °C. [d] The identity of the products was verified by ¹H-NMR spectroscopy. [e] Reaction time: 92 h.

imine was completely converted into the corresponding tertiary amine (**3p**) after increasing the reaction temperature, which confirms the observation by Feringa et al. that the catalyst is capable of converting secondary amines as well.^[14f] The exploration of an intramolecular reaction with 2-aminophenethyl alcohol showed a complete consumption of the starting material; however, only 36 % of 1*H*-indoline (**3q**) were formed and 1*H*-indole (**4q**) was detected as the major product, independent of the reaction conditions. Obviously, tautomerization of the imine intermediate is more facile than reduction to **3q**, driven by the rearomatization of **4q**. The reaction of benzyl alcohol with hexylamine produced amine **3r** in good yield under the closed system conditions, while under atmospheric conditions a 1:1 mixture of amine **3r** and imine **4r** was observed. The analogous reaction with benzylamine gave the amine **3s** preferentially under both sets of conditions.

With the knowledge that allylic alcohols have been successfully applied in iron-catalyzed hydrogen borrowing *N*-alkylation^[14e] and cascade processes^[3] and that imines derived from cinnamaldehyde are well-suited for the enantioselective hydrophosphonylation with chiral phosphoric acids,^[13] we decided to subject allylic alcohols to our *N*-alkylation and imine formation conditions (Table 3). The reaction of cinnamyl alcohol and crotyl alcohol with either aniline or *p*-anisidine gave mixtures of 4 possible amine and imine products with or without α,β -unsaturation. Interestingly, the application of crotyl alcohol in a closed system provided the fully saturated amines **3't** and **3'u** as major product, whereas cinnamyl alcohol led predominantly to the α,β -unsaturated amines **3v** and **3w**. Under atmospheric condi-

Table 3. Investigation of allylic alcohols in the *N*-alkylation and imine formation.^[a]



#	R	Ar	Conversion [%] ^[b]				
			Overall	3	3'	4	4'
(A) closed system under argon							
1	CH ₃	Ph	> 99	2	83	2	13
2	CH ₃	PMB	> 99	3	48	33	16
3	Ph	Ph	> 99	61	30	9	< 1
4	Ph	PMB	> 99	68	17	15	< 1
(B) open system in air							
5	CH ₃	Ph	> 99	2	43	50	5
6	CH ₃	PMB	94	3	31	53	8
7	Ph	Ph	90	46	5	39	< 1
8	Ph	PMB	95	47	10	38	< 1

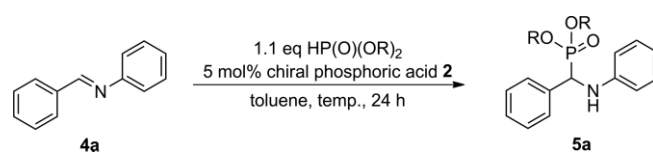
[a] Reaction conditions: A) selective formation of amine: 5 mol-% **1b**, 150 mg of molecular sieves (3Å), 0.250 mmol alcohol, 0.250 mmol aniline, 0.3 mL of *p*-xylene, 110 °C, 24 h, closed system, argon. B) selective formation of imine: 7.5 mol-% **1b**, 150 mg of molecular sieves (3Å), 0.300 mmol alcohol, 0.250 mmol aniline, 0.3 mL of *p*-xylene, 140 °C, 24 h, open system, air. [b] Conversions and product ratios were determined via GC/FID and GC/MS using mesitylene as internal standard.

tions the amount of α,β -unsaturated imine **4t-w** significantly increased for all substrates, although the selectivity remained moderate.

Enantioselective Hydrophosphonylation

In order to promote the enantioselective hydrophosphonylation, we focused on chiral phosphoric acids, which are known to be efficient organocatalysts for various selective additions to imines,^[21] including the hydrophosphonylation.^[9b,13] Akiyama^[13a,13b] and Ma^[13c] studied the enantioselective hydrophosphonylation of *N*-benzylidene *p*-anisidine and aldimines derived from cinnamaldehyde derivatives using the BINOL-based phosphoric acids **2a-g**. As a test reaction, we therefore decided to investigate the addition of various phosphites to *N*-benzylideneaniline (**4a**) (Table 4).

Table 4. Influence of the acid catalyst, structure of phosphite and reaction temperature on the enantioselective hydrophosphonylation of imine **4a**.^[a]



#	Product	2	HP(O)(OR) ₂	Temp. [°C]	Yield [%] ^[b]	ee [%] ^[c]
Different phosphoric acids 2						
1	5a	–	HP(O)(OEt) ₂	25	21	– ^[d]
2	5a	2a	HP(O)(OEt) ₂	25	94	< 5
3	5a	2b	HP(O)(OEt) ₂	25	91	23
4	5a	2c	HP(O)(OEt) ₂	25	93	52
5	5a	2d	HP(O)(OEt) ₂	25	89	9
6	5a	2e	HP(O)(OEt) ₂	25	84 ^[e]	45
7	5a	2f	HP(O)(OEt) ₂	25	90	8
8	5a	2g	HP(O)(OEt) ₂	25	91	35
Different phosphites						
9	5aa	2c	HP(O)(OMe) ₂	25	91	47
10	5ab	2c	HP(O)(OiPr) ₂	25	95	39
11	5ac	2c	HP(O)(OPh) ₂	25	98 ^[f]	< 5
Varying temperatures						
12	5a	2c	HP(O)(OEt) ₂	0	91 ^[g]	51
13	5a	2c	HP(O)(OEt) ₂	60	95 ^[h]	47
14	5a	–	HP(O)(OEt) ₂	100	94	< 5

[a] Reaction conditions: 5 mol-% **2**, 0.250 mmol *N*-benzylideneaniline, 0.275 mmol phosphite, 0.3 mL of toluene. [b] Isolated yield. [c] Determined via chiral HPLC. [d] Not applicable. [e] Reaction time: 48 h. [f] The reaction proceeded to completion within 15 min also in the absence of an acid catalyst or when 1 equiv. hydroquinone (relative to **4a**) was added. [g] Reaction time: 90 h. [h] Reaction time: 5 h.

In general, decent yields were obtained for all phosphoric acids and phosphites, while enantioselectivities remained moderate. In agreement to results obtained for *N*-benzylidene *p*-anisidine,^[13] the sterically hindered 3,5-bis(trifluoromethyl)phenyl-substituted acid **2c** gave the highest selectivity (52 % ee). Despite its bulkiness, the anthracene-substituted phosphoric acid **2g** was significantly less enantioselective (35 % ee). Interestingly, the sterically more demanding diisopropyl and diphenyl phosphite led to a diminished enantioselectivity

as well. In particular, diphenyl phosphite gave essentially a racemic product. This observation can be explained by a fast uncatalyzed background reaction for this substrate. The reaction is complete within 15 min even in the absence of an acid catalyst. In order to rule out a radical process, the reaction of diphenyl phosphite with **4a** was repeated in the presence of 1 equiv. hydroquinone with and without added phosphoric acid **2a**, leading also to complete conversion within 15 min in both cases.

Varying the reaction temperature solely influenced the rate of the reaction, but hardly showed any impact on the enantioselectivity (Table 4, entries 4, 12, 13). Lower reaction temperatures required longer reaction times, whereas higher temperatures led to a faster completion of the reaction. In general, the addition of diethyl phosphite to the imine proceeded also in the absence of catalyst when the reactions were conducted at 100 °C.

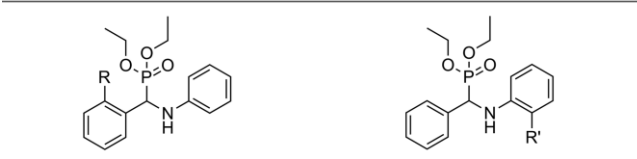
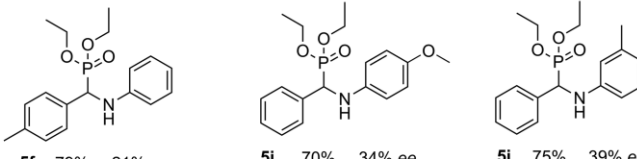
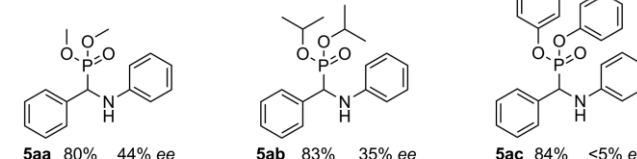
Attempts to extend the substrate scope of the enantioselective hydrophosphonylation of imines to the aliphatic imine *N*-phenylhexanimine were frustrated by its instability in the presence of either diethyl phosphite ($pK_A \approx 13.0$)^[22a] or chiral phosphoric acid ($pK_A \approx 3.0$)^[22b] leading to facile cleavage of the imine.

One-Pot Synthesis of α -*N*-Alkylaminophosphonates

Since we wanted to couple the *N*-alkylation with the hydrophosphonylation, we performed compatibility studies as well. We found that aniline hampers the addition of diethyl phosphite to *N*-benzylideneaniline, whereas phosphoric acids **2** suppress the *N*-alkylation. This led us to the conclusion that a one-pot cascade reaction is not feasible, but the synthesis of α -*N*-alkylaminophosphonates can be achieved in a sequential one-pot procedure (for detailed experimental data see supplementary information, Tables S4 and S5). With the optimized reaction conditions for each reaction step, we were able to carry out the synthesis of diethyl [phenyl(phenylamino)methyl]phosphonate (**5a**) in 80 % isolated yield with 50 % ee via one-pot condensation of aniline, benzyl alcohol and diethyl phosphite (Table 5). Fractional crystallization from heptane, leaving the enantioenriched form in the supernatant and increasing the enantiomeric excess up to 81 %. However, none of the other products showed a similar fractionation.

After showing the proof of principle with the benchmark reaction, we chose suitable substrates to investigate the influence of steric and electronic changes on the hydrophosphonylation. We found that steric hindrance in the *ortho*-position, either in the alcohols or the amines, did not improve the selectivity of the reaction and the enantiomeric excess remained in the 30–40 % range in most cases. However, the addition of diethyl phosphite to the imines derived from *ortho*-methyl- and *ortho*-fluoro-aniline were hampered, and no reaction was observed at ambient temperature. Only heating to 60 °C, respectively 100 °C, produced the desired products **5g** and **5h** in decent yields.

Table 5. One-pot two step synthesis of α -*N*-alkylaminophosphonates **5**.^[a]

$R-OH + R'-NH_2$		1) 7.5 mol% 1b , MS (3Å), <i>p</i> -xylene, 55 h, 140 °C 2) 10 mol% 2c , 1.1 eq HP(O)(OR) ₂ , 24 h, 25 °C		5a–5j	
1.2 eq	1.0 eq				
					
5a	R = H	81%	50% ee	5g	R' = CH ₃ 68% 21% ee ^[b]
5b	R = CH ₃	83%	41% ee	5h	R' = F 58% 7% ee ^[c]
5c	R = OCH ₃	63%	40% ee		
5d	R = Cl	59%	32% ee		
					
5f		79%	21% ee	5i	70% 34% ee
				5j	75% 39% ee
					
5aa		80%	44% ee	5ab	83% 35% ee
				5ac	84% <5% ee

[a] Reaction conditions: 1) 7.5 mol-% **1b**, 150 mg of molecular sieves (3Å), 0.300 mmol alcohol, 0.250 mmol aniline, 0.3 mL of *p*-xylene, open system, air; 2) 10 mol-% **2c**, 0.275 mmol phosphite; Isolated yields. Enantiomeric excess was determined via chiral HPLC. [b] Reaction temperature: 60 °C. [c] Reaction temperature: 100 °C.

During purification of products **5a–5j** we managed to recover the valuable chiral phosphoric acid catalysts **2** from the last fraction of the column chromatography.

Conclusions

In brief, the *N*-alkylation of anilines with benzylic alcohols catalyzed by the highly reactive acetonitrile-ligated Knölker complex **1b** can be switched in favor of imine formation. While the hydrogen borrowing process is achieved in a closed system under argon, the dehydrogenative condensation occurs at a higher temperature in an open system in air. Both reactions do not require activation by a base additive. The highly reactive C=N-bond of the in situ formed imine can be used for the atom-efficient synthesis of α -*N*-alkylaminophosphonates by a one-pot three-component condensation of alcohols, amines and phosphites. Notably, this tandem reaction can be performed under atmospheric conditions, forming water as the only by-product and the applied chiral phosphoric acid can be recovered. However, this protocol appears to be only amenable to aniline and benzyl alcohol derivatives, as aliphatic alcohols and amines either lead to predominant amine formation under both sets of

reaction conditions or the resulting aliphatic imines are unstable under the conditions of hydrophosphonylation.

Experimental Section

General Considerations: Toluene and *p*-xylene were distilled from sodium benzophenone ketyl. Alcohols and phosphites used as substrates for catalysis were distilled from Na₂SO₄. Amines used as substrates for catalysis were distilled from CaH₂. If not mentioned differently all commercially available starting materials were used without further purification. All ¹H, ¹³C, ³¹P, and ¹⁹F NMR spectra were recorded on a Bruker UltrashieldTM 400 or 600 Plus instrument, whereby the ¹H NMR spectra were measured at 400.3 MHz or 600.2 MHz, the ¹³C NMR spectra at 100.6 or 150.9 MHz, and the ³¹P NMR spectra at 162.0 MHz. All chemical shifts are noted in ppm. ¹H and ³¹C chemical shifts are indicated relative to TMS and were referenced to residual signals of the solvent [¹H NMR (CDCl₃): 7.27 ppm, ¹³C NMR (CDCl₃): 77.0 ppm]. ³¹P chemical shifts were referenced to H₃PO₄ (0.00 ppm). Column chromatography was performed by using Biotage® SP4 and Isolera flash systems and the applied columns were packed with silica gel 60 Å or aluminium oxide 90 standardised (activity II–III). TLC was performed with commercial Kieselgel 60 F254 or ALOX N/UV254 and visualized via UV lamp. GC/MS measurements were conducted on an Agilent Technologies with 5977B MSD High Efficiency Source and 7820A GC-system. GC/FID measurements were conducted on a Shimadzu GC-2010 system. HPLC measurements were conducted on an Agilent Technologies Series 1200 system with 61379B Degasser, 61311A QuatPump, 61329A LLS, 61316A TCC, G1315D DAD. The Knölker's complexes **1a**,^[14d] **1b**,^[6b,16a,16b] and **1c**^[6c,18] were synthesized according to the literature, as well as the chiral BINOL-based phosphoric acids **2a**,^[23] **2b**,^[23] **2c**,^[23] **2d**,^[24] **2e**,^[25] **2f**,^[26] and **2g**.^[27]

Synthesis of *N*-Benzylaniline (3a): In an argon filled glovebox, a PTFE-lined screw-cap vial (1.5 mL), equipped with a magnetic stirring bar and molecular sieves (3 Å, 150 mg), Knölker's complex **1b** (5.3 mg, 0.013 mmol, 0.05 equiv.) was dissolved in *p*-xylene (0.3 mL). Benzyl alcohol (26 µL, 1.04 g/mL, 0.250 mmol, 1.0 equiv.) and aniline (23 µL, 1.03 g/mL, 0.250 mmol, 1.0 equiv.) were added and the vial was closed tightly and sealed with Teflon tape. The vial was placed in an aluminum block, covered with aluminum foil, and the resulting reaction mixture was heated to 110 °C with magnetic stirring for 24 h. After cooling to room temperature the reaction was quenched by addition of H₂O (0.5 mL) and the water layer was extracted with EtOAc (3 × 2 mL). The combined organic layers were dried with MgSO₄ and the solvent was removed under vacuum. Purification via column chromatography (silica, hept:CH₂Cl₂/Et₃N = 9:1:0.1) led to 42 mg (93 %) of *N*-benzylaniline as a slightly yellow oil.

Synthesis of *N*-Benzylideneaniline (4a): In a PTFE-lined screw-cap vial (1.5 mL), equipped with a magnetic stirring bar and molecular sieves (3 Å, 150 mg), Knölker's complex **1b** (8.1 mg, 0.019 mmol, 0.075 equiv.) was dissolved in *p*-xylene (0.3 mL). Benzyl alcohol (31 µL, 1.04 g/mL, 0.300 mmol, 1.2 equiv.) and aniline (23 µL, 1.03 g/mL, 0.250 mmol, 1.0 equiv.) were added. The vial was placed in an aluminum block, and the resulting reaction mixture was heated in the vial opened to air to 60 °C with magnetic stirring for 15 min, then the vial was loosely capped in order for hydrogen to be able to escape, covered with aluminum foil, and heated to 140 °C for 55 h. After cooling to room temperature, the reaction was quenched by addition of H₂O (0.5 mL) and the water layer was extracted with EtOAc (3 × 2 mL). The combined organic layers were dried with MgSO₄ and the solvent was removed under vacuum.

Purification via pipette chromatography (silica, hept/CH₂Cl₂/Et₃N = 9:1:0.1) led to 37 mg (82 %) of *N*-benzylideneaniline as a slightly yellow solid.

Synthesis of Diethyl [Phenyl(phenylamino)methyl] Phosphonate (5a): In a PTFE-lined screw-cap vial (1.5 mL), equipped with a magnetic stirring bar and molecular sieves (3 Å, 150 mg), Knölker's complex **1b** (8.1 mg, 0.019 mmol, 0.075 equiv.) was dissolved in *p*-xylene (0.3 mL). Then benzyl alcohol (31 µL, 1.04 g/mL, 0.300 mmol, 1.2 equiv.) and aniline (23 µL, 1.03 g/mL, 0.250 mmol, 1.0 equiv.) were added. The vial was placed in an aluminum block and the resulting reaction mixture was heated in the vial opened to air to 60 °C with magnetic stirring for 15 min, then the vial was loosely capped in order for hydrogen to be able to escape, covered with aluminum foil, and heated to 140 °C for 55 h. After cooling to room temperature, chiral phosphoric acid **2c** (19.3 mg, 0.025 mmol, 0.10 equiv.) was added, followed by the addition of HP(O)(OEt)₂ (35 µL, 1.07 g/mL, 0.275 mmol, 1.1 equiv.). The mixture was stirred for additional 24 h at ambient temperature. The reaction was quenched by addition of sat. NaHCO₃ solution (0.5 mL) and the water layer was extracted with EtOAc (3 × 3 mL). The combined organic layers were dried with MgSO₄ and the solvent was removed under vacuum. Purification via column chromatography (silica, 20–50 % EtOAc in heptane, 0.5 % Et₃N) led to 64 mg (81 %) of diethyl [phenyl(phenylamino)-methyl]phosphonate as white solid.

Acknowledgments

We would like to thank Mr. Adam ElBataoui for the synthesis of phosphoric acids **2d** and **2f** and intermediates for **2g**.

Keywords: Homogeneous catalysis · Organocatalysis · Tandem catalysis · α-Aminophosphonates · Chiral phosphoric acids

- [1] a) R. A. Sheldon, I. W. C. E. Arends, U. Hanefeld, *Green Chemistry and Catalysis*, Wiley-VCH, Weinheim, **2007**; b) R. A. Sheldon, *Chem. Commun.* **2008**, 3352–3365.
- [2] a) M. H. Hamid, P. A. Slatford, J. M. J. Williams, *Adv. Synth. Catal.* **2007**, 349, 1555–1575; b) T. D. Nixon, M. K. Whittlesey, J. M. J. Williams, *Dalton Trans.* **2009**, 753–762; c) M. H. S. A. Hamid, C. L. Allen, G. W. Lamb, A. C. Maxwell, H. C. Maytum, A. J. A. Watson, J. M. J. Williams, *J. Am. Chem. Soc.* **2009**, 131, 1766–1774; d) G. Guillena, D. J. Ramón, M. Yus, *Chem. Rev.* **2010**, 110, 1611–1641; e) G. E. Dobreiner, R. H. Crabtree, *Chem. Rev.* **2010**, 110, 681–703; f) Y. Obora, *ACS Catal.* **2014**, 4, 3972–3981; g) A. Corma, J. Navas, M. J. Sabater, *Chem. Rev.* **2018**, 118, 1410–1459; h) T. Irrgang, R. Kempe, *Chem. Rev.* **2019**, 119, 2524–2549; i) B. G. Reed-Berendt, K. Polidano, L. C. Morrill, *Org. Biomol. Chem.* **2019**, 17, 1595–1607.
- [3] a) A. Quintard, T. Constantieux, J. Rodriguez, *Angew. Chem. Int. Ed.* **2013**, 52, 12883–12887; *Angew. Chem.* **2013**, 125, 13121–13125; b) M. Roudier, T. Constantieux, A. Quintard, J. Rodriguez, *Org. Lett.* **2014**, 16, 2802–2805; c) M. Roudier, T. Constantieux, A. Quintard, J. Rodriguez, *ACS Catal.* **2016**, 6, 5236–5244; d) M. Roudier, T. Constantieux, J. Rodriguez, A. Quintard, *Chimia* **2016**, 70, 97–101; e) A. Quintard, J. Rodriguez, *ChemSusChem* **2016**, 9, 28–30; f) A. Quintard, M. Roudier, J. Rodriguez, *Synthesis* **2018**, 50, 785–792.
- [4] a) S. Zhou, S. Fleischer, K. Junge, M. Beller, *Angew. Chem. Int. Ed.* **2011**, 50, 5120–5124; *Angew. Chem.* **2011**, 123, 5226–5230; b) S. Fleischer, S. Zhou, S. Werkmeister, K. Junge, M. Beller, *Chem. Eur. J.* **2013**, 19, 4997–5003.
- [5] a) Y. Zhang, C. S. Lim, D. S. B. Sim, H. J. Pan, Y. Zhao, *Angew. Chem. Int. Ed.* **2014**, 53, 1399–1403; *Angew. Chem.* **2014**, 126, 1423–1427; b) Z.-Q. Rong, Y. Zhang, R. H. B. Chua, H.-J. Pan, Y. Zhao, *J. Am. Chem. Soc.* **2015**, 137, 4944–4947; c) C. S. Lim, T. T. Quach, Y. Zhao, *Angew. Chem. Int. Ed.* **2017**, 56, 7176–7180; *Angew. Chem.* **2017**, 129, 7282–7286.

- [6] a) H.-J. Knölker, J. Heber, C. H. Mahler, *Synlett* **1992**, 12, 1002–1004; b) H.-J. Knölker, H. Goesmann, R. Klauss, *Angew. Chem. Int. Ed.* **1999**, 38, 702–705; *Angew. Chem.* **1999**, 111, 727–731; c) H.-J. Knölker, E. Baum, H. Goesmann, R. Klauss, *Angew. Chem. Int. Ed.* **1999**, 38, 2064–2066; *Angew. Chem.* **1999**, 111, 2196–2199. For a review specifically on iron cyclopentadienone complexes see: A. Quintard, J. Rodriguez, *Angew. Chem. Int. Ed.* **2014**, 53, 4044–4055; *Angew. Chem.* **2014**, 126, 4124–4136.
- [7] a) C. Bolm, J. Legros, J. Le Pailh, L. Zani, *Chem. Rev.* **2004**, 104, 6217–6254; b) E. B. Bauer, *Curr. Org. Synth.* **2008**, 5, 1341–1369; c) K. Junge, K. Schröder, M. Beller, *Chem. Commun.* **2011**, 47, 4849–4859; d) I. Bauer, H.-J. Knölker, *Chem. Rev.* **2015**, 115, 3170–3387; e) A. Fürstner, *ACS Cent. Sci.* **2016**, 2, 778–789; f) J.-L. Renaud, S. Gaillard, *Synthesis* **2016**, 48, 3659–3683; g) F. Kallmeier, R. Kempe, *Angew. Chem. Int. Ed.* **2018**, 57, 46–60; *Angew. Chem.* **2018**, 130, 48–63; h) D. Wei, C. Darcel, *Chem. Rev.* **2019**, 119, 2550–2610.
- [8] a) K. S. Egorova, V. P. Ananikov, *Angew. Chem. Int. Ed.* **2016**, 55, 12150–12162; *Angew. Chem.* **2016**, 128, 12334–12347; b) K. S. Egorova, V. P. Ananikov, *Organometallics* **2017**, 36, 4071–4090.
- [9] a) A. C. Rafael, I. G. Vladimir, *Russ. Chem. Rev.* **1998**, 67, 857–882; b) X. Cheng, R. Goddard, G. Buth, B. List, *Angew. Chem. Int. Ed.* **2008**, 47, 5079–5081; *Angew. Chem.* **2008**, 120, 5157–5159; c) N. S. Zefirov, E. D. Matveeva, *ARKIVOC* **2008**, 1–17; d) G. Keglevich, E. Bálint, *Molecules* **2012**, 17, 12821–12835.
- [10] For references on the application of α -aminophosphonates see: a) F. R. Atherton, M. J. Hall, C. H. Hassall, R. W. Lambert, W. J. Lloyd, P. S. Ringrose, *Antimicrob. Agents Chemother.* **1979**, 15, 696–705; b) A. B. Smith, K. M. Yager, C. M. Taylor, *J. Am. Chem. Soc.* **1995**, 117, 10879–10888; c) F. Orsini, G. Sello, M. Sisti, *Curr. Med. Chem.* **2010**, 17, 264–289. For references on the synthesis of α -aminophosphonates see: d) C. Qian, T. Huang, *J. Org. Chem.* **1998**, 63, 4125–4128; e) E. Haak, I. Bytschkov, S. Doye, *Eur. J. Org. Chem.* **2002**, 457–463; f) G. D. Joly, E. N. Jacobsen, *J. Am. Chem. Soc.* **2004**, 126, 4102–4103; g) L. O. Irina, E. V. Matveeva, *Russ. Chem. Rev.* **2012**, 81, 221–238.
- [11] B. Kaboudin, F. Kazemi, N. K. Hosseini, *Res. Chem. Intermed.* **2017**, 43, 4475–4486.
- [12] H. Sun, F.-Z. Su, J. Ni, Y. Cao, H.-Y. He, K.-N. Fan, *Angew. Chem. Int. Ed.* **2009**, 48, 4390–4393; *Angew. Chem.* **2009**, 121, 4454–4457.
- [13] a) T. Akiyama, H. Morita, J. Itoh, K. Fuchibe, *Org. Lett.* **2005**, 7, 2583–2585; b) T. Akiyama, H. Morita, P. Bachu, K. Mori, M. Yamanaka, T. Hirata, *Tetrahedron* **2009**, 65, 4950–4956; c) L. Wang, S. Cui, W. Meng, G. Zhang, J. Nie, J. Ma, *Chin. Sci. Bull.* **2010**, 55, 1729–1731.
- [14] For the application of Knölker's complex and related iron cyclopentadienone complexes in the N-alkylation of amines with alcohols see: a) T. Yan, B. L. Feringa, K. Barta, *Nat. Commun.* **2014**, 5, 5602–5609; b) A. J. Rawlings, L. J. Diorazio, M. Wills, *Org. Lett.* **2015**, 17, 1086–1089; c) H.-J. Pan, T. W. Ng, Y. Zhao, *Chem. Commun.* **2015**, 51, 11907–11910; d) T. Yan, B. L. Feringa, K. Barta, *ACS Catal.* **2016**, 6, 381–388; e) B. Emayavaramban, M. Roy, B. Sundararaju, *Chem. Eur. J.* **2016**, 22, 3952–3955; f) T. Yan, B. L. Feringa, K. Barta, *Sci. Adv.* **2017**, 3, eaao6494; g) T. J. Brown, M. Cumbe, L. J. Diorazio, G. J. Clarkson, M. Wills, *J. Org. Chem.* **2017**, 82, 10489–10503; h) A. Lator, S. Gaillard, A. Poater, J. L. Renaud, *Org. Lett.* **2018**, 20, 5985–5990; i) K. Polidano, B. D. W. Allen, J. M. J. Williams, L. C. Morrill, *ACS Catal.* **2018**, 8, 6440–6445. For the application of iron cyclopentadienone complexes in the reductive ethylation of Imines with ethanol see: M. Vayer, S. P. Morcillo, J. Dupont, V. Gandon, C. Bour, *Angew. Chem. Int. Ed.* **2018**, 57, 3228–3232; *Angew. Chem.* **2018**, 130, 3282–3286. For the application of Knölker's complex in the synthesis of pyrrols via dehydrogenative condensation see: B. Emayavaramban, M. Sen, B. Sundararaju, *Org. Lett.* **2017**, 19, 6–9.
- [15] a) M. Mastalir, M. Glatz, N. Gorgas, B. Stöger, E. Pittenauer, G. Allmaier, L. F. Veiros, K. Kirchner, *Chem. Eur. J.* **2016**, 22, 12316–12320; b) A. Mukherjee, A. Nerush, G. Leitun, L. J. W. Shimon, Y. Ben-David, N. A. E. Jalapa, D. Milstein, *J. Am. Chem. Soc.* **2016**, 138, 4298–4301.
- [16] a) T. N. Plank, J. L. Drake, D. K. Kim, T. W. Funk, *Adv. Synth. Catal.* **2012**, 354, 597–601; b) T. N. Plank, J. L. Drake, D. K. Kim, T. W. Funk, *Adv. Synth. Catal.* **2012**, 354, 1179–1179; c) M. Kamitani, Y. Nishiguchi, R. Tada, M. Itazaki, H. Nakazawa, *Organometallics* **2014**, 33, 1532–1535.
- [17] S. Elangovan, J.-B. Sortais, M. Beller, C. Darcel, *Angew. Chem. Int. Ed.* **2015**, 54, 14483–14486; *Angew. Chem.* **2015**, 127, 14691–14694.
- [18] A. Chakraborty, R. G. Kinney, J. A. Krause, H. Guan, *ACS Catal.* **2016**, 6, 7855–7864.
- [19] It should be noted that the hydride species **1c** is prone to decomposition when exposed to air and daylight, see ref.^[6c] however, decomposition of complex **1b** is much slower, see ref.^[6b] As a precaution the reaction vials were heated in an aluminum block and covered with aluminum foil to reduce exposure to daylight. Although partial decomposition of the catalyst in the open system cannot be ruled out, catalytic turnover was noticeable for at least 55 h and some substrates form N-alkylation products even in the open system. These observations suggest a greater robustness of the catalyst system in air under the catalytic conditions.
- [20] For examples of oxidative quenching of bifunctional iridium catalysts see: a) Z. M. Heiden, T. B. Rauchfuss, *J. Am. Chem. Soc.* **2007**, 129, 14303–14310; b) S. Arita, T. Koike, Y. Kayaki, T. Ikariya, *Angew. Chem. Int. Ed.* **2008**, 47, 2447–2449; *Angew. Chem.* **2008**, 120, 2481–2483; c) S. Arita, T. Koike, Y. Kayaki, T. Ikariya, *Chem. Asian J.* **2008**, 3, 1479–1485. The oxidation of alcohols by the related Shvo catalyst requires the application of electron-transfer mediators, see for example: d) G.-Z. Wang, U. Andreasson, J.-E. Bäckvall, *J. Chem. Soc., Chem. Commun.* **1994**, 1037–1038; e) G. Csajnyik, A. H. Éll, L. Fadini, B. Pugin, J.-E. Bäckvall, *J. Org. Chem.* **2002**, 67, 1657–1662; f) E. V. Johnston, E. A. Karlsson, L.-H. Tran, B. Åkermark, J.-E. Bäckvall, *Eur. J. Org. Chem.* **2010**, 1971–1976; g) B. P. Babu, Y. Endo, J.-E. Bäckvall, *Chem. Eur. J.* **2012**, 18, 11524–11527. For a review see: h) J. Piera, J.-E. Bäckvall, *Angew. Chem. Int. Ed.* **2008**, 47, 3506–3523; *Angew. Chem.* **2008**, 120, 3558–3576.
- [21] a) S. J. Connon, *Angew. Chem. Int. Ed.* **2006**, 45, 3909–3912; *Angew. Chem.* **2006**, 118, 4013–4016; b) T. Akiyama, J. Itoh, K. Fuchibe, *Adv. Synth. Catal.* **2006**, 348, 999–1010; c) M. Terada, *Synthesis* **2010**, 1929–1982.
- [22] a) K. D. Troev, *Polyphosphoesters*, Elsevier, Oxford, **2012**, pp. 1–127; b) P. Christ, A. G. Lindsay, S. S. Vormittag, J.-M. Neudörfl, A. Berkessel, A. C. O'Donoghue, *Chem. Eur. J.* **2011**, 17, 8524–8528.
- [23] L. Qin, P. Wang, Y. Zhang, Z. Ren, X. Zhang, C.-S. Da, *Synlett* **2016**, 27, 571–574.
- [24] M. Yamanaka, J. Itoh, K. Fuchibe, T. Akiyama, *J. Am. Chem. Soc.* **2007**, 129, 6756–6764.
- [25] X.-L. Liu, Z.-B. Yu, B.-W. Pan, L. Chen, T.-T. Feng, Y. Zhou, *J. Heterocycl. Chem.* **2015**, 52, 628–634.
- [26] M. Rueping, E. Sugiono, C. Azap, T. Theissmann, M. Bolte, *Org. Lett.* **2005**, 7, 3781–3783.
- [27] F. Romanov-Mikhailidis, M. Romanova-Michaelides, M. Pupier, A. Alexakis, *Chem. Eur. J.* **2015**, 21, 5561–5583.

Received: February 7, 2019

Supporting Information

1. General Information

Toluene and *p*-xylene were distilled from sodium benzophenone ketyl. Alcohols and phosphites used as substrates for catalysis were distilled from Na₂SO₄. Amines used as substrates for catalysis were distilled from CaH₂. If not mentioned differently all commercially available starting materials were used without further purification.

All ¹H, ¹³C and ³¹P NMR spectra were recorded on a Bruker Ultrashield™ 400 or 600 Plus instrument, whereby the ¹H NMR spectra were measured at 400.3 MHz or 600.2 MHz, the ¹³C NMR spectra at 100.6 or 150.9 MHz and the ³¹P NMR spectra at 162.0 MHz. All chemical shifts are noted in ppm. ¹H and ¹³C chemical shifts are indicated relative to TMS and were referenced to residual signals of the solvent (¹H NMR (CDCl₃): 7.27 ppm, ¹³C NMR (CDCl₃): 77.0 ppm). ³¹P chemical shifts were referenced to H₃PO₄ (0.00 ppm). Column chromatography was performed by using Biotage® SP4 and Isolera flash systems and the applied columns were packed with silica gel 60 Å or aluminium oxide 90 standardised (activity II-III). TLC was performed with commercial Kieselgel 60 F₂₅₄ or ALOX N/UV₂₅₄ and visualized *via* UV lamp. GC/MS measurements were conducted on an Agilent Technologies with 5977B MSD High Efficiency Source and a 7820A GC-system equipped with a *HP-5MS* column (30 m, 250 µm, 0.25 µm). GC/FID measurements were conducted on a Shimadzu GC-2010 system equipped with a *HP-5* column (30 m, 320 µm, 0.25 µm). HPLC measurements were conducted on an Agilent Technologies Series 1200 system with 61379B Degasser, 61311A QuatPump, 61329A LLS, 61316A TCC, G1315D DAD.

The Knölker complexes **1a**,^[1] **1b**,^[2,3] and **1c**^[4] were synthesized according to the literature, as well as the chiral BINOL-based phosphoric acids **2a**,^[5] **2b**,^[5] **2c**,^[5] **2d**,^[6] **2e**,^[7] **2f**,^[8] **2g**.^[9]

2. Catalytic Screenings

2.1. Catalytic Activity

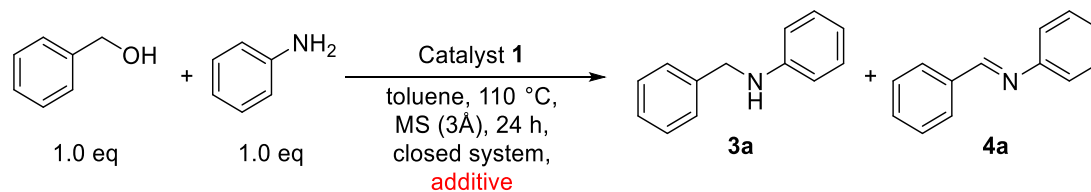


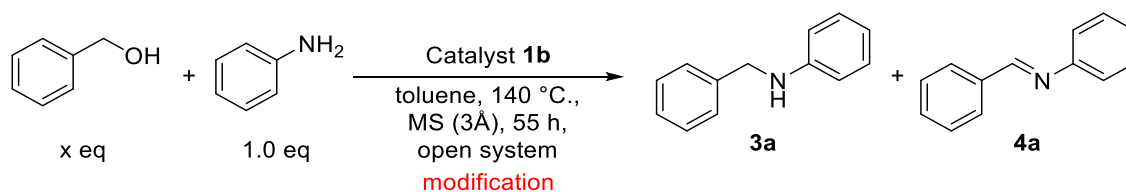
Table S1. Comparison of Catalytic Activity of Complexes **1a**, **1b** and **1c**.

#	Catalyst ([mol%])	Additive ([mol%])	Conversion ^[a] [%]		
			Overall	Amine 3a	Imine 4a
1	1a (10)	---	<1	<1	<1
2	1a (10)	<i>KOtBu</i> (100)	92	77	15
3	1a (10)	<i>KOtBu</i> (20)	18	8	10
4	1a (10)	KH (100)	quant.	94	6
5	1a (10)	KH (50)	79	72	7
6	1b (5)	---	quant.	>99	<1
7	1b (3)	---	93	93	<1
8	1b (5)	KH (50)	47	25	22
9	1c (5)	---	95	95	<5
10	1c (3)	---	74	59	15

Reaction conditions: x mol% **1**, 150 mg molecular sieves (3 Å), 0.250 mmol benzyl alcohol, 0.250 mmol aniline, 0.3 mL toluene, 110 °C, 24 h, closed system under inert conditions.

[a] Conversion was determined via GC/MS and GC/FID using mesitylene as internal standard.

2.2. Selectivity Studies

**Table S2.** Selective imine formation.

#	Catalyst 1b [mol%]	Alcohol [equiv]	Modification	Conversion ^[a] [%]		
				Overall	Amine 3a	Imine 4a
1	5.0	1.0	24 h	47	7	40
2	7.5	1.0	24 h	63	9	54
3	7.5	1.0	---	94	16	78
4	7.5	1.0	<i>p</i>-xylene (solvent)	quant.	17	83
5	7.5	1.0	without MS (3Å)	10	6	4
6	7.5	1.2	---	93	20	73
7	7.5	1.5	---	91	25	66
8	7.5	1.0	48 h	87	14	73
9	10.0	1.0	48 h	94	15	79
10	5.0	1.0	110°C, 24 h, closed, argon	quant.	>99	<1
11	5.0	1.0	110°C, 24 h, closed, <i>L</i> -proline (10 mol%) argon	quant.	86	14
12	5.0	1.0	110°C, 24 h, closed, argon, KH (10 mol%)	47	25	22

Reaction conditions: x mol% **1b**, 150 mg molecular sieves (3 Å), x equiv benzyl alcohol, 0.250 mmol aniline, 0.3 mL toluene, open system under atmospheric conditions.

[a] Conversion was determined *via* GC/FID using mesitylene as internal standard.

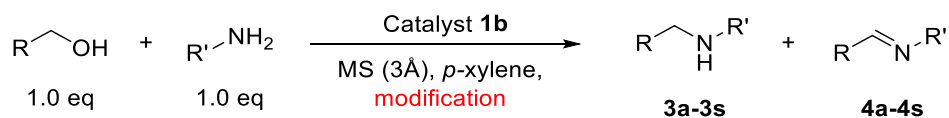


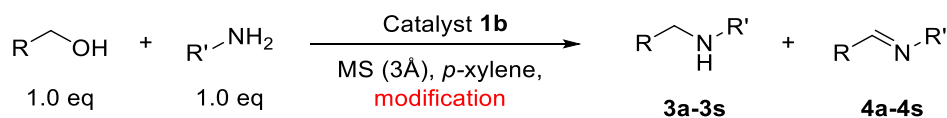
Table S3A. Substrate Screening 1 – selective amine formation.

#	Amine (product)	Conversion ^[a] [%]	Imine (by-product)	Conversion ^[a] [%]	Ratio 3 : 4
1	3a	>99	4a	<1	only 3
2	3b	75	4b	15	5.0 : 1
3	3c	100	4c	<1	only 3
4	3d	24	4d	30	0.8 : 1
5	3e ^[b]	94	4e	<1	only 3
6	3f	96	4f	4	24.0 : 1
7	3g	91	4g	5	18.2 : 1
8	3h	71	4h	11	6.5 : 1
9	3i	>99	4i	<1	only 3
10	3j	97	4j	3	32.3 : 1
11	3k	67	4k	<1	only 3
12	3l	47	4l	<1	only 3
13	3m ^[c]	91	4m	<1	only 3
14	3n	>99	4n	<1	only 3
15	3o	95	4o	<1	only 3
16	3p ^[c]	100	4p	<1	only 3
17	3q	36	4q	64	0.6 : 1
18	3r	85	4r	5	10.6 : 1
19	3s	86	4s	10	8.6 : 1

Reaction conditions:

A) selective formation of amine: 5 mol% Knölker's complex **1b**, 150 mg molecular sieves (3Å), 0.250 mmol alcohol, 0.250 mmol aniline, 0.3 mL *p*-xylene, 110 °C, 24 h, closed system under inert conditions.

[a] Conversion was determined *via* GC/FID using mesitylene as internal standard. [b] NMR-yield. [c] Reaction temperature: 130 °C.

**Table S3B.** Substrate Screening 1 – selective imine formation.(B) Selective formation of imines **3**

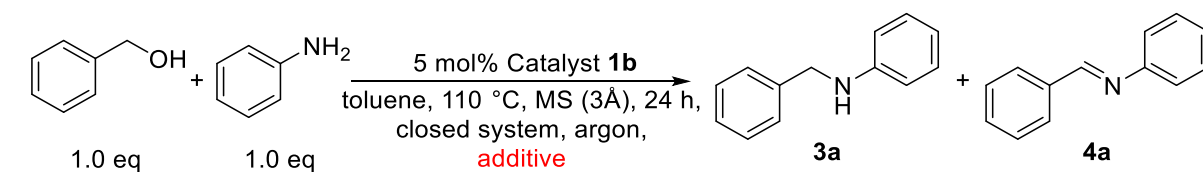
#	Amine (by-product)	Conversion ^[a] [%]	Imine (product)	Conversion ^[a] [%]	Ratio 3 : 4
1	3a	17	4a	83	1 : 4.9
2	3b	10	4b	90	1 : 9.0
3	3c	21	4c	69	1 : 3.3
4	3d	8	4d ^[c]	70	1 : 8.8
5	3e	89	4e ^[b]	11	1 : 0.1
6	3f	14	4f	86	1 : 6.1
7	3g	13	4g	72	1 : 5.5
8	3h	19	4h ^[c]	67	1 : 3.5
9	3i	25	4i	75	1 : 3.0
10	3j	13	4j	77	1 : 5.9
11	3k	51	4k	6	1 : 0.1
12	3l	47	4l	13	1 : 0.3
13	3m	91	4m	9	1 : 0.1
14	3n	63	4n	5	1 : 0.8
15	3o	61	4o ^[d]	<1	only 3
16	3p	60	4p ^[d]	<1	only 3
17	3q	25	4q	75	1 : 3.0
18	3r	51	4r	49	1 : 1.0
19	3s	62	4s	23	1 : 0.4

Reaction conditions:

B) selective formation of imine: 7.5 mol% Knölker's complex **1b**, 150 mg molecular sieves (3Å), 0.300 mmol alcohol, 0.250 mmol aniline, 0.3 mL *p*-xylene, 140 °C, 55 h, open system under atmospheric conditions.

[a] Conversion was determined *via* GC/FID using mesitylene as internal standard. [b] NMR-yield. [c] Reaction time: 92 h. [d] Polymerization products of the imine were found as by-products.

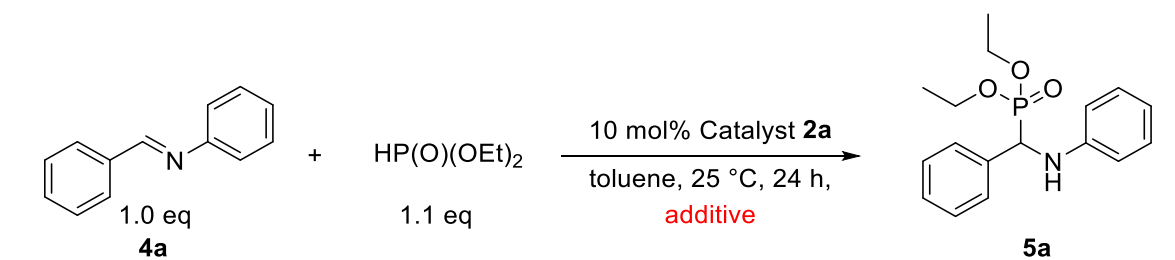
2.3. Compatibility Studies

**Table S4.** Compatibility Studies – N-alkylation.

#	Additive ([equiv])	Conversion ^[a] [%]		
		Overall	Amine 3a	Imine 4a
1	none	>99	>99	<1
2	HP(O)(OEt) ₂ (1.1)	72	72	<1
3	2a (0.1)	28	22	6
4	HP(O)(OEt) ₂ (1.1) 2a (0.1)	77	77	<1

Reaction conditions: 5 mol% **1b**, 150 mg molecular sieves (3 Å), 0.250 mmol benzyl alcohol, 0.250 mmol aniline, 0.3 mL, toluene, 110 °C, 24 h, closed system under inert conditions.

[a] Conversion was determined *via* GC/FID using mesitylene as internal standard.

**Table S5.** Compatibility Studies – hydrophosphonylation.

#	Additive ([mol%])	Conversion ^[a] [%]
1	none	91
2	aniline (30)	18
3	benzyl alcohol (30)	95
4	1a (5)	89

Reaction conditions: 10 mol% **2a**, 0.250 mmol N-benzylideneaniline, 0.275 mmol diethyl phosphite, 0.3 mL, toluene, 25 °C, 24 h.

[a] Isolated Yield.

3. Optimized Procedures for the tunable *N*-alkylation

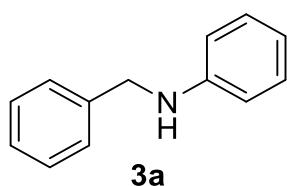
3.1. General procedure for the synthesis of secondary amines **3**

In an argon filled glovebox, a PTFE-lined screw-cap vial (1.5 mL, \varnothing 1 cm, height 3 cm) was charged with Knölker's complex **1b** (5.3 mg, 0.013 mmol, 0.05 equiv), molecular sieves (3 Å, 150 mg), and *p*-xylene (0.3 mL). The complex was dissolved with stirring and then the alcohol (0.250 mmol, 1.0 equiv) and amine (0.250 mmol, 1.0 equiv) were added. The vial was closed tightly, sealed with Teflon tape. The vial was placed in an aluminum block, covered with aluminum foil, and the resulting reaction mixture was heated to 110°C with magnetic stirring for 24 h. After cooling to room temperature, the reaction was quenched by addition of H₂O (0.5 mL). The reactions were analyzed *via* GC/MS and GC/FID analysis. Mesitylene (50 μ L) was used as internal standard.

Exemplary *N*-benzylaniline (**3a**) was isolated and purified:

The water layer was extracted with EtOAc (3 \times 2 mL). The combined organic layers were dried over MgSO₄ and the solvent was removed under vacuum. Purification *via* column chromatography (silica, hept:CH₂Cl₂:Et₃N = 9:1:0.1) led to 42 mg (93%) of *N*-benzylaniline as a slightly yellow oil.

The reaction was scaled up to a 1.000 mmol scale, performed in a tightly closed Schlenk tube, yielding 166 mg (91%) of **3a**.



¹H NMR (400.3 MHz, CDCl₃): δ = 7.31 – 7.46 (m, 4H, aryl-H), 7.28 – 7.32 (m, 1H, aryl-H), 7.11 – 7.24 (m, 2H, aryl-H), 6.73 (t, ³*J*_{H-H} = 7.3 Hz, 1H, aryl-H), 6.58 – 6.69 (m, 2H, aryl-H), 4.37 (d, ³*J*_{H-H} = 5.6 Hz, 2H, CH₂), 4.02 (br s, 1H);

¹³C{¹H} NMR (100.6 MHz, CDCl₃): δ = 148.2 (C_q), 139.4 (C_q), 129.2 (2 CH), 128.6 (2 CH), 127.5 (2 CH), 127.2 (CH), 117.6 (CH), 112.8 (2 CH, aryl-C), 48.3 (CH₂).

HRMS (ESI): *m/z* Calcd. [C₁₃H₁₄N, M+H]⁺: 184.1121 found; 184.1121.

The NMR spectroscopic data is in agreement with the literature.^[10]

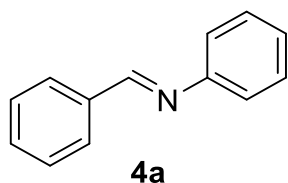
3.2. General procedure for the synthesis of aldimines **4**

In a PTFE-lined screw-cap vial (1.5 mL, \varnothing 1 cm, height 3 cm), equipped with a magnetic stirring bar and molecular sieves (3 Å, 150 mg), Knölker's complex **1b** (8.1 mg, 0.019 mmol, 0.075 equiv) was dissolved in *p*-xylene (0.3 mL). Then, the alcohol (0.300 mmol, 1.2 equiv) and amine (0.250 mmol, 1.0 equiv) were added. The vial was placed in an aluminum block, and the resulting reaction mixture was heated in the vial opened to air to 60°C with magnetic stirring for 15 min, then the vial was loosely capped in order for hydrogen to be able to escape, covered with aluminum foil, and heated to 140°C for 55 h. After cooling to room temperature, the reaction was quenched by addition of H₂O (0.5 mL). The reactions were analyzed *via* GC/MS and GC/FID analysis. Mesitylene (50 μ L) was used as internal standard.

Exemplary *N*-benzylideneaniline (**4a**) was isolated and purified:

The water layer was extracted with EtOAc (3 \times 2 mL). The combined organic layers were dried over MgSO₄ and the solvent was removed under vacuum. Purification *via* column chromatography (silica, hept:CH₂Cl₂:Et₃N = 9:1:0.1) led to 37 mg (82%) of *N*-benzylideneaniline as a slightly yellow solid.

The reaction was scaled up to a 1.000 mmol scale, performed in a round bottom flask equipped with a condenser, yielding 147 mg (81%) of **4a**.



¹H NMR (400.3 MHz, CDCl₃): δ = 8.48 (s, 1H, CHN), 7.85 – 8.01 (m, 2H, aryl-H), 7.46 – 7.59 (m, 3H, aryl-H), 7.36 – 7.46 (m, 2H, aryl-H), 7.14 – 7.30 (m, 3H, aryl-H);

¹³C{¹H} NMR (100.6 MHz, CDCl₃): δ = 160.4 (CHN), 152.1 (C_q), 136.2 (C_q), 131.4 (CH), 129.1 (2 CH), 128.8 (2 CH), 128.7 (2 CH), 125.9 (CH), 120.9 (2 CH, aryl-C).

HRMS (ESI): m/z Calcd. [C₁₃H₁₂N, M+H]⁺: 182.0964 found; 182.0967.

The NMR spectroscopic data is in agreement with the literature.^[11]

4. Hydrophosphonylation of *N*-benzylideneaniline

4.1. General procedure for the hydrophosphonylation of *N*-benzylideneaniline

In a PTFE-lined screw-cap vial (1.5 mL, \varnothing 1 cm, height 3 cm), equipped with a magnetic stirring bar *N*-benzylideneaniline (45.3 mg, 0.250 mmol, 1.0 equiv) was dissolved in toluene (0.3 mL). Then, chiral phosphoric acid **2** (0.025 mmol, 0.10 equiv) was added, followed by the addition of phosphite (0.275 mmol, 1.1 equiv). The mixture was stirred for additional 24 h at ambient temperature. The reaction was quenched by addition of sat. NaHCO₃-solution (0.5 mL) and the water layer was extracted with EtOAc (3 \times 3 mL). The combined organic layers were dried over MgSO₄ and the solvent was removed under vacuum. Purification *via* column chromatography (silica, 20 – 50% EtOAc in heptane, 0.5% Et₃N) led to the respective α -amino phosphonate.

5. Synthesis and characterization of α -amino phosphonates

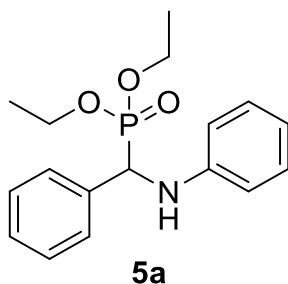
5.1. General procedure for the synthesis of α -amino phosphonates:

In a PTFE-lined screw-cap vial (1.5 mL, \varnothing 1 cm, height 3 cm), equipped with a magnetic stirring bar and molecular sieves (3 Å, 150 mg), Knölker's complex **1b** (8.1 mg, 0.019 mmol, 0.075 equiv) was dissolved in *p*-xylene (0.3 mL). Then alcohol (0.300 mmol, 1.2 equiv) and amine (0.250 mmol, 1.0 equiv) were added. The vial was placed in an aluminum block and the resulting reaction mixture was heated in the vial opened to air to 60 °C with magnetic stirring for 15 min, then the vial was loosely capped in order for hydrogen to be able to escape, covered with aluminum foil, and heated to 140°C for 55 h. After cooling to room temperature, chiral phosphoric acid **2c** (19.3 mg, 0.025 mmol, 0.10 equiv) was added, followed by the addition of phosphite (0.275 mmol, 1.1 equiv). The mixture was stirred for additional 24 h at ambient temperature. The reaction was quenched by addition of sat. NaHCO₃-solution (0.5 mL) and the water layer was extracted with EtOAc (3 × 3 mL). The combined organic layers were dried over MgSO₄ and the solvent was removed under vacuum. Purification *via* column chromatography (silica, 20 – 50% EtOAc in heptane, 0.5% Et₃N) led to the respective α -amino phosphonate.

5.2. Spectroscopic data for α -amino phosphonates

Diethyl (phenyl(phenylamino)methyl)phosphonate (**5a**)

81% yield;



¹H NMR (400.3 MHz, CDCl₃): δ = 7.44 – 7.52 (m, 2H, aryl-H), 7.31 – 7.38 (m, 2H, aryl-H), 7.27 – 7.31 (m, 1H, aryl-H), 7.06 – 7.17 (m, 2H, aryl-H), 6.67 – 6.73 (m, 1H, aryl-H), 6.57 – 6.63 (m, 2H, aryl-H), 4.68 – 4.86 (m, 2H, CHP, NH), 4.04 – 4.20 (m, 2H, CH₂CH₃), 3.95 (dt, ³J_{H-P} = 10.1 Hz, ³J_{H-H} = 7.1 Hz, 1H, CH₂CH₃), 3.61 – 3.76 (m, 1H, CH₂CH₂CH₃), 1.29 (td, ³J_{H-H} = 7.1 Hz, ⁴J_{H-P} = 0.6 Hz, 3H, CH₂CH₃), 1.12 (td, ³J_{H-H} = 7.1, ⁴J_{H-P} = 0.6 Hz, 3H, CH₂CH₃);

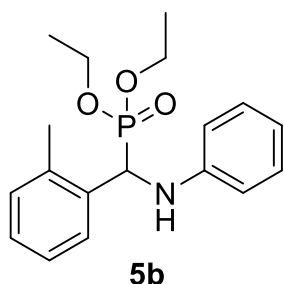
¹³C{¹H} NMR (100.7 MHz, CDCl₃): δ = 146.3 (d, ³J_{C-P} = 14.7 Hz, C_q), 135.9 (d, ²J_{C-P} = 2.9 Hz, C_q), 129.2 (2 CH), 128.6 (d, ⁴J_{C-P} = 2.9 Hz, 2 CH), 127.9 (CH), 127.8 (d, ³J_{C-P} = 5.1 Hz, 2 CH), 118.4 (CH), 113.9 (2 CH, aryl-C), 63.3 (d, ²J_{C-P} = 2.9 Hz, CH₂CH₃), 63.2 (d, ²J_{C-P} = 2.9, CH₂CH₃), 56.1 (d, ¹J_{C-P} = 150.4 Hz, CHP), 16.4 (d, ³J_{C-P} = 5.9 Hz, CH₂CH₃), 16.2 (d, ³J_{C-P} = 5.9 Hz, CH₂CH₃);

³¹P NMR (162.0 MHz, CDCl₃): δ = 22.8.

HRMS (ESI): *m/z* calcd. for [C₁₇H₂₂NO₃PNa, M+Na]⁺: 342.1235; found 342.1234.

The NMR spectroscopic data is in agreement with the literature.^[12]

The reaction was scaled up to a 1.000 mmol scale, performed in a round bottom flask equipped with a condenser, yielding 249 mg (78%) of **5a**.



Diethyl ((phenylamino)(*o*-tolyl)methyl)phosphonate (**5b**)

83% yield;

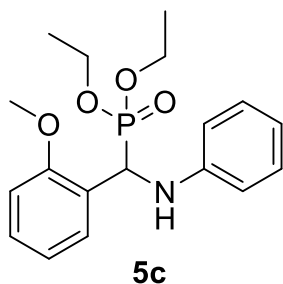
¹H NMR (400.3 MHz, CDCl₃): δ = 7.44 – 7.55 (m, 1H, aryl-H), 7.01 – 7.22 (m, 5H, aryl-H), 6.64 – 6.75 (m, 1H, aryl-H), 6.50 – 6.59 (m, 2H, aryl-H), 5.01 (dd, ²J_{H-P} = 23.7 Hz, ³J_{H-H} = 8.07 Hz, 1H, CHP), 4.83 (t, ³J_{H-H} = 8.7 Hz, 1H, NH), 4.04 – 4.24 (m, 2H, CH₂CH₃), 3.85 – 3.92 (m, 1H, CH₂CH₃), 3.48 – 3.64 (m, 1H, CH₂CH₃), 2.54 (s, 3H, CH₃), 1.31 (t, ³J_{H-H} = 7.0 Hz, 3H, CH₂CH₃), 1.07 (t, *J* = 7.0 Hz, 3H, CH₂CH₃);

$^{13}\text{C}\{^1\text{H}\}$ NMR (100.7 MHz, CDCl_3): δ = 146.3 (d, $^3J_{\text{C-P}}$ = 14.7 Hz, C_q), 136.3 (d, $^3J_{\text{C-P}}$ = 6.6 Hz, C_q), 134.2 (d, $^2J_{\text{C-P}}$ = 2.9 Hz, C_q), 130.5 (d, $^4J_{\text{C-P}}$ = 2.2 Hz, CH), 129.2 (2 CH), 127.7 (d, $^3J_{\text{C-P}}$ = 3.7 Hz, CH), 127.1 (d, $^5J_{\text{C-P}}$ = 4.4 Hz, CH), 126.5 (d, $^4J_{\text{C-P}}$ = 2.9 Hz, CH), 118.3 (CH), 113.5 (2 CH, aryl-C), 63.3 (d, $^2J_{\text{C-P}}$ = 6.6, CH_2CH_3), 63.1 (d, $^2J_{\text{C-P}}$ = 7.3, CH_2CH_3), 52.1 (d, $^1J_{\text{C-P}}$ = 150.1 Hz, CHP), 19.7 (CH₃), 16.4 (d, $^3J_{\text{C-P}}$ = 5.9 Hz, CH_2CH_3), 16.1 (d, $^3J_{\text{C-P}}$ = 5.9 Hz, CH_2CH_3);

^{31}P NMR (162.0 MHz, CDCl_3): δ = 23.6.

HRMS (ESI): m/z Calcd. for $[\text{C}_{18}\text{H}_{24}\text{NO}_3\text{PNa}, \text{M}+\text{Na}]^+$: 356.1386; found 356.1389.

The NMR spectroscopic data is in agreement with the literature.^[13]



Diethyl ((2-methoxyphenyl)(phenylamino)methyl)phosphonate (5c)

63% yield;

^1H NMR (400.3 MHz, CDCl_3): δ = 7.44 – 7.52 (m, 1H, aryl-H), 7.21 – 7.27 (m, 1H, aryl-H), 7.04 – 7.16 (m, 2H, aryl-H), 6.83 – 6.98 (m, 2H, aryl-H), 6.56 – 6.74 (m, 3H, aryl-H), 5.51 (dd, $^2J_{\text{H-H}}$ = 24.6 Hz, $^3J_{\text{H-H}}$ = 9.2 Hz, 1H, CHP), 4.83 (t, $^3J_{\text{H-H}}$ = 8.9 Hz, 1H, NH), 4.05 – 4.28 (m, 2H, CH_2CH_3), 3.79 – 4.03 (m, 1H, CH_2CH_3), 3.94 (s, 3H, CH₃), 3.52 – 3.74 (m, 1H, CH_2CH_3), 1.32 (td, $^3J_{\text{H-H}}$ = 7.1, Hz, $^4J_{\text{H-P}}$ = 0.6 Hz, 3H, CH_2CH_3), 1.05 (td, $^3J_{\text{H-H}}$ = 7.1, Hz,

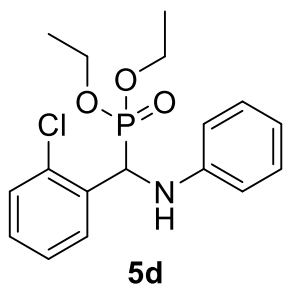
$^4J_{\text{H-P}}$ = 0.6 Hz, 3H, CH_2CH_3);

$^{13}\text{C}\{^1\text{H}\}$ NMR (151.9 MHz, CDCl_3): δ = 157.3 (d, $^3J_{\text{C-P}}$ = 6.1 Hz, C_q), 146.3 (d, $^3J_{\text{C-P}}$ = 14.6 Hz, C_q), 129.1 (2 CH), 128.9 (d, $^5J_{\text{C-P}}$ = 3.0 Hz, CH), 128.2 (d, $^3J_{\text{C-P}}$ = 4.4 Hz, CH), 124.5 (d, $^2J_{\text{C-P}}$ = 1.1 Hz, C_q), 121.0 (d, $^4J_{\text{C-P}}$ = 2.8 Hz, CH), 118.1 (CH), 113.5 (2 CH), 110.4 (d, $^4J_{\text{C-P}}$ = 2.2 Hz, CH, aryl-C), 63.1 (d, $^2J_{\text{C-P}}$ = 7.2 Hz, CH_2CH_3), 63.0 (d, $^2J_{\text{C-P}}$ = 6.9 Hz, CH_2CH_3), 55.7 (OCH₃), 48.0 (d, $^1J_{\text{C-P}}$ = 151.5 Hz, CHP), 16.4 (d, $^3J_{\text{C-P}}$ = 5.8 Hz, CH_2CH_3), 16.1 (d, $^3J_{\text{C-P}}$ = 5.8 Hz, CH_2CH_3);

^{31}P NMR (162.0 MHz, CDCl_3): δ = 23.7.

HRMS (ESI): m/z Calcd. for $[\text{C}_{18}\text{H}_{24}\text{NO}_4\text{PNa}, \text{M}+\text{Na}]^+$: 372.1335; found 372.1340.

The NMR spectroscopic data is in agreement with the literature.^[14]



Diethyl ((2-chlorophenyl)(phenylamino)methyl)phosphonate (5d)

59% yield;

^1H NMR (400.3 MHz, CDCl_3): δ = 7.54 – 7.60 (m, 1H, aryl-H), 7.37 – 7.42 (m, 1H, aryl-H), 7.18 – 7.25 (m, 2H, aryl-H), 7.10 – 7.15 (m, 2H, aryl-H), 6.68 – 6.73 (m, 1H, aryl-H), 6.56 – 6.63 (m, 2H, aryl-H), 5.38 (dd, $^2J_{\text{H-P}}$ = 24.6 Hz, $^3J_{\text{H-H}}$ = 8.6 Hz, 1H, CHP), 4.93 (t, $^3J_{\text{H-H}}$ = 9.2 Hz, 1H, NH), 4.18 – 4.28 (m, 2H, CH_2CH_3), 3.88 – 3.99 (m, 1H, CH_2CH_3), 3.61 – 3.69 (m, 1H, CH_2CH_3),

1.55 (s, 2H, H₂O)*, 1.35 (td, $^3J_{\text{H-H}}$ = 7.1 Hz, $^4J_{\text{H-P}}$ = 0.6 Hz, 3H, CH_2CH_3), 1.08 (td, $^3J_{\text{H-H}}$ = 7.1 Hz, $^4J_{\text{H-P}}$ = 0.6 Hz, 3H, CH_2CH_3);

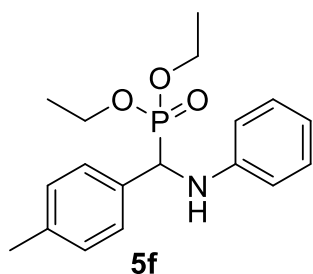
*crystallizes with water from heptane

$^{13}\text{C}\{^1\text{H}\}$ NMR (100.7 MHz, CDCl_3): δ = 145.7 (d, $^3J_{\text{C-P}}$ = 14.7 Hz, C_q), 134.1 (d, $^2J_{\text{C-P}}$ = 2.9 Hz, C_q), 129.4 (d, $^4J_{\text{C-P}}$ = 2.2 Hz, 1 CH), 129.3 (2 CH), 129.1 (d, $^5J_{\text{C-P}}$ = 3.7 Hz, 1 CH), 128.9 (d, $^3J_{\text{C-P}}$ = 4.4 Hz, 1 CH), 128.0 (d, $^3J_{\text{C-P}}$ = 2.2 Hz, C_q), 127.3 (d, $^4J_{\text{C-P}}$ = 2.9 Hz, 1 CH), 118.5 (CH), 113.6 (2 CH, aryl-C), 63.5 (d, $^2J_{\text{C-P}}$ = 2.9 Hz, CH_2CH_3), 63.4 (d, $^2J_{\text{C-P}}$ = 2.9 Hz, CH_2CH_3), 51.6 (d, $^1J_{\text{C-P}}$ = 152.5 Hz, CHP), 16.4 (d, $^3J_{\text{C-P}}$ = 5.9 Hz, CH_2CH_3), 16.1 (d, $^3J_{\text{C-P}}$ = 5.9 Hz, CH_2CH_3);

^{31}P NMR (162.0 MHz, CDCl_3): δ = 22.2.

HRMS (ESI): m/z Calcd. for $[\text{C}_{17}\text{H}_{21}\text{NO}_3\text{PClNa}, \text{M}+\text{Na}]^+$: 376.0840; found 376.0830.

The NMR spectroscopic data is in agreement with the literature.^[15]

Diethyl ((phenylamino)(p-tolyl)methyl)phosphonate (5f)

79% yield;

¹H NMR (400.3 MHz, CDCl₃): δ = 7.31 – 7.40 (m, 2H, aryl-H), 7.09 – 7.15 (m, 4H, aryl-H), 6.64 – 6.75 (m, 1H, aryl-H), 6.60 (m, 2H, aryl-H), 4.64 – 4.87 (m, 2H, CHP, NH), 4.03 – 4.22 (m, 2H, CH₂CH₃), 3.91 – 4.01 (m, 1H, CH₂CH₃), 3.71 (m, 1H, CH₂CH₃), 3.32 (s, 3H, CH₃), 1.29 (t, ³J_{H-H} = 7.1 Hz, 3H, CH₂CH₃), 1.14 (t, ³J_{H-H} = 7.1 Hz, 3H, CH₂CH₃);

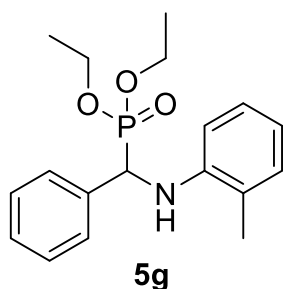
¹³C{¹H} NMR (100.7 MHz, CDCl₃): δ = 146.4 (d, ³J_{C-P} = 14.7 Hz, C_q), 137.6 (d, ⁵J_{C-P} = 3.7 Hz, C_q), 132.7 (d, ²J_{C-P} = 2.9 Hz, C_q), 129.3 (d, ⁴J_{C-P} = 2.9 Hz, 2 CH), 129.1 (2 CH), 127.7

(d, ³J_{C-P} = 5.9 Hz, 2 CH), 118.3 (CH), 113.9 (2 CH, aryl-C), 63.22 (d, ²J_{C-P} = 2.9 Hz, CH₂CH₃), 63.16 (d, ²J_{C-P} = 2.9 Hz, CH₂CH₃), 55.8 (d, ¹J_{C-P} = 151.1 Hz, CHP), 21.1 (CH₃), 16.4 (d, ³J_{C-P} = 5.9 Hz, CH₂CH₃), 16.2 (d, ³J_{C-P} = 5.1 Hz, CH₂CH₃);

³¹P NMR (162.0 MHz, CDCl₃): δ = 23.0.

HRMS (ESI): m/z Calcd. for [C₁₈H₂₄NO₃PNa, M+Na]⁺: 356.1386; found 356.1393.

The NMR spectroscopic data is in agreement with the literature.^[16]

Diethyl (phenyl(o-tolylamino)methyl)phosphonate (5g)

68% yield;

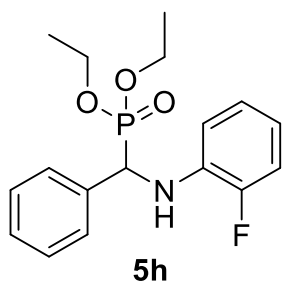
¹H NMR (400.3 MHz, CDCl₃): δ = 7.47 – 7.49 (m, 2H, aryl-H), 7.25 – 7.36 (m, 3H, aryl-H), 7.06 – 7.08 (m, 1H, aryl-H), 6.94 – 6.98 (m, 1H, aryl-H), 6.63 – 6.67 (m, 1H, aryl-H), 6.40 – 6.42 (m, 1H, aryl-H), 4.81 (dd, ²J_{H-P} = 24.0 Hz, ³J_{H-H} = 7.1 Hz, 1H, CHP), 4.65 – 4.69 (m, 1H, NH), 4.05 – 4.19 (m, 2H, CH₂CH₃), 3.92 – 4.00 (m, 1H, CH₂CH₃), 3.67 – 3.77 (m, 1H, CH₂CH₃), 2.29 (s, 3H), 1.29 (t, ³J_{H-H} = 7.1 Hz, 3H, CH₂CH₃), 1.14 (t, ³J_{H-H} = 7.1 Hz, 3H, CH₂CH₃);

¹³C{¹H} NMR (100.7 MHz, CDCl₃): δ = 144.3 (d, ³J_{C-P} = 13.9 Hz, C_q), 136.0 (d, ²J_{C-P} = 2.9 Hz, C_q), 130.2 (CH), 128.6 (d, ⁴J_{C-P} = 2.9 Hz, 2 CH), 127.9 (d, ⁵J_{C-P} = 3.7 Hz, CH), 127.7 (d, ³J_{C-P} = 5.1 Hz, 2 CH), 126.9 (CH), 126.0 (C_q), 118.0 (CH), 111.3 (CH, aryl-C), 63.3 (d, ²J_{C-P} = 2.2 Hz, CH₂CH₃), 63.2 (d, ²J_{C-P} = 2.2 Hz, CH₂CH₃), 56.1 (d, ¹J_{C-P} = 150.3 Hz, CHP), 17.5 (CH₃), 16.4 (d, ³J_{C-P} = 5.9 Hz, CH₂CH₃), 16.2 (d, ³J_{C-P} = 5.1 Hz, CH₂CH₃);

³¹P NMR (162.0 MHz, CDCl₃): δ = 22.0.

HRMS (ESI): m/z Calcd. for [C₁₈H₂₄NO₃PNa, N+Na]⁺: 356.1386; found 356.1388.

The NMR spectroscopic data is in agreement with the literature.^[17]

**Diethyl (((2-fluorophenyl)amino)(phenyl)methyl)phosphonate (5h)**

58% yield;

¹H NMR (400.3 MHz, CDCl₃): δ = 7.47 – 7.49 (m, 2H, aryl-H), 7.33 – 7.38 (m, 3H, aryl-H), 6.95 – 7.00 (m, 1H, aryl-H), 6.83 – 6.87 (m, 1H, aryl-H), 6.60 – 6.66 (m, 1H, aryl-H), 6.49 – 6.53 (m, 1H, aryl-H), 4.97 – 5.02 (m, 1H, NH), 4.75 (dd, ²J_{H-P} = 24.0 Hz, ³J_{H-H} = 7.8 Hz, 1H, CHP), 4.05 – 4.17 (m, 2H, CH₂CH₃), 3.94 – 4.02 (m, 1H, CH₂CH₃), 3.74 – 3.80 (m, 1H, CH₂CH₃), 1.29 (td, ³J_{H-H} = 7.1, ⁴J_{H-P} = 0.6 Hz, 3H, CH₂CH₃), 1.16 (td, ³J_{H-H} = 7.1,

⁴J_{H-P} = 0.6 Hz, 3H, CH₂CH₃);

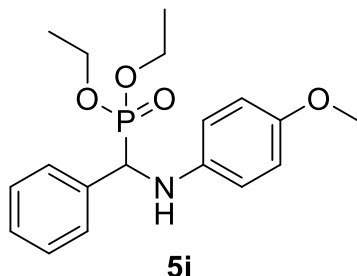
¹³C{¹H} NMR (100.7 MHz, CDCl₃): δ = 151.9 (d, ¹J_{C-F} = 239.6 Hz, C_q), 135.5 (d, ²J_{C-P} = 2.9 Hz, C_q), 134.8 (dd, ³J_{C-P} = 14.6 Hz, ²J_{C-F} = 11.6 Hz, C_q), 128.6 (d, ⁴J_{C-P} = 2.5 Hz, 2 CH), 128.1 (d, ⁵J_{C-P} = 3.0 Hz, CH), 127.8 (d, ³J_{C-P} = 5.5 Hz, 2 CH), 124.4 (d, ⁴J_{C-F} = 3.3 Hz, CH), 118.0 (d, ³J_{C-F} = 7.2 Hz, CH), 114.6 (d, ²J_{C-F} = 18.4 Hz, CH), 113.5 (d, ³J_{C-F} = 2.8 Hz, CH),

aryl-C), 63.4 (d, $^2J_{C-P}$ = 7.0 Hz, CH_2CH_3), 63.3 (d, $^2J_{C-P}$ = 7.0 Hz, CH_2CH_3), 55.9 (d, $^1J_{C-P}$ = 151.1 Hz, CHP), 16.4 (d, $^3J_{C-P}$ = 5.8 Hz, CH_2CH_3), 16.2 (d, $^3J_{C-P}$ = 5.8 Hz, CH_2CH_3);

^{31}P NMR (162.0 MHz, CDCl_3): δ = 22.1.

^{19}F $\{^1\text{H}\}$ NMR (659.0 MHz, CDCl_3): δ = -135.2;

HRMS (ESI): m/z Calcd. for $[\text{C}_{17}\text{H}_{21}\text{NO}_3\text{PNa}, \text{M}+\text{Na}]^+$ 360.1135; found 360.1132.



Diethyl (((4-methoxyphenyl)amino)(phenyl)methyl)phosphonate (**5i**)
70% yield;

^1H NMR (400.3 MHz, CDCl_3): δ = 7.42 – 7.52 (m, 2H, aryl-H), 7.30 – 7.39 (m, 2H, aryl-H), 7.25 – 7.29 (m, 1H, aryl-H), 6.67 – 6.74 (m, 2H, aryl-H), 6.50 – 6.59 (m, 2H, aryl-H), 4.70 (dd, $^2J_{H-P}$ = 23.8 Hz, $^3J_{H-H}$ = 7.68 Hz, 1H, CHP), 4.54 (t, $^3J_{H-H}$ = 8.6 Hz, 1H, NH), 4.04 – 4.20 (m, 2H, CH_2CH_3), 3.86 – 4.02 (m, 1H, CH_2CH_3), 3.66 – 3.74 (m,

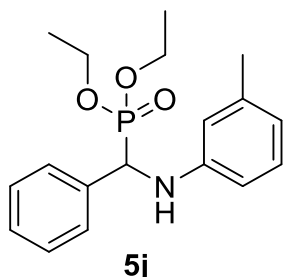
1H, CH_2CH_3), 3.69 (s, 3H, CH₃), 1.29 (t, $^3J_{H-H}$ = 7.0 Hz, 3H, CH_2CH_3), 1.12 (t, $^3J_{H-H}$ = 6.8 Hz, 3H, CH_2CH_3);

$^{13}\text{C}\{^1\text{H}\}$ NMR (100.7 MHz, CDCl_3): δ = 152.7 (C_q), 140.4 (d, $^3J_{C-P}$ = 15.4 Hz, C_q), 136.1 (d, $^2J_{C-P}$ = 2.9 Hz, C_q), 128.6 (d, $^4J_{C-P}$ = 2.9 Hz, 2 CH), 127.87 (d, $^3J_{C-P}$ = 5.9 Hz, 2 CH), 127.86 (CH), 115.2 (2 CH), 114.8 (2 CH, aryl-C), 63.2 (d, $^2J_{C-P}$ = 7.3 Hz, 2 CH_2CH_3), 57.0 (d, $^1J_{C-P}$ = 150.5 Hz, CHP), 55.6 (OCH_3), 16.4 (d, $^3J_{C-P}$ = 5.9 Hz, CH_2CH_3), 16.2 (d, $^3J_{C-P}$ = 5.9 Hz, CH_2CH_3);

^{31}P NMR (162.0 MHz, CDCl_3): δ = 22.9.

HRMS (ESI): m/z Calcd. for $[\text{C}_{18}\text{H}_{24}\text{NO}_4\text{PNa}, \text{M}+\text{Na}]^+$: 372.1335; found 372.1333.

The NMR spectroscopic data is in agreement with the literature.^[18]



Diethyl (phenyl(m-tolylamino)methyl)phosphonate (**5j**)
75% yield;

^1H NMR (400.3 MHz, CDCl_3): δ = 7.34 – 7.56 (m, 2H, aryl-H), 7.23 – 7.38 (m, 3H, aryl-H), 6.96 – 7.03 (m, 1H, aryl-H), 6.36 – 6.60 (m, 3H, aryl-H), 4.65 – 4.85 (m, 2H, CHP, NH), 4.03 – 4.20 (m, 2H, CH_2CH_3), 3.88 – 4.00 (m, 1H, CH_2CH_3), 3.60 – 3.72 (m, 1H, CH_2CH_3), 2.22 (s, 3H, CH₃), 1.29 (t, $^3J_{H-H}$ = 7.1 Hz, 3H), 1.12

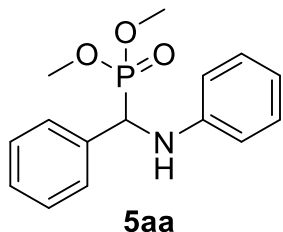
(t, $^3J_{H-H}$ = 7.1 Hz, 3H);

$^{13}\text{C}\{^1\text{H}\}$ NMR (100.7 MHz, CDCl_3): δ = 146.3 (d, $^3J_{C-P}$ = 13.9 Hz, C_q), 138.9 (C_q), 136.0 (d, $^2J_{C-P}$ = 2.9 Hz, C_q), 129.0 (CH), 128.5 (d, $^4J_{C-P}$ = 2.9 Hz, 2 CH), 127.83 (d, $^3J_{C-P}$ = 5.9 Hz, 2 CH), 127.77 (CH), 119.3 (CH), 114.7 (CH), 110.8 (CH, aryl-C), 63.2 (d, $^2J_{C-P}$ = 6.6 Hz, 2 CH_2CH_3), 56.0 (d, $^1J_{C-P}$ = 150.7 Hz, CHP), 21.5 (CH₃), 16.4 (d, $^3J_{C-P}$ = 5.9 Hz, CH_2CH_3), 16.2 (d, $^3J_{C-P}$ = 5.9 Hz, CH_2CH_3);

^{31}P NMR (162.0 MHz, CDCl_3): δ = 22.8.

HRMS (ESI): m/z Calcd. for $[\text{C}_{18}\text{H}_{24}\text{NO}_3\text{PNa}, \text{M}+\text{Na}]^+$: 356.1386, found 356.1386.

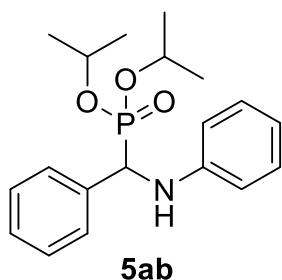
The NMR spectroscopic data is in agreement with the literature.^[15]



Dimethyl (phenyl(phenylamino)methyl)phosphonate (**5aa**)
80% yield;

^1H NMR (400.3 MHz, CDCl_3): δ = 7.44 – 7.52 (m, 2H, aryl-H), 7.32 – 7.41 (m, 2H, aryl-H), 7.28 – 7.32 (m, 1H, aryl-H), 7.08 – 7.18 (m, 2H, aryl-H), 6.67 – 6.75 (m, 1H, aryl-H), 6.58 – 6.64 (m, 2H, aryl-H), 4.81 (d, $^3J_{H-H}$ = 24.4 Hz, 1H, CHP), 4.79 (br s, 1H, NH), 3.75 (d, $^3J_{H-P}$ = 10.6 Hz, 3H, CH₃), 3.49 (d, $^3J_{H-P}$ = 10.5 Hz, 3H, CH₃);

$^{13}\text{C}\{^1\text{H}\}$ NMR (100.7 MHz, CDCl_3): δ = 146.1 (d, $^3J_{\text{C-P}} = 14.7$ Hz, C_q), 135.6 (d, $^2J_{\text{C-P}} = 2.9$ Hz, C_q), 129.2 (2 CH), 128.7 (d, $^4J_{\text{C-P}} = 2.2$ Hz, 2 CH), 128.1 (d, $^5J_{\text{C-P}} = 2.9$ Hz, CH), 127.8 (d, $^3J_{\text{C-P}} = 5.1$ Hz, 2 CH), 118.6 (CH), 113.9 (2 CH, aryl-C), 55.7 (d, $^1J_{\text{C-P}} = 151.3$ Hz, CHP), 53.82 (CH_3), 53.76 (CH_3);



^{31}P NMR (162.0 MHz, CDCl_3): δ = 25.1.

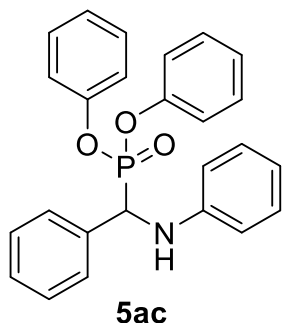
HRMS (ESI): m/z Calcd. for $[\text{C}_{15}\text{H}_{18}\text{NO}_3\text{PNa}, \text{M}+\text{Na}]^+$: 314.0917; found 314.0921.

The NMR spectroscopic data is in agreement with the literature.^[12]

Diisopropyl (phenyl(phenylamino)methyl)phosphonate (5ab)
83% yield;

^1H NMR (400.3 MHz, CDCl_3): δ = 7.44 – 7.52 (m, 2H, aryl-H), 7.29 – 7.37 (m, 2H, aryl-H), 7.22 – 7.29 (m, 1H, aryl-H), 7.06 – 7.16 (m, 2H, aryl-H), 6.65 – 6.73 (m, 1H, aryl-H), 6.57 – 6.62 (m, 2H, aryl-H), 4.63 – 4.86 (m, 3H, $\text{CH}(\text{CH}_3)_2$, CHP, NH), 4.41 – 4.54 (m, 1H, $\text{CH}(\text{CH}_3)_2$), 1.33 (d, $^3J_{\text{H-H}} = 6.2$ Hz, 3H, $\text{CH}(\text{CH}_3)_2$), 1.27 (d, $^3J_{\text{H-H}} = 6.1$ Hz, 3H, $\text{CH}(\text{CH}_3)_2$), 1.23 (d, $^3J_{\text{H-H}} = 6.1$ Hz, 3H, $\text{CH}(\text{CH}_3)_2$), 0.94 (d, $^3J_{\text{H-H}} = 6.1$ Hz, 3H, $\text{CH}(\text{CH}_3)_2$);

$^{13}\text{C}\{^1\text{H}\}$ NMR (100.7 MHz, CDCl_3): δ = 146.6 (d, $^3J_{\text{C-P}} = 14.7$ Hz, C_q), 136.3 (d, $^2J_{\text{C-P}} = 2.9$ Hz, C_q), 129.1 (2 CH), 128.4 (d, $^4J_{\text{C-P}} = 2.9$ Hz, 2 CH), 128.0 (d, $^3J_{\text{C-P}} = 5.1$ Hz, 2 CH), 127.7 (d, $^5J_{\text{C-P}} = 2.9$ Hz, CH), 118.2 (CH), 113.8 (2 CH, aryl-C), 72.0 (d, $^1J_{\text{C-P}} = 7.3$ Hz, CH, $\text{CH}(\text{CH}_3)_2$), 71.9 (d, $^1J_{\text{C-P}} = 7.3$ Hz, CH, $\text{CH}(\text{CH}_3)_2$), 56.6 (d, $^1J_{\text{C-P}} = 151.7$ Hz, CHP), 24.2 (d, $^2J_{\text{C-P}} = 3.7$ Hz, 2 $\text{CH}(\text{CH}_3)_2$), 23.8 (d, $^3J_{\text{C-P}} = 5.1$ Hz, $\text{CH}(\text{CH}_3)_2$), 23.2 (d, $^3J_{\text{C-P}} = 5.9$ Hz, $\text{CH}(\text{CH}_3)_2$);



^{31}P NMR (162.0 MHz, CDCl_3): δ = 21.0.

HRMS (ESI): m/z Calcd. for $[\text{C}_{19}\text{H}_{26}\text{NO}_3\text{PNa}, \text{M}+\text{Na}]^+$: 370.1543; found 370.1551.

The NMR spectroscopic data is in agreement with the literature.^[19]

Diphenyl (phenyl(phenylamino)methyl)phosphonate (5ac)
84% yield;

^1H NMR (400.3 MHz, CDCl_3): δ = 7.50 – 7.67 (m, 2H, aryl-H), 7.26 – 7.42 (m, 5H, aryl-H), 7.04 – 7.25 (m, 8H, aryl-H), 6.83 – 6.93 (m, 2H, aryl-H), 6.72 – 6.80 (m, 1H, aryl-H), 6.62 – 6.70 (m, 2H, aryl-H), 5.16 (dd, $^2J_{\text{H-P}} = 24.6$ Hz, $^3J_{\text{H-H}} = 8.3$ Hz, 1H, CHP), 4.91 (t, $^3J_{\text{H-H}} = 8.9$ Hz, 1H, NH);

$^{13}\text{C}\{^1\text{H}\}$ NMR (100.7 MHz, CDCl_3): δ = 150.3 (d, $^2J_{\text{C-P}} = 9.9$ Hz, C_q), 150.2 (d, $^2J_{\text{C-P}} = 9.9$ Hz, C_q), 145.9 (d, $^3J_{\text{C-P}} = 15.4$ Hz, C_q), 134.8 (d, $^2J_{\text{C-P}} = 2.2$ Hz, C_q), 129.7 (2 CH), 129.6 (2 CH), 129.3 (2 CH), 128.8 (d, $^4J_{\text{C-P}} = 2.9$ Hz, 2 CH), 128.4 (d, $^5J_{\text{C-P}} = 2.9$ Hz, CH), 128.1 (d, $^3J_{\text{C-P}} = 5.9$ Hz, 2 CH), 125.4 (CH), 125.2 (CH), 120.7 (d, $^3J_{\text{C-P}} = 4.1$ Hz, 2 CH), 120.3 (d, $^3J_{\text{C-P}} = 4.1$ Hz, 2 CH), 118.9 (CH), 114.0 (2 CH, aryl-C), 56.1 (d, $^1J_{\text{C-P}} = 153.9$ Hz, CH);

^{31}P NMR (162.0 MHz, CDCl_3): δ = 15.4.

HRMS (ESI): m/z Calcd. for $[\text{C}_{25}\text{H}_{22}\text{NO}_3\text{PNa}, \text{M}+\text{Na}]^+$: 438.1230; found 438.1220.

The NMR spectroscopic data is in agreement with the literature.^[20]

6. Literature

- [1] T. Yan, B. L. Feringa, K. Barta, *ACS Catal.* **2016**, 6, 381–388.
- [2] H.-J. Knölker, H. Goesmann, R. Klauss, *Angew. Chem. Int. Ed.* **1999**, 38, 702–705; *Angew. Chem.* **1999**, 111, 727–731.
- [3] T. N. Plank, J. L. Drake, D. K. Kim, T. W. Funk, *Adv. Synth. Catal.* **2012**, 354, 597–601.
- [4] A. Chakraborty, R. G. Kinney, J. A. Krause, H. Guan, *ACS Catal.* **2016**, 6, 7855–7864.
- [5] L. Qin, P. Wang, Y. Zhang, Z. Ren, X. Zhang, C.-S. Da, *Synlett* **2016**, 27, 571–574.
- [6] M. Yamanaka, J. Itoh, K. Fuchibe, T. Akiyama, *J. Am. Chem. Soc.* **2007**, 129, 6756–6764.
- [7] X.-L. Liu, Z.-B. Yu, B.-W. Pan, L. Chen, T.-T. Feng, Y. Zhou, *J. Heterocyclic Chem.* **2015**, 52, 628–634.
- [8] L. Bernardi, G. Bolzoni, M. Fochi, M. Mancinelli, A. Mazzanti, *Eur. J. Org. Chem.* **2016**, 2016, 3208–3216.
- [9] F. Romanov-Michailidis, M. Romanova-Michaelides, M. Pupier, A. Alexakis, *Chem. Eur. J.* **2015**, 21, 5561–5583.
- [10] J. Zheng, T. Roisnel, C. Darcel, J.-B. Sortais, *ChemCatChem* **2013**, 5, 2861–2864.
- [11] M. De Rosa, G. Vigliotta, G. Palma, C. Saturnino, A. Soriente, *Molecules* **2015**, 20, 22044–22057.
- [12] X.-C. Li, S.-S. Gong, D.-Y. Zeng, Y.-H. You, Q. Sun, *Tetrahedron Lett.* **2016**, 57, 1782–1785.
- [13] X. Wang, Y. Cai, J. Chen, F. Verpoort, *Phosphorus, Sulfur Silicon Relat. Elem.* **2016**, 191, 1268–1273.
- [14] Z. P. Zhan, J. P. Li, *Synth. Commun.* **2005**, 35, 2501–2508.
- [15] K. Ramakrishna, J. M. Thomas, C. Sivasankar, *J. Org. Chem.* **2016**, 81, 9826–9835.
- [16] K. Babak, Z. Hazegh, *Chem. Lett.* **2008**, 37, 540–541.
- [17] M. Zahouily, A. Elmakssoudi, A. Mezdar, A. Rayadh, S. Sebti, *J. Chem. Res.* **2005**, 2005, 324–327.
- [18] J. Wu, W. Sun, H.-G. Xia, X. Sun, *Org. Biomol. Chem.* **2006**, 4, 1663–1666.
- [19] S. Sobhani, E. Safaei, M. Asadi, F. Jalili, *J. Organomet. Chem.* **2008**, 693, 3313–3317.
- [20] M. Rostamizadeh, M. T. Maghsoodlou, N. Hazeri, S. M. Habibi-khorassani, L. Keishams, *Phosphorus, Sulfur Silicon Relat. Elem.* **2011**, 186, 334–337.

7. NMR Spectroscopic Data

NMR spectra (^1H -, ^{13}C -, and ^{31}P - NMR spectra) and HPLC traces of the synthesized products are available on the *Eur. J. Org. Chem. website* at DOI:

[10.1002/ejoc.201900209](https://doi.org/10.1002/ejoc.201900209).

3.2. Publication 3

Synthesis of Tetrahydroquinolines via Borrowing Hydrogen Methodology Using a Manganese PN³ Pincer Catalyst

Natalie Hofmann^[a] Leonard Homberg^[a] and Kai C. Hultzsch^{*,[a]}

^[a] Universität Wien, Fakultät für Chemie, Institut für Chemische Katalyse
Währinger Straße 38, 1090 Wien
<https://chemcat@univie.ac.at/>

* Corresponding author; email: kai.hultzsch@univie.ac.at

Org. Lett. **2020**, 22, 7964–7970; doi: 10.1021/acs.orglett.0c02905.

The manganese PN³ pincer complex was synthesized according to the procedure which was previously reported by our research group. Then a broad screening was conducted in order to find suitable reaction conditions for the selective synthesis of 1,2,3,4-tetrahydroquinolines starting from secondary alcohols and 2-aminobenzyl alcohols. After finding the optimized reaction conditions a substrate screening was performed and initial experiments were done to get insights into the reaction mechanism.

As first author I designed the described selective synthesis of 1,2,3,4-tetrahydroquinolines. Besides, I planned and conducted the experimental work, processed the acquired data and prepared the draft of the manuscript.

Synthesis of Tetrahydroquinolines via Borrowing Hydrogen Methodology Using a Manganese PN³ Pincer Catalyst

Natalie Hofmann, Leonard Homberg, and Kai C. Hultsch*



Cite This: *Org. Lett.* 2020, 22, 7964–7970



Read Online

ACCESS |



Metrics & More

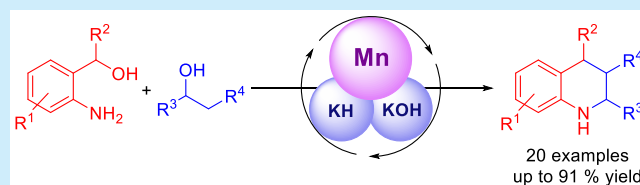


Article Recommendations



Supporting Information

ABSTRACT: A straightforward and selective synthesis of 1,2,3,4-tetrahydroquinolines starting from 2-aminobenzyl alcohols and simple secondary alcohols is reported. This one-pot cascade reaction is based on the borrowing hydrogen methodology promoted by a manganese(I) PN³ pincer complex. The reaction selectively leads to 1,2,3,4-tetrahydroquinolines thanks to a targeted choice of base. This strategy provides an atom-efficient pathway with water as the only byproduct. In addition, no further reducing agents are required.

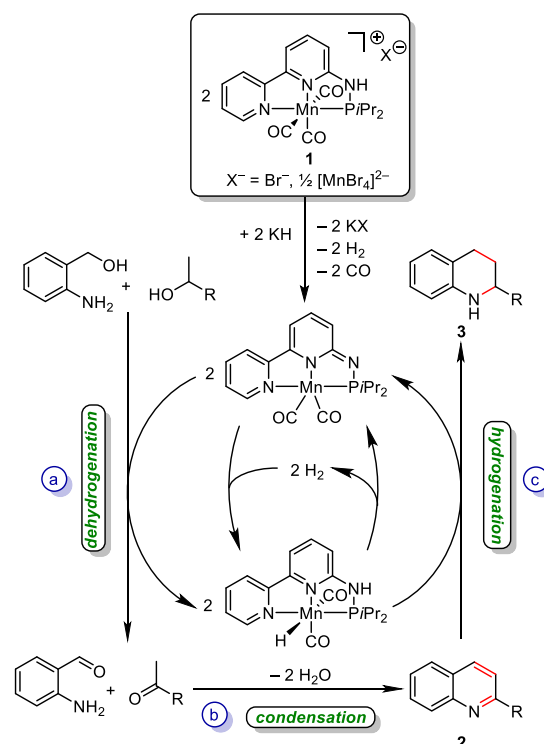


Nitrogen-containing heterocycles are indispensable substructures of important pharmaceuticals and agrochemicals.¹ Within this important substance class, the 1,2,3,4-tetrahydroquinoline² scaffold represents a particularly relevant building block for various natural products and pharmacologic active substances. While a number of synthetic approaches to tetrahydroquinolines exist,² the development of new catalytic processes that provide a faster and more (atom-) efficient access are highly desirable to reach the goals of a sustainable development.³ The borrowing hydrogen (BH) methodology⁴ offers an atom-economical pathway for the formation of carbon–carbon and carbon–nitrogen bonds utilizing inexpensive, abundant, and renewable starting materials.⁵ Key to many BH processes is the catalytic acceptorless dehydrogenation^{6,7} of an alcohol to form a carbonyl compound that can subsequently undergo further transformations, such as imine formation or aldol condensation. Finally, the catalyst returns the hydrogen to the condensation product to complete the BH cycle. While most catalyst systems have relied on precious metals, such as Ru and Ir,^{4c} more abundant and less expensive base metal catalysts, including Mn, Fe, Co, and Ni, have received significant attention recently.^{4d,7,8}

The BH methodology offers a simple opportunity to construct tetrahydroquinolines in an atom- and step-economical manner starting from 2-aminobenzyl alcohols and a second alcohol (Scheme 1, steps a–c) with water as the only byproduct.

However, previous attempts in the condensation of 2-aminobenzyl alcohols and alcohols have produced only quinolines via an acceptorless dehydrogenative coupling (corresponding to Scheme 1, steps a and b) utilizing precious^{9–11} and recently also base metal^{12–16} catalysts, thus falling short of completing the whole BH cycle. Quinolines can be reduced to tetrahydroquinolines via catalytic hydrogenation;^{10d,17–19} however, the additional reduction step

Scheme 1. Proposed Borrowing Hydrogen (BH) Cycle for the Synthesis of Tetrahydroquinolines (3)



Received: August 29, 2020

Published: September 24, 2020



reduces the efficiency of the overall process and reactions with molecular hydrogen often depend on higher pressure (≥ 15 atm) for catalytic turnover.^{17a,d,f-i}

Curiously, efforts to combine the dehydrogenative coupling with catalytic hydrogenation to a full BH cycle are scarce and limited in scope to primary alcohols using a heterogeneous Ni catalyst²⁰ or the Ru-catalyzed synthesis of tetrahydronaphthyridines.²¹ Tetrahydroquinolines have been prepared in an intramolecular N-alkylation reaction via BH,²² but the necessary amino alcohols have to be prepared in a multistep reaction sequence.

Herein, we disclose the direct synthesis of 1,2,3,4-tetrahydroquinolines starting from 2-aminobenzyl alcohols and secondary alcohols based on the BH strategy utilizing the manganese PN³ pincer complex **1** (Scheme 1), which exhibited high activity in the N-alkylation of amines with alcohols when activated with KH as base.^{23,24}

During our investigations, we observed that the reaction temperature and the applied base influence the outcome of the reaction of 2-aminobenzyl alcohol with 1-phenylethanol drastically. The usage of KOtBu at 140 °C leads to the selective formation of the corresponding 2-phenylquinoline (**2a**) (Table 1, entry 3), with significantly lower catalyst and

A screening was conducted in order to identify the most suitable conditions for the selective formation of the hydrogenated product (Table 1, see also Tables S1–S5). The influence of different solvents (Table S1) revealed that DME combined the highest activity with good selectivity for **3a**.

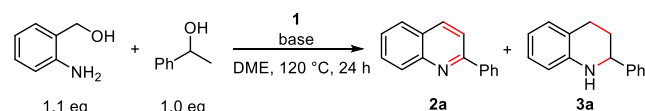
Among the tested bases (Table 1, entries 1–5), KH led to the highest selectivity for **3a**. The application of 150 mol % of KH is the best choice (Table 1, entry 7), while lower amounts of base decrease the reactivity (Table 1, entries 5 and 6) and higher amounts (Table 1, entry 8) hamper the selectivity of the system for **3a**. The concentration as well as the ratio between reaction volume and headspace have an additional impact on the success of the system (Table 1, entry 7 vs entry 10; Table S3). A substrate concentration of 1.0 M and a 1:5 ratio between volume of reaction mixture and headspace led to the best results. Increasing the catalyst loading to 3.0 mol % only led to a minor improvement in conversion (Table 1, entry 11), whereas a reduction to 1.5 mol % impairs the outcome more clearly (Table 1, entry 9). Attempts to increase the conversion to **3a** further by extending the reaction time had only a minor effect (Table S2).

A challenging problem is the suppression of the self-condensation of 2-aminobenzyl alcohol,^{10b} which led to the formation of oligomeric products. In our case, the additional application of KOH (30 mol %) and the order of addition seem to be crucial to minimize this competing side reaction (Table 1, entry 12 and Table S4). No conversion was observed with Mn(CO)₅Br in the absence of the pincer ligand (Table 1, entry 13).

With the optimized reaction conditions in hand, the selectivity of the catalytic system for a broader range of substrates was explored (Table 2). We started our investigations by applying different aromatic secondary alcohols. Generally good yields were obtained.^{25–27} The catalytic system tolerates an alcohol containing a ferrocene moiety (**3c**), though a higher catalyst loading (5 mol %) was required when an additional nitrogen atom was present in order to obtain a decent yield (**3d**). A significant decrease in yield was observed when higher substituted alcohols were applied (**3e–3g**). Aliphatic alcohols provided moderate to good conversions in general, providing a facile and atom-efficient access to norangustureine (**3k**), a precursor of the important Hancock alkaloid (\pm)-angustureine.²⁸ For products **3i–3k**, the corresponding regioisomers were detected as minor products in diminishing amounts with increasing chain length. A higher catalyst loading was required for the sterically more demanding aliphatic alcohol 3-methylbutan-2-ol to obtain a satisfactory yield of **3l**. Small amounts of 2-(*tert*-butyl)quinoline (**2m**) were observed as the only product for the bulkier 3,3-dimethylbutan-2-ol and no conversion to the corresponding tetrahydroquinoline **3m** was observed. An additional methyl group at the 2-aminobenzyl alcohol was well tolerated, which is reflected by the good yields of **3o–3r**. Even the electron-rich heterocyclic (3-aminopyridin-4-yl)methanol readily reacted with 1-phenylethanol, yielding the corresponding 1,2,3,4-tetrahydro-1,7-naphthyridine **3s** in moderate yield. The conversion of 2-aminobenzyl alcohol to **3t** and **3u** was low, though the dehydrogenative quinoline products were observed as byproducts in relatively large amounts.

In order to prove the feasibility of the catalyst system, the benchmark reaction of 2-aminobenzyl alcohol with 1-phenyl-

Table 1. Optimization of Reaction Conditions for the Synthesis of 2-Phenyl-1,2,3,4-tetrahydroquinoline (3a**)^a**



no.	base		cat. loading (mol %)	conversion ^b (%)		
	type	amt (equiv)		2a	3a	Σ
1	KOH ^c	1.00	2.0	57	2	59
2	KOtBu ^c	1.00	2.0	40	10	50
3	KOtBu ^{c,e}	0.50	2.0	98	<1	98
4	NaH ^c	1.00	2.0	35	8	43
5	KH ^c	1.00	2.0	18	46	64
6	KH ^c	1.25	2.0	18	56	74
7	KH ^c	1.50	2.0	15	59	74
8	KH ^c	1.75	2.0	44	36	80
9	KH ^d	1.50	1.5	5	50	55
10	KH ^d	1.50	2.0	10	65	75
11	KH ^d	1.50	3.0	13	67	80
12	KH + KOH ^d	1.50, 0.30	2.0	12	84	96
13	KH + KOH ^d	1.50, 0.30	2.0 ^f	<1	<1	<1

^aReaction conditions: 0.275 mmol of 2-aminobenzyl alcohol, 0.250 mmol of 1-phenylethanol, stock solution of **1** in DME (0.005 mmol), closed system, Ar. ^bGC conversion referenced to *p*-xylene.

^cConcentration: 0.3 M, ratio volume reaction mixture/headspace = 1:2. ^dConcentration: 1.0 M, ratio volume reaction mixture/headspace = 1:5. ^eAt 140 °C. ^fCat. = 2 mol % Mn(CO)₅Br. Note: Using KH as base led to traces of 1-phenylethanol self-condensation products (<5%).

base loadings in comparison to previous manganese-based catalyst systems.¹² However, catalyst **1** produces preferentially the reduced form (2-phenyl-1,2,3,4-tetrahydroquinoline, **3a**) when a combination of bases, KH and KOH, is employed at 120 °C. As the synthesis of quinolines via dehydrogenative coupling has already been reported with various catalytic systems,^{9–16} we decided to focus on the undeveloped formation of 1,2,3,4-tetrahydroquinolines **3**.

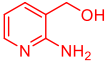
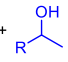
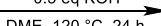
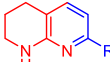
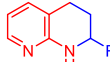
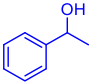
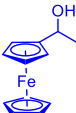
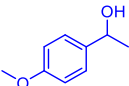
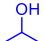
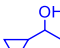
Table 2. Substrate Screening in the Synthesis of 1,2,3,4-Tetrahydroquinolines^a

3a 84% (78%) ^b 4 mmol scale: 603 mg (72 %) yield	3b 71% (67%) ^c	3c 98% (91%)
3d 86% (70%) ^d	3e 20% (10%)	3f 24% (21%)
3g 23% (14%)	3h 84% (74%)	3i 61% (54%) ^e
3j 61% (57%) ^e	norangustureine (3k) 64% (62%) ^e	3l 66% (61%) ^d
3m no product ^f	3n 81% (69%)	3o 81% (71%)
3p 81% (79%)	3q 94% (91%)	3r 94% (79%)
3s 54% (43%)	3t 53% (28%) ^g	3u 30% (20%) ^h

^aReaction conditions: 0.880 mmol aminobenzyl alcohol, 0.800 mmol alcohol (1.0 M), stock solution of **1** in DME (0.016 mmol), closed system, Ar, GC conversion referenced to *p*-xylene. Isolated yields are given in parentheses. ^b2% of self-condensation products of 1-phenylethanol. ^c7% of self-condensation products of 4-methyl-1-phenylethanol. ^d5 mol % of **1**. ^eThe corresponding regioisomers (**3i'**) were detected as minor products: **3i'**: 28% 2,3-dimethyl-1,2,3,4-tetrahydroquinoline (for results of the respective quinoline, see ref 10b); **3j'**: 10% 3-ethyl-2-methyl-1,2,3,4-tetrahydroquinoline; **3k'**: 2% 3-butyl-2-methyl-1,2,3,4-tetrahydroquinoline. ^f12% of 2-(*tert*-butyl)-quinoline (**2m**) was observed. ^gByproduct: 41% 2,4-diphenylquinoline (**2t**). ^hByproduct: 67% 2-methyl-4-phenylquinoline (**2u**).

ethanol was performed on a 4 mmol scale to give **3a** in 72% of isolated yield (Table 2).

Table 3. Synthesis of 1,2,3,4-Tetrahydro-1,8-naphthyridines^a

<div><div><div><div><div></div><div>1.1 eq</div></div><div><div></div><div>1.0 eq</div></div></div><div><div><div>2 mol% 1 1.5 eq KH 0.3 eq KOH</div><div></div><div><div></div><div>4</div></div><div><div></div><div>4'</div></div></div><div>DME, 120 °C, 24 h</div></div></div></div>				
no.	sec. alcohol	Conversion ^b (Yield) ^c [%]		
		4	4'	
1		4a 89 (73)	4a'	<1
2		4b 96 (71)	4b'	4
3		4c n.d. ^d (24)	4c'	n.d. ^d (3)
4		4d 59 (51)	4d'	27 (15)
5		4e 82 (63)	4e'	12

^aReaction conditions: 0.880 mmol of aminobenzyl alcohol, 0.800 mmol of alcohol (1.0 M), stock solution of **1** in DME (0.016 mmol), closed system, Ar. ^bGC conversion referenced to *p*-xylene. ^cIsolated yield. ^dFull conversion of *p*-methoxy-1-phenylethanol into naphthyridine **4c**, **4c'** and yet unidentified byproducts. n.d. = not detected.

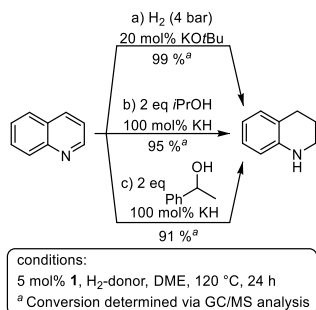
Intrigued by our finding that (3-aminopyridin-4-yl)methanol led to 1,2,3,4-tetrahydro-1,7-naphthyridine **3s**, we explored the reaction with (2-aminopyridin-3-yl)methanol as well (Table 3). Here, the transfer hydrogenation occurs predominantly at the pre-existing pyridyl ring, as noted for the ruthenium-promoted process,²¹ leading to 7-substituted 1,2,3,4-tetrahydro-1,8-naphthyridines **4** when the newly formed pyridyl ring bears a conjugated aromatic substituent (Table 3, entries 1–3). The 2-substituted 1,2,3,4-tetrahydro-1,8-naphthyridine **4'** was only observed as a significant byproduct when small aliphatic secondary alcohols were employed (Table 3, entries 4 and 5).

Interestingly, the reaction with *p*-methoxy-1-phenylethanol produced **4c** in 24% yield (Table 3, entry 3) and some yet unidentified byproducts. However, formation of 4-ethylanisole was not observed, in contrast to the respective reaction of *p*-methoxy-1-phenylethanol with 2-aminobenzyl alcohol.²⁶

Preliminary mechanistic investigations revealed that 2-ferrocenylquinoline (**2c**) was formed as major product (via GC analysis) within the first 2 h in the reaction of 2-aminobenzyl alcohol with 1-ferrocenylethanol (Table S8, Figure S2).²⁹ Then the amount of **2c** started to decrease concomitant with formation of the hydrogenated 2-ferrocenyl-1,2,3,4-tetrahydroquinoline (**3c**). No other intermediates of the reaction were detected.

The hydrogenation of quinoline proceeds efficiently using catalyst **1** with external hydrogen (Scheme 2a, Table S9,

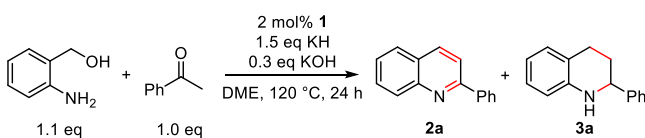
Scheme 2. Catalytic Hydrogenation of Quinoline with **1** Using Different Hydrogen Sources



entries 1–4) requiring significantly lower H₂ pressure (4 bar) compared to known Mn-based catalyst systems (15–80 bar).^{17g–i} Furthermore, transfer hydrogenation occurred smoothly with *i*PrOH (Scheme 2b, Table S9, entries 5–8) and 1-phenylethanol (Scheme 2c). Under optimal conditions, 2 equiv of *i*PrOH are employed, whereas larger amounts significantly impaired the result. Transfer hydrogenation of 2-phenylquinoline (**2a**) with *i*PrOH went smoothly (Table S9, entry 12), while 1-phenylethanol was less efficient (Table S9, entry 13), arguably due to the increased steric hindrance and conjugation of the aromatic heterocycle to the 2-phenyl substituent in **2a**.

Furthermore, the influence of hydrogen atmosphere or hydrogen pressure on the reduction step of the borrowing hydrogen process was investigated using acetophenone as substrate instead of 1-phenylethanol (Table 4). The reaction proceeded under the optimized conditions to form an approximate 1:1 mixture of 2-phenylquinoline (**2a**) and 2-phenyl-1,2,3,4-tetrahydroquinoline (**3a**) (Table 4, entry 1).

Table 4. Influence of Acetophenone on the Distribution of Dehydrogenated and Hydrogenated Product^a



no.	conditions	conversion ^b (%)		
		2a	3a	Σ
1	argon (pressurized vial)	49	47	96 ^c
2	H ₂ (balloon, 1 atm)	75	8	83
3	H ₂ (autoclave, 4 bar)	1	76	77

^aReaction conditions: 0.250 mmol of acetophenone, 0.275 mmol of 2-aminobenzyl alcohol, concentration 1.0 M, stock solution of **1** in DME (0.005 mmol), Ar. ^bGC/MS conversion. ^cByproducts: 1,3-diphenylpropan-1-one and chalcone.

This observation can be explained by the presence of an insufficient amount of reducing equivalents, as acetophenone is not a hydrogen donor. Introduction of additional hydrogen with a balloon under atmospheric pressure led to a large excess of quinoline **2a**, while performing the reaction under increased H₂ pressure produced the hydrogenated form **3a** as the major product (Table 4, entry 2 vs entry 3). These observations indicate that catalyst **1** requires a certain pressure of hydrogen

for the hydrogenation step, which is attained in our established procedure for the formation of 1,2,3,4-tetrahydroquinolines through heating of the tightly closed vial to 120 °C.

In summary, we have developed a homogeneous catalytic system which facilitates the atom-efficient and selective synthesis of 1,2,3,4-tetrahydroquinolines via a BH process. The combination of the PN³ manganese pincer complex **1** with the bases KH and KOH allows the formation of a C–C and a C–N single bond in a one-pot reaction. Notably, this cascade reaction can be performed without any additional reducing agent, and the only byproduct generated is water. Various aromatic and aliphatic alcohols lead to good conversions, enabling the straightforward synthesis of valuable nitrogen-containing heterocycles, as exemplified in the synthesis of norangustureine. Besides, the catalytic system shows high activity in the hydrogenation of quinolines by using external hydrogen or via transfer hydrogenation with secondary alcohols as hydrogen donor.

■ ASSOCIATED CONTENT

Supporting Information

The Supporting Information is available free of charge at <https://pubs.acs.org/doi/10.1021/acs.orglett.0c02905>.

Experimental procedures, spectral data, ¹H and ¹³C NMR spectra of all organic products, results of additional catalytic screening reactions, representative GC/FID traces (PDF)

■ AUTHOR INFORMATION

Corresponding Author

Kai C. Hultzsich – University of Vienna, Faculty of Chemistry, Institute of Chemical Catalysis, 1090 Vienna, Austria;
kai.hultzsich@univie.ac.at; Email: kai.hultzsich@univie.ac.at

Authors

Natalie Hofmann – University of Vienna, Faculty of Chemistry, Institute of Chemical Catalysis, 1090 Vienna, Austria
 Leonard Homberg – University of Vienna, Faculty of Chemistry, Institute of Chemical Catalysis, 1090 Vienna, Austria

Complete contact information is available at:
<https://pubs.acs.org/doi/10.1021/acs.orglett.0c02905>

Notes

The authors declare no competing financial interest.

■ REFERENCES

- (1) *Amino Group Chemistry: From Synthesis to the Life Sciences*; Ricci, A., Ed.; Wiley-VCH: Weinheim, 2008.
- (2) (a) Sridharan, V.; Suryavanshi, P. A.; Menéndez, J. C. *Advances in the Chemistry of Tetrahydroquinolines*. *Chem. Rev.* **2011**, *111*, 7157–7259. (b) Muthukrishnan, I.; Sridharan, V.; Menéndez, J. C. *Progress in the Chemistry of Tetrahydroquinolines*. *Chem. Rev.* **2019**, *119*, 5057–5191.
- (3) (a) Sheldon, R. A.; Arends, I.; Hanefeld, U. *Green Chemistry and Catalysis*; Wiley-VCH: Weinheim, Germany, 2007. (b) Sheldon, R. A. E. factors, green chemistry and catalysis: an odyssey. *Chem. Commun.* **2008**, 3352–3365.
- (4) (a) Watson, A. J.; Williams, J. M. The give and take of alcohol activation. *Science* **2010**, *329*, 635–636. (b) Gunanathan, C.; Milstein, D. Applications of acceptorless dehydrogenation and related trans-

formations in chemical synthesis. *Science* **2013**, *341*, 1229712. (c) Corma, A.; Navas, J.; Sabater, M. J. Advances in One-Pot Synthesis through Borrowing Hydrogen Catalysis. *Chem. Rev.* **2018**, *118*, 1410–1459. (d) Irrgang, T.; Kempe, R. 3d-Metal Catalyzed N- and C-Alkylation Reactions via Borrowing Hydrogen or Hydrogen Autotransfer. *Chem. Rev.* **2019**, *119*, 2524–2549.

(5) (a) Deuss, P. J.; Barta, K.; de Vries, J. G. Homogeneous catalysis for the conversion of biomass and biomass-derived platform chemicals. *Catal. Sci. Technol.* **2014**, *4*, 1174–1196. (b) Li, H.; Guo, H.; Fang, Z.; Aida, T. M.; Smith, R. L. Cycloamination strategies for renewable N-heterocycles. *Green Chem.* **2020**, *22*, 582–611.

(6) Selected reviews on (de)hydrogenations: (a) Dobereiner, G. E.; Crabtree, R. H. Dehydrogenation as a substrate-activating strategy in homogeneous transition-metal catalysis. *Chem. Rev.* **2010**, *110*, 681–702. (b) Gunanathan, C.; Milstein, D. Metal-ligand cooperation by aromatization-dearomatization: a new paradigm in bond activation and “green” catalysis. *Acc. Chem. Res.* **2011**, *44*, 588–602. (c) Obora, Y. Recent Advances in α -Alkylation Reactions using Alcohols with Hydrogen Borrowing Methodologies. *ACS Catal.* **2014**, *4*, 3972–3981. (d) Werkmeister, S.; Neumann, J.; Junge, K.; Beller, M. Pincer-Type Complexes for Catalytic (De)Hydrogenation and Transfer (De)Hydrogenation Reactions: Recent Progress. *Chem. - Eur. J.* **2015**, *21*, 12226–12250. (e) Crabtree, R. H. Homogeneous Transition Metal Catalysis of Acceptorless Dehydrogenative Alcohol Oxidation: Applications in Hydrogen Storage and to Heterocycle Synthesis. *Chem. Rev.* **2017**, *117*, 9228–9246.

(7) Selected reviews on base metal-catalyzed (de)hydrogenation reactions: (a) Zell, T.; Milstein, D. Hydrogenation and Dehydrogenation Iron Pincer Catalysts Capable of Metal-Ligand Cooperation by Aromatization/Dearomatization. *Acc. Chem. Res.* **2015**, *48*, 1979–1994. (b) Garbe, M.; Junge, K.; Beller, M. Homogeneous Catalysis by Manganese-Based Pincer Complexes. *Eur. J. Org. Chem.* **2017**, *2017*, 4344–4362. (c) Maji, B.; Barman, M. Recent Developments of Manganese Complexes for Catalytic Hydrogenation and Dehydrogenation Reactions. *Synthesis* **2017**, *49*, 3377–3393. (d) Kallmeier, F.; Kempe, R. Manganese Complexes for (De)Hydrogenation Catalysis: A Comparison to Cobalt and Iron Catalysts. *Angew. Chem., Int. Ed.* **2018**, *57*, 46–60. (e) Filonenko, G. A.; van Putten, R.; Hensen, E. J. M.; Pidko, E. A. Catalytic (de)hydrogenation promoted by non-precious metals - Co, Fe and Mn: recent advances in an emerging field. *Chem. Soc. Rev.* **2018**, *47*, 1459–1483. (f) Gorgas, N.; Kirchner, K. Isoelectronic Manganese and Iron Hydrogenation/Dehydrogenation Catalysts: Similarities and Divergences. *Acc. Chem. Res.* **2018**, *51*, 1558–1569. (g) Liu, W.; Sahoo, B.; Junge, K.; Beller, M. Cobalt Complexes as an Emerging Class of Catalysts for Homogeneous Hydrogenations. *Acc. Chem. Res.* **2018**, *51*, 1858–1869. (h) Mukherjee, A.; Milstein, D. Homogeneous Catalysis by Cobalt and Manganese Pincer Complexes. *ACS Catal.* **2018**, *8*, 11435–11469. (i) Wei, D.; Darcel, C. Iron Catalysis in Reduction and Hydro-metalation Reactions. *Chem. Rev.* **2019**, *119*, 2550–2610. (j) Junge, K.; Papa, V.; Beller, M. Cobalt-Pincer Complexes in Catalysis. *Chem. - Eur. J.* **2019**, *25*, 122–143. (k) Waiba, S.; Maji, B. Manganese Catalyzed Acceptorless Dehydrogenative Coupling Reactions. *ChemCatChem* **2020**, *12*, 1891–1902.

(8) Selected examples for applications of Mn in BH and acceptorless dehydrogenative coupling reactions: (a) Mukherjee, A.; Nerush, A.; Leitun, G.; Shimon, L. J.; Ben-David, Y.; Espinosa Jalapa, N. A.; Milstein, D. Manganese-Catalyzed Environmentally Benign Dehydrogenative Coupling of Alcohols and Amines to Form Aldimines and H₂: A Catalytic and Mechanistic Study. *J. Am. Chem. Soc.* **2016**, *138*, 4298–4301. (b) Elangovan, S.; Neumann, J.; Sortais, J. B.; Junge, K.; Darcel, C.; Beller, M. Efficient and selective N-alkylation of amines with alcohols catalyzed by manganese pincer complexes. *Nat. Commun.* **2016**, *7*, 12641. (c) Pena-Lopez, M.; Piehl, P.; Elangovan, S.; Neumann, H.; Beller, M. Manganese-Catalyzed Hydrogen-Autotransfer C-C Bond Formation: α -Alkylation of Ketones with Primary Alcohols. *Angew. Chem., Int. Ed.* **2016**, *55*, 14967–14971. (d) Mastalir, M.; Pittenauer, E.; Allmaier, G.; Kirchner, K. Manganese-Catalyzed Aminomethylation of Aromatic Compounds

with Methanol as a Sustainable C1 Building Block. *J. Am. Chem. Soc.* **2017**, *139*, 8812–8815. (e) Fu, S.; Shao, Z.; Wang, Y.; Liu, Q. Manganese-Catalyzed Upgrading of Ethanol into 1-Butanol. *J. Am. Chem. Soc.* **2017**, *139*, 11941–11948. (f) Deibl, N.; Kempe, R. Manganese-Catalyzed Multicomponent Synthesis of Pyrimidines from Alcohols and Amidines. *Angew. Chem., Int. Ed.* **2017**, *56*, 1663–1666. (g) Kallmeier, F.; Dudziec, B.; Irrgang, T.; Kempe, R. Manganese-Catalyzed Sustainable Synthesis of Pyrroles from Alcohols and Amino Alcohols. *Angew. Chem., Int. Ed.* **2017**, *56*, 7261–7265. (h) Zhang, G.; Irrgang, T.; Dietel, T.; Kallmeier, F.; Kempe, R. Manganese-Catalyzed Dehydrogenative Alkylation or α -Olefination of Alkyl-Substituted N-Heteroarenes with Alcohols. *Angew. Chem., Int. Ed.* **2018**, *57*, 9131–9135. (i) Wang, Y.; Shao, Z.; Zhang, K.; Liu, Q. Manganese-Catalyzed Dual-Deoxygenative Coupling of Primary Alcohols with 2-Arylethanol. *Angew. Chem., Int. Ed.* **2018**, *57*, 15143–15147. (j) Barman, M. K.; Jana, A.; Maji, B. Phosphine-Free NNN-Manganese Complex Catalyzed α -Alkylation of Ketones with Primary Alcohols and Friedländer Quinoline Synthesis. *Adv. Synth. Catal.* **2018**, *360*, 3233–3238. (k) Daw, P.; Kumar, A.; Espinosa-Jalapa, N. A.; Diskin-Posner, Y.; Ben-David, Y.; Milstein, D. Synthesis of Pyrazines and Quinoxalines via Acceptorless Dehydrogenative Coupling Routes Catalyzed by Manganese Pincer Complexes. *ACS Catal.* **2018**, *8*, 7734–7741. (l) Masdemont, J.; Luque-Urrutia, J. A.; Gimferrer, M.; Milstein, D.; Poater, A. Mechanism of Coupling of Alcohols and Amines To Generate Aldimines and H₂ by a Pincer Manganese Catalyst. *ACS Catal.* **2019**, *9*, 1662–1669. (m) Freitag, F.; Irrgang, T.; Kempe, R. Mechanistic Studies of Hydride Transfer to Imines from a Highly Active and Chemoselective Manganate Catalyst. *J. Am. Chem. Soc.* **2019**, *141*, 11677–11685. (n) Bruneau-Voisine, A.; Pallova, L.; Bastin, S.; César, V.; Sortais, J.-B. Manganese catalyzed α -methylation of ketones with methanol as a C1 source. *Chem. Commun.* **2019**, *55*, 314–317. (o) Borghs, J. C.; Lebedev, Y.; Rueping, M.; El-Sepelgy, O. Sustainable Manganese-Catalyzed Solvent-Free Synthesis of Pyrroles from 1,4-Diols and Primary Amines. *Org. Lett.* **2019**, *21*, 70–74. (p) Das, K.; Mondal, A.; Pal, D.; Srimani, D. Sustainable Synthesis of Quinazoline and 2-Aminoquinoline via Dehydrogenative Coupling of 2-Aminobenzyl Alcohol and Nitrile Catalyzed by Phosphine-Free Manganese Pincer Complex. *Org. Lett.* **2019**, *21*, 3223–3227. (q) Kaithal, A.; Gracia, L. L.; Camp, C.; Quadrelli, E. A.; Leitner, W. Direct Synthesis of Cycloalkanes from Diols and Secondary Alcohols or Ketones Using a Homogeneous Manganese Catalyst. *J. Am. Chem. Soc.* **2019**, *141*, 17487–17492. (r) Shao, Z.; Li, Y.; Liu, C.; Ai, W.; Luo, S.-P.; Liu, Q. Reversible interconversion between methanol-diamine and diamide for hydrogen storage based on manganese catalyzed (de)hydrogenation. *Nat. Commun.* **2020**, *11*, 591. (s) Kaithal, A.; van Bonn, P.; Hölscher, M.; Leitner, W. Manganese(I)-Catalyzed β -Methylation of Alcohols Using Methanol as C₁ Source. *Angew. Chem., Int. Ed.* **2020**, *59*, 215–220. (t) Jana, A.; Das, K.; Kundu, A.; Thorve, P. R.; Adhikari, D.; Maji, B. A Phosphine-Free Manganese Catalyst Enables Stereoselective Synthesis of (1 + n)-Membered Cycloalkanes from Methyl Ketones and 1,n-Diols. *ACS Catal.* **2020**, *10*, 2615–2626.

(9) Re: (a) Mastalir, M.; Glatz, M.; Pittenauer, E.; Allmaier, G.; Kirchner, K. Rhodium-Catalyzed Dehydrogenative Coupling of Alcohols and Amines to Afford Nitrogen-Containing Aromatics and More. *Org. Lett.* **2019**, *21*, 1116–1120. (b) Wei, D.; Dorcet, V.; Darcel, C.; Sortais, J.-B. Synthesis of Quinolines Through Acceptorless Dehydrogenative Coupling Catalyzed by Rhodium PN(H)P Complexes. *ChemSusChem* **2019**, *12*, 3078–3082.

(10) Selected examples for Ru: (a) Chai, H.; Wang, L.; Liu, T.; Yu, Z. A Versatile Ru(II)-NNP Complex Catalyst for the Synthesis of Multisubstituted Pyrroles and Pyridines. *Organometallics* **2017**, *36*, 4936–4942. (b) Guo, B.; Yu, T.-Q.; Li, H.-X.; Zhang, S.-Q.; Braunstein, P.; Young, D. J.; Li, H.-Y.; Lang, J.-P. Phosphine Ligand-Free Ruthenium Complexes as Efficient Catalysts for the Synthesis of Quinolines and Pyridines by Acceptorless Dehydrogenative Coupling Reactions. *ChemCatChem* **2019**, *11*, 2500–2510. (c) Donthireddy, S. N. R.; Mathoor Illam, P.; Rit, A. Ruthenium(II) Complexes of Heteroditopic N-Heterocyclic Carbene Ligands: Efficient Catalysts

for C–N Bond Formation via a Hydrogen-Borrowing Strategy under Solvent-Free Conditions. *Inorg. Chem.* **2020**, *59*, 1835–1847. (d) Yun, X.-J.; Zhu, J.-W.; Jin, Y.; Deng, W.; Yao, Z.-J. Half-Sandwich Ruthenium Complexes for One-Pot Synthesis of Quinolines and Tetrahydroquinolines: Diverse Catalytic Activity in the Coupled Cyclization and Hydrogenation Process. *Inorg. Chem.* **2020**, *59*, 7841–7851.

(11) Ir: Ruch, S.; Irrgang, T.; Kempe, R. New Iridium Catalysts for the Selective Alkylation of Amines by Alcohols under Mild Conditions and for the Synthesis of Quinolines by Acceptor-less Dehydrogenative Condensation. *Chem. - Eur. J.* **2014**, *20*, 13279–13285.

(12) Mn: (a) Mastalir, M.; Glatz, M.; Pittenauer, E.; Allmaier, G.; Kirchner, K. Sustainable Synthesis of Quinolines and Pyrimidines Catalyzed by Manganese PNP Pincer Complexes. *J. Am. Chem. Soc.* **2016**, *138*, 15543–15546. (b) Das, K.; Mondal, A.; Srimani, D. Phosphine free Mn-complex catalyzed dehydrogenative C–C and C–heteroatom bond formation: a sustainable approach to synthesize quinoxaline, pyrazine, benzothiazole and quinoline derivatives. *Chem. Commun.* **2018**, *54*, 10582–10585. (c) Azizi, K.; Akrami, S.; Madsen, R. Manganese(III) Porphyrin-Catalyzed Dehydrogenation of Alcohols to form Imines, Tertiary Amines and Quinolines. *Chem. - Eur. J.* **2019**, *25*, 6439–6446.

(13) Fe: Elangovan, S.; Sortais, J.-B.; Beller, M.; Darcel, C. Iron-Catalyzed α -Alkylation of Ketones with Alcohols. *Angew. Chem., Int. Ed.* **2015**, *54*, 14483–14486.

(14) Co: (a) Zhang, G.; Wu, J.; Zeng, H.; Zhang, S.; Yin, Z.; Zheng, S. Cobalt-Catalyzed α -Alkylation of Ketones with Primary Alcohols. *Org. Lett.* **2017**, *19*, 1080–1083. (b) Midya, S. P.; Landge, V. G.; Sahoo, M. K.; Rana, J.; Balaraman, E. Cobalt-catalyzed acceptorless dehydrogenative coupling of aminoalcohols with alcohols: direct access to pyrrole, pyridine and pyrazine derivatives. *Chem. Commun.* **2018**, *54*, 90–93. (c) Shee, S.; Ganguli, K.; Jana, K.; Kundu, S. Cobalt complex catalyzed atom-economical synthesis of quinoxaline, quinoline and 2-alkylaminoquinoline derivatives. *Chem. Commun.* **2018**, *54*, 6883–6886.

(15) Ni: (a) Das, S.; Maiti, D.; De Sarkar, S. Synthesis of Polysubstituted Quinolines from α -2-Aminoaryl Alcohols Via Nickel-Catalyzed Dehydrogenative Coupling. *J. Org. Chem.* **2018**, *83*, 2309–2316. (b) Parua, S.; Sikari, R.; Sinha, S.; Das, S.; Chakraborty, G.; Paul, N. D. A nickel catalyzed acceptorless dehydrogenative approach to quinolines. *Org. Biomol. Chem.* **2018**, *16*, 274–284.

(16) Cu: Tan, D.-W.; Li, H.-X.; Zhu, D.-L.; Li, H.-Y.; Young, D. J.; Yao, J.-L.; Lang, J.-P. Ligand-Controlled Copper(I)-Catalyzed Cross-Coupling of Secondary and Primary Alcohols to α -Alkylated Ketones, Pyridines, and Quinolines. *Org. Lett.* **2018**, *20*, 608–611.

(17) Selected examples using molecular hydrogen: (a) Wang, D. S.; Chen, Q. A.; Lu, S. M.; Zhou, Y. G. Asymmetric Hydrogenation of Heteroarenes and Arenes. *Chem. Rev.* **2012**, *112*, 2557–2590. See also references cited therein. (b) Chakraborty, S.; Brennessel, W. W.; Jones, W. D. A Molecular Iron Catalyst for the Acceptorless Dehydrogenation and Hydrogenation of N-Heterocycles. *J. Am. Chem. Soc.* **2014**, *136*, 8564–8567. (c) Xu, R.; Chakraborty, S.; Yuan, H.; Jones, W. D. Acceptorless, Reversible Dehydrogenation and Hydrogenation of N-Heterocycles with a Cobalt Pincer Catalyst. *ACS Catal.* **2015**, *5*, 6350–6354. (d) Luo, Y. E.; He, Y. M.; Fan, Q. H. Asymmetric Hydrogenation of Quinoline Derivatives Catalyzed by Cationic Transition Metal Complexes of Chiral Diamine Ligands: Scope, Mechanism and Catalyst Recycling. *Chem. Rec.* **2016**, *16*, 2697–2711. (e) Adam, R.; Cabrero-Antonino, J. R.; Spannenberg, A.; Junge, K.; Jackstell, R.; Beller, M. A General and Highly Selective Cobalt-Catalyzed Hydrogenation of N-Heteroarenes under Mild Reaction Conditions. *Angew. Chem., Int. Ed.* **2017**, *56*, 3216–3220. (f) Sahoo, B.; Kreyenschulte, C.; Agostini, G.; Lund, H.; Bachmann, S.; Scalone, M.; Junge, K.; Beller, M. A robust iron catalyst for the selective hydrogenation of substituted (iso)quinolones. *Chem. Sci.* **2018**, *9*, 8134–8141. (g) Wang, Y.; Zhu, L.; Shao, Z.; Li, G.; Lan, Y.; Liu, Q. Unmasking the Ligand Effect in Manganese-Catalyzed Hydrogenation: Mechanistic Insight and Catalytic Application. *J.*

Am. Chem. Soc. **2019**, *141*, 17337–17349. (h) Papa, V.; Cao, Y.; Spannenberg, A.; Junge, K.; Beller, M. Development of a practical non-noble metal catalyst for hydrogenation of N-heteroarenes. *Nat. Catal.* **2020**, *3*, 135. (i) Wang, Z.; Chen, L.; Mao, G.; Wang, C. Simple manganese carbonyl catalyzed hydrogenation of quinolines and imines. *Chin. Chem. Lett.* **2020**, *31*, 1890–1894.

(18) Selected examples using transfer hydrogenation: (a) Cabrero-Antonino, J. R.; Adam, R.; Junge, K.; Jackstell, R.; Beller, M. Cobalt-catalyzed transfer hydrogenation of quinolines and related heterocycles using formic acid under mild conditions. *Catal. Sci. Technol.* **2017**, *7*, 1981–1985. (b) Dubey, A.; Rahaman, S. M. W.; Fayzullin, R. R.; Khusnutdinova, J. R. Transfer Hydrogenation of Carbonyl Groups, Imines and N-Heterocycles Catalyzed by Simple, Bipyridine-Based Mn^I Complexes. *ChemCatChem* **2019**, *11*, 3844–3852.

(19) For the Mn-catalyzed (de)hydrogenation of other N-heterocycles, see: Zubar, V.; Borghs, J. C.; Rueping, M. Hydrogenation or Dehydrogenation of N-Containing Heterocycles Catalyzed by a Single Manganese Complex. *Org. Lett.* **2020**, *22*, 3974–3978.

(20) Zhang, J.; An, Z.; Zhu, Y.; Shu, X.; Song, H.; Jiang, Y.; Wang, W.; Xiang, X.; Xu, L.; He, J. Ni⁰/Ni^{δ+} Synergistic Catalysis on a Nanosized Ni Surface for Simultaneous Formation of C–C and C–N Bonds. *ACS Catal.* **2019**, *9*, 11438–11446.

(21) Xiong, B.; Li, Y.; Lv, W.; Tan, Z.; Jiang, H.; Zhang, M. Ruthenium-Catalyzed Straightforward Synthesis of 1,2,3,4-Tetrahydronaphthyridines via Selective Transfer Hydrogenation of Pyridyl Ring with Alcohols. *Org. Lett.* **2015**, *17*, 4054–4057.

(22) (a) Fujita, K.; Yamamoto, K.; Yamaguchi, R. Oxidative cyclization of amino alcohols catalyzed by a CpIr complex. Synthesis of indoles, 1,2,3,4-tetrahydroquinolines, and 2,3,4,5-tetrahydro-1-benzazepine. *Org. Lett.* **2002**, *4*, 2691–2694. (b) Lim, C. S.; Quach, T. T.; Zhao, Y. Enantioselective Synthesis of Tetrahydroquinolines by Borrowing Hydrogen Methodology: Cooperative Catalysis by an Achiral Iridacycle and a Chiral Phosphoric Acid. *Angew. Chem., Int. Ed.* **2017**, *56*, 7176–7180.

(23) Homberg, L.; Roller, A.; Hultsch, K. C. A Highly Active PN³ Manganese Pincer Complex Performing N-Alkylation of Amines under Mild Conditions. *Org. Lett.* **2019**, *21*, 3142–3147.

(24) In complex **1**, the metal and the ligand are thought to be involved in the bond activation of the (de)hydrogenation process. For a review on this concept of metal–ligand cooperation, see: Khusnutdinova, J. R.; Milstein, D. Metal-Ligand Cooperation. *Angew. Chem., Int. Ed.* **2015**, *54*, 12236–12273.

(25) Attempts to use *p*-bromo-1-phenylethanol led to loss of bromine during the reaction, and the dehydrogenated 2-phenylquinoline (**2a**) was detected as the major product (53%). Similar results were also obtained at lower reaction temperatures (80 °C). Further investigations revealed that bromobenzene was hydrodehalogenated under the general reaction conditions, whereas no reaction was observed under these conditions in the absence of the Mn pincer complex. Besides, hydrodehalogenation was also observed for (2-amino-5-chlorophenyl)methanol as starting material, indicating that aryl chlorides and bromides are not tolerated under these reactions conditions in general. This stands in marked contrast to our finding that aromatic halide substituents are generally tolerated under conditions applied in the N-alkylation of alcohols; see ref **23**. However, hydrodehalogenation can be facilitated by a number of catalyst systems, and it is a known competition reaction during the catalytic hydrogenation of halogenated compounds; see: (a) Sisak, A.; Simon, O. B. In *Handbook of Homogeneous Hydrogenation*; de Vries, J. G., Elsevier, C. J., Eds.; Wiley-VCH: Weinheim, Germany, 2007; Vol. 3, pp 513–546. (b) Formenti, D.; Ferretti, F.; Scharnagl, F. K.; Beller, M. Reduction of Nitro Compounds Using 3d-Non-Noble Metal Catalysts. *Chem. Rev.* **2019**, *119*, 2611–2680.

(26) The reaction with *p*-methoxy-1-phenylethanol produced 4-ethylanisole (83% conv by GC/MS analysis) rather than the corresponding quinoline or 1,2,3,4-tetrahydroquinoline, suggesting that the alcohol is acting as a PMB-protecting group that is cleaved under the prevalent reaction conditions.

(27) 1-(2-Furanyl)ethanol and 1-(2-thienyl)ethanol were tested as substrates as well. However, these reactions only led to traces of the corresponding tetrahydroquinolines (<5% based on GC/MS analysis) and yet unidentified byproducts.

(28) Davies, S. G.; Fletcher, A. M.; Roberts, P. M.; Thomson, J. E. The Hancock Alkaloids Angustureine, Cuspareine, Galipinine, and Galipeine: A Review of their Isolation, Synthesis, and Spectroscopic Data. *Eur. J. Org. Chem.* **2019**, 2019, 5093–5119.

(29) Similar observations were made for the reaction of 2-aminobenzyl alcohol with *i*PrOH in which the reaction rate decreased significantly after 4 h (Table S7, Figure S1).

1. General Information

p-Xylene was distilled from sodium benzophenone ketyl. DME was distilled from CaH₂. Alcohols used as substrates for catalysis were distilled from Na₂SO₄. Ferrocene-1-ethanol was synthesized *via* reduction of acetylferrocene according to the literature.¹ Aminoalcohols used as substrates for catalysis were dried under high vacuum. If not mentioned otherwise all commercially available starting materials were used without further purification.

All ¹H, and ¹³C spectra were recorded on a Bruker Ultrashield™ 400 instrument, whereby the ¹H NMR spectra were measured at 400.3 MHz and the ¹³C NMR spectra at 100.7 MHz. All chemical shifts are noted in ppm. ¹H and ³¹C chemical shifts are indicated relative to TMS and were referenced to residual signals of the solvent (¹H NMR (CDCl₃): 7.27 ppm, ¹³C NMR (CDCl₃): 77.0 ppm). All HRMS measurements were conducted on a Bruker maXis UHR-TOF instrument. Column chromatography was performed by using Biotage® SP4 and Isolera flash systems and the applied columns were packed with silica gel 60 Å. TLC was performed with commercial Kieselgel 60 F₂₅₄ and visualized *via* UV lamp. GC/MS measurements were conducted on an Agilent Technologies instrument with 5977B MSD High Efficiency Source and a 7820A GC-system equipped with a *HP-5MS* column (30 m, 250 µm, 0.25 µm) (GC-MS conditions: Inlet temp.: 270 °C, carrier gas flow: He at 39.8 cm/s; oven temperature: 45 °C (2.25 min) to 300 °C at 25 °C/min (hold 0.55 min) for a total run time of 14 min). GC/FID measurements were conducted on a Shimadzu GC-2010 system equipped with a *HP-5* column (30 m, 320 µm, 0.25 µm) (GC-FID conditions: Inlet temp.: 270 °C, carrier gas flow: He at 34.9 cm/s; oven temperature: 50 °C (2.25 min) to 300 °C at 25 °C/min (hold 5 min) for a total run time of 17.25 min).

Mn(CO)₅Br was commercially purchased and bpy-⁶NH-^{iPr}P was synthesized according to the literature.²

2. Catalytic screenings

Table S1: Influence of different solvents.^a

Nc1ccccc1CO + CC(O)c1ccccc1
 $\xrightarrow[\text{solvent, 120 } ^\circ\text{C, 24 h}]{2 \text{ mol\% } \mathbf{1}, 100 \text{ mol\% KH}}$
c1ccc2c(c1)c(c[nH]2)c3ccccc3 + c1ccc2c(c1)c(c[nH]2)CCc3ccccc3

1.1 eq 1.0 eq **2a** **3a**

#	solvent	Conversion ^b [%]		
		2a	3a	Σ
1	DME	18	46	64
2	toluene	45	10	55
3	<i>tert</i> -amyl alcohol	25	0	25
4	bromobenzene	55	2	57
5	dioxane	10	35	45
6	THF	23	22	55

^a Reaction conditions: 0.250 mmol scale, concentration: 0.31 M. ^b Conversion determined via GC/MS analysis.

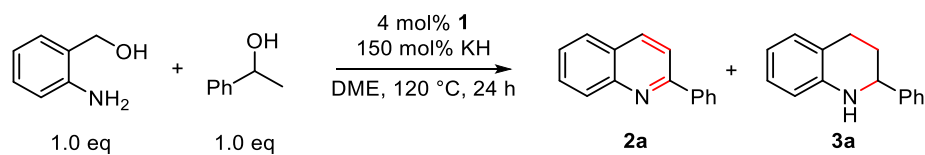
Table S2: Influence of reaction time.^a

Nc1ccccc1CO + CC(O)c1ccccc1
 $\xrightarrow[\text{reaction time}]{2 \text{ mol\% } \mathbf{1}, 150 \text{ mol\% KH, DME, 120 } ^\circ\text{C}}$
c1ccc2c(c1)c(c[nH]2)c3ccccc3 + c1ccc2c(c1)c(c[nH]2)CCc3ccccc3

1.1 eq 1.0 eq **2a** **3a**

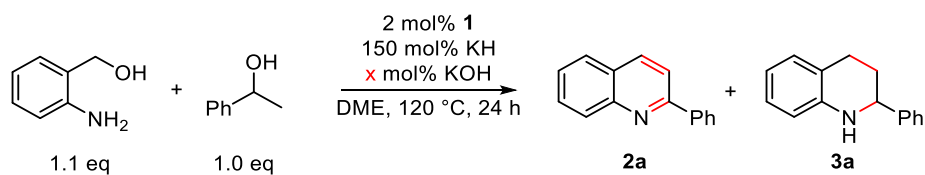
#	Reaction time [h]	Conversion ^b [%]		
		2a	3a	Σ
1	24	15	59	74
2	48	13	62	75
3	65	12	63	75

^a Reaction conditions: 0.250 mmol scale, concentration: 0.31 M. ^b Conversion determined via GC/MS analysis.

Table S3: Ratio between reaction volume and headspace.^a

#	Size of reaction vessel [mL]	Ratio volume : headspace	Conversion ^b [%]		
			2a	3a	Σ
1	1.8	1.0 : 0.5	7	40	47
2	2.5	1.0 : 1.1	14	69	83
3	5.0	1.0 : 3.1	11	73	84
4	15.0	1.0 : 11.1	82	19	quant.

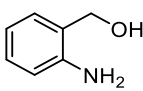
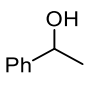
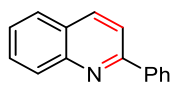
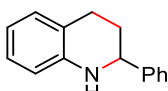
^a Reaction conditions: 1.200 mmol scale, concentration: 1.00 M. ^b Conversion determined *via* GC/MS analysis.

Table S4: Application of KOH.^a

#	Amount of KOH [mol%]	Conversion ^b [%]		
		2a	3a	Σ
1	---	10	65	75
2	20	10	78	88
3	30	12	84	96
4	50	14	80	93

^a Reaction conditions: 0.250 mmol scale, concentration: 1.00 M. ^b Conversion determined *via* GC/FID analysis referenced to *p*-xylene as internal standard.

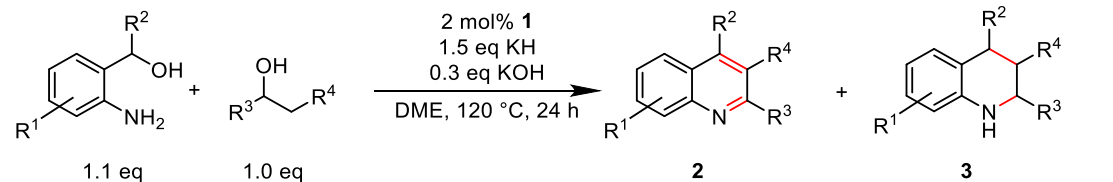
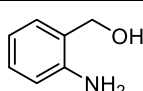
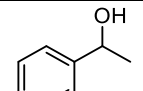
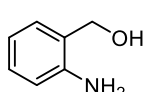
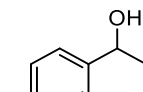
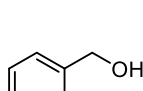
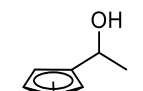
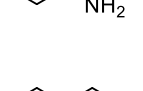
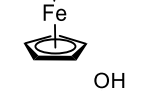
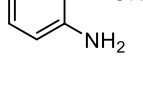
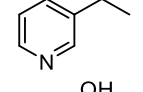
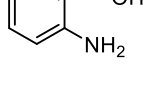
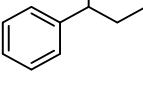
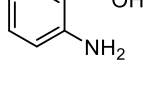
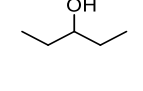
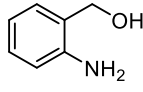
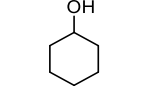
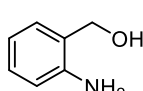
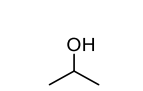
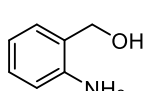
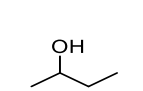
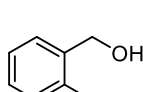
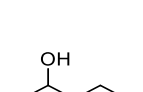
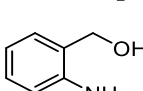
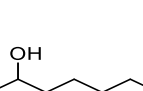
Table S5: Different amounts of 1-phenylethanol.^a

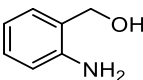
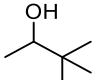
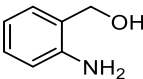
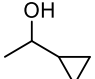
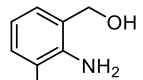
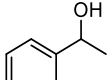
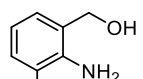
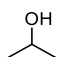
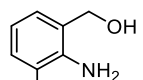
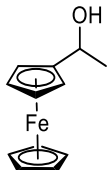
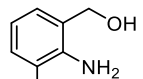
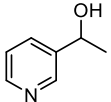
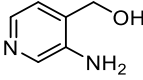
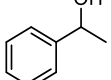
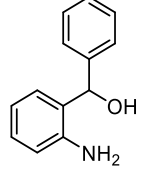
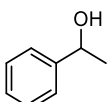
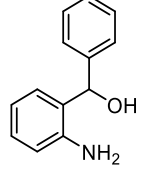
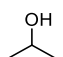
<div style="display: flex; align-items: center; justify-content: center;"> <div style="text-align: center;">  <p>1.0 eq</p> </div> <div style="margin: 0 10px;">+</div> <div style="text-align: center;">  <p>x eq</p> </div> <div style="margin-left: 20px;"> <p>2 mol% 1 150 mol% KH 30 mol% KOH</p> <p>→</p> <p>DME, 120 °C, 24 h</p> </div> <div style="text-align: center;">  <p>2a</p> </div> <div style="margin: 0 10px;">+</div> <div style="text-align: center;">  <p>3a</p> </div> </div>				
#	Amount of 1-phenylethanol [eq]	Conversion ^b [%]		
		2a	3a	Σ
1	1.0	12	84	96
2	1.5	11	35	91 ^c
3	2.0	18	29	92 ^d

^a Reaction conditions: 0.250 mmol scale, concentration: 1.00 M. ^b Conversion determined via GC/FID analysis referenced to *p*-xylene as internal standard. If KH was applied as base, traces of the self-condensation products of 1-phenylethanol (<5 %) were detected.

^c 45 % of the self-condensation products of 1-phenylethanol were detected. ^d 52 % of the self-condensation products of 1-phenylethanol were detected.

Table S6: Substrate Screening: Selectivity for 1,2,3,4-tetrahydroquinolines^a (supplement to Table 2).

						
#	2-aminobenzyl alcohol	secondary alcohol	Desired Product	Conversion ^b [%]		
				2	3	Σ
1			3a	12	84	98 ^c
2			3b	3	71	81 ^d
3			3c	2	98	>99
4			3d	<1	86	86 ^e
5			3e	1	20	21
6			3f	7	24	31
7			3g	0	23	23
8			3h	<1	84	84
9			3i	<1	61	61 ^f
10			3j	<1	61	71 ^g
11			3k	2	64	66 ^h
12			3l	32	66	98 ^e

13			3m	12	<1	12 ⁱ
14			3n	8	81	89
15			3o	2	81	83
16			3p	<1	81	81
17			3q	6	94	>99
18			3r	6	94	>99
19			3s	<1	54	54
20			3t	41	53	94 ^j
21			3u	67	30	97 ^k

^a Reaction conditions: 0.880 mmol aminobenzyl alcohol, 0.800 mmol alcohol, closed system, argon atmosphere, concentration: 1.0 M, ^b Conversion was determined *via* GC/FID analysis referenced to *p*-xylene. ^c 2 % of the self-condensation products of 1-phenylethanol were observed. ^d 7 % of the self-condensation products of 4-methyl-1-phenylethanol were observed. ^e 5 mol% **1**. ^f Formation of 24 % 2,3-dimethyl-1,2,3,4-tetrahydroquinoline as by-product. ^g Formation of 10 % 3-ethyl-2-methyl-1,2,3,4-tetrahydroquinoline as by-product. ^h 2% 3-butyl-2-methyl-1,2,3,4-tetrahydroquinoline. ⁱ 12% of 2-(tert-butyl)-quinoline (**2m**) was observed. ^j Byproduct: 41% 2,4-diphenylquinoline (**2t**). ^k Byproduct: 67% 2-methyl-4-phenylquinoline (**2u**).

Table S7: Reaction monitoring via GC/FID analysis of the reaction of 2-aminobenzyl alcohol with isopropanol.^a

<chem>Nc1ccccc1CO</chem> (1.1 eq) + <chem>CC(C)O</chem> (1.0 eq) $\xrightarrow[\text{DME, 120 } ^\circ\text{C}]{\substack{2 \text{ mol\% } \mathbf{1} \\ 150 \text{ mol\% KH} \\ 30 \text{ mol\% KOH}}}$ <chem>Cc1ccc2c(c1)c(c[nH]2)C</chem> (2h) + <chem>Cc1ccc2c(c1)CN(C)CC2</chem> (3h)					
#	Reaction time [h]	Conversion ^b [%]			Σ
		2h	3h		
1	2	16	24		40
2	4	17	52		68
3	18	13	71		81
4	24	2	81		83

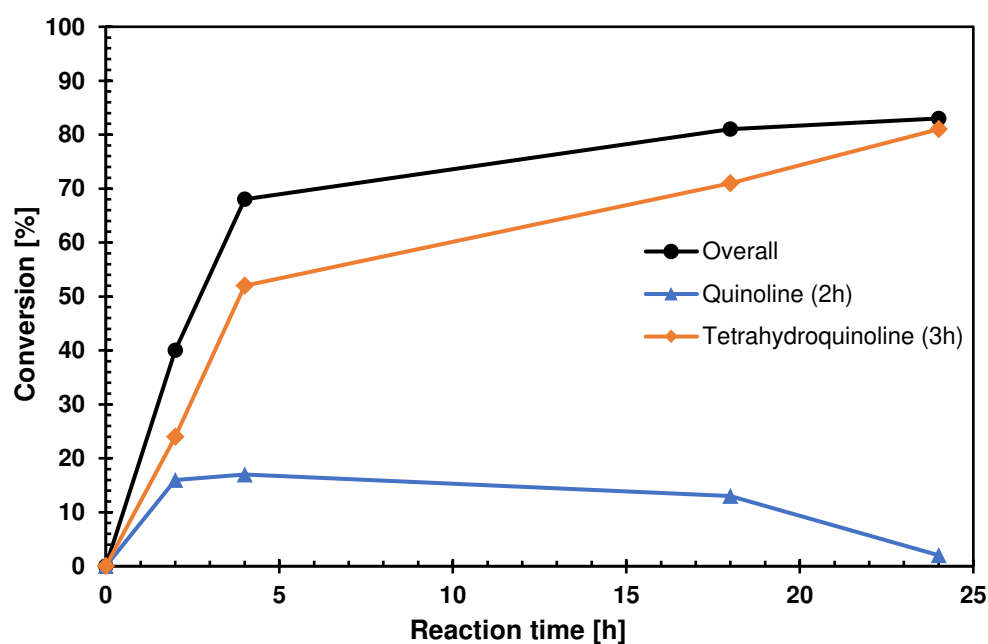
^a 0.500 mmol scale – divided into 4 vials (à 250 µL), concentration: 0.50 M.^b Conversion determined *via* GC/FID analysis referenced to *p*-xylene as internal standard.

Figure S1: Reaction monitoring via GC/FID analysis of the reaction of 2-aminobenzyl alcohol with isopropanol.

Table S8: Reaction monitoring via GC/FID analysis of the reaction of 2-aminobenzyl alcohol with 1-ferrocenylethanol.^a

#	Reaction time [h]	Conversion ^b [%]		
		2c	3c	Σ
1	0	0	0	0
2	1	62	12	74
3	2	65	19	84
4	3	59	32	91
5	4	56	38	94
6	5	51	43	94
7	6	50	48	98
8	8	41	57	98
9	14	35	64	99
10	19	31	68	99
11	24	30	70	>99

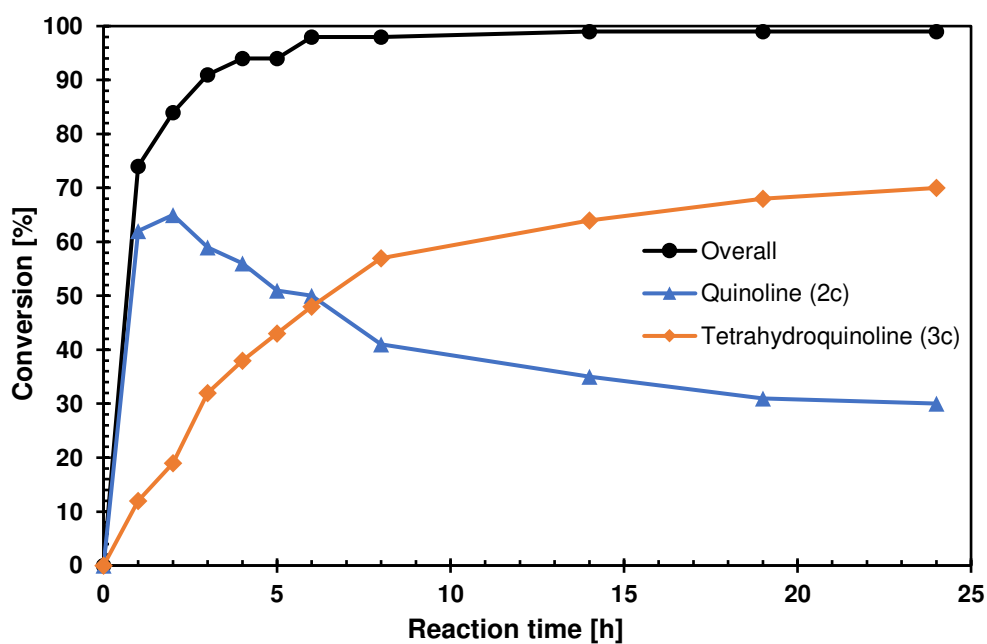
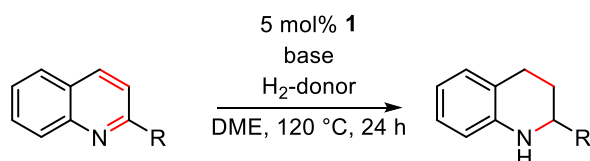
^a 3.000 mmol scale – divided into 12 vials (à 250 µL), concentration: 1.00 M.^b Conversion determined *via* GC/FID analysis referenced to *p*-xylene as internal standard.

Figure S2: Reaction monitoring via GC/FID analysis of the reaction of 2-aminobenzyl alcohol with 1-ferrocenylethanol.

Table S9: Investigation of the reduction of quinoline and 2-phenylquinoline using different hydrogen donors.^a

#	R =	Base		H ₂ -donor		Conversion ^b [%]
		Type	Amount	Type	Amount	
1	H	KH	100	H ₂ ^c	20 bar ^c	94
2	H	KH	100	H ₂ ^c	4 bar ^c	12 ^d
3	H	KH	20	H ₂ ^c	4 bar ^c	59 ^d
4	H	KOtBu	20	H ₂ ^c	4 bar ^c	99
5	H	KH	100	<i>i</i> PrOH	1 eq	93
6	H	KH	100	<i>i</i> PrOH	2 eq	95
7	H	KH	100	<i>i</i> PrOH	5 eq	87
8	H	KH	100	<i>i</i> PrOH	10 eq	58
9	H	KH	100	1-phenylethanol	2 eq	91 ^e
10	Ph	KH	100	H ₂ ^c	4 bar ^c	95
11	Ph	KOtBu	20	H ₂ ^c	4 bar ^c	16
12	Ph	KH	100	<i>i</i> PrOH	2 eq	99
13	Ph	KH	100	1-phenylethanol	2 eq	22 ^e

^a Reaction conditions: 0.250 mmol quinoline, concentration 1.0 M, argon atmosphere. ^b Conversion determined *via* GC/MS analysis. ^c Reaction conducted in a steel autoclave. ^d The starting material was fully converted into 1,2,3,4-tetrahydroquinoline and yet unidentified by-products. ^e The condensation products of 1-phenylethanol 1,3-diphenylpropan-1-one and chalcone were observed as by-products.

3. Experimental procedures

3.1. Procedure for the preparation of a stock solution of catalyst **1**

In an argon filled glovebox, a PTFE-lined screw-cap vial (4.0 mL, \varnothing 1.5 cm, height 4 cm), equipped with a magnetic stirring bar, was charged with $\text{Mn}(\text{CO})_5\text{Br}$ (44.0 mg, 0.16 mmol, 1.0 equiv) and bpy- $^6\text{NH-}i\text{Pr}_2\text{P}$ (46.0 mg, 0.16 mmol, 1.0 equiv). Then DME (2.150 mL) was added. The resulting yellow suspension was stirred in a preheated aluminum block at 30 °C until a light brown solution was formed (15 min). The obtained stock solution was used without further purification.

3.2. General procedure for the synthesis of 1,2,3,4-tetrahydroquinolines

In an argon filled glovebox, a PTFE-lined screw-cap vial (4.0 mL, \varnothing 1.5 cm, height 4 cm), equipped with a magnetic stirring bar, was charged with KH (48.1 mg, 1.20 mmol, 1.5 equiv) and a stock solution of catalyst **1** (215 μL , 0.075 M, 0.016 mmol, 0.02 equiv), then closed with a cap with a septum. After cooling to -5 °C in a cold aluminum block the secondary alcohol (0.800 mmol, 1.0 equiv) was added dropwise through the septum *via* syringe and the resulting mixture was stirred for 5 min. In a second vial (1.5 mL) aminobenzyl alcohol (0.880 mmol, 1.1 equiv) and KOH (13.5 mg, 0.24 mmol, 0.3 equiv) were dissolved in DME (285 μL). Both mixtures were combined and diluted with DME (300 μL). The vial was closed tightly and the resulting reaction mixture was stirred in a preheated aluminum block at 120 °C for 24 h. After cooling to room temperature, the reaction mixture was quenched with H_2O (0.1 mL) and extracted with EtOAc (3×1.5 mL). The combined organic layers were dried over MgSO_4 and the solvent was removed under reduced pressure. The crude product was purified *via* column chromatography (silica, 0 – 20 % DCM in heptane).

3.3. Procedure for the 4 mmol scale synthesis of 2-phenyl-1,2,3,4-tetrahydroquinoline (**3a**)

In an argon filled glovebox, a PTFE-lined screw-cap vial (21.0 mL, \varnothing 2.5 cm, height 5.5 cm), equipped with a magnetic stirring bar, was charged with KH (240 mg, 6.0 mmol, 1.5 equiv) and a stock solution of catalyst **1** (1075 μL , 0.075 M, 0.08 mmol, 0.02 equiv), then closed with a cap with a septum. After cooling to -5 °C in a cold aluminum block the 1-phenylethanol (484 μL , 489 mg, 4.0 mmol, 1.0 equiv) was added dropwise *via* syringe and the resulting mixture was stirred for 5 min. In a second vial (4.0 mL) 2-aminobenzyl alcohol (542 mg, 4.4 mmol, 1.1 equiv) and KOH (67 mg, 1.2 mmol, 0.3 equiv) were dissolved in DME (2 mL). Both mixtures were combined and diluted with DME (1 mL). The vial was closed tightly and the resulting reaction mixture was stirred in a preheated oil bath at 120 °C for 24 h. After cooling to room temperature, the reaction mixture was

quenched with H₂O (5 mL) and extracted with EtOAc (3 × 15 mL). The combined organic layers were dried over MgSO₄ and the solvent was removed under reduced pressure. The crude product was purified *via* column chromatography (silica, 0 – 40 % DCM in heptane) yielding in 603 mg (72 %) of **3a** as slightly yellow oil.

3.4. General procedure for the synthesis of quinolines

In an argon filled glovebox, a PTFE-lined screw-cap vial (4.0 mL, ø 1.5 cm, height 4 cm), equipped with a magnetic stirring bar, was charged with *t*BuOK (44.9 mg, 0.40 mmol, 0.5 equiv) and aminobenzyl alcohol (0.880 mmol, 1.1 equiv). Then a stock solution of catalyst **1** (215 µL, 0.075 M, 0.016 mmol, 0.02 equiv) and secondary alcohol (0.800 mmol, 1.0 equiv) were added. The vial was closed tightly and the resulting reaction mixture was stirred in a preheated aluminum block at 140 °C for 12 h. After cooling to room temperature, the reaction mixture was quenched with H₂O (0.1 mL) and extracted with EtOAc (3 × 1.5 mL). The combined organic layers were dried over MgSO₄ and the solvent was removed under reduced pressure. The crude product was purified *via* column chromatography (silica, 0 – 20 % DCM in heptane).

3.5. General procedure for the synthesis of 1,2,3,4-tetrahydronaphthyridines

In an argon filled glovebox, a PTFE-lined screw-cap vial (4.0 mL, ø 1.5 cm, height 4 cm), equipped with a magnetic stirring bar was charged with KH (48.1 mg, 1.20 mmol, 1.5 equiv) and a stock solution of catalyst **1** (215 µL, 0.075 M, 0.016 mmol, 0.02 equiv), then closed with a cap with a septum. After cooling to –5 °C the secondary alcohol (0.800 mmol, 1.0 equiv) was added dropwise through the septum *via* syringe and the resulting mixture was stirred for 5 min. In a second vial (1.5 mL) (2-aminopyridin-3-yl)methanol (109.2 mg, 0.880 mmol, 1.1 equiv) and KOH (13.5 mg, 0.24 mmol, 0.3 equiv) were dissolved in DME (285 µL). Both mixtures were combined and diluted with DME (300 µL). The vial was closed tightly and the resulting reaction mixture was stirred in a preheated aluminum block at 120 °C for 24 h. After cooling to room temperature, the reaction mixture was quenched with H₂O (0.1 mL) and extracted with EtOAc (3 × 1.5 mL). The combined organic layers were dried over MgSO₄ and the solvent was removed under reduced pressure. The crude product was purified *via* column chromatography (silica, 0 – 10 % EtOAc in heptane).

3.6. General procedure for the hydrogenation of quinolines

Procedure A – hydrogenation with external hydrogen:

In an argon filled glovebox, in a vial (3.0 mL, ø 2.0 cm, height 3 cm), equipped with a magnetic stirring bar, quinoline (0.250 mmol, 1.0 equiv) and KH (10.0 mg, 0.250 mmol, 1.0 equiv) were dissolved in DME (80 µL). A stock solution of catalyst **1** (168 µL, 0.075 M, 0.0125 mmol, 0.05 equiv) was added. The open vial was placed in a steel autoclave and the autoclave was closed

tightly. Outside of the glovebox the autoclave was flushed three times with H₂. Then a pressure of 20 bar (H₂) was applied and the reaction was heated by using an oil bath to 120 °C for 24 h. After cooling to room temperature, the reaction mixture was quenched with H₂O (0.1 mL) and extracted with EtOAc (0.5 mL). 40 µL of the organic layer were diluted with EtOAc (1.0 mL) and analyzed *via* GC/MS analysis.

Procedure B – transfer hydrogenations:

In an argon filled glovebox, in a PTFE-lined screw-cap vial (1.5 mL, ø 1.0 cm, height 3 cm), equipped with a magnetic stirring bar, quinoline (0.250 mmol, 1.0 equiv) and KH (10.0 mg, 0.250 mmol, 1.0 equiv) were dissolved in DME (80 µL). A stock solution of catalyst **1** (168 µL, 0.075 M, 0.0125 mmol, 0.05 equiv) was added, followed by the addition of alcohol (1 – 10 equiv). The vial was closed tightly and the resulting reaction mixture was stirred in a preheated aluminum block at 120 °C for 24 h. After cooling to room temperature, the reaction mixture was quenched with H₂O (0.1 mL) and extracted with EtOAc (0.5 mL). 40 µL of the organic layer were diluted with EtOAc (1.0 mL) and analyzed *via* GC/MS analysis.

3.7. Procedure for the reactions with bromobenzene

Reaction with KH in presence of catalyst **1**:

In an argon filled glovebox, in a PTFE-lined screw-cap vial (4.0 mL, ø 1.5 cm, height 4 cm), equipped with a magnetic stirring bar, bromobenzene (84 µL, 0.80 mmol, 1.0 equiv, d = 1.495 g/mL) and KH (48.1 mg, 1.20 mmol, 1.5 equiv) were dissolved in DME (585 µL). Then a stock solution of catalyst **1** (215 µL, 0.075 M, 0.016 mmol, 0.02 equiv) was added. The vial was closed tightly and the resulting reaction mixture was stirred in a preheated aluminum block at 120 °C for 24 h. After cooling to room temperature, *p*-xylene (70 µL) was added as internal standard, then the reaction mixture was quenched with H₂O (0.1 mL) and extracted with EtOAc (2 mL). 40 µL of the organic layer were diluted with EtOAc (1.0 mL) and analyzed *via* GC/MS analysis. Hydrodebromination was observed, leading to benzene as major product (72 %).

Reaction with KH in absence of catalyst **1**:

In an argon filled glovebox, in a PTFE-lined screw-cap vial (4.0 mL, ø 1.5 cm, height 4 cm), equipped with a magnetic stirring bar, bromobenzene (84 µL, 0.800 mmol, 1.0 equiv, d = 1.495 g/mL) and KH (48.1 mg, 1.20 mmol, 1.5 equiv) were dissolved in DME (800 µL). The vial was closed tightly and the resulting reaction mixture was stirred in a preheated aluminum block at 120 °C for 24 h. After cooling to room temperature, *p*-xylene (70 µL) was added as internal standard, then the reaction mixture was quenched with H₂O (0.1 mL) and extracted with EtOAc (2 mL). 40 µL of the organic layer were diluted with EtOAc (1.0 mL) and analyzed *via* GC/MS analysis. No hydrodebromination of bromobenzene was detected.

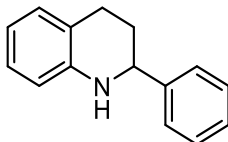
3.8. General procedure for the preparation of samples for GC/FID and GC/MS analysis

The reaction was allowed to reach room temperature. Then *p*-xylene (70 μ L) was added as internal standard. The reaction mixture was quenched with H₂O (0.1 mL) and extracted with EtOAc (2 mL). 40 μ L of the organic layer were diluted with EtOAc (1.0 mL) and analyzed *via* GC/FID or GC/MS analysis.

4. Characterization of products

4.1. Spectroscopic data of 1,2,3,4-tetrahydroquinolines

2-Phenyl-1,2,3,4-tetrahydroquinoline (3a)



Following the general procedure for the synthesis of 1,2,3,4-tetrahydroquinolines, 2-aminobenzyl alcohol (108 mg, 0.880 mmol) and 1-phenylethanol (97 μ l, 98 mg, 0.800 mmol) were used.

Pale yellow oil, GC-Yield: 84 %, Isolated yield: 130 mg, 78 %

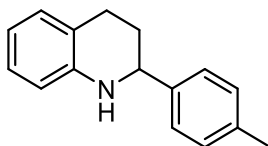
Larger scale synthesis: The reaction was scaled up to a 4.0 mmol scale, yielding 603 mg (72 %) of **3a** (For detailed experimental procedure see Section 3.3).

R_f (silica, Hept/DCM = 1:1) = 0.33

^1H NMR (400.3 MHz, CDCl_3): δ = 7.33 – 7.45 (m, 4H, aryl-H), 7.28 – 7.33 (m, 1H, aryl-H), 6.96 – 7.09 (m, 2H, aryl-H), 6.67 (td, $^3J_{\text{H-H}}$ = 7.4 Hz, $^4J_{\text{H-H}}$ = 1.0 Hz, 1H, aryl-H), 6.56 (d, $^3J_{\text{H-H}}$ = 7.47 Hz, 1H, aryl-H), 4.46 (dd, $^3J_{\text{H-H}}$ = 9.3 Hz, $^3J_{\text{H-H}}$ = 3.3 Hz, 1H, CHNH), 4.05 (br s, 1H, NH), 2.87 – 3.02 (m, 1H, CH_2), 2.68 – 2.82 (m, 1H, CH_2), 2.09 – 2.22 (m, 1H, CH_2), 1.93 – 2.07 (m, 1H, CH_2); $^{13}\text{C}\{^1\text{H}\}$ NMR (100.7 MHz, CDCl_3): δ = 144.8 (Cq), 144.7 (Cq), 129.3 (CH), 128.6 (2 CH), 127.4 (CH), 126.9 (CH), 126.5 (2 CH), 120.9 (Cq), 117.2 (CH), 114.0 (CH, aryl-C), 56.3 (CH, CHNH), 30.7 (CH_2), 20.4 (CH_2). The NMR spectroscopic data is in agreement with the literature.³

HRMS (ESI): m/z Calcd. for $[\text{C}_{15}\text{H}_{16}\text{N}, \text{M}+\text{H}]^+$: 210.1277; found 210.1277.

2-(p-Tolyl)-1,2,3,4-tetrahydroquinoline (3b)



Following the general procedure for the synthesis of 1,2,3,4-tetrahydroquinolines, 2-aminobenzyl alcohol (108 mg, 0.880 mmol) and 1-(p-tolyl)ethan-1-ol (111 μ l, 109 mg, 0.800 mmol) were used.

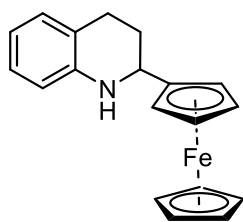
Pale yellow oil, GC-Yield: 71 %, Isolated yield: 119 mg, 67 %

R_f (silica, Hept/DCM = 1:4) = 0.82

^1H NMR (400.3 MHz, CDCl_3): δ = 7.24 – 7.31 (m, 2H, aryl-H), 7.16 (d, $^3J_{\text{H-H}}$ = 7.9 Hz, 2H, aryl-H), 6.96 – 7.04 (m, 2H, aryl-H), 6.60 – 6.68 (m, 1H, aryl-H), 6.53 (d, $^3J_{\text{H-H}}$ = 8.0 Hz, 1H, aryl-H), 4.40

(dd, $^3J_{H-H} = 9.4$ Hz, $^3J_{H-H} = 3.2$ Hz, 1H, CHNH), 4.00 (br s, 1H, NH), 2.86 – 2.98 (m, 1H, CH₂), 2.69 – 2.79 (m, 1H, CH₂), 2.35 (s, 3H, CH₃), 2.05 – 2.14 (m, 1H, CH₂), 1.99 – 2.03 (m, 1H, CH₂); $^{13}\text{C}\{^1\text{H}\}$ NMR (100.7 MHz, CDCl₃): $\delta = 144.8$ (Cq), 141.8 (Cq), 137.1 (Cq), 129.3 (CH), 129.2 (2 CH), 126.9 (CH), 126.4 (2 CH), 120.9 (Cq), 117.1 (CH), 113.9 (CH, aryl-C), 56.0 (CH, CHNH), 31.0 (CH₂), 26.5 (CH₂), 21.1 (CH₃). The NMR spectroscopic data is in agreement with the literature.⁴
HRMS (ESI): m/z Calcd. for [C₁₆H₁₈N, M+H]⁺: 224.1434; found 224.1435.

2-Ferrocenyl-1,2,3,4-tetrahydroquinoline (**3c**)



Following the general procedure for the synthesis of 1,2,3,4-tetrahydroquinolines, 2-aminobenzyl alcohol (108 mg, 0.880 mmol) and α -methylferrocenemethanol (184 mg, 0.800 mmol) were used.

Orange oil, GC-Yield: 98 %, Isolated yield: 231 mg, 91 %

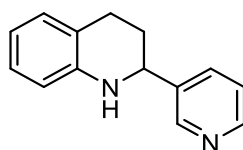
Larger scale synthesis: The reaction was scaled up to a 1.5 mmol scale, performed in a Schlenk tube (10 mL) and heated by using an oil bath, yielding 366 mg (77 %) of **3c**.

R_f (silica, Hept/DCM = 1:4) = 0.78

^1H NMR (400.3 MHz, CDCl₃): $\delta = 6.70$ – 7.09 (m, 2H, aryl-H), 6.62 – 6.68 (m, 1H, aryl-H), 6.56 – 6.62 (m, 1H, aryl-H), 4.22 (s, 5H, C₅H₅), 4.10 – 4.29 (m, 6H, C₅H₄, NH, CHNH, partially obstructed by other signals), 2.84 – 2.96 (m, 1H, CH₂), 2.69 – 2.80 (m, 1H, CH₂), 2.09 – 2.17 (m, 1H, CH₂), 1.72 – 1.88 (m, 1H, CH₂); $^{13}\text{C}\{^1\text{H}\}$ NMR (100.7 MHz, CDCl₃): $\delta = 144.6$ (Cq), 129.2 (CH), 126.8 (CH), 121.0 (Cq), 117.0 (CH), 113.8 (CH, aryl-C), 92.8 (Cq, Fc), 68.3 (C₅H₅), 67.8 (CH), 67.0 (CH), 66.8 (CH), 65.7 (CH, ferrocenyl-C), 51.1 (CH, CHNH), 30.9 (CH₂), 26.8 (CH₂).

HRMS (ESI): m/z Calcd. for [C₁₉H₁₉FeN, M]⁺: 317.0861; found 317.0867.

2-(Pyridin-3-yl)-1,2,3,4-tetrahydroquinoline (**3d**)



Following the general procedure for the synthesis of 1,2,3,4-tetrahydroquinolines, 2-aminobenzyl alcohol (108 mg, 0.880 mmol) and 1-(pyridin-3-yl)ethan-1-ol (99 mg, 0.91 μL , 0.800 mmol) were used.

A different workup procedure was applied to obtain this product in satisfying yields:

The reaction was quenched with water, then all volatiles were removed under reduced pressure. The solids were suspended in Et₂O, then NH₄Cl was added in portions until a pH of 7 was reached. After filtration, the solvent was removed under reduced pressure. The crude product was purified *via* column chromatography (silica, 0 – 50 % EtOAc in heptane).

Yellow oil, GC-Yield: 86 %, Isolated yield: 117 mg, 70 %

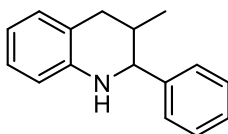
R_f (silica, Hept/DCM = 1:4) = 0.04

¹H NMR (400.3 MHz, CDCl₃): δ = 8.64 (d, ⁴J_{H-H} = 2.0 Hz, 1H, aryl-H), 8.56 (dd, ⁴J_{H-H} = 4.6 Hz, ⁴J_{H-H} = 1.5 Hz, 1H, aryl-H), 7.74 (d, ³J_{H-H} = 7.9 Hz, 1H, aryl-H), 7.29 (dd, ³J_{H-H} = 7.9 Hz, ⁴J_{H-H} = 4.8 Hz, 1H, aryl-H) 6.98 – 7.09 (m, 2H, aryl-H), 6.66 – 6.73 (m, 1H, aryl-H), 6.58 (d, ³J_{H-H} = 7.9 Hz, 1H, aryl-H), 4.50 (dd, ³J_{H-H} = 7.9 Hz, ³J_{H-H} = 4.8 Hz, 1H, CHNH), 4.05 (br s, 1H, NH), 2.90 – 2.96 (m, 1H, CH₂), 2.70 – 2.80 (m, 1H, CH₂), 2.11 – 2.19 (m, 1H, CH₂), 1.95 – 2.09 (m, 1H, CH₂). The ¹H NMR spectroscopic data is in agreement with the literature.⁵

¹³C{¹H} NMR (100.7 MHz, CDCl₃): δ = 149.0 (CH), 148.6 (CH), 144.2 (Cq), 140.0 (Cq), 134.2 (CH), 129.4 (CH), 127.0 (CH), 123.6 (CH), 120.7 (Cq), 117.7 (CH), 114.2 (CH, aryl-C), 53.9 (CH), 30.8 (CH₂), 26.0 (CH₂).

HRMS (ESI): m/z Calcd. for [C₁₄H₁₅N₂, M+H]⁺: 211.1230; found 211.1230.

3-Methyl-2-phenyl-1,2,3,4-tetrahydroquinoline (3e)

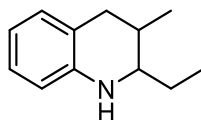


Following the general procedure for the synthesis of 1,2,3,4-tetrahydroquinolines, 2-aminobenzyl alcohol (108 mg, 0.880 mmol) and 1-phenylpropan-1-ol (109 mg, 110 μL, 0.800 mmol) were used. Pale yellow oil, GC-Yield: 20 %, Isolated yield: 18 mg, 10 %

R_f (silica, Hept/DCM = 1:4) = 0.66

¹H NMR (400.3 MHz, CDCl₃): δ = 7.24 – 7.43 (m, 5H, aryl-H), 6.98 – 7.09 (m, 2H, aryl-H), 6.77 (td, ³J_{H-H} = 7.4 Hz, ⁴J_{H-H} = 1.2 Hz, 1H, aryl-H), 6.58 (td, ³J_{H-H} = 7.9 Hz, ⁴J_{H-H} = 0.8 Hz, 1H, aryl-H), 4.54 (d, ³J_{H-H} = 3.6 Hz, 1H, CHNH), 4.14 (br s, 1H, NH), 2.99 (dd, ²J_{H-H} = 16.2 Hz, ³J_{H-H} = 5.0 Hz, 1H, CH₂), 2.52 (dd, ²J_{H-H} = 16.1 Hz, ³J_{H-H} = 6.6 Hz, 1H, CH₂), 2.26 – 2.38 (m, 1H, CH), 0.84 (d, ³J_{H-H} = 7.0 Hz, 3H, CH₃); ¹³C{¹H} NMR (100.7 MHz, CDCl₃): δ = 144.2 (Cq), 142.9 (Cq), 129.7 (CH), 128.1 (2 CH), 127.2 (2 CH), 127.1 (CH), 126.9 (CH), 120.0 (Cq), 117.1 (CH), 113.7 (CH, aryl-C), 59.4 (CH, CHNH), 33.4 (CH₂), 31.9 (CH), 15.1 (CH₃). The NMR spectroscopic data is in agreement with the literature.⁶

HRMS (ESI): m/z Calcd. for [C₁₆H₁₈N, M+H]⁺: 224.1434; found 224.1433.

2-Ethyl-3-methyl-1,2,3,4-tetrahydroquinoline (3f)

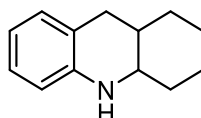
Following the general procedure for the synthesis of 1,2,3,4-tetrahydroquinolines, 2-aminobenzyl alcohol (108 mg, 0.880 mmol) and pentan-3-ol (71 mg, 86 μ L, 0.800 mmol) were used.

Pale yellow oil, GC-Yield: 24 %, Isolated yield: 29 mg, 21 %

R_f (silica, Hept/DCM = 1:4) = 0.70

^1H NMR (400.3 MHz, CDCl_3): δ = 6.91 – 7.03 (m, 2H, aryl-H), 6.61 (td, $^3J_{\text{H-H}} = 7.4$ Hz, $^4J_{\text{H-H}} = 1.2$ Hz, 1H, aryl-H), 6.50 (d, $^3J_{\text{H-H}} = 7.9$ Hz, 1H, aryl-H), 3.78 (br s, 1H, NH), 3.07 – 3.26 (m, 1H, CHNH), 2.94 (dd, $^2J_{\text{H-H}} = 16.1$ Hz, $^3J_{\text{H-H}} = 5.4$ Hz, 1H, CH_2), 2.49 (dd, $^2J_{\text{H-H}} = 16.1$ Hz, $^3J_{\text{H-H}} = 4.9$ Hz, 1H, CH_2), 2.09 – 2.14 (m, 1H, CH), 1.39 – 1.57 (m, 2H, CH_2CH_3), 0.99 (t, $^3J_{\text{H-H}} = 7.5$ Hz, 3H, CH_2CH_3), 0.92 (d, $^3J_{\text{H-H}} = 4.9$ Hz, 3H, CH_3); $^{13}\text{C}\{^1\text{H}\}$ NMR (100.7 MHz, CDCl_3): δ = 144.0 (Cq), 129.9 (CH), 126.6 (CH), 120.3 (Cq), 116.9 (CH), 113.7 (CH, aryl-C), 56.3 (CH, CHNH), 34.5 (CH_2), 28.9 (CH), 24.8 (CH_2CH_3), 13.7 (CH_3), 10.5 (CH_3). The NMR spectroscopic data is in agreement with the literature.⁷

HRMS (ESI): m/z Calcd. for $[\text{C}_{12}\text{H}_{18}\text{N}, \text{M}+\text{H}]^+$: 176.1434; found 176.1437.

1,2,3,4,4a,9,9a,10-Octahydroacridine (3g)

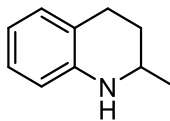
Following the general procedure for the synthesis of 1,2,3,4-tetrahydroquinolines, 2-aminobenzyl alcohol (108 mg, 0.880 mmol) and cyclohexanol (80 mg, 84 μ L, 0.800 mmol) were used.

Pale yellow oil, GC-Yield: 23%, Isolated yield: 21 mg, 14%

R_f (silica, Hept/DCM = 1:4) = 0.66

^1H NMR (400.3 MHz, CDCl_3): δ = 6.88 – 7.02 (m, 2H, aryl-H), 6.57 (td, $^3J_{\text{H-H}} = 7.4$ Hz, $^4J_{\text{H-H}} = 1.2$ Hz, 1H, aryl-H), 6.45 (td, $^3J_{\text{H-H}} = 7.8$ Hz, $^4J_{\text{H-H}} = 0.9$ Hz, 1H, aryl-H), 3.40 – 3.67 (m, 2H, NH, CHNH), 2.91 (dd, $^2J_{\text{H-H}} = 16.2$ Hz, $^3J_{\text{H-H}} = 5.7$ Hz, 1H, CH_2), 2.53 (dd, $^2J_{\text{H-H}} = 16.3$ Hz, $^3J_{\text{H-H}} = 4.1$ Hz, 1H, CH_2), 2.04 (m, 1H, CH), 1.57 – 1.74 (m, 4H, 2 CH_2), 1.30 – 1.51 (m, 4H, 2 CH_2); $^{13}\text{C}\{^1\text{H}\}$ NMR (100.7 MHz, CDCl_3): δ = 143.9 (Cq), 129.7 (CH), 126.6 (CH), 119.3 (Cq), 116.4 (CH), 113.2 (CH, aryl-C), 50.0 (CHNH), 32.9 (CH), 32.5 (CH_2), 31.8 (CH_2), 27.3 (CH_2), 24.7 (CH_2), 20.7 (CH_2). The NMR spectroscopic data is in agreement with the literature.⁶

HRMS (ESI): m/z Calcd. for $[\text{C}_{13}\text{H}_{18}\text{N}, \text{M}+\text{H}]^+$: 188.1434; found 188.1434.

2-Methyl-1,2,3,4-tetrahydroquinoline (3h)

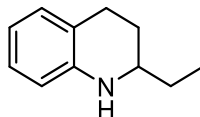
Following the general procedure for the synthesis of 1,2,3,4-tetrahydroquinolines, 2-aminobenzyl alcohol (108 mg, 0.880 mmol) and propan-2-ol (48 mg, 62 μ L, 0.800 mmol) were used.

Pale yellow oil, GC-Yield: 84 %, Isolated yield: 87 mg, 74 %

R_f (silica, Hept/DCM = 1:1) = 0.34

^1H NMR (400.3 MHz, CDCl_3): δ = 6.95 – 7.02 (m, 2H, aryl-H), 6.63 (t, $^3J_{\text{H-H}}$ = 7.4 Hz, 1H, aryl-H), 6.49 (d, $^3J_{\text{H-H}}$ = 8.2 Hz, 1H, aryl-H), 3.69 (br s, 1H, NH), 3.39 – 3.46 (m, 1H, CHNH), 2.81 – 2.87 (m, 1H, CH_2), 2.70 – 2.79 (m, 1H, CH_2), 1.92 – 1.99 (m, 1H, CH_2), 1.59 – 1.65 (m, 1H, CH_2), 1.23 (d, $^3J_{\text{H-H}}$ = 6.2 Hz, CH_3); $^{13}\text{C}\{^1\text{H}\}$ NMR (100.7 MHz, CDCl_3): δ = 144.7 (Cq), 129.2 (CH), 126.7 (CH), 121.1 (Cq), 117.0 (CH), 114.0 (CH, aryl-C), 47.2 (CH, CHNH), 30.1 (CH_2), 26.6 (CH_2), 22.6 (CH_3). The NMR spectroscopic data is in agreement with the literature.⁸

HRMS (ESI): m/z Calcd. for $[\text{C}_{10}\text{H}_{14}\text{N}, \text{M}+\text{H}]^+$: 148.1121; found 148.1121.

2-Ethyl-1,2,3,4-tetrahydroquinoline (3i)

Following the general procedure for the synthesis of 1,2,3,4-tetrahydroquinolines, 2-aminobenzyl alcohol (108 mg, 0.880 mmol) and butan-2-ol (59 mg, 73 μ L, 0.800 mmol) were used.

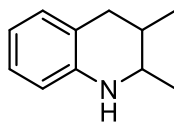
Pale yellow oil, GC-Yield: 61 %, NMR yield of **3i**: 70 mg, 54 %

R_f (silica, Hept/DCM = 1:3) = 0.53

Attempts to separate **3i** and **3i'** by column chromatography have been unsuccessful so far.

^1H NMR (400.3 MHz, CDCl_3): δ = 6.95 – 7.00 (m, 2H, aryl-H), 6.59 – 6.63 (m, 1H, aryl-H), 6.47 – 6.50 (m, 1H, aryl-H), 3.77 (br s, 1H, NH), 3.14 – 3.23 (m, 1H, CHNH), 2.70 – 2.88 (m, 2H, CH_2), 1.94 – 2.02 (m, 1H, CH_2), 1.50 – 1.64 (m, 3H, CH_2), 1.01 (t, $^3J_{\text{H-H}}$ = 7.5 Hz, 3H, CH_3); $^{13}\text{C}\{^1\text{H}\}$ NMR (100.7 MHz, CDCl_3): δ = 144.7 (Cq), 129.2 (CH), 126. (CH), 121.4 (Cq), 116.8 (CH), 114.0 (CH, aryl-C), 53.0 (CHNH), 29.4 (CH_2), 27.6 (CH_2), 26.4 (CH_2), 10.0 (CH_3). The NMR spectroscopic data is in agreement with the literature⁹

HRMS (ESI): m/z Calcd. for $[\text{C}_{11}\text{H}_{16}\text{N}, \text{M}+\text{H}]^+$: 162.1277; found 162.1279.

2,3-dimethyl-1,2,3,4-tetrahydroquinoline (3i')

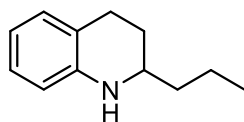
Following the general procedure for the synthesis of 1,2,3,4-tetrahydroquinolines, 2-aminobenzyl alcohol (108 mg, 0.880 mmol) and butan-2-ol (59 mg, 73 μ L, 0.800 mmol) were used.

Yellow oil, GC-Yield: 28 %, NMR yield of **3i'**: 31 mg, 24 %

R_f (silica, Hept/DCM = 1:3) = 0.50

Attempts to separate **3i** and **3i'** by column chromatography have been unsuccessful so far.

^1H NMR (400.3 MHz, CDCl_3): δ = 6.95 – 7.00 (m, 2H, aryl-H), 6.59 – 6.63 (m, 1H, aryl-H), 6.47 – 6.50 (m, 1H, aryl-H), 3.71 (br s, 1H, NH), 3.43 – 3.51 (m, 1H, CHNH), 2.85 – 2.95 (m, 2H, CH_2), 2.49 (dd, $^1J_{\text{H-H}}$ = 16.1 Hz, $^3J_{\text{H-H}}$ = 6.0 Hz, 1H, CH_2), (2.03 – 2.09 (m, 1H, CH), 1.13 (d, $^3J_{\text{H-H}}$ = 6.6 Hz, 3H, CH_3), 0.95 (d, $^3J_{\text{H-H}}$ = 6.6 Hz, 3H, CH_3); $^{13}\text{C}\{^1\text{H}\}$ NMR (100.7 MHz, CDCl_3): δ = 143.9 (Cq), 129.8 (CH), 126.6 (CH), 120.9 (Cq), 116.9 (CH), 113.8 (CH, aryl-C), 49.9 (CHNH), 33.8 (CH_2), 30.5 (CH), 18.1 (CH_3), 14.4 (CH_3). The NMR spectroscopic data is in agreement with the literature.¹⁰

2-Propyl-1,2,3,4-tetrahydroquinoline (3j)

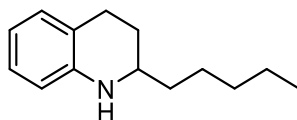
Following the general procedure for the synthesis of 1,2,3,4-tetrahydroquinolines, 2-aminobenzyl alcohol (108 mg, 0.880 mmol) and pentan-2-ol (71 mg, 87 μ L, 0.800 mmol) were used.

Pale yellow oil, GC-Yield: 61 %, Isolated yield: 80 mg, 57 %

R_f (silica, Hept/DCM = 1:4) = 0.68

^1H NMR (400.3 MHz, CDCl_3): δ = 6.94 – 7.02 (m, 2H, aryl-H), 6.61 (dt, $^3J_{\text{H-H}}$ = 7.4 Hz, $^4J_{\text{H-H}}$ = 0.9 Hz, 1H, aryl-H), 6.49 (dd, $^3J_{\text{H-H}}$ = 8.4 Hz, $^4J_{\text{H-H}}$ = 0.9 Hz, 1H, aryl-H), 3.78 (br s, 1H, NH), 3.23 – 3.31 (m, 1H, CHNH), 2.70 – 2.89 (m, 2H, CH_2), 1.93 – 2.04 (m, 1H, CH_2), 1.56 – 1.68 (m, 1H, CH_2), 1.39 – 1.55 (m, 4H, 2 CH_2), 0.98 (t, $^3J_{\text{H-H}}$ = 6.9 Hz, 3H, CH_3); $^{13}\text{C}\{^1\text{H}\}$ NMR (100.7 MHz, CDCl_3): δ = 144.7 (Cq), 129.2 (CH), 126.7 (CH), 121.4 (Cq), 116.9 (CH), 114.0 (CH, aryl-C), 51.3 (CHNH), 38.9 (CH_2), 28.1 (CH_2), 26.4 (CH_2), 18.9 (CH_2), 14.2 (CH_3). The NMR spectroscopic data is in agreement with the literature.¹¹

HRMS (ESI): m/z Calcd. for $[\text{C}_{12}\text{H}_{18}\text{N}, \text{M}+\text{H}]^+$: 176.1434; found 176.1437.

2-Pentyl-1,2,3,4-tetrahydroquinoline (3k)

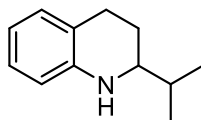
Following the general procedure for the synthesis of 1,2,3,4-tetrahydroquinolines, 2-aminobenzyl alcohol (108 mg, 0.880 mmol) and heptan-2-ol (93 mg, 113 μ L, 0.800 mmol) were used.

Pale yellow oil, GC-Yield: 64 %, Isolated yield: 101 mg, 62 %

R_f (silica, Hept/DCM = 1:5) = 0.85

^1H NMR (400.3 MHz, CDCl_3): δ = 6.94 – 7.02 (m, 2H, aryl-H), 6.52 (td, $^3J_{\text{H-H}} = 7.3$ Hz, $^4J_{\text{H-H}} = 0.9$ Hz, 1H, aryl-H), 6.40 (d, $^3J_{\text{H-H}} = 8.1$ Hz, 1H, aryl-H), 3.77 (br s, 1H, NH), 3.21 – 3.29 (m, 1H, CHNH), 2.70 – 2.90 (m, 2H, CH_2), 1.92 – 2.02 (m, 1H, CH_2), 1.56 – 1.67 (m, 1H, CH_2), 1.47 – 1.55 (m, 2H, CH_2), 1.31 – 1.46 (m, 6H, 3 CH_2), 0.93 (t, $^3J_{\text{H-H}} = 6.9$ Hz, 3H, CH_3); $^{13}\text{C}\{^1\text{H}\}$ NMR (100.7 MHz, CDCl_3): δ = 144.7 (Cq), 129.2 (CH), 126.7 (CH), 121.4 (Cq), 116.8 (CH), 114.0 (CH, aryl-C), 51.6 (CHNH), 36.7 (CH_2), 31.9 (CH_2), 28.1 (CH_2), 26.4 (CH_2), 25.4 (CH_2), 22.6 (CH_2), 14.0 (CH_3). The NMR spectroscopic data is in agreement with the literature.¹²

HRMS (ESI): m/z Calcd. for $[\text{C}_{14}\text{H}_{22}\text{N}, \text{M}+\text{H}]^+$: 204.1747; found 204.1749.

2-Isopropyl-1,2,3,4-tetrahydroquinoline (3l)

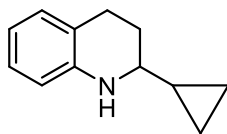
Following the general procedure for the synthesis of 1,2,3,4-tetrahydroquinolines, 2-aminobenzyl alcohol (108 mg, 0.880 mmol) and 3-methylbutan-2-ol (71 mg, 86 μ L, 0.800 mmol) were used.

Yellow oil, GC-Yield: 66 %, Isolated yield: 85 mg, 61 %

R_f (silica, Hept/DCM = 1:4) = 0.80

^1H NMR (400.3 MHz, CDCl_3): δ = 6.88 – 7.04 (m, 2H, aryl-H), 6.59 (t, $^3J_{\text{H-H}} = 7.3$ Hz, 1H, aryl-H), 6.49 (d, $^3J_{\text{H-H}} = 7.8$ Hz, 1H, aryl-H), 3.78 (br s, 1H, NH), 2.98 – 3.11 (m, 1H, CHNH), 2.60 – 2.87 (m, 2H, CH_2), 1.84 – 1.99 (m, 1H, CH), 1.61 – 1.79 (m, 2H, CH_2), 0.95 – 1.03 (m, 6H, 2 CH_3); $^{13}\text{C}\{^1\text{H}\}$ NMR (100.7 MHz, CDCl_3): δ = 145.0 (Cq), 129.1 (CH), 126.7 (CH), 121.4 (Cq), 116.7 (CH), 113.9 (CH, aryl-C), 57.3 (CHNH), 32.5 (CH_2), 26.6 (CH), 24.5 (CH_2), 18.6 (CH_3), 18.2 (CH_3). The NMR spectroscopic data is in agreement with the literature.¹¹

HRMS (ESI): m/z Calcd. for $[\text{C}_{12}\text{H}_{18}\text{N}, \text{M}+\text{H}]^+$: 176.1434; found 176.1433.

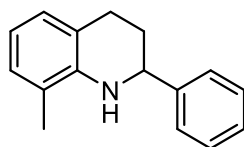
2-Cyclopropyl-1,2,3,4-tetrahydroquinoline (3n)

Following the general procedure for the synthesis of 1,2,3,4-tetrahydroquinolines, 2-aminobenzyl alcohol (108 mg, 0.880 mmol) and 1-cyclopropylethan-1-ol (69 mg, 78 μ L, 0.800 mmol) were used. Yellow oil, GC-Yield: 81 %, Isolated yield: 95 mg, 69 %

R_f (silica, Hept/DCM = 1:4) = 0.70

^1H NMR (400.3 MHz, CDCl_3): δ = 6.91 – 7.02 (m, 2H, aryl-H), 6.61 (td, $^3J_{\text{H-H}} = 7.3$ Hz, $^4J_{\text{H-H}} = 0.9$ Hz, 1H, aryl-H), 6.50 (d, $^3J_{\text{H-H}} = 7.9$ Hz, 1H, aryl-H), 3.99 (br s, 1H, NH), 2.73 – 2.83 (m, 2H, CHNH, CH_2), 2.37 – 2.44 (m, 1H, CH_2), 2.04 – 2.16 (m, 1H, CH_2), 1.73 – 1.87 (m, 1H, CH_2), 0.88 – 0.98 (m, 1H, CH), 0.49 – 0.59 (2H, CH_2), 0.20 – 0.31 (2H, CH_2); $^{13}\text{C}\{^1\text{H}\}$ NMR (100.7 MHz, CDCl_3): δ = 144.6 (Cq), 129.2 (CH), 126.7 (CH), 121.2 (Cq), 116.8 (CH), 113.8 (CH, aryl-C), 57.5 (CHNH), 28.3 (CH_2), 26.7 (CH_2), 17.0 (CH), 2.9 (CH_2), 1.9 (CH_2). The NMR spectroscopic data is in agreement with the literature.⁴

HRMS (ESI): m/z Calcd. for $[\text{C}_{12}\text{H}_{16}\text{N}, \text{M}+\text{H}]^+$: 174.1277; found 174.1277.

8-Methyl-2-phenyl-1,2,3,4-tetrahydroquinoline (3o)

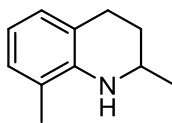
Following the general procedure for the synthesis of 1,2,3,4-tetrahydroquinolines, 2-amino-3-methylbenzyl alcohol (121 mg, 0.880 mmol) and 1-phenylethanol (97 μ L, 98 mg, 0.800 mmol) were used.

Pale yellow oil, GC-Yield: 81 %, Isolated yield: 126 mg, 71 %

R_f (silica, Hept/DCM = 1:4) = 0.75

^1H NMR (400.3 MHz, CDCl_3): δ = 7.29 – 7.51 (m, 5H, aryl-H), 6.94 (t, $^3J_{\text{H-H}} = 8.3$ Hz, 2H, aryl-H), 6.63 (t, $^3J_{\text{H-H}} = 7.4$ Hz, 1H, aryl-H), 4.52 (dd, $^3J_{\text{H-H}} = 9.4$ Hz, $^3J_{\text{H-H}} = 3.1$ Hz, 1H, CHNH), 3.89 (br s, 1H, NH), 2.91 – 3.06 (m, 1H, CH_2), 2.72 – 2.82 (m, 1H, CH_2), 2.10 – 2.23 (m, 1H, CH_2 , obscured by other signal), 2.13 (s, 3H, CH_3), 1.95 – 2.09 (m, 1H, CH_2); $^{13}\text{C}\{^1\text{H}\}$ NMR (100.7 MHz, CDCl_3): δ = 145.1 (Cq), 142.7 (Cq), 128.6 (2 CH), 128.0 (CH), 127.4 (CH), 127.1 (CH), 126.5 (2 CH), 120.9 (Cq), 120.3 (Cq), 116.6 (CH, aryl-C), 56.6 (CH, CHNH), 31.0 (CH_2), 26.7 (CH_2), 17.2 (CH_3).

HRMS (ESI): m/z Calcd. for $[\text{C}_{16}\text{H}_{18}\text{N}, \text{M}+\text{H}]^+$: 224.1434; found 224.1437.

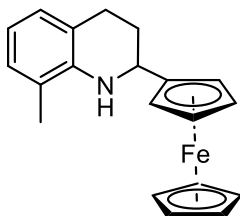
2,8-Dimethyl-1,2,3,4-tetrahydroquinoline (3p)

Following the general procedure for the synthesis of 1,2,3,4-tetrahydroquinolines, 2-amino-3-methylbenzyl alcohol (121 mg, 0.880 mmol) and propan-2-ol (48 mg, 62 μ L, 0.800 mmol) were used.

Pale yellow oil, GC-Yield: 81 %, Isolated yield: 101 mg, 79 %

R_f (silica, Hept/DCM = 1:1) = 0.30

^1H NMR (400.3 MHz, CDCl_3): δ = 6.89 (t, $^3J_{\text{H-H}}$ = 6.4 Hz, 2H, aryl-H), 6.57 (t, $^3J_{\text{H-H}}$ = 7.4 Hz, 1H, aryl-H), 3.42 – 3.51 (m, 2H, NH, CHNH), 2.82 – 2.96 (m, 1H, CH_2), 2.70 – 2.82 (m, 1H, CH_2), 2.11 (s, 3H, aryl- CH_3), 1.88 – 2.01 (m, 1H, CH_2), 1.51 – 1.69 (m, 1H, CH_2), 1.28 (d, $^3J_{\text{H-H}}$ = 6.2 Hz, 3H, CH_3); $^{13}\text{C}\{^1\text{H}\}$ NMR (100.7 MHz, CDCl_3): δ = 142.7 (Cq), 127.8 (CH), 127.1 (CH), 120.8 (Cq), 120.5 (Cq), 116.3 (CH, aryl-C), 47.4 (CH, CHNH), 30.0 (CH_2), 26.9 (CH_2), 22.8 (CH_3), 17.2 (CH_3). **HRMS** (ESI): m/z Calcd. for $[\text{C}_{11}\text{H}_{15}\text{N}, \text{M}+\text{H}]^+$: 162.1277; found 162.1279.

2-Ferrocenyl-8-methyl-1,2,3,4-tetrahydroquinoline (3q)

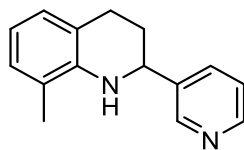
Following the general procedure for the synthesis of 1,2,3,4-tetrahydroquinolines, 2-amino-3-methylbenzyl alcohol (121 mg, 0.880 mmol) and α -methylferrocenemethanol (184 mg, 0.800 mmol) were used.

Orange oil, GC-Yield: 94%, Isolated yield: 241 mg, 91 %

R_f (silica, Hept/DCM = 1:4) = 0.80

^1H NMR (400.3 MHz, CDCl_3): δ = 6.97 (d, $^3J_{\text{H-H}}$ = 7.4 Hz, 1H, aryl-H), 6.92 (d, $^3J_{\text{H-H}}$ = 7.4 Hz, 1H, aryl-H), 6.61 (t, $^3J_{\text{H-H}}$ = 7.4 Hz, 1H, aryl-H), 4.25 (s, 5H, C_5H_5), 4.10 – 4.34 (m, 6H, C_5H_4 , NH, CHNH, partially obstructed by other signals), 2.89 – 3.01 (m, 1H, CH_2), 2.73 – 2.83 (m, 1H, CH_2), 2.25 (s, CH_3), 2.05 – 2.16 (m, 1H, CH_2), 1.68 – 1.85 (m, 1H, CH_2); $^{13}\text{C}\{^1\text{H}\}$ NMR (100.7 MHz, CDCl_3): δ = 142.7 (Cq), 128.0 (CH), 127.1 (CH), 120.4 (Cq), 120.2 (Cq), 116.3 (CH, aryl-C), 93.2 (Cq, Fc), 68.3 (C_5H_5), 67.8 (CH), 67.6 (CH), 67.1 (CH), 65.3 (CH, ferrocenyl-C), 51.3 (CH, CHNH), 31.4 (CH_2), 27.2 (CH_2), 17.3 (CH_3).

HRMS (ESI): m/z Calcd. for $[\text{C}_{20}\text{H}_{21}\text{FeN}, \text{M}]^+$: 331.1023; found 331.1016.

8-Methyl-2-(pyridin-3-yl)-1,2,3,4-tetrahydroquinoline (3r)

Following the general procedure for the synthesis of 1,2,3,4-tetrahydroquinolines, 2-amino-3-methylbenzyl alcohol (121 mg, 0.880 mmol) and 1-(pyridin-3-yl)ethan-1-ol (99 mg, 0.91 μ L, 0.800 mmol) were used.

A different workup procedure was applied to obtain this product in satisfying yields:

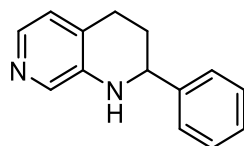
The reaction was quenched with water, then all volatiles were removed under reduced pressure. The solids were suspended in Et₂O, then NH₄Cl was added in portions until a pH of 7 was reached. After filtration, the solvent was removed under reduced pressure. The crude product was purified *via* column chromatography (silica, 0 – 50 % EtOAc in heptane).

Dark yellow oil, GC-Yield: 94 %, Isolated yield: 142 mg, 79 %

R_f (silica, Hept/DCM = 1:4) = 0.05

¹H NMR (400.3 MHz, CDCl₃): δ = 8.68 (d, ⁴J_{H-H} = 2.0 Hz, 1H, aryl-H), 8.58 (dd, ³J_{H-H} = 4.8 Hz, ⁴J_{H-H} = 1.6 Hz, 1H, aryl-H), 7.76 (dt, ³J_{H-H} = 7.9 Hz, ⁴J_{H-H} = 1.8 Hz, 1H, aryl-H), 7.31 (dd, ³J_{H-H} = 7.8 Hz, ³J_{H-H} = 4.8 Hz, 1H, aryl-H), 6.96 (d, ³J_{H-H} = 7.4 Hz, 1H, aryl-H), 6.93 (d, ³J_{H-H} = 7.4 Hz, 1H, aryl-H), 6.65 (t, ³J_{H-H} = 7.4 Hz, 1H, aryl-H), 4.55 (dd, ³J_{H-H} = 9.3 Hz, ³J_{H-H} = 3.3 Hz, 1H, CHNH), 3.85 (br s, 1H, NH), 2.91 – 3.05 (m, 1H, CH₂), 2.76 – 3.00 (m, 1H, CH₂), 2.10 – 2.23 (m, 1H, CH₂), 2.13 (s, 3H, CH₃), 1.95 – 2.10 (m, 1H, CH₂); ¹³C{¹H} NMR (100.7 MHz, CDCl₃): δ = 148.9 (CH), 148.5 (CH), 142.2 (Cq), 140.3 (Cq), 134.2 (CH), 128.1 (CH), 127.2 (CH), 123.6 (CH), 121.3 (Cq), 120.2 (Cq), 117.1 (CH, aryl-C), 54.2 (CH), 30.8 (CH₂), 26.3 (CH₂), 17.2 (CH₃).

HRMS (ESI): m/z Calcd. for [C₁₅H₁₇N₂, M+H]⁺: 225.1386; found 225.1393.

2-Phenyl-1,2,3,4-tetrahydro-1,7-naphthyridine (3s)

Following the general procedure for the synthesis of 1,2,3,4-tetrahydroquinolines, (3-aminopyridin-4-yl)methanol (109 mg, 0.880 mmol) and 1-phenylethanol (97 μ L, 98 mg, 0.800 mmol) were used.

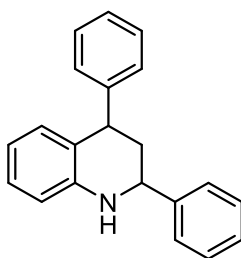
R_f (silica, Hept/EtOAc = 1:1) = 0.27

Dark yellow oil, GC-Yield: 54 %, Isolated yield: 73 mg, 43 %

^1H NMR (400.3 MHz, CDCl_3): δ = 7.94 (s, 1H, aryl-H), 7.88 (d, $^3J_{\text{H-H}}$ = 4.8 Hz, 1H, aryl-H), 7.34 – 7.41 (m, 4H, aryl-H), 7.29 – 7.34 (m, 1H, aryl-H), 6.90 (d, $^3J_{\text{H-H}}$ = 4.8 Hz, 1H, aryl-H), 4.48 (dd, $^3J_{\text{H-H}}$ = 9.1 Hz, $^3J_{\text{H-H}}$ = 2.4 Hz, 1H, CHNH), 4.17 (br s, 1H, NH), 2.84 – 2.95 (m, 1H, CH_2), 2.68 – 2.76 (m, 1H, CH_2), 2.10 – 2.20 (m, 1H, CH_2), 1.93 – 2.07 (m, 1H, CH_2); $^{13}\text{C}\{^1\text{H}\}$ NMR (100.7 MHz, CDCl_3): δ = 143.9 (Cq), 141.6 (Cq), 138.4 (CH), 136.0 (CH), 128.69 (2 CH), 128.67 (Cq), 127.7 (CH), 126.4 (2 CH), 123.5 (CH, aryl-C), 55.7 (CHNH), 29.9 (CH_2), 25.5 (CH_2).

HRMS (ESI): m/z Calcd. for $[\text{C}_{14}\text{H}_{15}\text{N}_2, \text{M}+\text{H}]^+$: 211.1230; found 211.1235.

2,4-Diphenyl-1,2,3,4-tetrahydroquinoline (**3t**)



Following the general procedure for the synthesis of 1,2,3,4-tetrahydroquinolines, 2-aminobenzhydrol (175 mg, 0.880 mmol) and 1-phenylethanol (97 μl , 98 mg, 0.800 mmol) were used.

Yellow oil, GC-Yield: 53 %, Isolated yield: 64 mg, 28 %

R_f (silica, Hept/DCM = 1:5) = 0.53

mixture of *cis*- and *trans*- isomer (ratio = 0.72:1)

cis-isomer:

^1H NMR (400.3 MHz, CDCl_3): δ = 7.42 (d, $^3J_{\text{H-H}}$ = 7.4 Hz, 2H, aryl-H), 7.26 – 7.35 (m, 5H, aryl-H), 7.19 – 7.24 (m, 2H, aryl-H), 6.95 – 7.00 (m, 1H, aryl-H), 6.59 – 6.64 (m, 2H, aryl-H), 6.52 – 6.55 (m, 2H, aryl-H), 4.58 (dd, $^3J_{\text{H-H}}$ = 11.2 Hz, $^4J_{\text{H-H}}$ = 2.7 Hz, 1H, CH), 4.26 – 4.29 (m, 1H, CH), 4.04 (br s, 1H, NH), 2.24 – 2.39 (m, 1H, CH_2), 2.12 – 2.19 (m, 1H, CH_2); $^{13}\text{C}\{^1\text{H}\}$ NMR (100.7 MHz, CDCl_3): δ = 145.34 (Cq), 145.30 (Cq), 143.9 (Cq), 129.7 (CH), 128.7 (2 CH), 128.6 (2 CH), 128.5 (2 CH), 127.7 (CH), 127.2 (CH), 126.6 (2 CH), 126.5 (CH), 124.7 (Cq), 117.6 (CH), 114.3 (CH, aryl-C), 57.3 (CHNH), 45.0 (CH), 42.1 (CH_2). The NMR spectroscopic data is in agreement with the literature.¹³

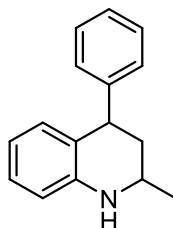
trans-isomer:

^1H NMR (400.3 MHz, CDCl_3): δ = 7.05 – 7.32 (m, 11H, aryl-H), 6.85 (dd, $^3J_{\text{H-H}}$ = 7.6 Hz, $^4J_{\text{H-H}}$ = 0.8 Hz, 1H, aryl-H), 6.60 – 6.65 (m, 1H, aryl-H), 6.49 – 6.54 (m, 1H, aryl-H), 4.26 – 4.29 (m, 1H, CH), 4.12 (t, $^3J_{\text{H-H}}$ = 4.6 Hz, 1H, CH), 4.04 (br s, 1H, NH), 2.24 – 2.39 (m, 1H, CH_2), 2.12 – 2.19 (m, 1H, CH_2); $^{13}\text{C}\{^1\text{H}\}$ NMR (100.7 MHz, CDCl_3): δ = 146.9 (Cq), 144.8 (Cq), 144.4 (Cq), 130.5 (CH),

128.7 (2 CH), 128.5 (2 CH), 128.3 (2 CH), 127.6 (CH), 127.4 (CH), 126.6 (2 CH), 126.1 (CH), 122.0 (Cq), 117.2 (CH), 114.0 (CH, aryl-C), 51.9 (CHNH), 41.7 (CH), 39.1 (CH₂). The NMR spectroscopic data is in agreement with the literature.³

HRMS (ESI): m/z Calcd. for [C₂₁H₂₀N, M+H]⁺: 286.1590; found 286.1587.

2-Methyl-4-phenyl-1,2,3,4-tetrahydroquinoline (**3u**)



Following the general procedure for the synthesis of 1,2,3,4-tetrahydroquinolines, 2-aminobenzhydrol (175 mg, 0.880 mmol) and propan-2-ol (48 mg, 62 μ L, 0.800 mmol) were used.

Yellow oil, GC-Yield: 30 %, Isolated yield: 36 mg, 20 %

R_f (silica, Hept/DCM = 1:5) = 0.59

mixture of *cis*- and *trans*-isomer (ratio = 0.04:1)

***cis*-isomer:**

Detected in traces.¹⁴

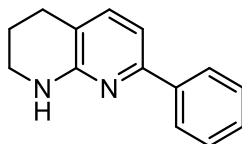
***trans*-isomer:**

¹H NMR (400.3 MHz, CDCl₃): δ = 7.26 – 7.32 (m, 2H, aryl-H), 7.16 – 7.23 (m, 1H, aryl-H), 7.00 – 7.14 (m, 3H, aryl-H), 6.87 (d, ³J_{H-H} = 6.9 Hz, 1H, aryl-H), 6.56 – 6.68 (m, 2H, aryl-H), 4.14 – 4.27 (m, 1H, CHNH), 3.84 (br s, 1H, NH), 3.25 – 3.39 (m, 1H, CH), 1.88 – 2.03 (m, 2H, CH₂), 1.17 (d, ³J_{H-H} = 6.3 Hz, CH₃); ¹³C{¹H} NMR (100.7 MHz, CDCl₃): δ = 147.7 (Cq), 145.0 (Cq), 130.7 (CH), 128.6 (2 CH), 128.1 (2 CH), 127.4 (CH), 125.9 (CH), 121.9 (Cq), 117.0 (CH), 114.0 (CH, aryl-C), 42.2 (CH), 42.0 (CH), 38.3 (CH₂), 22.4 (CH₃). The NMR spectroscopic data is in agreement with the literature.¹⁴

HRMS (ESI): m/z Calcd. for [C₁₆H₁₈N, M+H]⁺: 224.1434; found 224.1436.

4.2. Spectroscopic data of 1,2,3,4-tetrahydronaphthyridines

7-Phenyl-1,2,3,4-tetrahydro-1,8-naphthyridine (**4a**)



Following the general procedure for the synthesis of 1,2,3,4-tetrahydronaphthyridines, (2-aminopyridin-3-yl)methanol (109 mg, 0.880 mmol) and 1-phenylethanol (97 μ l, 98 mg, 0.800 mmol) were used.

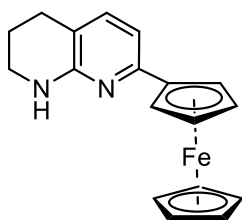
Pale yellow solid, GC-Yield: 89 %, Isolated yield: 122 mg, 73 %

R_f (silica, Hept/EtOAc = 1:1) = 0.61

^1H NMR (400.3 MHz, CDCl_3): δ = 7.86 – 7.95 (m, 2H, aryl-H), 7.39 – 7.47 (m, 2H, aryl-H), 7.31 – 7.39 (m, 1H, aryl-H), 7.23 (d, $^3J_{\text{H-H}}$ = 7.5 Hz, 1H, aryl-H), 6.95 (d, $^3J_{\text{H-H}}$ = 7.5 Hz, 1H, aryl-H), 5.10 (br s, 1H, NH), 3.41 (td, $^3J_{\text{H-H}}$ = 5.5 Hz, $^3J_{\text{H-H}}$ = 2.5 Hz, 2H, CH_2), 2.77 (t, $^3J_{\text{H-H}}$ = 6.3 Hz, 2H, CH_2), 1.95 (quin, $^3J_{\text{H-H}}$ = 7.5 Hz, 2H, CH_2); $^{13}\text{C}\{^1\text{H}\}$ NMR (100.7 MHz, CDCl_3): δ = 156.0 (Cq), 154.0 (Cq), 140.0 (Cq), 136.8 (CH), 128.4 (2 CH), 128.1 (CH), 126.6 (2 CH), 114.8 (Cq), 109.6 (CH, aryl-C), 41.6 (CH_2), 26.5 (CH_2), 21.5 (CH_2). The NMR spectroscopic data is in agreement with the literature.¹⁵

HRMS (ESI): m/z Calcd. for $[\text{C}_{14}\text{H}_{15}\text{N}, \text{M}+\text{H}^+]^+$: 211.1231; found 211.1230.

7-Ferrocenyl-1,2,3,4-tetrahydro-1,8-naphthyridine (**4b**)



Following the general procedure for the synthesis of 1,2,3,4-tetrahydronaphthyridines, (2-aminopyridin-3-yl)methanol (109 mg, 0.880 mmol) and α -methylferrocenemethanol (184 mg, 0.800 mmol) were used.

Orange solid, GC-Yield: 96 %, Isolated yield: 181 mg, 71 %

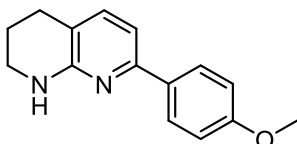
R_f (silica, Hept/EtOAc = 1:1) = 0.55

^1H NMR (400.3 MHz, CDCl_3): δ = 7.08 (d, $^3J_{\text{H-H}}$ = 7.5 Hz, 1H, aryl-H), 6.71 (d, $^3J_{\text{H-H}}$ = 7.5 Hz, 1H, aryl-H), 4.80 (t, $^3J_{\text{H-H}}$ = 1.6 Hz, 2H, ferrocenyl-H), 4.77 (br s, 1H, NH), 4.30 (t, $^3J_{\text{H-H}}$ = 1.8 Hz, 2H, ferrocenyl-H), 4.06 (s, 5H, C_5H_5), 3.43 (td, $^3J_{\text{H-H}}$ = 5.5 Hz, $^3J_{\text{H-H}}$ = 2.4 Hz, 2H, CH_2), 2.70 (t, $^3J_{\text{H-H}}$ = 6.3 Hz, 2H, CH_2), 1.94 (quin, $^3J_{\text{H-H}}$ = 5.9 Hz, 2H, CH_2); $^{13}\text{C}\{^1\text{H}\}$ NMR (100.7 MHz, CDCl_3): δ =

155.6 (Cq), 155.0 (Cq), 136.2 (CH), 112.9 (Cq), 109.6 (CH, aryl-C), 85.1 (Cq, Fc), 69.5 (C₅H₅), 69.0 (2 CH), 67.0 (2 CH, ferrocenyl-C), 41.6 (CH₂), 26.5 (CH₂), 21.6 (CH₂).

HRMS (ESI): *m/z* Calcd. for [C₁₈H₁₉FeN₂, M+H]⁺: 319.0892; found 319.0895.

7-(4-Methoxyphenyl)-1,2,3,4-tetrahydro-1,8-naphthyridine (4c)



Following the general procedure for the synthesis of 1,2,3,4-tetrahydronaphthyridines, (2-aminopyridin-3-yl)methanol (109 mg, 0.880 mmol) and 1-(4-methoxyphenyl)ethan-1-ol (122 mg, 0.800 mmol) were used.

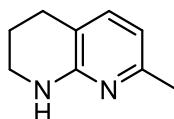
Pale yellow solid, GC-Yield: not determined, NMR yield of **4c**: 46 mg, 24 %

R_f (silica, Hept/EtOAc = 1:1) = 0.20

¹H NMR (400.3 MHz, CDCl₃): δ = 8.09 (d, ⁴*J*_{H-H} = 2.0 Hz, 1H, aryl-H), 6.95 (d, ³*J*_{H-H} = 8.6 Hz, 2H, aryl-H), 7.36 (s, 1H, aryl-H), 6.95 (d, ³*J*_{H-H} = 8.9 Hz, 2H, aryl-H), 4.91 (br s, 1H, NH), 3.84 (s, 3H, CH₃), 3.46 (td, ³*J*_{H-H} = 5.4 Hz, ³*J*_{H-H} = 2.5 Hz, 2H, CH₂), 2.80 (t, ³*J*_{H-H} = 6.3 Hz, 2H, CH₂), 1.96 (quin, ³*J*_{H-H} = 5.9 Hz, 2H, CH₂); ¹³C{¹H} NMR (100.7 MHz, CDCl₃): δ = 158.5 (Cq), 155.2 (Cq), 143.8 (CH), 134.7 (CH), 127.1 (2 CH), 125.9 (Cq), 115.8 (Cq), 114.3 (2 CH, aryl-C), 55.5 (CH₃), 41.7 (CH₂), 26.7 (CH₂), 21.4 (CH₂).

HRMS (ESI): *m/z* Calcd. for [C₁₅H₁₇N₂O, M+H]⁺: 241.1335; found 241.1337.

7-Methyl-1,2,3,4-tetrahydro-1,8-naphthyridine (4d)



Following the general procedure for the synthesis of 1,2,3,4-tetrahydronaphthyridines, (2-aminopyridin-3-yl)methanol (109 mg, 0.880 mmol) and propan-2-ol (48 mg, 62 μL, 0.800 mmol) were used.

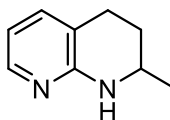
Yellow solid, GC-Yield: 59 %, Isolated yield: 60 mg, 51 %

R_f (silica, Hept/EtOAc = 1:1) = 0.24

¹H NMR (400.3 MHz, CDCl₃): δ = 7.04 (d, ³*J*_{H-H} = 7.3 Hz, 1H, aryl-H), 6.35 (d, ³*J*_{H-H} = 7.3 Hz, 1H, aryl-H), 4.83 (br s, 1H, NH), 3.40 (td, ³*J*_{H-H} = 5.5 Hz, ³*J*_{H-H} = 2.5 Hz, 2H, CH₂), 2.69 (t, ³*J*_{H-H} = 6.3 Hz, 2H, CH₂), 2.32 (s, 3H, CH₃), 1.90 (quint, ³*J*_{H-H} = 6.1 Hz, 2H, CH₂); ¹³C{¹H} NMR (100.7 MHz, CDCl₃): δ = 155.6 (Cq), 154.3 (Cq), 136.7 (CH), 112.8 (Cq), 111.8 (CH, aryl-C), 41.6 (CH₂), 26.3 (CH₂), 23.8 (CH₃), 21.5 (CH₂). The NMR spectroscopic data is in agreement with the literature.¹⁵

HRMS (ESI): m/z Calcd. for $[C_9H_{13}N_2, M+H]^+$: 149.1073; found 149.1072.

2-Methyl-1,2,3,4-tetrahydro-1,8-naphthyridine (4d')



Following the general procedure for the synthesis of 1,2,3,4-tetrahydronaphthyridines, (2-aminopyridin-3-yl)methanol (109 mg, 0.880 mmol) and propan-2-ol (48 mg, 62 μ L, 0.800 mmol) were used.

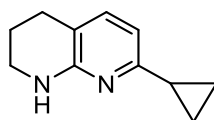
Yellow solid, GC-Yield: 27 %, Isolated yield: 18 mg, 15 %

R_f (silica, Hept/EtOAc = 1:1) = 0.40

1H NMR (400.3 MHz, $CDCl_3$): δ = 7.86 (d, $^3J_{H-H}$ = 4.9 Hz, 1H, aryl-H), 7.16 (d, $^3J_{H-H}$ = 7.1 Hz, 1H, aryl-H), 6.49 (dd, $^3J_{H-H}$ = 7.2 Hz, $^3J_{H-H}$ = 5.1 Hz, 1H, aryl-H), 4.76 (br s, 1H, NH), 3.49 – 3.63 (m, 1H, CHNH), 2.64 – 2.81 (m, 2H, CH_2), 1.86 – 2.00 (m, 1H, CH_2), 1.48 – 1.64 (m, 1H, CH_2), 1.25 (d, $^3J_{H-H}$ = 6.4 Hz, 3H, CH_3); $^{13}C\{^1H\}$ NMR (100.7 MHz, $CDCl_3$): δ = 156.2 (Cq), 145.9 (CH), 136.0 (CH), 115.7 (Cq), 112.6 (CH, aryl-C), 47.1 (CHNH), 29.3 (CH_2), 25.9 (CH_2), 22.4 (CH_3). The NMR spectroscopic data is in agreement with the literature.¹⁵

HRMS (ESI): m/z Calcd. for $[C_9H_{13}N_2, M+H]^+$: 149.1073; found 149.1073.

7-Cyclopropyl-1,2,3,4-tetrahydro-1,8-naphthyridine (4e)



Following the general procedure for the synthesis of 1,2,3,4-tetrahydronaphthyridines, (2-aminopyridin-3-yl)methanol (109 mg, 0.880 mmol) and 1-cyclopropylethan-1-ol (69 mg, 78 μ L, 0.800 mmol) were used.

Pale yellow solid, GC-Yield: 82 %, Isolated yield: 88 mg, 63 %

R_f (silica, Hept/EtOAc = 1:1) = 0.16

1H NMR (400.3 MHz, $CDCl_3$): δ = 7.02 (d, $^3J_{H-H}$ = 7.4 Hz, 1H, aryl-H), 6.33 (d, $^3J_{H-H}$ = 7.4 Hz, 1H, aryl-H), 4.69 (br s, 1H, NH), 3.38 (td, $^3J_{H-H}$ = 5.5 Hz, $^3J_{H-H}$ = 2.5 Hz, 2H, CH_2), 2.67 (t, $^3J_{H-H}$ = 6.3 Hz, 2H, CH_2), 1.89 (quin, $^3J_{H-H}$ = 5.9 Hz, 2H, CH_2), 1.79 – 1.86 (m, 1H, CH), 0.78 – 0.90 (m, 4H, 2 CH_2); $^{13}C\{^1H\}$ NMR (100.7 MHz, $CDCl_3$): δ = 159.0 (Cq), 155.7 (Cq), 136.3 (CH), 112.5 (Cq), 109.5 (CH, aryl-C), 41.6 (CH_2), 26.3 (CH_2), 21.6 (CH_2), 16.6 (CH), 8.5 (2 CH_2).

HRMS (ESI): m/z Calcd. for $[C_{11}H_{15}N, M+H]^+$: 175.1230; found 175.1235.

5. Literature

1. Plevová, K.; Mudráková, B.; Šebesta, R., A Practical Three-Step Synthesis of Vinylferrocene. *Synthesis* **2018**, 50 (04), 760–763.
2. Homberg, L.; Roller, A.; Hultsch, K. C., A Highly Active PN^3 Manganese Pincer Complex Performing N-Alkylation of Amines under Mild Conditions. *Org. Lett.* **2019**, 21 (9), 3142–3147.
3. Ueda, M.; Kawai, S.; Hayashi, M.; Naito, T.; Miyata, O., Efficient Entry into 2-Substituted Tetrahydroquinoline Systems through Alkylative Ring Expansion: Stereoselective Formal Synthesis of (\pm)-Martinellie Acid. *J. Org. Chem.* **2010**, 75 (3), 914–921.
4. Wang, Y.; Dong, B.; Wang, Z.; Cong, X.; Bi, X., Silver-Catalyzed Reduction of Quinolines in Water. *Org. Lett.* **2019**, 21 (10), 3631–3634.
5. Brough, P. A.; Baker, L.; Bedford, S.; Brown, K.; Chavda, S.; Chell, V.; D'Alessandro, J.; Davies, N. G. M.; Davis, B.; Le Strat, L.; Macias, A. T.; Maddox, D.; Mahon, P. C.; Massey, A. J.; Matassova, N.; McKenna, S.; Meissner, J. W. G.; Moore, J. D.; Murray, J. B.; Northfield, C. J.; Parry, C.; Parsons, R.; Roughley, S. D.; Shaw, T.; Simmonite, H.; Stokes, S.; Surgenor, A.; Stefaniak, E.; Robertson, A.; Wang, Y.; Webb, P.; Whitehead, N.; Wood, M., Application of Off-Rate Screening in the Identification of Novel Pan-Isoform Inhibitors of Pyruvate Dehydrogenase Kinase. *J. Med. Chem.* **2017**, 60 (6), 2271–2286.
6. Chen, F.; Surkus, A.-E.; He, L.; Pohl, M.-M.; Radnik, J.; Topf, C.; Junge, K.; Beller, M., Selective Catalytic Hydrogenation of Heteroarenes with N-Graphene-Modified Cobalt Nanoparticles ($\text{Co}_3\text{O}_4\text{-Co/NGr}@ \alpha\text{-Al}_2\text{O}_3$). *J. Am. Chem. Soc.* **2015**, 137 (36), 11718–11724.
7. Wang, D.-W.; Wang, X.-B.; Wang, D.-S.; Lu, S.-M.; Zhou, Y.-G.; Li, Y.-X., Highly Enantioselective Iridium-Catalyzed Hydrogenation of 2-Benzylquinolines and 2-Functionalized and 2,3-Disubstituted Quinolines. *J. Org. Chem.* **2009**, 74 (7), 2780–2787.
8. Sridharan, V.; Avendaño, C.; Menéndez, J. C., CAN-catalyzed three-component reaction between anilines and alkyl vinyl ethers: stereoselective synthesis of 2-methyl-1,2,3,4-tetrahydroquinolines and studies on their aromatization. *Tetrahedron* **2007**, 63 (3), 673–681.
9. Yang, T.; Yin, Q.; Gu, G.; Zhang, X., A one-pot process for the enantioselective synthesis of tetrahydroquinolines and tetrahydroisoquinolines via asymmetric reductive amination (ARA). *Chem. Commun.* **2018**, 54 (52), 7247–7250.
10. Hu, X.-H.; Hu, X.-P., Highly Diastereo- and Enantioselective Ir-Catalyzed Hydrogenation of 2,3-Disubstituted Quinolines with Structurally Fine-Tuned Phosphine–Phosphoramidite Ligands. *Org. Lett.* **2019**, 21 (24), 10003–10006.
11. Wu, J.; Wang, C.; Tang, W.; Pettman, A.; Xiao, J., The Remarkable Effect of a Simple Ion: Iodide-Promoted Transfer Hydrogenation of Heteroaromatics. *Chem. Eur. J.* **2012**, 18 (31), 9525–9529.

12. Diaz-Muñoz, G.; Isidorio, R. G.; Miranda, I. L.; de Souza Dias, G. N.; Diaz, M. A. N., A concise and efficient synthesis of tetrahydroquinoline alkaloids using the phase transfer mediated Wittig olefination reaction. *Tetrahedron Lett.* **2017**, 58 (33), 3311–3315.
13. Zhang, Z.; Du, H., Enantioselective Metal-Free Hydrogenations of Disubstituted Quinolines. *Org. Lett.* **2015**, 17 (24), 6266–6269.
14. Youn, S. W.; Yoo, H. J.; Lee, E. M.; Lee, S. Y., Metal-Free One-Pot Synthesis of (Tetrahydro)Quinolines through Three-Component Assembly of Arenediazonium Salts, Nitriles, and Styrenes. *Adv. Synth. Catal.* **2018**, 360 (2), 278–283.
15. Xiong, B.; Li, Y.; Lv, W.; Tan, Z.; Jiang, H.; Zhang, M., Ruthenium-Catalyzed Straightforward Synthesis of 1,2,3,4-Tetrahydronaphthyridines via Selective Transfer Hydrogenation of Pyridyl Ring with Alcohols. *Org. Lett.* **2015**, 17 (16), 4054–4057.

6. NMR Spectra

NMR spectra (^1H -, ^{13}C -, and ^{31}P - NMR spectra) and HPLC traces of the synthesized products are available on the *Org. Lett. website* at <https://doi.org/10.1021/acs.orglett.0c02905>

7. GC/FID Traces

7.1. Representative GC/FID traces

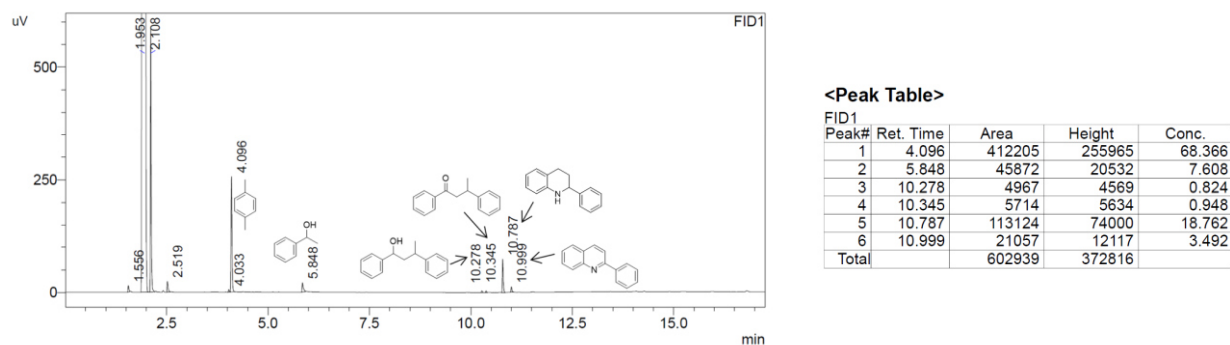


Figure S53: Representative GC/FID trace of the synthesis of 2-phenyl-1,2,3,4-tetrahydroquinoline (**3a**).

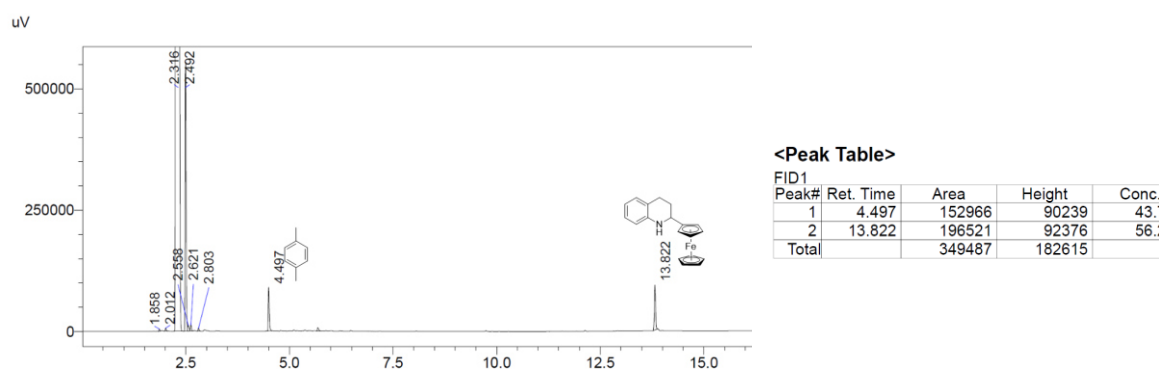


Figure S54: Representative GC/FID trace of the synthesis of 2-ferrocenyl-1,2,3,4-tetrahydroquinoline (**3c**).

7.2. GC/FID traces of reaction monitoring of the synthesis of 2-ferrocenyl-1,2,3,4-tetrahydroquinoline (**3c**)

Table S10: Retention times of GC/FID traces in the synthesis of 2-ferrocenyl-1,2,3,4-tetrahydroquinoline (**3c**)

Retention time [min]	Compound
4.50	<i>p</i> -xylene
7.75	2-aminobenzyl alcohol
9.73	1-(ferrocenyl)ethanol
13.82	2-ferrocenyl-1,2,3,4-tetrahydroquinoline (3c)

13.89

2-ferrocenyl-quinoline (2c)

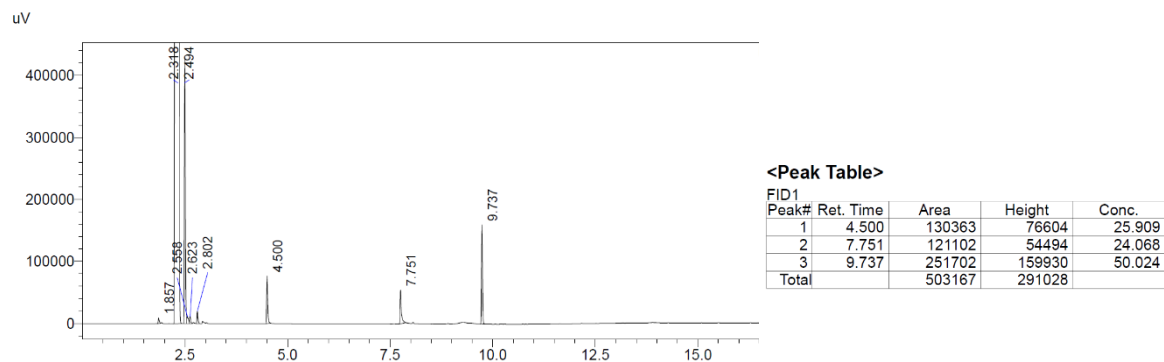


Figure S55: GC/FID trace of reaction monitoring after 0 h.

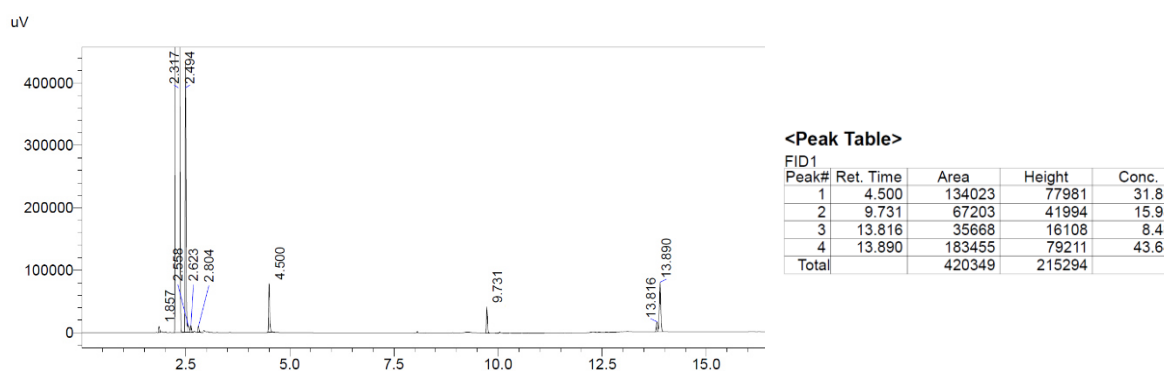


Figure S56: GC/FID trace of reaction monitoring after 1 h.

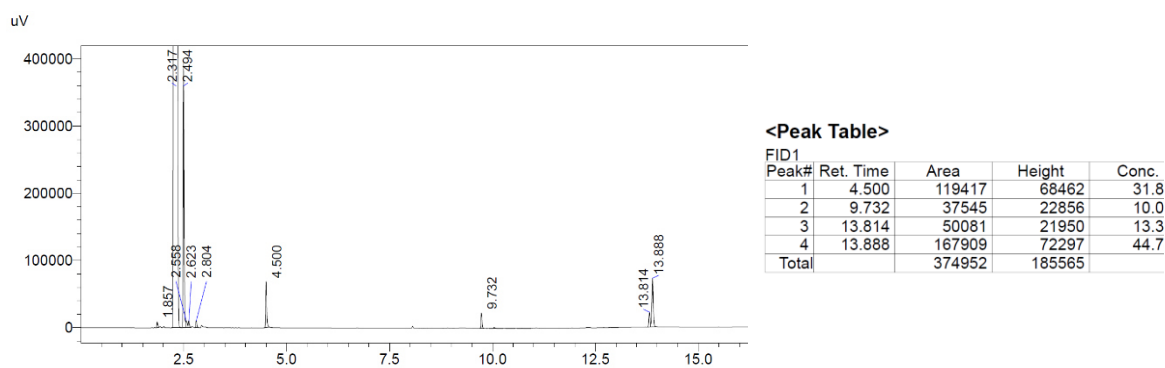


Figure S57: GC/FID trace of reaction monitoring after 2 h.

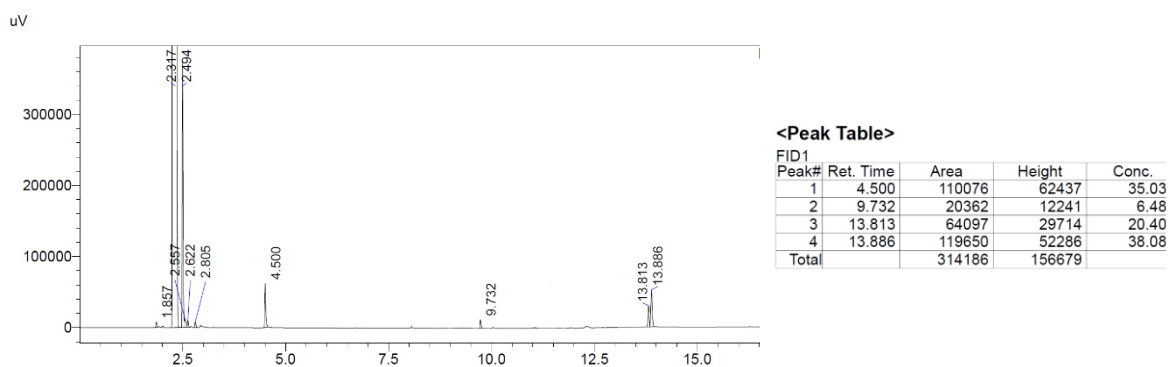


Figure S58: GC/FID trace of reaction monitoring after 3 h.

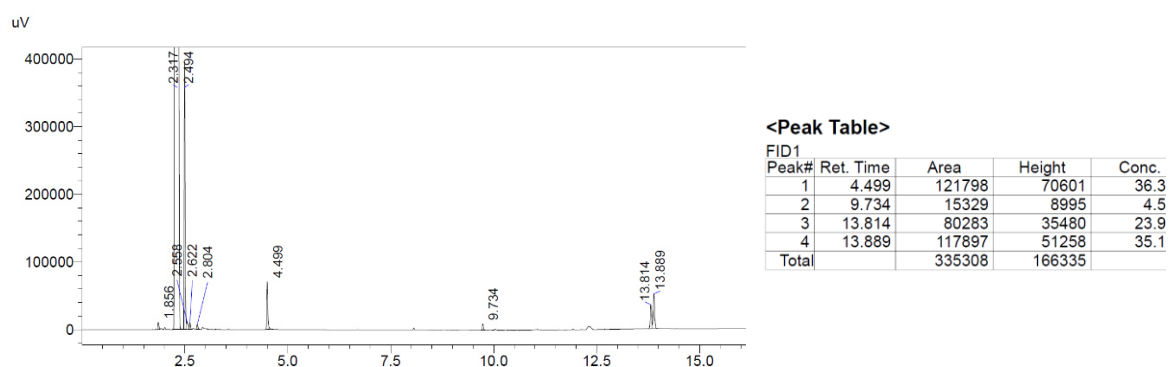


Figure S59: GC/FID trace of reaction monitoring after 4 h.

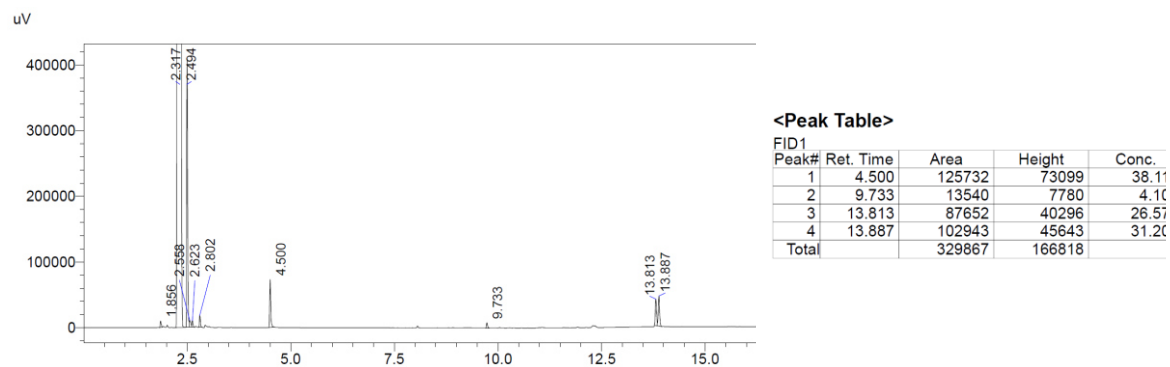


Figure S60: GC/FID trace of reaction monitoring after 5 h.

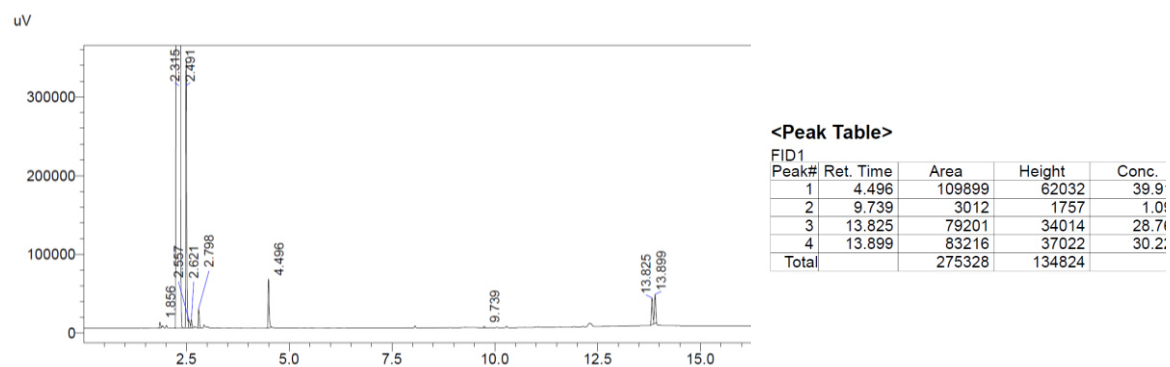


Figure S61: GC/FID trace of reaction monitoring after 6 h.

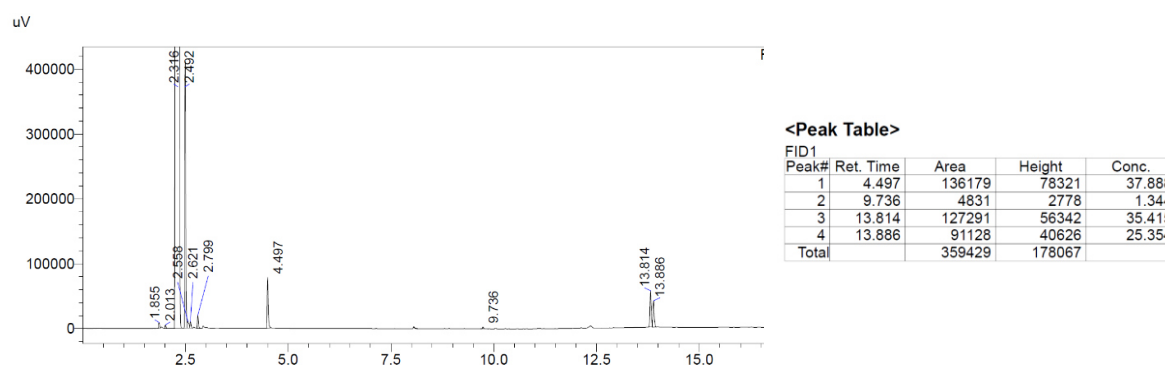


Figure S62: GC/FID trace of reaction monitoring after 8 h.

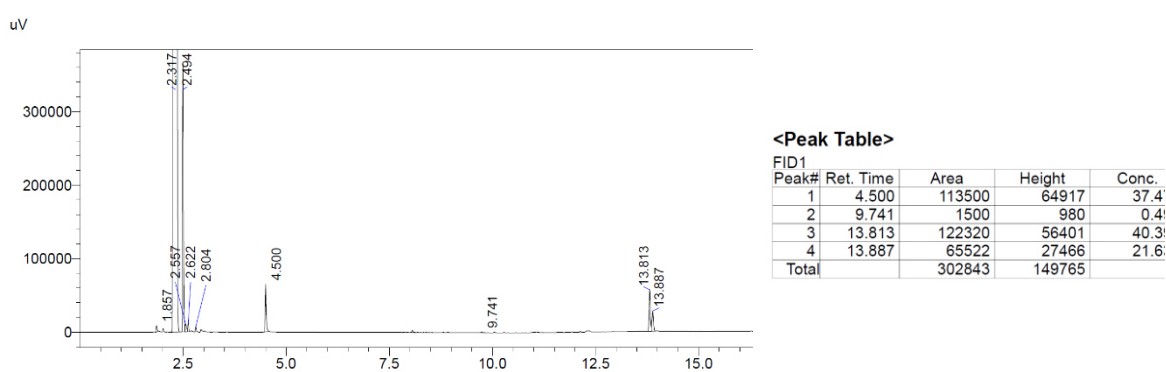


Figure S63: GC/FID trace of reaction monitoring after 14 h.

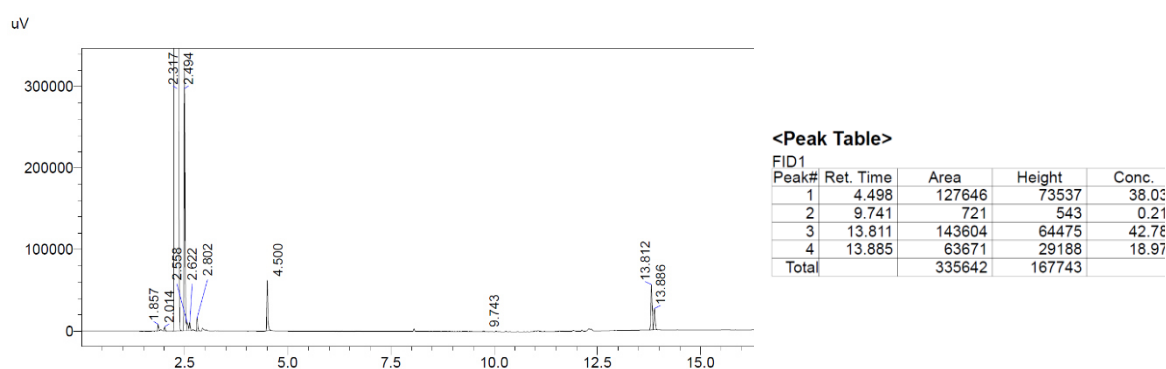


Figure S64: GC/FID trace of reaction monitoring after 19 h.

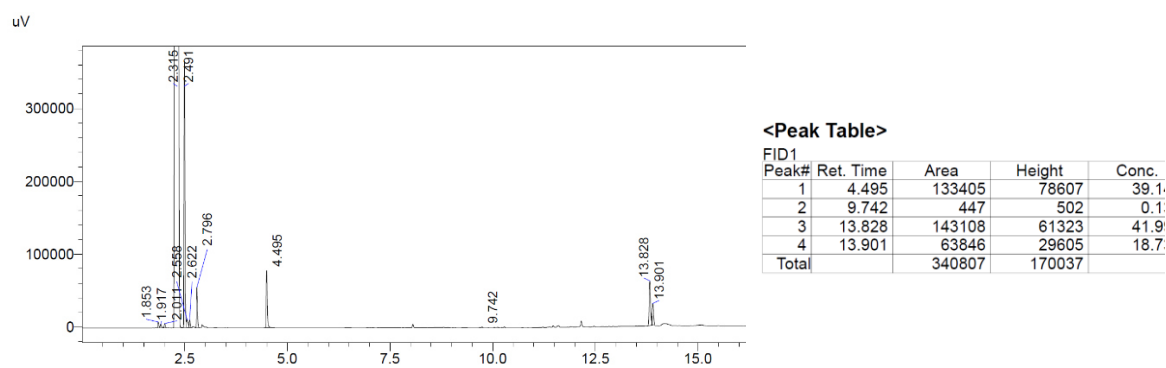
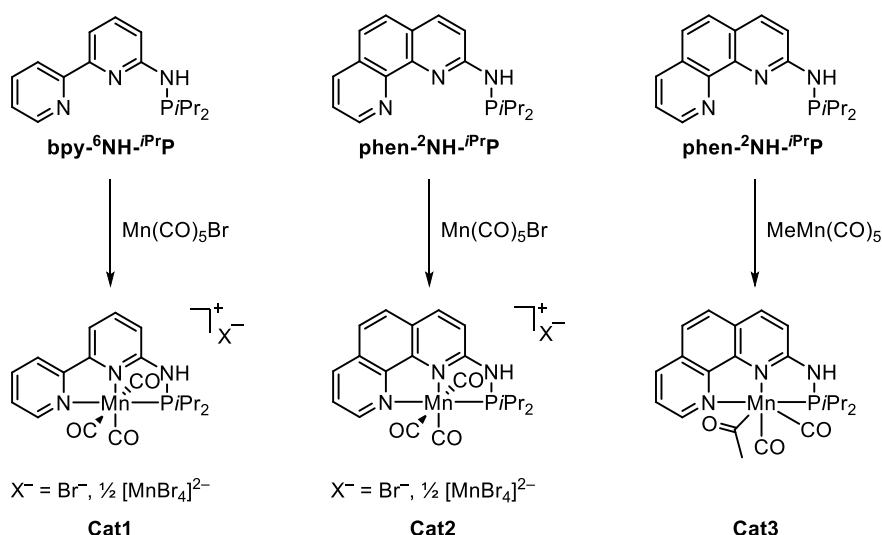


Figure S65: GC/FID trace of reaction monitoring after 24 h.

3.4. Unpublished Results

In this part further investigations concerning the catalytic activity of manganese based PNN-pincer complexes were conducted. On the one hand the reaction scope of **Cat1** was broadened and on the other hand the new PN^3 manganese pincer complexes **Cat2** and **Cat3** (Scheme 14) were synthesized and characterized. Besides, the catalytic activities of **Cat1** – **Cat3** in borrowing hydrogen reactions and hydrogenations were examined and compared. **Cat1** and **Cat2** have different backbones but are based on the same metal precursor. Thus, the influence of the highly conjugated phenanthroline backbone was examined. **Cat2** and **Cat3** have the same phenanthroline-backbone but are formed from different precursors. In this way the effect of the acyl-ligand on the stability and catalytic activity was evaluated.



Scheme 14: Investigated PN^3 manganese pincer complexes.

3.4.1. Results and Discussion

Synthesis of 2-aminoquinolines

The aminoquinoline scaffold represents an interesting precursor for various biologically important and pharmacologically active substances.^[51] Hence, we investigated the activity of the PN^3 manganese pincer complex **Cat1** in the dehydrogenative coupling of 2-aminobenzyl alcohols and nitriles. The strategy was adapted from recent publications by Sortais,^[52] Kundu,^[53] Srimani^[54] and Paul.^[55] Compared to the reported base metal containing systems^[53-55] our manganese-based system allows lower catalyst and base loadings. Thus, a substrate screening was started (Table 1). In general, 2-aminobenzyl alcohols and benzyl nitriles led to good conversions (Table 1, Entries 1–3, 7–9), whereas aliphatic aminoalcohols and aliphatic nitriles did not allow the formation of the desired

product (Table 1, Entries 10–12). Nitrogen heteroatoms in the 2-aminobenzyl alcohol backbone were not tolerated leading to a mixture of unidentified products (Table 1, Entries 4 and 5).

Table 1: Substrate Screening for the synthesis of 2-amino quinolines

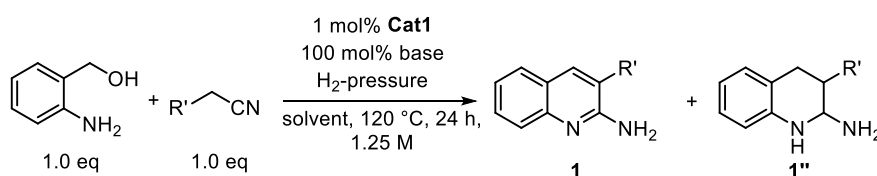
$ \begin{array}{c} \text{1.0 eq} \quad \text{1.0 eq} \\ \text{DME, 120 } ^\circ\text{C, 24 h,} \\ \text{1.25 M} \end{array} \xrightarrow[10 \text{ mol\% KOtBu}]{1 \text{ mol\% Cat1}} \begin{array}{c} \text{1} \quad \text{1'} \\ \text{by-products} \end{array} $						
#			Conversion ^a [%]			Isolated Yield [%]
			1	1'	by-products	
1			72	<1	<1	64
2			80	<1	<1	72
3			83	<1	<1	66
4			product mixture			not found
5			product mixture			not found
6			<1	<1	10 ^b	---
7			54	<1	<1	36
8			16	<1	<1	10
9			77	<1	9 ^c	70
10			<1	45	45 ^d	---
11			nothing detected			---
12			<1	<1	<1 ^e	---

^a Conversion determined via GC/MS analysis. ^b 5 % of 2-phenylacetamide and 5 % of (2-aminophenyl)-(phenyl)methanone were detected. ^c 2-(4-methoxyphenyl)acetamide was detected as by-product. ^d So far unidentified by-product (m/z=161.1). ^e 3-aminopropan-1-ol was not detected in the GC/MS trace. It is assumed to undergo oligomerization reactions.

2-Aminobenzhydrol did not lead to the corresponding 2-aminoquinoline, only a small amount of the corresponding (2-aminophenyl)-(phenyl)methanone was detected (Table 1, Entry 6). Using bromine-substituted benzyl nitriles, similar results compared to the rhenium-based system developed by Sortais^[52] were observed. A bromine in *para*-position is well tolerated, whereas a bromine in *ortho*-position diminished the yield significantly (Table 1, Entries 7 and 8). This screening revealed first insights into the substrate tolerance of the catalytic system and showed the weaknesses which still need to be addressed.

Unfortunately, the idea to refine the coupling of 2-aminobenzyl alcohols and nitriles by performing the reaction under a hydrogen atmosphere with the aim to form the reduced 2-amino-1,2,3,4-tetrahydroquinolines failed. The reactions shown in Table 2 were conducted in a steel autoclave using 6, respectively 50 bar of hydrogen. Experiments with different nitriles, bases, solvents and H₂-pressures were unsuccessful so far, only leading to the dehydrogenated 2-aminoquinolines **1**. Interestingly, the reaction using propionitrile as substrate in combination with 100 mol% KH and a hydrogen pressure of 50 bar formed the corresponding 3-methyl-2-aminoquinoline in high yield (Table 2, Entry 5), whereas the reaction in combination with 10 mol% KO^tBu under argon atmosphere led to 2-ethylquinazoline (Table 1, Entry 10). This observation could be traced back on the change in type and amount of base, though further examinations need to be conducted in order to confirm this assumption.

Table 2: Attempted synthesis of 2-amino-1,2,3,4-tetrahydroquinolines.

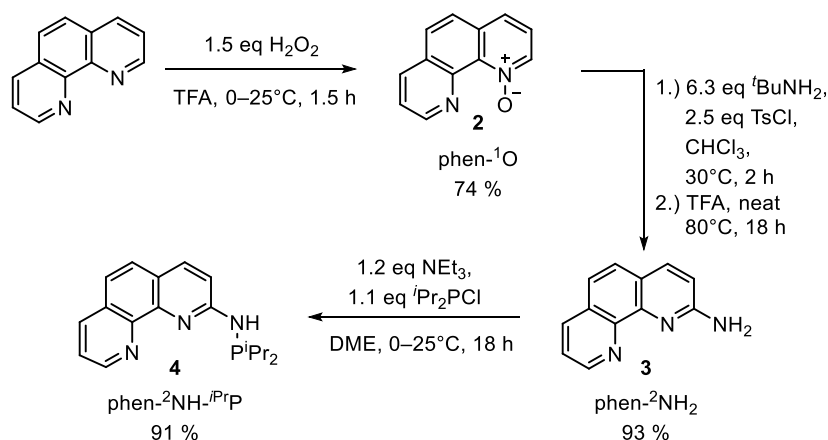


#	R' =	H ₂ -pressure [bar]	base	solvent	Conversion [%] ^a	
					1	1''
1	Ph	6	KO ^t Bu	toluene	72	<1
2	Ph	6	KH	toluene	97	<1
3	CH ₃	6	KH	toluene	<1	<1
4	Ph	50	KH	DME	83	<1
5	CH ₃	50	KH	DME	91	<1

^a Conversion determined via GC/MS analysis.

Synthesis of phen-²NH-ⁱPrP

The synthesis of phen-²NH-ⁱPrP (**4**) was performed following the described procedure for the synthesis of bpy-⁶NH-ⁱPrP which was developed in our group.^[33, 56] The protocol was slightly modified in order to obtain the ligand in good yields (Scheme 15). The formation of phen-²NH₂ (**3**) was performed in a two-step synthesis. After introducing the amine, the solvent was removed and the deprotection step was conducted neat. As phen-²NH₂ (**3**) was poorly soluble in THF, the addition of the phosphine, forming desired phen-²NH-ⁱPrP (**4**), was conducted in DME. The detailed experimental procedure is described in the experimental section (see Section 3.4.3).

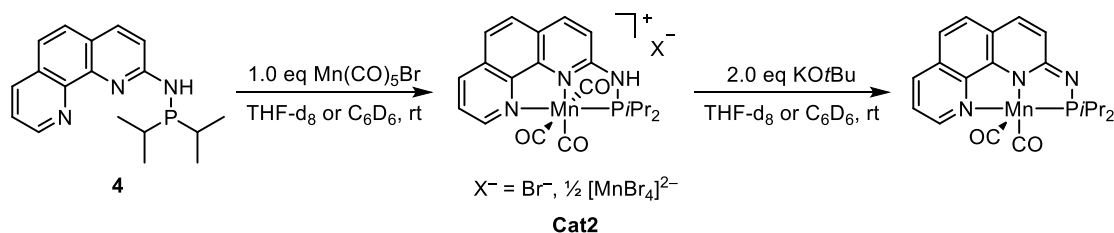


Scheme 15: Optimized synthesis of the phenanthroline-based NNP pincer ligand **4**.

Complexations

Complexation and activation of phen-²NH-ⁱPrP (**4**) with Mn(CO)₅Br

With the pure ligand in hand different complexation strategies were investigated. The complexation of phen-²NH-ⁱPrP (**4**) with Mn(CO)₅Br was performed at room temperature in THF-*d*₈ and C₆D₆ (Scheme 16) and monitored *via* ¹H and ³¹P NMR spectroscopy.



Scheme 16: Complexation of phen-²NH-ⁱPrP (**4**) with Mn(CO)₅Br.

The ^1H NMR spectra showed small, broad and overlapping signals, making them unsuitable for closer examination. Thus, the ^{31}P NMR spectra were used for detailed investigation and comparison with the complexation of $\text{bpy-}^6\text{NH-}^i\text{PrP}$ with $\text{Mn}(\text{CO})_5\text{Br}$ to form **Cat1**.^[33] As it is the case for the formation of **Cat1** in THF-d_8 , first a broad signal at 99 ppm (**A**) was formed within 2 h. However, additional species around 58 ppm (**B**) were monitored (ratio **A**:**B**=1:1), which were not found for **Cat1** (Figure 8). The species then converted into a single species at 158 ppm (**C**) within 24 h and only a small residual signal at 58 ppm remained (ratio **C**:**B** = 16.7:1). In contrast, however, for **Cat1** two species were formed. After addition of 2 equivalents of KO^tBu the catalytically active species (**D**) was formed, showing a signal at 146 ppm.

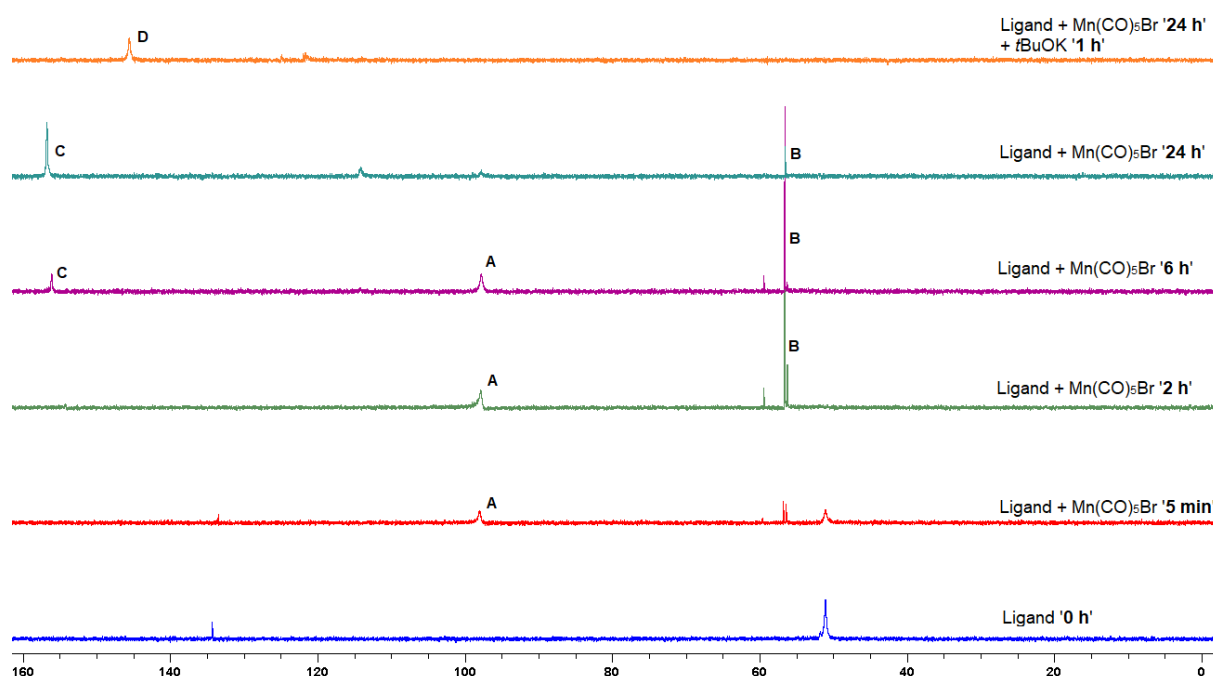


Figure 8: Complexation of $\text{phen-}^2\text{NH-}^i\text{PrP}$ (**4**) with $\text{Mn}(\text{CO})_5\text{Br}$ in THF-d_8 monitored via ^{31}P NMR spectroscopy.

Similar results were obtained when C_6D_6 was used as solvent, although the intermediate **B** at 58 ppm was only formed in very small amounts (ratio **A**:**B** = 14.3:1) and the complexation process required more time (compare Figure 8 vs. Figure 9 & 10). After 24 h only 46 % of intermediate **A** were converted into species **C** and after 48 h 9 % of species **A** were still remaining. Nevertheless, further investigations showed that the time of addition of base does not influence the final species, as in both studies the activated single species **D** at 146 ppm was obtained. During activation of the complex with KO^tBu an additional intermediate **E** at 124 ppm was observed. In addition, the complexation was successful in CDCl_3 as well, though an elevated temperature of 50 °C (4 h) was required.

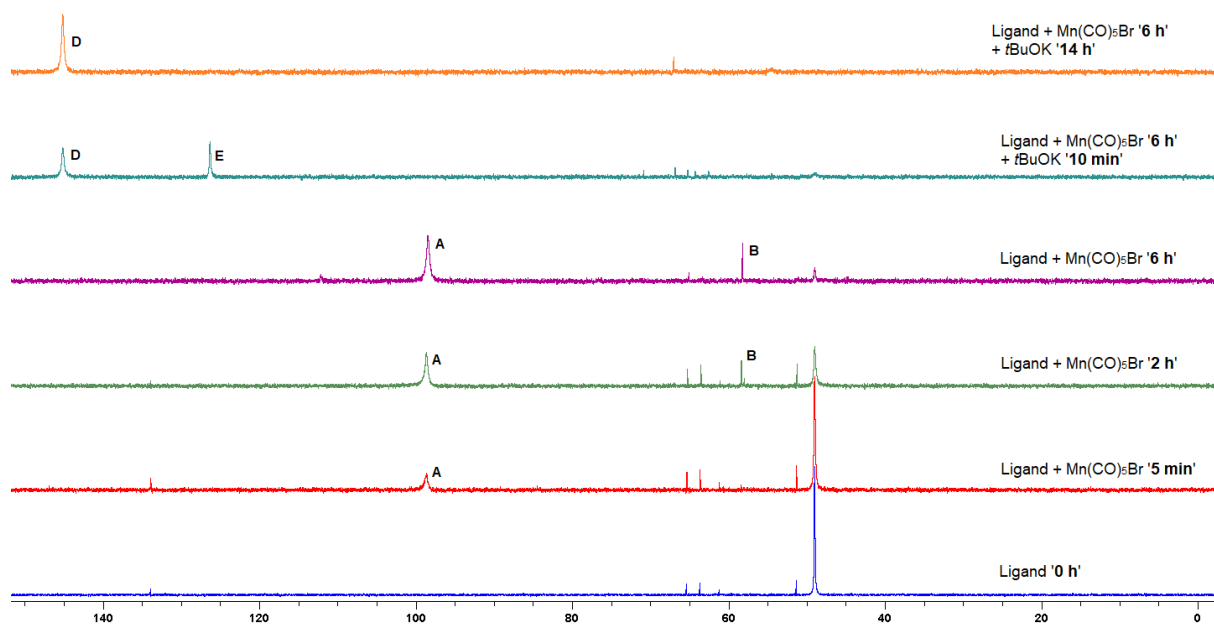


Figure 9: Complexation of phen-²NH-ⁱPrP (**4**) with Mn(CO)₅Br in C₆D₆ monitored via ³¹P NMR spectroscopy.

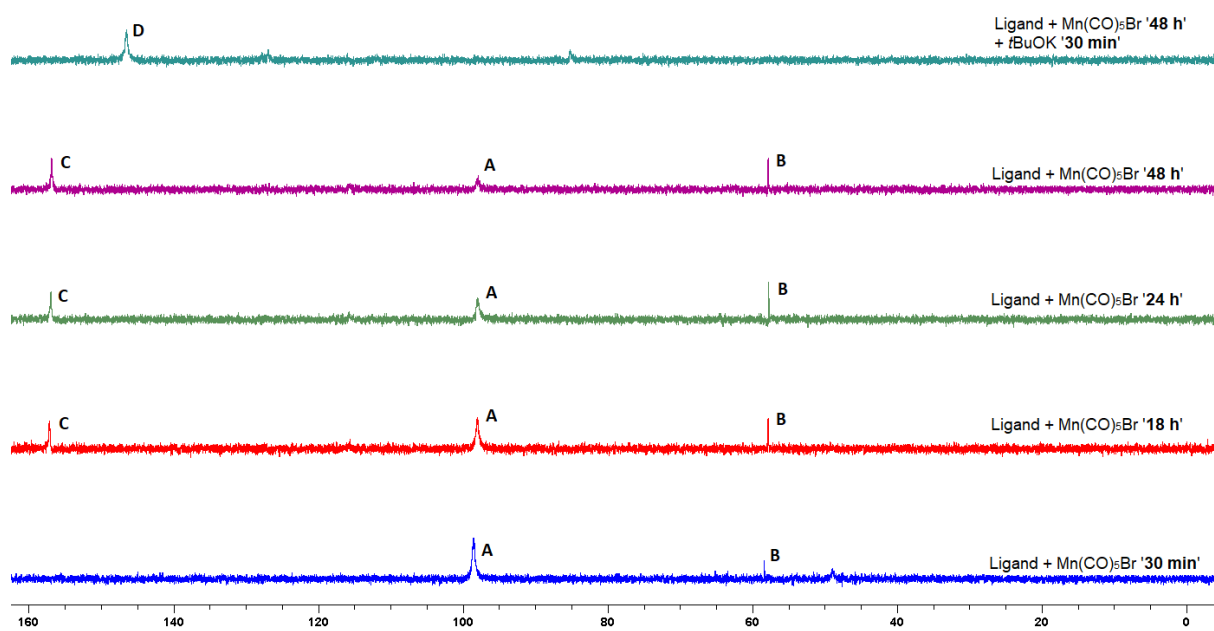


Figure 10: Complexation of phen-²NH-ⁱPrP (**4**) with Mn(CO)₅Br in C₆D₆ monitored via ³¹P NMR spectroscopy over a longer period of time.

The change of the vibrations of the CO-ligands upon complexation was observed *via* FT-IR spectroscopy (Figure 11). The spectra were recorded in a NaCl-cuvette using CHCl₃ as solvent. A clear change in the spectrum of the Mn(CO)₅Br precursor and the pincer complex **Cat2** was observed. The signals are significantly broadened and shifted to lower

wavenumbers, which can be explained by the increased π -backdonation obtained through complexation of the strong σ -donating PN^3 -ligand.

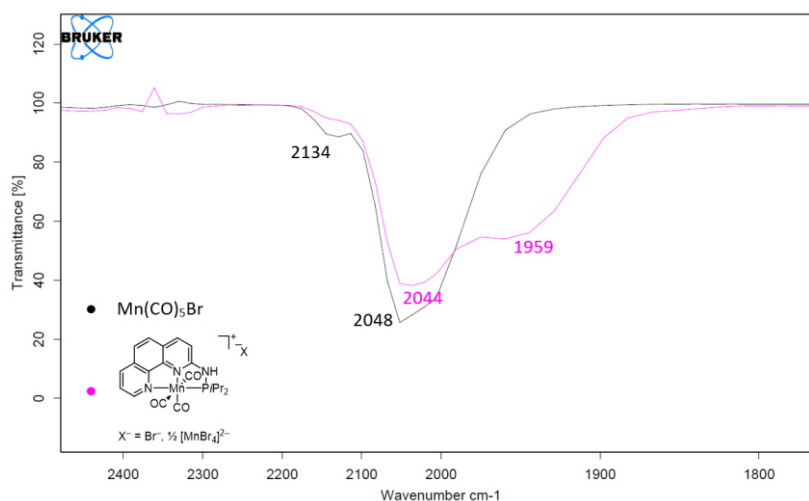
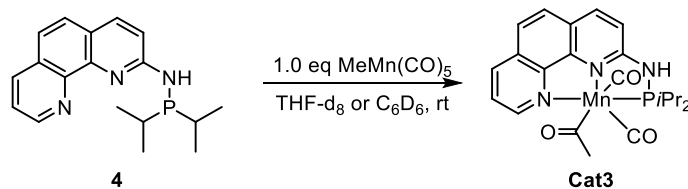


Figure 11: FT-IR spectrum of **Cat2** and its precursor ($\text{Mn}(\text{CO})_5\text{Br}$) recorded using a NaCl cuvette in CHCl_3 .

Complexation and activation of $\text{phen-}^2\text{NH-}i\text{PrP}$ (**4**) with $\text{MeMn}(\text{CO})_5$



Scheme 17: Complexation of $\text{phen-}^2\text{NH-}i\text{PrP}$ (**4**) with $\text{MeMn}(\text{CO})_5$.

Based on the recent success of metal alkyl complexes in promoting additive-free hydrogenations,^[57] the complexation of $\text{phen-}^2\text{NH-}i\text{PrP}$ (**4**) with $\text{MeMn}(\text{CO})_5$ was investigated (Scheme 17). The reaction was performed at room temperature in THF-d_8 and C_6D_6 and monitored *via* ^1H and ^{31}P NMR spectroscopy (Figures 12 – 15). The complexation in THF-d_8 was completed within 1 h (Figures 12 & 13), whereas the complexation in C_6D_6 required 24 h (Figures 14 & 15). In both cases only the final complex (**Cat3**, **A**) but no intermediates were detected. Furthermore, this complexation was successful in CDCl_3 as well, though an elevated temperature of $50\text{ }^\circ\text{C}$ (8 h) was required.

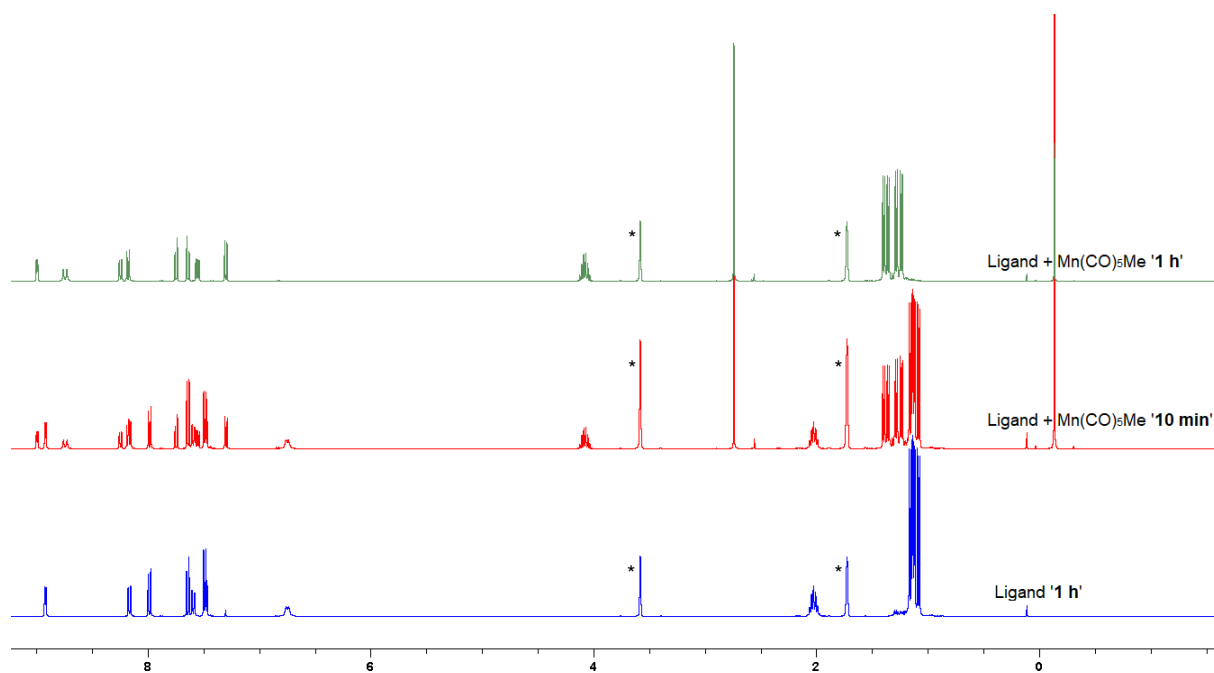


Figure 12: Complexation of phen-²NH-ⁱPrP (**4**) with MeMn(CO)₅ in THF-*d*₈ (*) monitored via ¹H NMR spectroscopy.

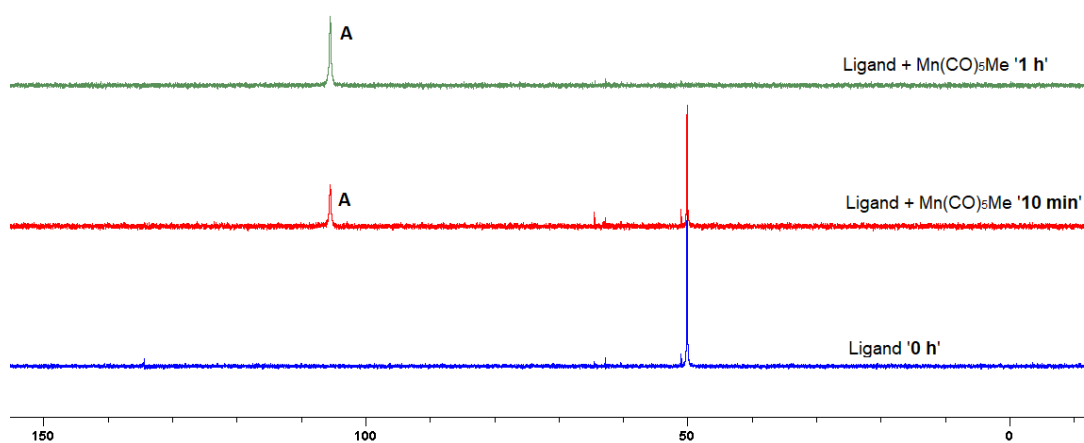


Figure 13: Complexation of phen-²NH-ⁱPrP (**4**) with MeMn(CO)₅ in THF-*d*₈ monitored via ³¹P NMR spectroscopy.

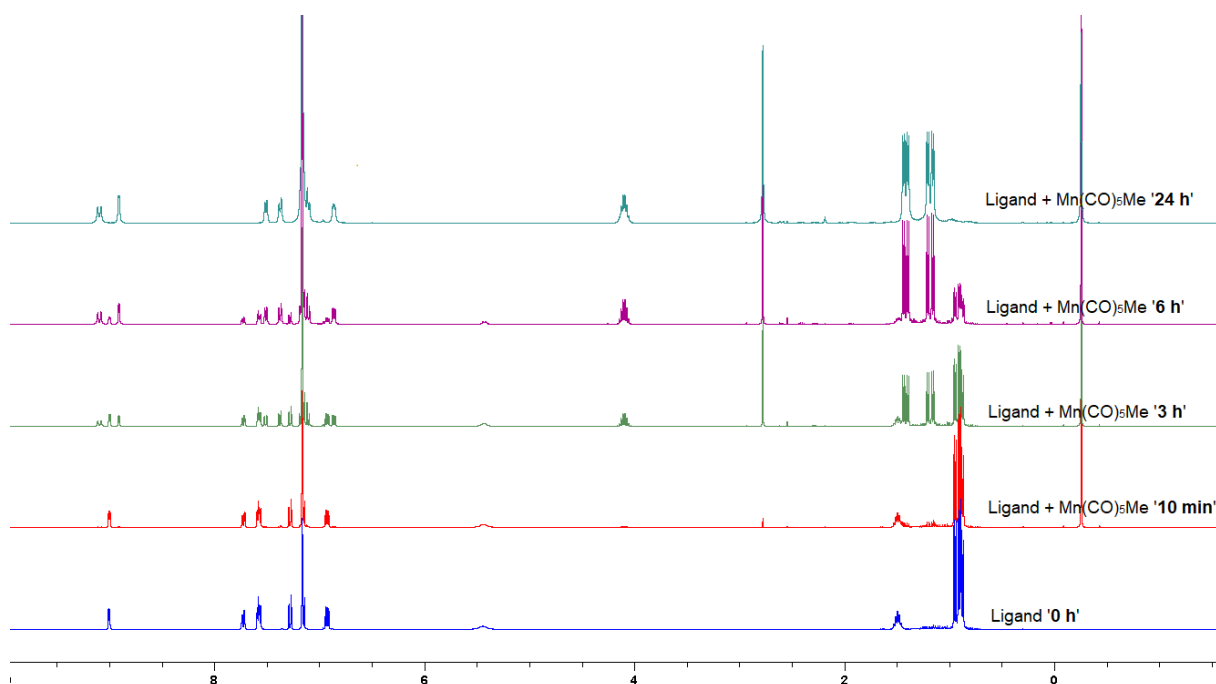


Figure 14: Complexation of phen-²NH-ⁱPrP (**4**) with MeMn(CO)₅ in C₆D₆ monitored via ¹H NMR spectroscopy.

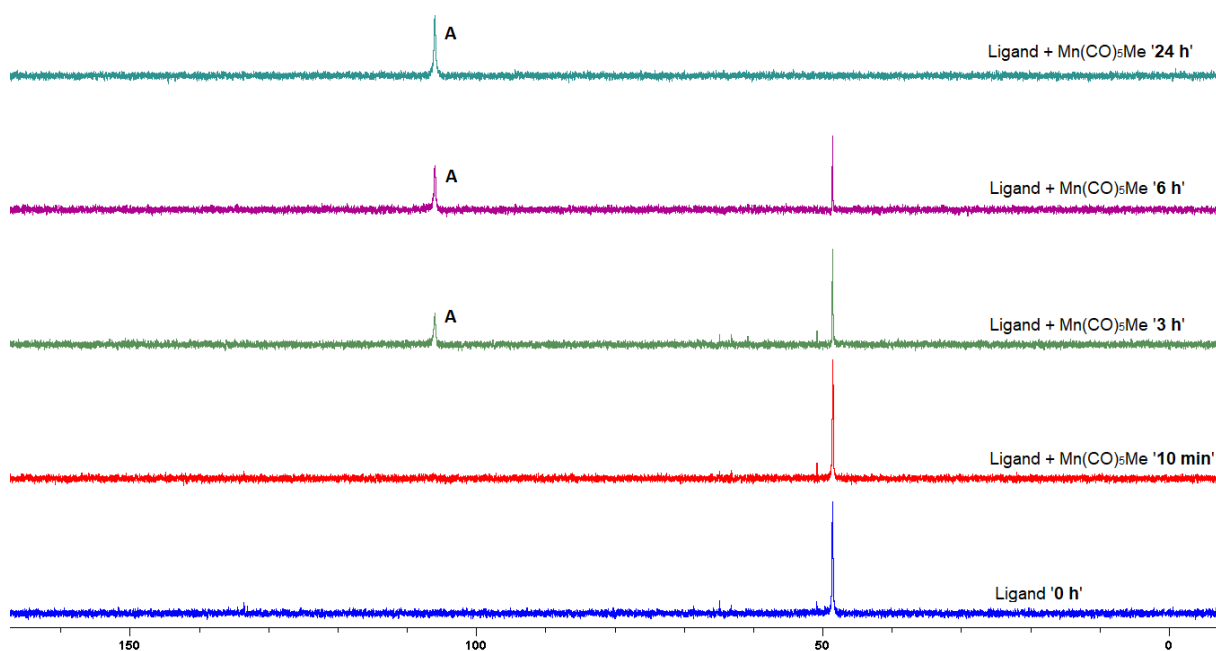


Figure 15: Complexation of phen-²NH-ⁱPrP (**4**) with MeMn(CO)₅ in C₆D₆ monitored via ³¹P NMR spectroscopy.

This complexation was monitored *via* FT-IR spectroscopy (Figure 16) as well. The metal precursor and the pincer complex were dissolved in CHCl₃ and the spectra were recorded in a NaCl-cuvette. Similar to **Cat2** a clear shift to lower wavenumbers is visible upon complexation. This observation can be explained by the increased π -backbonding through complexation of the manganese precursor to the strong σ -donating phen-²NH-ⁱPrP ligand.

However, in contrast to the complexation with the $\text{Mn}(\text{CO})_5\text{Br}$ precursor, the complexation with $\text{MeMn}(\text{CO})_5$ did not lead to a broadening of the absorption bands.

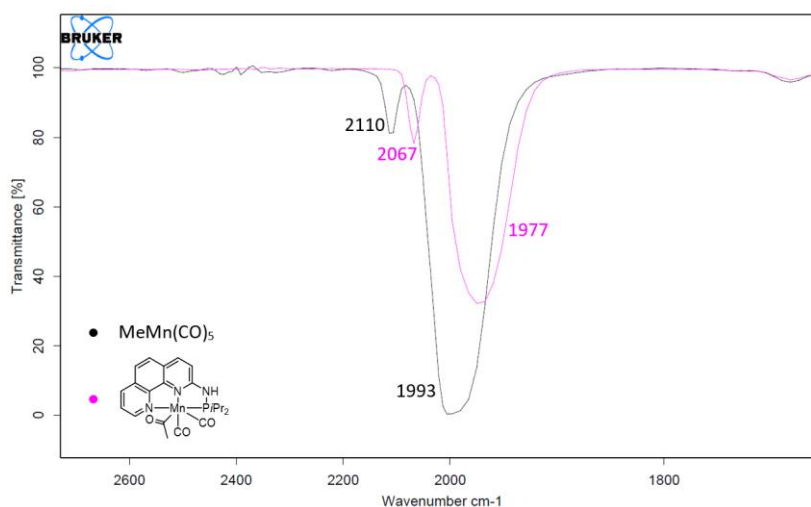


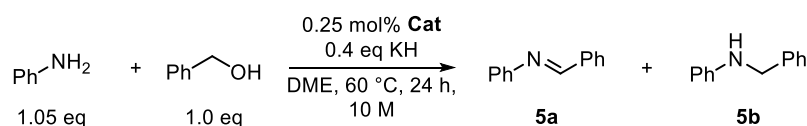
Figure 16: FT-IR spectrum of **Cat3** and its precursor ($\text{MeMn}(\text{CO})_5$) recorded using a NaCl cuvette in CHCl_3 .

Catalytic Activity

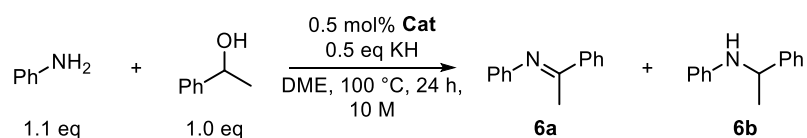
After performing the synthesis of the phenanthroline-based ligand **4** and its complexation with manganese successfully, the catalytic activity of the two new complexes (**Cat2** and **Cat3**) was investigated.

Comparison of the catalytic activity of **Cat1** and **Cat2**

At first, the influence of the highly conjugated phenanthroline backbone on the catalytic activity in borrowing hydrogen reactions was examined. Therefore, **Cat1** with the bipyridine backbone and **Cat2** with the phenanthroline backbone were applied in test reactions (Scheme 18). In general, **Cat1** provided better results. In the *N*-alkylation of aniline with benzyl alcohol (Scheme 18a) **Cat1** led to a significantly higher conversion. In the *N*-alkylation of aniline with 1-phenylethanol the conversion was low for both catalysts, however **Cat1** again demonstrated a higher activity (Scheme 18b). In contrast, **Cat2** produced a higher yield of desired product **7b** in the aldol-type reaction of benzyl alcohol and 1-phenylethanol (Scheme 18c). The reaction of 2-aminobenzyl alcohol with 1-phenylethanol led to product mixtures in both cases. However, when **Cat1** was applied, a higher selectivity for the desired reduced 1,2,3,4-tetrahydroquinoline **8b** was observed (Scheme 18d).

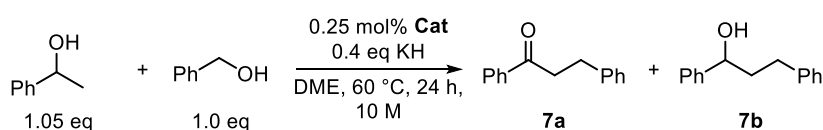
a) *N*-alkylation of aniline with benzyl alcohol

	Conversion* [%]	
	5a	5b
Cat1	<1	81
Cat2	<1	32

b) *N*-alkylation of aniline with 1-phenylethanol

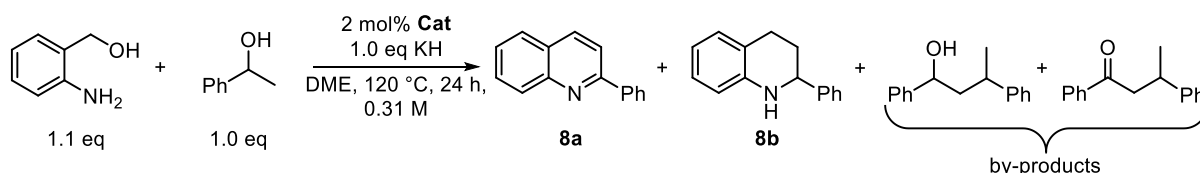
	Conversion* [%]	
	6a	6b
Cat1	3	12
Cat2	5	5

c) aldol condensation of 1-phenylethanol with benzyl alcohol



	Conversion* [%]	
	7a	7b
Cat1	<1	15
Cat2	<1	25

d) quinoline / tetrahydroquinoline synthesis



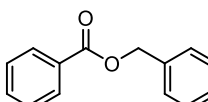
	Conversion* [%]		
	8a	8b	by-products
Cat1	12	47	39
Cat2	22	36	21

Scheme 18: Comparison of the catalytic activity of **Cat1** and **Cat2** (*Conversion determined via GC/MS analysis).

Comparison of the catalytic activity of **Cat2** and **Cat3**

Next, the catalytic activity of **Cat2** and **Cat3** in the *N*-alkylation of aniline with benzyl alcohol was compared (Table 3). Two different bases for activation were tested and in both cases **Cat2** (complex with $\text{Mn}(\text{CO})_5\text{Br}$) showed significantly higher conversions. However, these experiments revealed that **Cat3** (complex with $\text{MeMn}(\text{CO})_5$) can be activated by KH or KO i Bu and thus allows decent conversions.

Table 5: Hydrogenation of methylbenzoate

$ \begin{array}{c} \text{2.0 mol\% Cat3} \\ 50 \text{ bar H}_2 \\ x \text{ mol\% KOtBu} \\ \hline \text{DME, 120 } ^\circ\text{C, 24 h,} \\ 0.5 \text{ M} \end{array} \rightarrow \begin{array}{c} \text{C}_6\text{H}_5\text{CH}_2\text{OH} \\ \text{10} \end{array} + \begin{array}{c} \text{CH}_3\text{OH} \\ \text{11} \end{array} $		
#	KOtBu [mol%]	Observation
1	none	product mixture
2	10	71% 

^a Conversion determined via GC/MS analysis.

In previous studies,^[30, 59] ketones tended to be more active to undergo hydrogenation reactions compared to nitriles and esters. Thus, acetophenone was chosen as test substrate for further examination. The results of different approaches are summarized in Table 6. **Cat3** allowed a quantitative conversion of acetophenone when 20 bars H₂ and a catalytic amount of KOtBu were applied (Table 6, Entry 4). **Cat2** was tested as well for comparison. This complex showed a significantly higher activity as a complete conversion was obtained when 6 bars of H₂ were used (Table 6, Entry 6).

Table 6: Hydrogenation of acetophenone

$ \begin{array}{c} \text{2.0 mol\% Cat} \\ x \text{ bar H}_2 \\ x \text{ mol\% KOtBu} \\ \hline \text{DME, 120 } ^\circ\text{C, 24 h,} \\ 0.5 \text{ M} \end{array} \rightarrow \begin{array}{c} \text{C}_6\text{H}_5\text{CH(OH)CH}_3 \\ \text{12} \end{array} $				
#	Cat	KOtBu [mol%]	H ₂ pressure [bar]	Conversion ^a [%] 12
1	Cat3	none	6	< 1
2	Cat3	2	6	< 1
3	Cat3	10	6	48
4	Cat3	10	20	> 99
5	Cat2	none	6	< 1
6	Cat2	10	6	> 99

^a Conversion determined via GC/MS analysis.

The hydrogenation of amides was investigated as well (Table 7). Initial experiments were conducted with acetamide (Table 7, Entries 1 and 2). Unfortunately, neither the substrate, nor the product were detected in the GC/MS trace, even after repeating the reaction twice. It is assumed that the huge capacity of the reactor led to distribution of the reagents. Hence, another amide with a higher molecular weight was tested. However, the hydrogenation of benzamide was not successful and the corresponding benzylamine was not detected, and only unreacted starting material was found.

Table 7: Hydrogenation of amides

#	R =	KOtBu [mol%]	Conversion ^a [%] 13
1	CH ₃	none	n.d.
2	CH ₃	10	n.d.
3	C ₆ H ₅	none	<1
4	C ₆ H ₅	10	<1

^a Conversion determined via GC/MS analysis. (n.d. = nothing detected)

The best results were obtained in the hydrogenation of quinoline (Table 8). **Cat2** and **Cat3** led to similar results compared to the highly active **Cat1**.

Table 8: Hydrogenation of quinoline

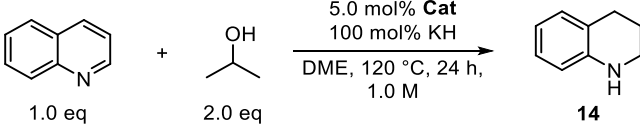
#	Cat	Conversion ^a [%] 14
1	Cat1	99
2	Cat2	93
3	Cat3	97

^a Conversion determined via GC/MS analysis.

Transfer hydrogenations promoted by **Cat3**

Based on the high reactivity in the hydrogenation of quinoline with external hydrogen, the capability of **Cat3** to promote transfer hydrogenations was examined as well. As test reaction, the hydrogenation of quinoline with *i*PrOH was chosen and compared to the catalytic activity of **Cat1** and **Cat2** (Table 9). All complexes showed to be suitable catalysts for this reaction. **Cat1** with the bipyridine backbone led to the highest conversion (Table 9, Entry 1). Comparison of the two phenanthroline-based complexes gave higher activity for the acyl ligated form (**Cat3**) (Table 9, Entries 2 and 3). This stands in remarkable contrast to the observations which were made for the *N*-alkylation of aniline, in which **Cat2** led to significantly higher conversions (see Table 3).

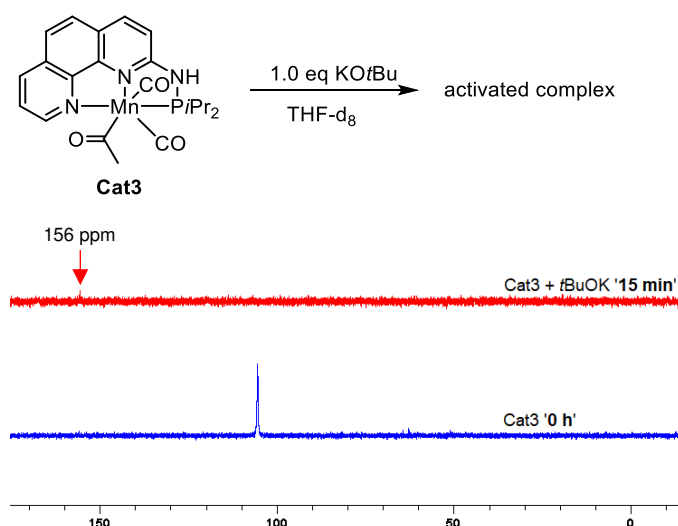
Table 9: Transfer hydrogenation of quinoline

		
#	Cat	Conversion ^a [%] 14
1	Cat1	95
2	Cat2	71
3	Cat3	80

^a Conversion determined via GC/MS analysis.

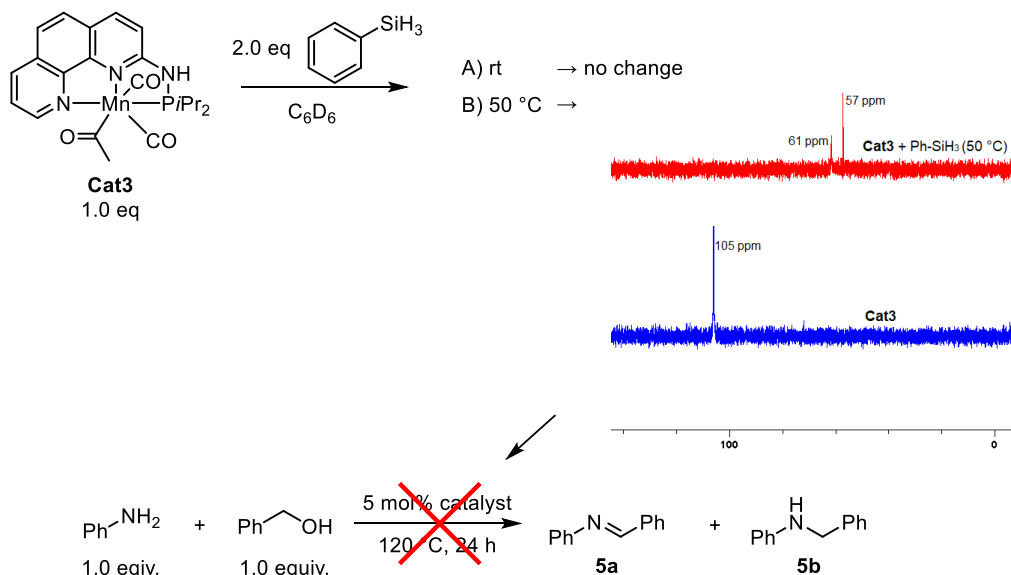
Activation of **Cat3**

Different strategies to activate **Cat3** were tested. Firstly, as KO^tBu can activate the complex for the *N*-alkylation of aniline (see Table 3), it was attempted to observe this activation *via* ³¹P NMR spectroscopy (Scheme 19, Figure 8). However, this activation could not be as easily monitored as the activation of **Cat1** and **Cat2** where a clear shift of the phosphorous signal was observed. 15 min after addition of KO^tBu the characteristic signal at 105 ppm disappeared and only a very small signal at 156 ppm appeared. Thus, additional studies should be performed, such as repeating this NMR experiment measuring a broader chemical shift range or applying other bases (e.g. KH or KOH).

Scheme 19: Activation of **Cat3** with KO^tBu in THF-*d*₈ at room temperature.

Additionally, based on the work by Cutler *et al.*^[60] the hydrosilylation strategy was tested for activation of **Cat3** (Scheme 20). However, these attempts did not lead to a successful activation so far. An NMR scale reaction in C₆D₆ was conducted. At room temperature no change was observed, just upon heating shifts of the signals were observed. In the ¹H NMR spectrum broad shifted signals appeared. The signal of the complex at 105 ppm in the ³¹P

NMR spectrum disappeared, whereas two new signals at 57 ppm and 61 ppm (ratio = 2.9:1) were observed. This solution was tested for catalytic activity in the *N*-alkylation of aniline with benzyl alcohol. However, no conversion of the starting materials was observed.



Scheme 20: Attempted activation via hydrosilylation of **Cat3**.

Stability test and catalytic activity of **Cat3**

The stability of **Cat3** under atmospheric conditions was tested. Therefore, the complex was prepared in C6D6 in a screw-cap NMR tube. After the complex was formed, the NMR tube was opened and air was allowed to get in. The slow decomposition process of the complex was followed by ¹H and ³¹P NMR spectroscopy (Figure 17 and 18). After the complex was exposed to air for 24 h, small amounts of precipitate were found and the signals in the ¹H NMR spectrum started to broaden. In the ³¹P NMR spectra the signal-to-noise ratio worsened, indicating decomposition. However, no new signals, which could be assigned to the decomposed phosphorous species, appeared. Over the course of 6 days the color of the complex solution slowly changed from slightly yellow to dark orange.

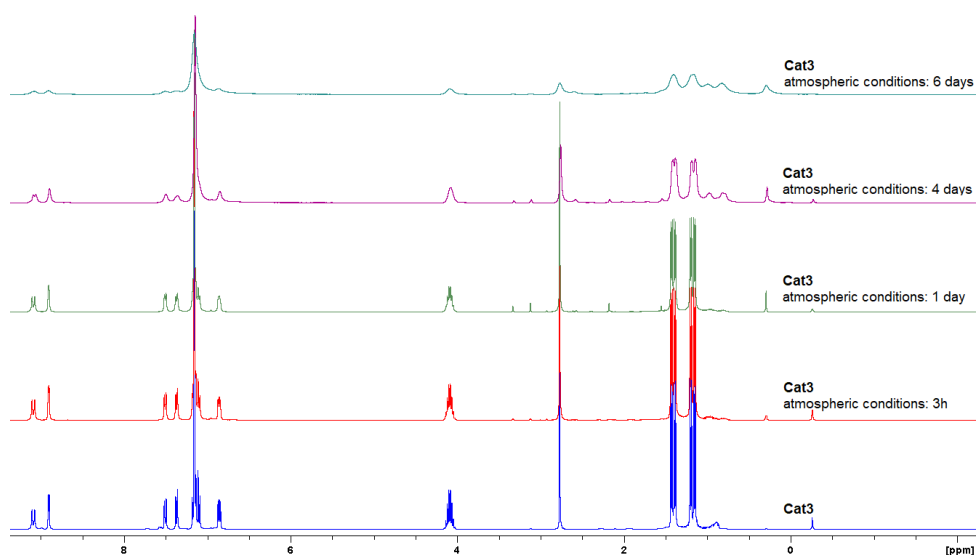


Figure 17: Decomposition of **Cat3** under atmospheric conditions monitored via ^1H -NMR spectroscopy in C_6D_6 .

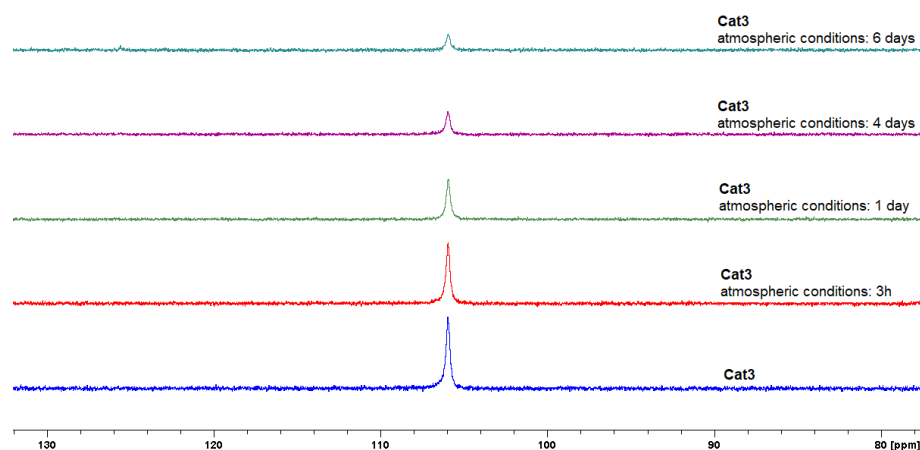
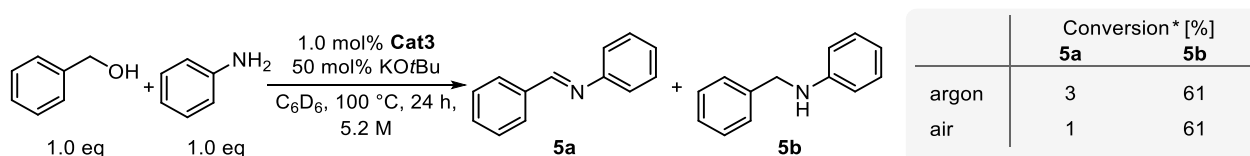


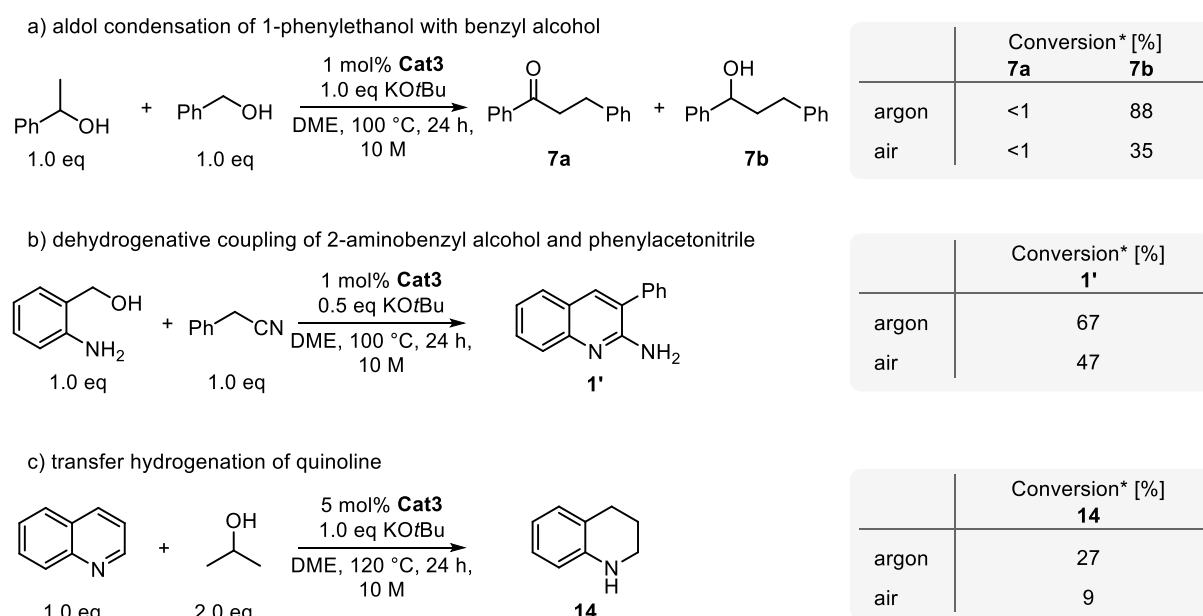
Figure 18: Decomposition of **Cat3** under atmospheric conditions monitored via ^{31}P -NMR spectroscopy in C_6D_6 .

After 24 h an aliquot was taken and used for catalysis. The *N*-alkylation of aniline with benzyl alcohol was conducted under atmospheric conditions. The catalyst showed remarkable activity. 61 % of the desired *N*-benzylaniline (**5b**) were detected via GC/MS analysis. For comparison, the reaction was conducted under the same reaction conditions with the freshly prepared complex under argon atmosphere. This reaction led to exactly the same conversion into the alkylated product **5b** (Scheme 21).



Scheme 21: *N*-alkylation of aniline under atmospheric conditions (*Conversion determined via GC/MS analysis).

Based on the success of the *N*-alkylation, three additional test reactions under aerobic conditions were examined (Scheme 22). For this screening a stock-solution of **Cat3** was freshly prepared under inert conditions. The observed reactivity was significantly higher when the reactions were conducted under argon atmosphere. However, even when the reactions were exposed to air, moderate conversions were achieved for the aldol reaction (Scheme 22a) and the dehydrogenative coupling (Scheme 22b). The transfer hydrogenation of quinoline led to relatively low conversions (Scheme 22c). The same reaction using KH as base allowed the formation of significantly higher amounts of product (see Table 9, Entry 3). However, as KH is pyrophoric in humid air, KO*t*Bu was chosen for this experiment. Despite the general lower conversions obtained under atmospheric conditions, these initial experiments proved that **Cat3** has the capability to promote borrowing hydrogen reactions and dehydrogenative couplings in air.



Scheme 22: Additional investigations on reactions under atmospheric conditions (Conversion determined via GC/MS analysis).

3.4.2. Conclusion

Various initial investigations concerning the stability and activity of PN^3 manganese pincer complexes were conducted in order to get a glimpse into the potential of these catalytic systems.

The synthesis of 2-aminoquinolines *via* dehydrogenative coupling of 2-aminobenzyl alcohols and nitriles was examined. The application of the bipyridine-based PN^3 manganese pincer complex **Cat1** allowed significantly milder reaction conditions compared to previously reported base metal catalysts. Early examinations concerning the substrate scope revealed that aromatic substrates are generally well tolerated, whereas aliphatic substrates did not lead to the formation of the desired products. Additional steps would be to further optimize the reaction conditions, in particular when more challenging substrates are applied, as well as to broaden the screening in order to highlight the unique potential of **Cat1**.

The synthetic procedure of the phenanthroline-based ligand (**4**, phen- $^2\text{NH-}^i\text{PrP}$) was optimized and the obtained ligand was successfully applied for complexation with $\text{Mn}(\text{CO})_5\text{Br}$ (**Cat2**) and $\text{Mn}(\text{CO})_5\text{Me}$ (**Cat3**), which could be monitored *via* NMR spectroscopy.

First investigations on the catalytic activity of the newly formed complexes were conducted as well. In combination with base, both catalytic systems can be used to promote various reactions based on the borrowing hydrogen strategy. However, in case of the benchmark reaction, i.e. *N*-alkylation of aniline with benzyl alcohol, the reactivity of the two new complexes (**Cat2**, **Cat3**) is significantly reduced compared to the already published bipyridine based complex (**Cat1**).

To get further information about the newly synthesized complexes **Cat2** and **Cat3**, IR spectra were recorded and the changes of the CO-vibrations were investigated. Moreover, attempts to crystallize **Cat2** and **Cat3** were conducted. However, until now crystals suitable for X-ray analysis have not been obtained.

The catalytic activity of **Cat3** in hydrogenation reactions was examined. In general, **Cat3** does not show activity without the application of base. Additional studies on this process should be conducted to allow more insights in this process. The catalytic activity of all complexes was compared in the transfer hydrogenation of quinoline with *i*PrOH. **Cat1** showed remarkable reactivity again, but **Cat2** and **Cat3** led to good conversions as well. For this particular reaction, **Cat3** led to a higher conversion than **Cat2**.

Stability tests of **Cat3** revealed that the complex only decomposes slowly in air in solution and that it has the potential to promote borrowing hydrogen reactions and dehydrogenative couplings under atmospheric conditions.

3.4.3. Experimental Part

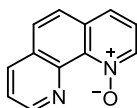
General

Unless otherwise noted all reactions were performed under inert conditions, either with a Schlenk line under argon in flame-dried glassware or in an argon filled glovebox. Solvents used for synthesis or catalysis were distilled from CaH₂ or sodium benzophenone ketyl. Alcohols and amines used as substrates for catalysis were distilled from Na₂SO₄. If not mentioned differently, all commercially available starting materials were used without further purification.

All ¹H, ¹³C and ³¹P NMR spectra were recorded on a Bruker Ultrashield™ 400 or 600 Plus instrument, whereby the ¹H NMR spectra were measured at 400.3 MHz or 600.2 MHz, the ¹³C NMR spectra at 100.6 or 150.9 MHz and the ³¹P NMR spectra at 162.0 MHz. All chemical shifts are noted in ppm. ¹H- and ³¹C- shifts are indicated relative to TMS and were referenced to residual signals of the solvent (¹H NMR (CDCl₃): 7.27 ppm, ¹H NMR (C₆D₆): 7.16 ppm, ¹³C NMR (CDCl₃): 77.0 ppm, ¹³C NMR (C₆D₆): 128.4 ppm).^[61] Column chromatography was performed by using Biotage® SP4 and Isolera Flash Systems and the applied columns were packed with silica gel 60 Å or aluminium oxide 90 standardised (activity II-III). TLC was performed with commercial Kieselgel 60 F₂₅₄ or ALOX N/UV₂₅₄ and visualised *via* UV lamp. GC/MS measurements were conducted on an Agilent Technologies with 5977B MSD High Efficiency Source and 7820A GC-system. GC/FID measurements were conducted on a Shimadzu GC-2010 Plus system.

Ligand Synthesis

Synthesis of 1,10-phenanthroline-1-oxide (phen-¹O, 2)



(Reaction was performed under atmospheric conditions)

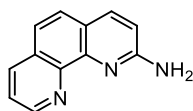
In a round bottom flask 1,10-phenanthroline (5.28 g, 29.3 mmol, 1.0 equiv) was dissolved in TFA (20 mL, d=1.489 g/mL, 261.2 mmol, 8.9 equiv). The solution was cooled to 0 °C and H₂O₂ (4.5 mL, 30 wt% in H₂O, 44.0 mmol, 1.5 equiv) was added dropwise. The reaction was allowed to reach room temperature and was stirred for 2 h. 6 M NaOH (30 mL) was added

slowly to quench the reaction. The layers were separated, and the aqueous phase was extracted with CH₂Cl₂ (3 × 50 mL). The combined organic layers were dried over MgSO₄, then all volatiles were removed under reduced pressure, leaving an off-white product. To increase the yield, NaCl was added to the aqueous layer, then the extraction with CH₂Cl₂ was repeated.

Yield: 4.3 g (74 %).

¹H NMR (400.3 MHz, CDCl₃): δ = 9.34 (dd, ³J_{H-H} = 4.4 Hz, ⁴J_{H-H} = 1.8 Hz, 1H, aryl-H), 8.77 (dd, ³J_{H-H} = 6.3 Hz, ⁴J_{H-H} = 1.0 Hz, 1H, aryl-H), 8.26 (dd, ³J_{H-H} = 8.0 Hz, ⁴J_{H-H} = 1.8 Hz, 1H, aryl-H), 7.83 (d, ³J_{H-H} = 8.9 Hz, 1H, aryl-H), 7.77 (d, ³J_{H-H} = 8.9 Hz, 1H, aryl-H), 7.76 (dd, ³J_{H-H} = 8.2 Hz, ⁴J_{H-H} = 1.0 Hz, 1H, aryl-H), 7.69 (dd, ³J_{H-H} = 8.0 Hz, ³J_{H-H} = 4.4 Hz, 1H, aryl-H), 7.48 (dd, ³J_{H-H} = 8.2 Hz, ³J_{H-H} = 6.3 Hz, 1H, aryl-H). The NMR spectroscopic data is in agreement with the literature.^[62]

Synthesis of 1,10-phenanthroline-2-amine (phen-2NH₂, **3**)



(Reaction was performed under atmospheric conditions)

bpy-¹O (2.20 g, 11.2 mmol, 1.0 equiv) and *t*BuNH₂ (7.3 mL, d=0.696 g/mL, 69.4 mmol, 6.2 equiv) were dissolved in CHCl₃ (50 mL). The mixture was cooled to 0 °C, then TsCl (5.30 g, 28.0 mmol, 2.5 equiv) was added in portions. The resulting reaction mixture was stirred at room temperature. After the reaction was completed (monitored *via* TLC: alox, 5% MeOH in EtOAc, 2.5 h), all volatiles were removed under reduced pressure. Then TFA (25 mL, d=1.489 g/mL, 326.4 mmol, 29.1 equiv) was added and the reaction was heated to 65 °C for 22 h. The reaction mixture was allowed to reach room temperature and all volatiles were removed under reduced pressure, leaving a brown oil. This was dissolved in CH₂Cl₂ (30 mL), treated with 6 M NaOH until a pH of 9 was reached. Then, the two phases were separated and the aqueous phase was extracted with CH₂Cl₂ (3 × 50 mL). The combined organic layers were dried over MgSO₄, then all volatiles were removed under reduced pressure, leaving a brown oil as crude product. Purification *via* flash chromatography (silica, 0 – 10% MeOH in DCM) provided the pure product as a slightly yellow foam.

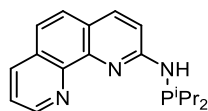
Yield: 2.05 mg (94 %).

R_f (silica, DCM) = 0.08.

¹H NMR (400.3 MHz, CDCl₃): δ = 9.02 (dd, ³J_{H-H} = 4.3 Hz, ³J_{H-H} = 1.7 Hz, 1H, aryl-H), 8.16 (dd, ³J_{H-H} = 8.0 Hz, ⁴J_{H-H} = 1.7 Hz, 1H, aryl-H), 7.95 (d, ³J_{H-H} = 8.7 Hz, 1H, aryl-H), 7.62 (d, ³J_{H-H} = 8.7 Hz, 1H, aryl-H), 7.51 (d, ³J_{H-H} = 8.7 Hz, 1H, aryl-H), 7.54 (d, ³J_{H-H} = 8.1 Hz, 1H, aryl-H), 6.92 (d, ³J_{H-H} = 8.5 Hz, 1H, aryl-H), 5.61 (br s, 2H, NH₂); ¹³C {¹H} NMR (100.7 MHz, CDCl₃): δ = 157.7 (Cq), 149.4 (CH), 145.6 (Cq), 145.0 (Cq), 138.0 (CH), 135.9 (CH), 129.2

(Cq), 126.4 (CH), 122.7 (Cq), 122.3 (CH), 121.8 (CH), 111.8 (CH). The NMR spectroscopic data is in agreement with the literature.^[62]

Synthesis of N-(diisopropylphosphanyl)-1,10-phenanthroline-2-amine
(*phen*-2NH-*i*PrP, **4**)



phen-2NH₂ (1.00 g, 5.12 mmol, 1.0 equiv) was suspended in THF (12 mL). Then NEt₃ (0.85 mL, d=0.726 g/mL, 6.10 mmol, 1.2 equiv) was added at once. The suspension was degassed with three freeze-pump-thaw cycles. After cooling to 0 °C, *i*Pr₂PCl (0.90 mL, d=0.959 g/mL, 5.66 mmol, 1.1 equiv) was added dropwise and the reaction mixture was allowed to reach room temperature. The suspension was heated to 60 °C for 16 h. Afterwards the reaction was cooled to 0 °C and the precipitates were filtered off. All volatiles were removed in *vacuo* yielding a yellow oil. The crude product was washed thoroughly with cold hexanes. Freeze-drying led to the product as a slightly yellow solid.

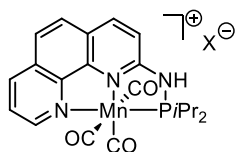
Yield: 1,46 mg (91 %).

¹H NMR (400.3 MHz, THF-*d*₈): δ = 8.98 (dd, ³*J*_{H-H} = 4.1 Hz, ⁴*J*_{H-H} = 1.8 Hz, 1H, aryl-H), 8.16 (dd, ³*J*_{H-H} = 8.1 Hz, ⁴*J*_{H-H} = 1.8 Hz, 1H, aryl-H), 7.99 (d, ³*J*_{H-H} = 8.8 Hz, 1H, aryl-H), 7.64 (d, ³*J*_{H-H} = 8.6 Hz, 1H, aryl-H), 7.59 (dd, ³*J*_{H-H} = 8.8 Hz, ⁴*J*_{H-H} = 2.9 Hz, 1H, aryl-H), 7.49 (d, ³*J*_{H-H} = 8.9 Hz, 1H, aryl-H), 7.47 (d, ³*J*_{H-H} = 8.2 Hz, 1H, aryl-H), 6.76 (br s, 1H, NH), 1.95 – 2.10 (m, 2H, CH(CH₃)₂), 1.04 – 1.18 (m, 12H, CH(CH₃)₂); ¹³C {¹H} NMR (100.7 MHz, THF-*d*₈): δ = 161.4 (d, ²*J*_{P-C} = 20.4 Hz, Cq), 149.2 (CH), 147.0 (Cq), 146.5 (Cq), 137.6 (d, ⁴*J*_{P-C} = 2.9 Hz, CH), 135.8 (CH), 129.9 (Cq), 127.0 (CH), 123.9 (Cq), 122.6 (CH), 122.1 (CH), 111.7 (d, ³*J*_{P-C} = 21.1 Hz, CH, aryl-C), 26.8 (d, ¹*J*_{P-C} = 11.6 Hz, 2 CH, CH(CH₃)₂), 19.1 (d, ²*J*_{P-C} = 20.4 Hz, 2 CH₃, CH(CH₃)₂), 17.7 (d, ²*J*_{P-C} = 8.0 Hz, 2 CH₃, CH(CH₃)₂); ³¹P {¹H} NMR (162.0 MHz, THF-*d*₈): δ = 50.1.

HRMS (ESI): *m/z* Calcd. for [C₁₈H₂₃PN₃, M+H]⁺: 312.1624; found 312.1624.

Complexations

Synthesis of Cat2 (Complexation of phen-2NH-*i*PrP with Mn(CO)₅Br)



X⁻ = Br⁻, ½ [MnBr₄]²⁻

Cat2

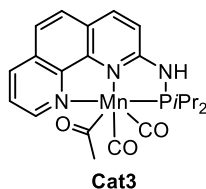
In a screw-cap NMR tube phen-²NH-ⁱPrP (15.9 mg, 0.051 mmol, 1.0 equiv) was dissolved in THF-d₈ or C₆D₆ (0.5 mL), then Mn(CO)₅Br (14.0 mg, 0.051 mmol, 1.0 equiv) was added. The tube was closed tightly, sealed with PTFE Teflon tape and shaken vigorously. Then the complexation was monitored *via* ³¹P{¹H} NMR spectroscopy. The ¹H and ¹³C {¹H} spectra showed small and broadened signals, thus they could not be used for detailed investigation.

³¹P{¹H} NMR (162.0 MHz, THF-d₈): δ = 156.0.

After the ³¹P NMR spectrum indicated a complete complexation (6 h), KO^tBu (11.4 mg, 0.102 mmol, 2.0 equiv) was added for activation. The activation was again monitored *via* ³¹P-NMR spectroscopy.

³¹P{¹H} NMR (162.0 MHz, THF-d₈): δ = 145.5.

Synthesis of **Cat3** (Complexation of phen-²NH-ⁱPrP with MeMn(CO)₅)



In a screw-cap NMR tube phen-²NH-ⁱPrP (14.0 mg, 0.045 mmol, 1.0 equiv) was dissolved in THF-d₈ or C₆D₆ (0.5 mL), then MeMn(CO)₅ (9.5 mg, 0.045 mmol, 1.0 equiv) was added. The tube was closed tightly, sealed with PTFE Teflon tape and shaken vigorously. Then the complexation was monitored *via* ¹H and ³¹P{¹H} NMR spectroscopy. The complexation was completed within 1 h in THF-d₈ whereas it required 18 h in C₆D₆. Removal of the solvent under reduced pressure gave the desired complex as a light brown solid.

Yield: 17.2 mg (82 %).

¹H NMR (400.3 MHz, THF-d₈): δ = 8.99 (dd, ³J_{H-H} = 4.2 Hz, ⁴J_{H-H} = 1.8 Hz, 1H, aryl-H), 8.74 (d, ²J_{P-H} = 12.8 Hz, 1H, NH), 8.24 (dd, ³J_{H-H} = 7.9 Hz, ⁴J_{H-H} = 1.7 Hz, 1H, aryl-H), 8.18 (d, ³J_{H-H} = 8.5 Hz, 1H, aryl-H), 7.74 (d, ³J_{H-H} = 8.7 Hz, 1H, aryl-H), 7.64 (d, ³J_{H-H} = 8.7 Hz, 1H, aryl-H), 7.55 (dd, ³J_{H-H} = 8.1 Hz, ⁴J_{H-H} = 4.1 Hz, 1H, aryl-H), 7.30 (d, ³J_{H-H} = 8.5 Hz, 1H, aryl-H), 4.02 – 4.13 (m, 2H, CH(CH₃)₂), 2.74 (s, 3H, CH₃), 1.38 (dd, ³J_{P-H} = 15.7 Hz, ³J_{H-H} = 7.1 Hz, 6H, CH(CH₃)₂), 1.26 (dd, ³J_{P-H} = 18.2 Hz, ³J_{H-H} = 7.1 Hz, 6H, CH(CH₃)₂); ¹³C {¹H} NMR (100.7 MHz, CDCl₃): δ = 217.9 (Cq), 216.3 (Cq), 214.5 (Cq, CO), 157.1 (d, ²J_{P-C} = 12.2 Hz, Cq), 150.7 (CH), 146.9 (Cq), 146.5 (Cq), 139.1 (CH), 136.4 (CH), 130.4 (Cq), 127.2 (CH), 124.9 (Cq), 124.1 (CH), 123.4 (CH), 115.2 (d, ³J_{P-C} = 6.6 Hz, CH, aryl-C), 51.8 (d, ³J_{P-C} = 2.2 Hz, CH₃), 30.3 (d, ¹J_{P-C} = 25.4 Hz, 2 CH, CH(CH₃)₂), 19.6 (d, ²J_{P-C} = 2.2 Hz, 2 CH₃, CH(CH₃)₂), 18.0 (d, ²J_{P-C} = 5.5 Hz, 2 CH₃, CH(CH₃)₂); ³¹P {¹H} NMR (162.0 MHz, THF-d₈): δ = 105.1.

Catalysis

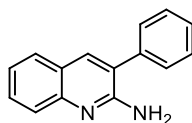
General procedure for the synthesis of 2-aminoquinolines (**1'**)

In an argon filled glovebox, in a PTFE-lined screw-cap vial (1.8 mL), equipped with a magnetic stirring bar, KO^tBu (5.6 mg, 0.05 mmol, 0.1 equiv) and aminobenzyl alcohol (0.500 mmol, 1.0 equiv) were dissolved in DME. Then a stock solution of **Cat1** (200 μ L, 0.025 M, 0.005 mmol, 0.01 equiv) and nitrile (0.500 mmol, 1.0 equiv) were added. The vial was closed tightly and the resulting reaction mixture was stirred in a preheated aluminum block at 120 °C for 24 h. After cooling to room temperature, the reaction mixture was quenched with H₂O (0.1 mL) and extracted with EtOAc (0.5 mL). 30 μ L of the organic layer were diluted in EtOAc (1.0 mL), filtered over MgSO₄ and analyzed *via* GC/MS analysis. To isolate the product, the aqueous layer was extracted with EtOAc (3 \times 0.5 mL) again. Then all organic layers were combined and dried over MgSO₄ and the solvent was removed under reduced pressure. The crude product was purified *via* column chromatography (alox, 5 – 30% EtOAc in heptanes).

Preparation of catalyst stock solution of **Cat1**:

In an argon filled glovebox, a PTFE-lined screw-cap vial (4.0 mL, \varnothing 1.5 cm, height 4 cm), equipped with a magnetic stirring bar, was charged with Mn(CO)₅Br (20.6 mg, 0.075 mmol, 1.0 equiv) and bpy-⁶NH-ⁱPrP (21.6 mg, 0.025 mmol, 1.0 equiv). Then DME (3.00 mL) was added. The resulting yellow suspension was stirred in a preheated aluminum block at 30 °C until a light brown solution was formed (15 min). The obtained stock solution was used without further purification.

3-phenylquinolin-2-amine



White solid, GC/MS-Yield: 84 %, Isolated yield: 75 mg, 64 %

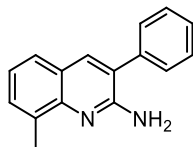
R_f (alox, EtOAc/Hept = 1:1) = 0.43

¹H NMR (400.3 MHz, CDCl₃): δ = 7.80 (s, 1H, aryl-H), 7.70 (d, ³J_{H-H} = 8.4 Hz, 1H, aryl-H), 7.66 (d, ³J_{H-H} = 8.0 Hz, 1H, aryl-H), 7.40 – 7.61 (m, 6H, aryl-H), 7.24 – 7.33 (m, 1H, aryl-H), 4.97 (br s, 2H, NH₂);

¹³C {¹H} NMR (100.7 MHz, CDCl₃): δ = 155.1 (Cq), 147.2 (Cq), 137.6 (Cq), 137.2 (CH), 129.6 (CH), 129.1 (2 CH), 128.9 (2 CH), 128.2 (CH), 127.5 (CH), 125.7 (CH), 125.0 (Cq), 124.2 (Cq), 122.8 (CH, aryl-C). The NMR spectroscopic data is in agreement with the literature.^[52]

HRMS (ESI): m/z Calcd. for $[C_{15}H_{13}N_2, M+H]^+$: 221.1073; found 221.1069.

8-methyl-3-phenylquinolin-2-amine



A different purification strategy was applied to obtain this product in satisfying yields: The crude product was purified *via* column chromatography (silica, 5 – 30% EtOAc in heptanes). White solid, GC/MS-Yield: 83 %, Isolated yield: 77 mg, 66 %

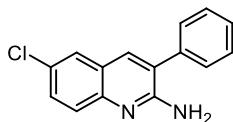
R_f (silica, EtOAc/Hept = 1:1) = 0.44

1H NMR (400.3 MHz, $CDCl_3$): δ = 7.78 (s, 1H, aryl-H), 7.47 – 7.58 (m, 5H, aryl-H), 7.38 – 7.47 (m, 2H, aryl-H), 7.18 (t, $^3J_{H-H}$ = 7.5 Hz, 1H, aryl-H), 4.92 (br s, 2H, NH_2), 2.71 (s, 3H, CH_3);

^{13}C $\{^1H\}$ NMR (100.7 MHz, $CDCl_3$): δ = 154.3 (Cq), 146.2 (Cq), 137.9 (Cq), 137.5 (CH), 133.7 (Cq), 129.8 (CH), 129.1 (2 CH), 128.9 (2 CH), 128.1 (CH), 125.5 (CH), 124.5 (Cq), 124.1 (Cq), 122.4 (CH, aryl-C), 17.9 (CH_3). The NMR spectroscopic data is in agreement with the literature.^[55]

HRMS (ESI): m/z Calcd. for $[C_{16}H_{15}N_2, M+H]^+$: 235.1230; found 235.1227.

6-chloro-3-phenylquinolin-2-amine



A different purification strategy was applied to obtain this product in satisfying yields: The crude product was purified *via* column chromatography (alox, 5 – 30% EtOAc in heptanes). The obtained yellow solid was recrystallized from heptanes/ CH_2Cl_2 (5:1).

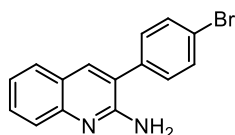
White crystals, GC/MS-Yield: 80 %, Isolated yield: 92 mg, 72 %

R_f (alox, EtOAc/Hept = 1:1) = 0.77

1H NMR (400.3 MHz, $CDCl_3$): δ = 7.70 (s, 1H, aryl-H), 7.63 (dd, $^3J_{H-H}$ = 6.5 Hz, $^4J_{H-H}$ = 3.3 Hz, 2H, aryl-H), 7.38 – 7.56 (m, 6H, aryl-H), 4.94 (br s, 2H, NH_2);

^{13}C $\{^1H\}$ NMR (100.7 MHz, $CDCl_3$): δ = 155.3 (Cq), 145.7 (Cq), 137.1 (Cq), 136.2 (CH), 130.2 (CH), 129.3 (2 CH), 128.8 (2 CH), 128.5 (CH), 127.9 (Cq), 127.3 (CH), 126.2 (CH), 125.9 (Cq), 124.8 (Cq).

HRMS (ESI): m/z Calcd. for $[C_{15}H_{12}ClN_2, M+H]^+$: 255.0684; found 255.0680.

3-(4-bromophenyl)quinolin-2-amine

A different purification strategy was applied to obtain this product in satisfying yields: The crude product was purified *via* column chromatography (alox, 5 – 30% EtOAc in heptanes). The obtained yellow solid was recrystallized from heptanes/CH₂Cl₂ (5:1).

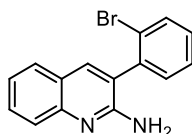
White crystals, GC/MS-Yield: 54 %, Isolated yield: 53 mg, 36 %

R_f (alox, EtOAc/Hept = 1:1) = 0.38

¹H NMR (400.3 MHz, CDCl₃): δ = 7.77 (s, 1H, aryl-H), 7.53 – 7.73 (m, 5H, aryl-H), 7.40 – 7.44 (m, 2H, aryl-H), 7.25 – 7.32 (m, 1H, aryl-H), 4.89 (br s, 2H, NH₂);

¹³C {¹H} NMR (100.7 MHz, CDCl₃): δ = 154.7 (Cq), 147.3 (Cq), 137.3 (CH), 136.5 (Cq), 132.3 (2 CH), 130.6 (2 CH), 129.9 (CH), 127.5 (CH), 125.8 (CH), 124.3 (Cq), 123.7 (Cq), 123.0 (CH), 122.5 (Cq). The NMR spectroscopic data is in agreement with the literature.^[55]

HRMS (ESI): m/z Calcd. for [C₁₅H₁₂BrN₂, M+H]⁺: 299.0178; found 299.0178.

3-(2-bromophenyl)quinolin-2-amine

A different purification strategy was applied to obtain this product in satisfying yields: The crude product was purified *via* column chromatography (alox, 5 – 30% EtOAc in heptanes). The obtained yellow solid was recrystallized from heptanes/CH₂Cl₂ (5:1).

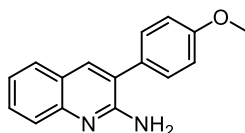
Yellow crystals, GC/MS-Yield: 16 %, Isolated yield: 59 mg, 10 %

R_f (alox, EtOAc/Hept = 1:1) = 0.33

¹H NMR (600.2 MHz, CDCl₃): δ = 7.71 – 7.78 (m, 3H, aryl-H), 7.67 (d, ³ J_{H-H} = 7.9 Hz, 1H, aryl-H), 7.61 (ddd, ³ J_{H-H} = 8.4 Hz, ³ J_{H-H} = 7.1 Hz, ⁴ J_{H-H} = 1.3 Hz, 1H, aryl-H), 7.43 – 7.48 (m, 1H, aryl-H), 7.38 – 7.42 (m, 1H, aryl-H), 7.28 – 7.35 (m, 2H, aryl-H), 4.68 (br s, 2H, NH₂);

¹³C {¹H} NMR (150.9 MHz, CDCl₃): δ = 154.7 (Cq), 147.6 (Cq), 138.0 (Cq), 137.8 (CH), 133.4 (CH), 131.7 (CH), 130.1 (CH), 129.9 (CH), 128.1 (CH), 127.7 (CH), 125.9 (CH), 124.2 (Cq), 124.0 (Cq), 123.7 (Cq), 122.9 (CH). The NMR spectroscopic data is in agreement with the literature.^[63]

HRMS (ESI): m/z Calcd. for [C₁₅H₁₂BrN₂, M+H]⁺: 299.0178; found 299.0176.

3-(4-methoxyphenyl)quinolin-2-amine

White solid, GC/MS-Yield: 77 %, Isolated yield: 87 mg, 70 %

R_f (alox, EtOAc/Hept = 1:1) = 0.35

^1H NMR (400.3 MHz, CDCl_3): δ = 7.76 (s, 1H, aryl-H), 7.69 (d, $^3J_{\text{H-H}}$ = 8.4 Hz, 1H, aryl-H), 7.65 (d, $^3J_{\text{H-H}}$ = 8.0 Hz, 1H, aryl-H), 7.57 (ddd, $^3J_{\text{H-H}}$ = 8.0 Hz, $^3J_{\text{H-H}}$ = 7.0 Hz, $^4J_{\text{H-H}}$ = 1.4 Hz, 1H, aryl-H), 7.42 – 7.49 (m, 2H, aryl-H), 7.23 – 7.32 (m, 1H, aryl-H), 7.00 – 7.07 (m, 2H, aryl-H), 4.90 (br s, 2H, NH_2), 3.98 (s, 3H, CH_3);

^{13}C $\{^1\text{H}\}$ NMR (100.7 MHz, CDCl_3): δ = 159.6 (Cq), 155.4 (Cq), 147.1 (Cq), 137.0 (CH), 136.1 (2 CH), 129.8 (Cq), 129.4 (CH), 127.4 (CH), 125.6 (CH), 124.7 (Cq), 124.3 (Cq), 122.7 (CH), 114.5 (2 CH, aryl-C), 55.4 (CH_3).

HRMS (ESI): m/z Calcd. for $[\text{C}_{16}\text{H}_{15}\text{N}_2\text{O}, \text{M}+\text{H}]^+$: 251.1179; found 251.1173.

General procedure for the attempted synthesis of 2-amino-1,2,3,4-tetrahydroquinolines

In an argon filled glovebox, in a reaction tube (10 mL), equipped with a magnetic stirring bar, base and aminobenzyl alcohol (0.500 mmol, 1.0 equiv) were dissolved in DME. Then a stock solution of **Cat1** (200 μL , 0.025 M, 0.005 mmol, 0.01 equiv) and nitrile (0.500 mmol, 1.0 equiv) were added. The tube was placed in a reactor, which was closed tightly. Outside of the glovebox the reactor was flushed with hydrogen (3 \times), then pressurized with hydrogen and heated in an oil bath to 120 $^\circ\text{C}$ for 24 h. After cooling to room temperature, the reaction mixture was quenched with H_2O (0.1 mL) and extracted with EtOAc (0.5 mL). 30 μL of the organic layer were diluted in EtOAc (1.0 mL), filtered over MgSO_4 and analyzed via GC/MS analysis.

General procedure for catalytic reactions based on the borrowing hydrogen strategy

In an argon filled glovebox, in a PTFE-lined screw-cap vial (1.5 mL, \varnothing 1 cm, height 3 cm) equipped with a magnetic stirring bar, ligand and metal precursor were dissolved in DME and stirred at 30 $^\circ\text{C}$ for 10 min. Afterwards, base was added and the resulting mixture was stirred for additional 5 min at room temperature. Then the substrates were added and the vial was closed tightly. Outside of the glovebox, the vial was placed in an aluminum block and heated at the required temperature for 24 h. After cooling to room temperature, the reaction was quenched by addition of H_2O (0.3 mL) and extracted with EtOAc (0.5 mL). 30 μL of the organic layer were diluted in EtOAc (1.0 mL), filtered over MgSO_4 and analyzed via GC/MS analysis.

Note: The reaction temperature and the amounts of ligand, metal precursor, base, substrates and solvent were adapted for each reaction.

General procedure for hydrogenation reactions

In an argon filled glovebox, in a reaction tube (10 mL), equipped with a magnetic stirring bar, **Cat3** (2.3 mg, 0.05 mmol, 0.02 equiv) and base were dissolved in DME (0.5 mL). Then the substrate (0.250 mmol, 1.0 equiv) was added. The tube was placed in a reactor, which was closed tightly. Outside of the glovebox the reactor was flushed with hydrogen (3×), pressurized with hydrogen and heated in an oil bath to 120 °C for 24 h. After cooling to room temperature, the reaction mixture was quenched with H₂O (0.1 mL) and extracted with EtOAc (0.5 mL). 30 µL of the organic layer were diluted in EtOAc (1.0 mL), filtered over MgSO₄ and analyzed *via* GC/MS analysis.

N-Alkylation of aniline with benzyl alcohol under atmospheric conditions

A PTFE-lined screw-cap vial (1.5 mL, ø 1 cm, height 3 cm), equipped with a magnetic stirring bar, was charged with aniline (89 µL, d=1.030 g/mL, 0.980 mmol, 1.0 equiv), benzyl alcohol (102 µL, d=1.045 g/mL, 0.980 mmol, 1.0 equiv) and KO^tBu (55.0 mg, 0.490 mmol, 0.5 equiv). Then **Cat3** (dissolved in C₆D₆, 0.052 M, 188 µL, 0.0098 mmol, 0.01 equiv) was added. The vial was closed, placed in an aluminum block and heated at 110 °C for 24 h. After cooling to room temperature, the reaction was quenched by addition of H₂O (0.3 mL) and extracted with EtOAc (0.5 mL). 30 µL of the organic layer were diluted in EtOAc (1.0 mL), filtered over MgSO₄ and analyzed *via* GC/MS analysis.

Aldol condensation of 1-phenylethanol with benzyl alcohol under atmospheric conditions

A PTFE-lined screw-cap vial (1.5 mL, ø 1 cm, height 3 cm), equipped with a magnetic stirring bar, was charged with 1-phenylethanol (121 µL, d=1.012 g/mL, 1.000 mmol, 1.0 equiv), benzyl alcohol (103.5 µL, d=1.045 g/mL, 1.000 mmol, 1.0 equiv) and KO^tBu (112.2 mg, 1.000 mmol, 1.0 equiv). Then **Cat3** (dissolved in DME, 0.10 M, 100 µL, 0.010 mmol, 0.01 equiv) was added. The vial was closed, placed in an aluminum block and heated at 100 °C for 24 h. After cooling to room temperature, the reaction was quenched by addition of H₂O (0.3 mL) and extracted with EtOAc (0.5 mL). 30 µL of the organic layer were diluted in EtOAc (1.0 mL), filtered over MgSO₄ and analyzed *via* GC/MS analysis.

Dehydrogenative coupling of 2-aminobenzyl alcohol and phenylacetonitrile under atmospheric conditions

A PTFE-lined screw-cap vial (1.5 mL, ø 1 cm, height 3 cm), equipped with a magnetic stirring bar, was charged with 2-aminobenzyl alcohol (123.5 mg, 1.000 mmol, 1.0 equiv),

phenylacetonitrile (117.15 mg, 1.000 mmol, 1.0 equiv) and KO^tBu (56.1 mg, 0.500 mmol, 0.5 equiv). Then **Cat3** (dissolved in DME, 0.10 M, 100 μ L, 0.010 mmol, 0.01 equiv) was added. The vial was closed, placed in an aluminum block and heated at 100 °C for 24 h. After cooling to room temperature, the reaction was quenched by addition of H₂O (0.3 mL) and extracted with EtOAc (0.5 mL). 30 μ L of the organic layer were diluted in EtOAc (1.0 mL), filtered over MgSO₄ and analyzed *via* GC/MS analysis.

Transfer hydrogenation of quinoline under atmospheric conditions

A PTFE-lined screw-cap vial (1.5 mL, \varnothing 1 cm, height 3 cm), equipped with a magnetic stirring bar, was charged with quinoline (118 μ L, d=1.093 g/mL, 1.000 mmol, 1.0 equiv), *i*PrOH (153 μ L, d=0.785 g/mL, 2.000 mmol, 2.0 equiv) and KO^tBu (112.2 mg, 1.000 mmol, 1.0 equiv). Then **Cat3** (dissolved in DME, 0.10 M, 100 μ L, 0.010 mmol, 0.01 equiv) was added. The vial was closed, placed in an aluminum block and heated at 100 °C for 24 h. After cooling to room temperature, the reaction was quenched by addition of H₂O (0.3 mL) and extracted with EtOAc (0.5 mL). 30 μ L of the organic layer were diluted in EtOAc (1.0 mL), filtered over MgSO₄ and analyzed *via* GC/MS analysis.

4. Conclusion and Outlook

In this work different strategies to broaden the applicability of the borrowing hydrogen principle were investigated.

First of all, the development of new reaction cascades was targeted. Thus, the combination of known abundant metal-based catalytic systems for borrowing hydrogen reactions with (chiral) organocatalysts that promote the transformation of the activated substrates was pursued. The combination of multiple catalytic species should open the way towards broader functionalized products and in the ideal case increase the enantioselectivity of these reaction sequences. Outstanding activities were observed with the acetonitrile-ligated analogue of the iron-based Knölker complex. Application of this catalyst allowed, on the one hand, the selective synthesis of higher substituted amines *via* *N*-alkylation and, on the other hand, the selective synthesis of imines *via* dehydrogenative condensation, starting from anilines and benzyl alcohols. The selectivity was demonstrated with 19 examples. Secondary amines were formed in a closed system under inert conditions. Quantitative conversions of the starting material were observed with 5 mol% of catalyst at 110 °C. Under aerobic conditions the selectivity switched in favor to the formation of imines. Conversions up to 86 % were achieved with a catalyst loading of 7.5 mol% and a reaction temperature of 140 °C. Both reactions were successfully performed without the application of base and the only formed by-product is water, which renders the developed strategy highly atom efficient. The newly formed highly reactive C=N-bond obtained through the dehydrogenative coupling process enabled the subsequent enantioselective functionalization with phosphites, promoted by chiral phosphoric acids (10 mol%). Thus, enantioenriched α -*N*-alkylamino phosphonates were successfully synthesized in up to 83 % yield with an enantiomeric excess up to 50 % *via* a one-pot two-step three component condensation. The only drawback of this strategy is that exclusively derivatives of anilines and benzyl alcohols can be used as substrates. The aromatic moiety seems to be crucial for the stability of the imines formed *in situ* under the reaction conditions.

Secondly, the possibility to change the outcome of a reaction, simply by tuning the reaction conditions, was examined. For these investigations a highly active PN³ manganese pincer complex with a bipyridine backbone (bpy-⁶NHⁱPrP) was chosen as catalyst. It was found that the application of this catalyst allows the selective synthesis of quinolines respectively 1,2,3,4-tetrahydroquinolines starting from secondary alcohols and aminobenzyl alcohols simply by adjusting the reaction temperature and switching between bases. 2 mol% of the manganese catalyst in combination with 50 mol% KO^tBu at 140 °C solely led to the formation of quinolines. Compared to the previously reported catalytic systems, the catalyst

and base loadings were significantly reduced. However, as the dehydrogenative coupling strategy has already been reported with various catalytic systems, we decided to focus on the selective synthesis of 1,2,3,4-tetrahydroquinolines. An activity screening revealed that the same amount of catalyst combined with 100 mol% of KH and 30 mol% of KOH at 120 °C leads to completion of the borrowing hydrogen cycle and thus favors the formation of the reduced 1,2,3,4-tetrahydroquinoline. Following the established procedure, 20 different 1,2,3,4-tetrahydroquinolines were synthesized in yields up to 91 %. Detailed investigations showed that it is crucial to conduct the reaction in a closed system under inert atmosphere. Moreover, the concentration and the ratio of reaction volume and headspace significantly influence the outcome of the reaction. Exemplary mechanistic studies demonstrated that the catalytic reaction starts with the formation of quinoline as the major product. After 4 h the amount of quinoline decreases while the hydrogenated tetrahydroquinoline is formed. During our studies we found that the PN^3 manganese complex is also able to form 1,2,3,4-tetrahydroquinolines starting from quinolines *via* hydrogenation with external hydrogen or transfer hydrogenation using *i*PrOH as hydrogen donor.

The third strategy comprised the synthesis and characterization of new manganese pincer complexes and first investigations of their catalytic activity. Thus, two manganese pincer complexes with a phenanthroline backbone ($\text{phen-}^2\text{NH}^i\text{PrP}$) were synthesized and compared. They are distinguished by their metal precursors, for one $\text{Mn}(\text{CO})_5\text{Br}$ was used as metal donor, for the other $\text{MeMn}(\text{CO})_5$. Both complexes were shown to be suitable catalysts to promote the *N*-alkylation of aniline, the hydrogenation of acetophenone and the transfer hydrogenation of quinoline, though the usage of additional base is required in any case. Particularly noteworthy results were obtained with the novel acyl manganese complex. Stability studies revealed that this complex decomposed only slowly in solution in air. Besides, it shows remarkable activity (conversion of 61 %) in promoting the *N*-alkylation of aniline under atmospheric conditions, opening new possibilities for manganese catalyzed borrowing hydrogen reactions. These early investigations reveal first insights into the potential and drawbacks of the synthesized manganese pincer complexes, though additional challenges still need to be addressed. Thus, to obtain further understandings in the mode of operation, an important point would be to crystallize the complexes and to examine their crystal structure. Furthermore, more catalytic studies should be conducted to broaden the reaction scope and to define the greatest strengths of the new complexes. Especially the studies under aerobic conditions have to be intensified, as they might open new possibilities for manganese catalyzed borrowing hydrogen reactions without the need to work in a glovebox or make use of Schlenk techniques .

5. References

- [1] R. A. Sheldon, *Chem. Commun.* **2008**, 3352–3365.
- [2] Sumit Bhaduri, D. Mukesh, *Homogeneous Catalysis: Mechanisms and Industrial Applications*, John Wiley & Sons, New Jersey, **2014**.
- [3] M. North, *Sustainable Catalysis: With Non-endangered Metals*, Royal Society of Chemistry, Cambridge, **2015**.
- [4] K. Hans Wedepohl, *Geochim. Cosmochim. Acta* **1995**, 59, 1217–1232.
- [5] M. Fritz, S. Schneider, in *The Periodic Table II: Catalytic, Materials, Biological and Medical Applications* Springer International Publishing, Cham, **2019**.
- [6] L. Alig, M. Fritz, S. Schneider, *Chem. Rev.* **2019**, 119, 2681–2751.
- [7] a) K. S. Egorova, V. P. Ananikov, *Angew. Chem. Int. Ed.* **2016**, 55, 12150–12162; b) K. S. Egorova, V. P. Ananikov, *Organometallics* **2017**, 36, 4071–4090.
- [8] Christoph Elschenbroich, A. Salzer, *Organometallchemie*, B. G. Teubner, Stuttgart, **1988**.
- [9] a) W. I. Dzik, J. I. Van der Vlugt, J. N. H. Reek, B. de Bruin, *Angew. Chem. Int. Ed.* **2011**, 50, 3356–3358; b) J. I. van der Vlugt, *Eur. J. Inorg. Chem.* **2012**, 2012, 363–375; c) V. Lyaskovskyy, B. de Bruin, *ACS Catal.* **2012**, 2, 270–279.
- [10] a) C. Gunanathan, D. Milstein, *Acc. Chem. Res.* **2011**, 44, 588–602; b) J. R. Khusnutdinova, D. Milstein, *Angew. Chem. Int. Ed.* **2015**, 54, 12236–12273.
- [11] A. Adrien Quintard, J. Rodriguez, *Angew. Chem. Int. Ed.* **2014**, 53, 4044 – 4055.
- [12] a) Y. Blum, Y. Shvo, *Isr. J. Chem.* **1984**, 24, 144–148; b) B. L. Conley, M. K. Pennington-Boggio, E. Boz, T. J. Williams, *Chem. Rev.* **2010**, 110, 2294–2312.
- [13] a) C. P. Casey, S. W. Singer, D. R. Powell, R. K. Hayashi, M. Kavana, *J. Am. Chem. Soc.* **2001**, 123, 1090–1100; b) J. B. Johnson, J.-E. Bäckvall, *J. Org. Chem.* **2003**, 68, 7681–7684.
- [14] G. N. Schrauzer, *J. Am. Chem. Soc.* **1959**, 81, 5307–5310.
- [15] a) H.-J. Knölker, J. Heber, C. H. Mahler, *Synlett* **1992**, 12, 1002–1004; b) H.-J. Knölker, E. Baum, H. Goesmann, R. Klauss, *Angew. Chem. Int. Ed.* **1999**, 38, 2064–2066; c) H.-J. Knölker, H. Goesmann, R. Klauss, *Angew. Chem. Int. Ed.* **1999**, 38, 702–705.
- [16] T. N. Plank, J. L. Drake, D. K. Kim, T. W. Funk, *Adv. Synth. Catal.* **2012**, 354, 597–601.
- [17] a) C. P. Casey, H. Guan, *J. Am. Chem. Soc.* **2007**, 129, 5816–5817; b) C. P. Casey, H. Guan, *J. Am. Chem. Soc.* **2009**, 131, 2499–2507.
- [18] L. Pignataro, C. Gennari, *Eur. J. Org. Chem.* **2020**, 3192–3205.

- [19] a) T. Yan, B. L. Feringa, K. Barta, *Nat. Commun.* **2014**, *5*, 5602–5609; b) S. Elangovan, J. Neumann, J. B. Sortais, K. Junge, C. Darcel, M. Beller, *Nat. Commun.* **2016**, *7*, 12641–12649; c) B. Emayavaramban, M. Roy, B. Sundararaju, *Chem. Eur. J.* **2016**, *22*, 3952–3955.
- [20] S. Elangovan, J.-B. Sortais, M. Beller, C. Darcel, *Angew. Chem. Int. Ed.* **2015**, *54*, 14483–14486.
- [21] a) T. Yan, K. Barta, *ChemSusChem* **2016**, *9*, 2321–2325; b) B. Emayavaramban, M. Sen, B. Sundararaju, *Org. Lett.* **2017**, *19*, 6–9.
- [22] a) J. Choi, A. H. R. MacArthur, M. Brookhart, A. S. Goldman, *Chem. Rev.* **2011**, *111*, 1761–1779; b) Gerard van Koten, D. Milstein, *Organometallic Pincer Chemistry*, Springer-Verlag, Berlin Heidelberg, **2013**; c) S. Werkmeister, J. Neumann, K. Junge, M. Beller, *Chem. Eur. J.* **2015**, *21*, 12226–12250; d) G. van Koten, R. A. Gossage, *The Privileged Pincer-Metal Platform: Coordination Chemistry and Applications*, Springer International Publishing, Cham, **2016**; e) E. Peris, R. H. Crabtree, *Chem. Soc. Rev.* **2018**, *47*, 1959–1968; f) M. A. W. Lawrence, K.-A. Green, P. N. Nelson, S. C. Lorraine, *Polyhedron* **2018**, *143*, 11–27.
- [23] a) C. J. Moulton, B. L. Shaw, *J. Chem. Soc., Dalton Trans.* **1976**, 1020–1024; b) G. van Koten, K. Timmer, J. G. Noltes, A. L. Spek, *J. Chem. Soc., Chem. Commun.* **1978**, 250–252; c) G. v. Koten, *Pure & Appl. Chem.* **1989**, *61*, 1681–1694.
- [24] H. Li, M. B. Hall, *ACS Catal.* **2015**, *5*, 1895–1913.
- [25] a) J. Zhang, G. Leituss, Y. Ben-David, D. Milstein, *J. Am. Chem. Soc.* **2005**, *127*, 10840–10841; b) E. Ben-Ari, G. Leituss, L. J. W. Shimon, D. Milstein, *J. Am. Chem. Soc.* **2006**, *128*, 15390–15391; c) J. Zhang, G. Leituss, Y. Ben-David, D. Milstein, *Angew. Chem. Int. Ed.* **2006**, *45*, 1113–1115; d) R. Langer, G. Leituss, Y. Ben-David, D. Milstein, *Angew. Chem. Int. Ed.* **2011**, *50*, 2120–2124; e) D. Srimani, Y. Ben-David, D. Milstein, *Chem. Commun.* **2013**, *49*, 6632–6634; f) P. Daw, S. Chakraborty, J. A. Garg, Y. Ben-David, D. Milstein, *Angew. Chem. Int. Ed.* **2016**, *55*, 14373–14377; g) A. Mukherjee, A. Nerush, G. Leituss, L. J. W. Shimon, Y. Ben David, N. A. Espinosa Jalapa, D. Milstein, *J. Am. Chem. Soc.* **2016**, *138*, 4298–4301; h) N. A. Espinosa-Jalapa, A. Kumar, G. Leituss, Y. Diskin-Posner, D. Milstein, *J. Am. Chem. Soc.* **2017**, *139*, 11722–11725; i) N. A. Espinosa-Jalapa, A. Nerush, L. J. W. Shimon, G. Leituss, L. Avram, Y. Ben-David, D. Milstein, *Chem. Eur. J.* **2017**, *23*, 5934–5938; j) P. Daw, A. Kumar, N. A. Espinosa-Jalapa, Y. Diskin-Posner, Y. Ben-David, D. Milstein, *ACS Catal.* **2018**, *8*, 7734–7741; k) U. K. Das, Y. Ben-David, G. Leituss, Y. Diskin-Posner, D. Milstein, *ACS Catal.* **2019**, *9*, 479–484; l) P. Daw, A. Kumar, N. A. Espinosa-Jalapa, Y. Ben-David, D. Milstein, *J. Am. Chem. Soc.* **2019**; m) A. Kumar, P. Daw, N. A. Espinosa-Jalapa, G. Leituss, L. J. W. Shimon, Y. Ben-

- David, D. Milstein, *Dalton Trans.* **2019**, 48, 14580–14584; n) S. Tang, D. Milstein, *Chem. Sci.* **2019**, 10, 8990–8994.
- [26] a) T. Zell, D. Milstein, *Acc. Chem. Res.* **2015**, 48, 1979–1994; b) S. Chakraborty, P. Bhattacharya, H. Dai, H. Guan, *Acc. Chem. Res.* **2015**, 48, 1995–2003; c) S. Murugesan, K. Kirchner, *Dalton Trans.* **2016**, 45, 416–439.
- [27] a) J. R. Carney, B. R. Dillon, S. P. Thomas, *Eur. J. Org. Chem.* **2016**, 2016, 3912–3929; b) D. A. Valyaev, G. Lavigne, N. Lugan, *Coord. Chem. Rev.* **2016**, 308, 191–235.
- [28] M. Garbe, K. Junge, M. Beller, *Eur. J. Org. Chem.* **2017**, 2017, 4344–4362.
- [29] a) D. Reardon, G. Aharonian, S. Gambarotta, G. P. A. Yap, *Organometallics* **2002**, 21, 786–788; b) H. Sugiyama, G. Aharonian, S. Gambarotta, G. P. A. Yap, P. H. M. Budzelaar, *J. Am. Chem. Soc.* **2002**, 124, 12268–12274; c) Q. Knijnenburg, S. Gambarotta, P. H. M. Budzelaar, *Dalton Trans.* **2006**, 5442–5448.
- [30] S. Elangovan, C. Topf, S. Fischer, H. Jiao, A. Spannenberg, W. Baumann, R. Ludwig, K. Junge, M. Beller, *J. Am. Chem. Soc.* **2016**, 138, 8809–8814.
- [31] F. Kallmeier, T. Irrgang, T. Dietel, R. Kempe, *Angew. Chem. Int. Ed.* **2016**, 55, 11806–11809.
- [32] N. H. Anderson, J. Boncella, A. M. Tondreau, *Chem. Eur. J.* **2019**, 25, 10557–10560.
- [33] L. Homberg, A. Roller, K. C. Hultsch, *Org. Lett.* **2019**, 21, 3142–3147.
- [34] a) A. Corma, J. Navas, M. J. Sabater, *Chem. Rev.* **2018**, 118, 1410–1459; b) T. Irrgang, R. Kempe, *Chem. Rev.* **2019**, 119, 2524–2549; c) B. G. Reed-Berendt, K. Polidano, L. C. Morrill, *Org. Biomol. Chem.* **2019**.
- [35] S. J. Pridmore, P. A. Slatford, A. Daniel, M. K. Whittlesey, J. M. J. Williams, *Tetrahedron Lett.* **2007**, 48, 5115–5120.
- [36] S. Waiba, B. Maji, *Chemcatchem* **2020**, 12, 1891–1902.
- [37] R. Fertig, T. Irrgang, F. Freitag, J. Zander, R. Kempe, *ACS Catal.* **2018**, 8, 8525–8530.
- [38] S. Zhou, S. Fleischer, K. Junge, M. Beller, *Angew. Chem. Int. Ed.* **2011**, 50, 5120–5124.
- [39] S. Fleischer, S. Zhou, S. Werkmeister, K. Junge, M. Beller, *Chem. Eur. J.* **2013**, 19, 4997–5003.
- [40] Y. Zhang, C. S. Lim, D. S. B. Sim, H. J. Pan, Y. Zhao, *Angew. Chem. Int. Ed.* **2014**, 53, 1399–1403.
- [41] A. Quintard, T. Constantieux, J. Rodriguez, *Angew. Chem. Int. Ed.* **2013**, 52, 12883–12887.
- [42] a) P. Merino, E. Marqués-López, R. P. Herrera, *Adv. Synth. Catal.* **2008**, 350, 1195–1208; b) R. P. Herrera, *Chem. Rec.* **2017**, 17, 833–840.

- [43] a) E. K. Fields, *J. Am. Chem. Soc.* **1952**, *74*, 1528–1531; b) A. C. Rafael, I. G. Vladimir, *Russ. Chem. Rev.* **1998**, *67*, 857; c) X. Cheng, R. Goddard, G. Buth, B. List, *Angew. Chem. Int. Ed.* **2008**, *47*, 5079–5081; d) Nikolay S. Zefirov, E. D. Matveeva, *ARKIVOC* **2008**, 1-17; e) G. Keglevich, E. Bálint, *Molecules* **2012**, *17*, 12821.
- [44] A. N. Pudovik, I. V. Konovalova, *Synthesis* **1979**, 1979, 81-96.
- [45] a) A. B. Smith, K. M. Yager, C. M. Taylor, *J. Am. Chem. Soc.* **1995**, *117*, 10879–10888; b) F. Orsini, G. Sello, M. Sisti, *Curr. Med. Chem.* **2010**, *17*, 264–289; c) M. Ordóñez, J. L. Viveros-Ceballos, C. Cativiela, F. J. Sayago, *Tetrahedron* **2015**, *71*, 1745–1784.
- [46] F. R. Atherton, M. J. Hall, C. H. Hassall, R. W. Lambert, W. J. Lloyd, P. S. Ringrose, *Antimicrob. Agents Chemother.* **1979**, *15*, 696–705.
- [47] Mario Ordóñez, José Luis Viveros-Ceballos, I. R. Estudillo, in *Amino Acids - New Insides and Roles in Plants and Animals* (Eds.: Thoshiki Asao, M. Asaduzzaman), InTech, **2017**, pp. 127–152.
- [48] a) W. F. Gilmore, H. A. McBride, *J. Am. Chem. Soc.* **1972**, *94*, 4361–4361; b) I. M. Lefebvre, S. A. Evans, *J. Org. Chem.* **1997**, *62*, 7532–7533; c) C. Qian, T. Huang, *J. Org. Chem.* **1998**, *63*, 4125–4128; d) F. A. Davis, S. Lee, H. Yan, D. D. Titus, *Org. Lett.* **2001**, *3*, 1757–1760.
- [49] a) H. Sasai, S. Arai, Y. Tahara, M. Shibasaki, *J. Org. Chem.* **1995**, *60*, 6656–6657; b) H. Gröger, Y. Saida, S. Arai, J. Martens, H. Sasai, M. Shibasaki, *Tetrahedron Lett.* **1996**, *37*, 9291–9292; c) H. Gröger, Y. Saida, H. Sasai, K. Yamaguchi, J. Martens, M. Shibasaki, *J. Am. Chem. Soc.* **1998**, *120*, 3089–3103; d) I. Schlemminger, Y. Saida, H. Gröger, W. Maison, N. Durot, H. Sasai, M. Shibasaki, J. Martens, *J. Org. Chem.* **2000**, *65*, 4818–4825; e) G. D. Joly, E. N. Jacobsen, *J. Am. Chem. Soc.* **2004**, *126*, 4102–4103; f) S. Kobayashi, H. Kiyohara, Y. Nakamura, R. Matsubara, *J. Am. Chem. Soc.* **2004**, *126*, 6558–6559; g) T. Akiyama, H. Morita, J. Itoh, K. Fuchibe, *Org. Lett.* **2005**, *7*, 2583–2585; h) D. Pettersen, M. Marcolini, L. Bernardi, F. Fini, R. P. Herrera, V. Sgarzani, A. Ricci, *J. Org. Chem.* **2006**, *71*, 6269–6272; i) L. Wang, S. Cui, W. Meng, G. Zhang, J. Nie, J. Ma, *Chin. Sci. Bull.* **2010**, *55*, 1729–1731; j) P. B. Thorat, S. V. Goswami, R. L. Magar, B. R. Patil, S. R. Bhusare, *Eur. J. Org. Chem.* **2013**, 5509–5516; k) P. S. Bhadury, Y. Zhang, S. Zhang, B. Song, S. Yang, D. Hu, Z. Chen, W. Xue, L. Jin, *Chirality* **2009**, *21*, 547–557; l) Y. Zhao, X. Li, F. Mo, L. Li, X. Lin, *RSC Adv.* **2013**, *3*, 11895–11901; m) F.-Q. Shi, B.-A. Song, *Org. Biomol. Chem.* **2009**, *7*, 1292–1298.

- [50] a) T. A. Mastryukova, I. M. Aladzheva, I. V. Leont'eva, P. V. Petrovski, E. I. Fedin, M. I. Kabachnik, *Pure Appl. Chem.* **1980**, *52*, 945–957; b) D. Parmar, E. Sugiono, S. Raja, M. Rueping, *Chem. Rev.* **2014**, *114*, 90479153.
- [51] a) J. P. Michael, *Nat. Prod. Rep.* **2008**, *25*, 166–187; b) Shagufta, I. Ahmad, *Med. Chem. Comm.* **2017**, *8*, 871–885.
- [52] D. Wei, V. Dorcet, C. Darcel, J.-B. Sortais, *ChemSusChem* **2019**, *12*, 3078–3082.
- [53] S. Shee, K. Ganguli, K. Jana, S. Kundu, *Chem. Commun.* **2018**, *54*, 6883–6886.
- [54] K. Das, A. Mondal, D. Pal, D. Srimani, *Org. Lett.* **2019**, *21*, 3223–3227.
- [55] G. Chakraborty, R. Sikari, S. Das, R. Mondal, S. Sinha, S. Banerjee, N. D. Paul, *J. Org. Chem.* **2019**, *84*, 2626–2641.
- [56] a) H. Li, Y. Wang, Z. Lai, K.-W. Huang, *ACS Catal.* **2017**, *7*, 4446–4450; b) L. Homberg, *Investigations on Base Metal-assisted Synthesis of Amines*, Doctoral thesis, University of Vienna, **2020**.
- [57] a) S. Weber, L. F. Veiros, K. Kirchner, *Adv. Synth. Catal.* **2019**, *361*, 5412–5420; b) S. Weber, B. Stöger, L. F. Veiros, K. Kirchner, *ACS Catal.* **2019**, *9*, 9715–9720; c) K. J. Kadassery, D. C. Lacy, *Dalton Trans.* **2019**, *48*, 4467–4470.
- [58] a) R. van Putten, E. A. Uslamin, M. Garbe, C. Liu, A. Gonzalez-de-Castro, M. Lutz, K. Junge, E. J. M. Hensen, M. Beller, L. Lefort, E. A. Pidko, *Angew. Chem. Int. Ed.* **2017**, *56*, 7531–7534; b) S. Elangovan, M. Garbe, H. Jiao, A. Spannenberg, K. Junge, M. Beller, *Angew. Chem. Int. Ed.* **2016**, *55*, 15364–15368; c) T. Chen, H. Li, S. Qu, B. Zheng, L. He, Z. Lai, Z.-X. Wang, K.-W. Huang, *Organometallics* **2014**, *33*, 4152–4155.
- [59] a) S. Weber, B. Stöger, K. Kirchner, *Org. Lett.* **2018**, *20*, 7212–7215; b) B. Maji, M. K. Barman, *Synthesis* **2017**, *49*, 3377–3393; c) M. B. Widegren, G. J. Harkness, A. M. Z. Slawin, D. B. Cordes, M. L. Clarke, *Angew. Chem. Int. Ed.* **2017**, *56*, 5825–5828.
- [60] a) B. T. Gregg, P. K. Hanna, E. J. Crawford, A. R. Cutler, *J. Am. Chem. Soc.* **1991**, *113*, 384–385; b) M. DiBiase Cavanaugh, B. T. Gregg, A. R. Cutler, *Organometallics* **1996**, *15*, 2764–2769; c) B. T. Gregg, A. R. Cutler, *J. Am. Chem. Soc.* **1996**, *118*, 10069–10084.
- [61] H. E. Gottlieb, V. Kotlyar, A. Nudelman, *J. Org. Chem.* **1997**, *62*, 7512–7515.
- [62] Y. Engel, A. Dahan, E. Rozenshine-Kemelmakher, M. Gozin, *J. Org. Chem.* **2007**, *72*, 2318–2328.
- [63] Wang Tao, Tang Xiaoli, G. Chenghao, CN104045599B, China, **2019**.

6. Appendix

6.1. Abbreviations

Alox	Aluminium oxide	NMR	Nuclear Magnetic Resonance
BINOL	1,1'-Binaphthyl-2,2'-diol	Ph	Phenyl
br	Broad signal	ppm	Parts per million
d	Doublet	quint	Quintet
dd	Doublet of doublet	rt	Room temperature
ddd	Doublet of doublet of doublet	s	Singlet
dH ₂ O	Deionised water	sept	Septet
dq	Doublet of quartet	t	Triplet
dquin	Doublet of quintet	td	Triplet of doublet
dsxt	Doublet of sextet	tt	Triplet of triplet
dt	Doublet of triplet	THF	Tetrahydrofurane
CH ₂ Cl ₂	Dichloromethane	TEMPO	(2,2,6,6-Tetramethylpiperidin-1-yl)oxyl
DMF	Dimethylformamide	TLC	Thin layer chromatography
ee	Enantiomeric excess		
eq	Equivalent		
Et ₂ O	Diethylether		
EtOAc	Ethylacetate		
EtOH	Ethanol		
FT-IR	Fourier-transform infrared spectroscopy		
GC/MS	Gas chromatography with mass spectrometry		
GC/FID	Gas chromatography with flame ionization detection		
h	Hour(s)		
hept	Heptane		
HPLC	High Pressure Liquid Chromatography		
<i>i</i> PrOH	Isopropylalcohol		
m	Multiplet		
MeOH	Methanol		
min	Minute(s)		
<i>n</i> BuLi	<i>n</i> -Butyllithium		

6.2. Figures

Figure 1: Concentration [ppm] of middle to late transitions metals in the continental earth crust.....	1
Figure 2: Tuning possibilities of pincer ligands.....	4
Figure 3: Different scaffolds of manganese-based pincer complexes.....	6
Figure 4: Important structural motifs obtained through ACD, ODC or BH strategies.....	9
Figure 5: Selected examples of biologically important α -amino phosphonates and phosphonic acids	13
Figure 6: a) Bifunctional activation mechanism of BINOL- based chiral phosphoric acids. b) Phosphonate-phosphite tautomerism.....	15
Figure 7: Strategies to broaden the applicability of borrowing hydrogen reactions and related methods.	16
Figure 8: Complexation of phen- ² NH- ⁱ PrP (4) with Mn(CO) ₅ Br in THF-d ₈ monitored <i>via</i> ³¹ P NMR spectroscopy.	102
Figure 9: Complexation of phen- ² NH- ⁱ PrP (4) with Mn(CO) ₅ Br in C ₆ D ₆ monitored <i>via</i> ³¹ P NMR spectroscopy.	103
Figure 10: Complexation of phen- ² NH- ⁱ PrP (4) with Mn(CO) ₅ Br in C ₆ D ₆ monitored <i>via</i> ³¹ P NMR spectroscopy over a longer period of time.....	103
Figure 11: FT-IR spectrum of Cat2 and its precursor (Mn(CO) ₅ Br) recorded using a NaCl cuvette in CHCl ₃	104
Figure 12: Complexation of phen- ² NH- ⁱ PrP with MeMn(CO) ₅ in THF-d ₈ (*) monitored <i>via</i> ¹ H NMR spectroscopy.	105
Figure 13: Complexation of phen- ² NH- ⁱ PrP with MeMn(CO) ₅ in THF-d ₈ monitored <i>via</i> ³¹ P NMR spectroscopy.	105
Figure 14: Complexation of phen- ² NH- ⁱ PrP with MeMn(CO) ₅ in C ₆ D ₆ monitored <i>via</i> ¹ H NMR spectroscopy.	106
Figure 15: Complexation of phen- ² NH- ⁱ PrP with MeMn(CO) ₅ in C ₆ D ₆ monitored <i>via</i> ³¹ P NMR spectroscopy.	106
Figure 16: FT-IR spectrum of Cat3 and its precursor (MeMn(CO) ₅) recorded using a NaCl cuvette in CHCl ₃	107
Figure 17: Decomposition of Cat3 under atmospheric conditions monitored <i>via</i> ¹ H-NMR spectroscopy in C ₆ D ₆	114
Figure 18: Decomposition of Cat3 under atmospheric conditions monitored <i>via</i> ³¹ P-NMR spectroscopy in C ₆ D ₆	114

6.3. Schemes

Scheme 1: Proposed mechanism for the dehydrogenation of alcohols promoted by ruthenium-based Shvo catalyst.	3
Scheme 2: Cyclopentadienyl-ligated iron complexes.	4
Scheme 3: Proposed aromatization dearomatization mechanism by using a non-innocent PNP pincer ligand for the hydrogenation of ketones.	5
Scheme 4: General principle of the borrowing hydrogen methodology.	7
Scheme 5: Ruthenium-promoted pyrrole synthesis from 1,4-alkynediols and amines.	8
Scheme 6: Mechanistic differences based on the role of hydrogen.	8
Scheme 7: Switchable selective synthesis of <i>N</i> -alkylated amines and imines.	9
Scheme 8: Enantioselective hydrogenation of imines and quinoxalines promoted by a cooperative catalytic system.	10
Scheme 9: Synthesis of chiral amines <i>via</i> cooperative catalysis by iridium and a chiral phosphoric acid.	11
Scheme 10: Enantioselective functionalization of allylic alcohols through dual catalysis by iron and an amino acid derivative.	12
Scheme 11: Synthesis of α -amino and α -hydroxy phosphonates.	13
Scheme 12: Asymmetric hydrophosphonylation of aldimines promoted by a chiral BINOL-based phosphoric acid.	14
Scheme 13: Direct asymmetric three- component Kabachnik-Fields reaction promoted by a chiral BINOL-based phosphoric acid.	14
Scheme 14: Investigated PN^3 manganese pincer complexes.	98
Scheme 15: Optimized synthesis of the phenanthroline-based NNP pincer ligand 4	101
Scheme 16: Complexation of phen- ² NH- ⁱ PrP (4) with $\text{Mn}(\text{CO})_5\text{Br}$	101
Scheme 17: Complexation of phen- ² NH- ⁱ PrP (4) with $\text{MeMn}(\text{CO})_5$	104
Scheme 18: Comparison of the catalytic activity of Cat1 and Cat2	108
Scheme 19: Activation of Cat3 with KOtBu in THF-d_8 at room temperature.	112
Scheme 20: Attempted activation via hydrosilylation of Cat3	113
Scheme 21: <i>N</i> -alkylation of aniline under atmospheric conditions.	114
Scheme 22: Additional investigations on reactions under atmospheric conditions.	115

6.4. Tables

Table 1: Substrate Screening for the synthesis of 2-amino quinolines	99
Table 2: Attempted synthesis of 2-amino-1,2,3,4-tetrahydroquinolines.	100
Table 3: Comparison of the catalytic activity of Cat2 and Cat3	109
Table 4: Hydrogenation of benzonitrile.....	109
Table 5: Hydrogenation of methylbenzoate.....	110
Table 6: Hydrogenation of acetophenone	110
Table 7: Hydrogenation of amides	111
Table 8: Hydrogenation of quinoline.....	111
Table 9: Transfer hydrogenation of quinoline	112